

Green Chemistry

Cutting-edge research for a greener sustainable future

www.rsc.org/greenchem

Volume 8 | Number 12 | December 2006 | Pages 1009–1088



ISSN 1463-9262

RSC Publishing

Ghule *et al.*
Antibacterial ZnO nanoparticle
coated paper

Kayaki *et al.*
Carboxylative cyclization of
propargylamines with supercritical
carbon dioxide

Bao and Wang
An effective synthesis of
bromoesters

Funatomi *et al.*
Pentafluorophenylammonium
triflate: an efficient, practical and cost
effective catalyst



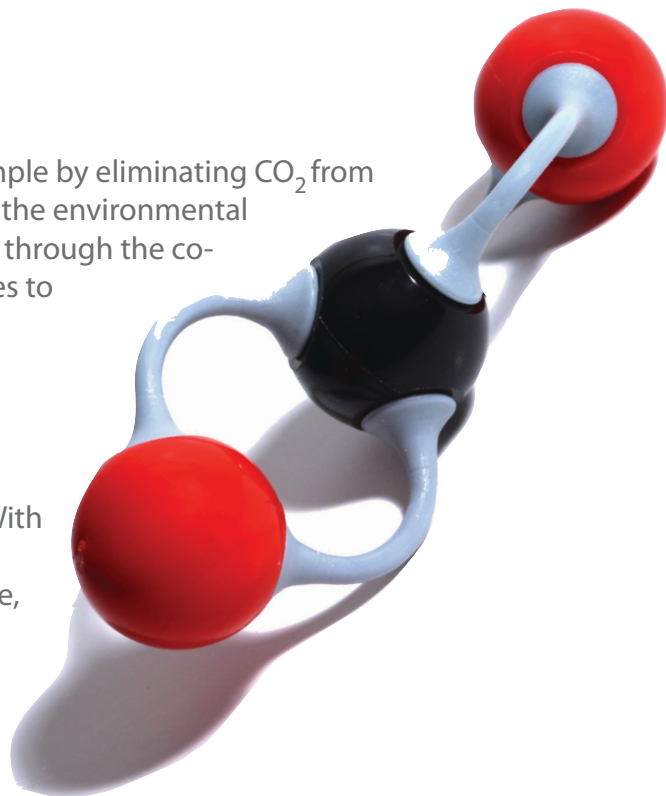
1463-9262(2006)8:12;1-X

Dalton Transactions web theme issue:

CO₂ at metal centres

Methods for decreasing excess atmospheric CO₂, for example by eliminating CO₂ from gas-streams during air purification processes, are high on the environmental agenda. The chemistry of carbon dioxide at metal centres through the co-ordination of CO₂ or by reacting CO₂ with metal complexes to prepare carbon containing derivatives may hold some of the answers.

This timely web theme issue, guest edited by Dr. Roger Guilard, Professor of Chemistry at the University of Bourgogne in Dijon, France addresses exactly this topic. With contributed articles printed in regular issues of *Dalton Transactions* and collected online on a dedicated webpage, this first web theme issue from a series to appear in *Dalton Transactions* hails a new age in dynamic and flexible special issue publishing.



Topics covered in CO₂ at metal centres include:

Study of CO₂ sequestration by various materials

Catalytic synthesis using CO₂ as a building block

CO₂ as a building block for supramolecular assemblies

Chemistry of CO₂ inspired by nature

Metal assisted catalytic reactions in compressed CO₂

Activation of CO₂ via formation of metal-CO₂ complexes or insertion into metal-heteroatom bonds

Visit the website to **read** the latest articles or to **contribute** your article to this issue

Registered Charity Number: 207890

RSC Publishing

www.rsc.org/dalton/CO2

Green Chemistry

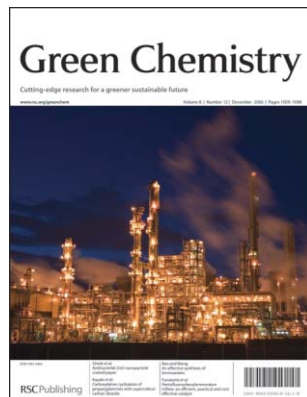
Cutting-edge research for a greener sustainable future

www.rsc.org/greenchem

RSC Publishing is a not-for-profit publisher and a division of the Royal Society of Chemistry. Any surplus made is used to support charitable activities aimed at advancing the chemical sciences. Full details are available from www.rsc.org

IN THIS ISSUE

ISSN 1463-9262 CODEN GRCHFJ 8(12) 1009-1088 (2006)



Cover

The novel green-chemical catalyst, pentafluorophenyl-ammonium triflate (PFPAT), is totally cost-effective for industrial scale condensations such as esterification, thioesterification, transesterification, and macrolactone formation. Image reproduced by permission of Yoo Tanabe, from *Green Chem.*, 2006, 8(12), 1022.

CHEMICAL TECHNOLOGY

T45

Chemical Technology highlights the latest applications and technological aspects of research across the chemical sciences.

Chemical Technology

December 2006/Volume 3/Issue 12

www.rsc.org/chemicaltechnology

HIGHLIGHT

1017

Highlights

Markus Hölscher reviews some of the recent literature in green chemistry.



EDITORIAL STAFF

Editor

Sarah Ruthven

News writer

Markus Hölscher

Publishing assistant

Emma Hacking

Team leader, serials production

Stephen Wilkes

Technical editor

Edward Morgan

Administration coordinator

Sonya Spring

Editorial secretaries

Lynne Braybrook, Jill Segev, Julie Thompson

Publisher

Emma Wilson

Green Chemistry (print: ISSN 1463-9262; electronic: ISSN 1463-9270) is published 12 times a year by the Royal Society of Chemistry, Thomas Graham House, Science Park, Milton Road, Cambridge, UK CB4 0WF.

All orders, with cheques made payable to the Royal Society of Chemistry, should be sent to RSC Distribution Services, c/o Portland Customer Services, Commerce Way, Colchester, Essex, UK CO2 8HP. Tel +44 (0) 1206 226050; E-mail sales@rscdistribution.org

2006 Annual (print + electronic) subscription price: £859; US\$1571. 2006 Annual (electronic) subscription price: £773; US\$1414. Customers in Canada will be subject to a surcharge to cover GST. Customers in the EU subscribing to the electronic version only will be charged VAT.

If you take an institutional subscription to any RSC journal you are entitled to free, site-wide web access to that journal. You can arrange access via Internet Protocol (IP) address at www.rsc.org/ip. Customers should make payments by cheque in sterling payable on a UK clearing bank or in US dollars payable on a US clearing bank. Periodicals postage paid at Rahway, NJ, USA and at additional mailing offices. Airfreight and mailing in the USA by Mercury Airfreight International Ltd., 365 Blair Road, Avenel, NJ 07001, USA.

US Postmaster: send address changes to Green Chemistry, c/o Mercury Airfreight International Ltd., 365 Blair Road, Avenel, NJ 07001. All despatches outside the UK by Consolidated Airfreight.

PRINTED IN THE UK

Advertisement sales: Tel +44 (0) 1223 432246; Fax +44 (0) 1223 426017; E-mail advertising@rsc.org

Green Chemistry

Cutting-edge research for a greener sustainable future

www.rsc.org/greenchem

Green Chemistry focuses on cutting-edge research that attempts to reduce the environmental impact of the chemical enterprise by developing a technology base that is inherently non-toxic to living things and the environment.

EDITORIAL BOARD

Chair

Professor Martyn Poliakoff,
Department of Chemistry
University of Nottingham,
Nottingham, UK
E-mail martyn.poliakoff@nottingham.ac.uk

Scientific editor

Professor Walter Leitner,
RWTH-Aachen, Germany
E-mail leitner@itmc.rwth-aachen.de

Members

Professor Joan Brennecke,
University of Notre Dame, USA

Dr Janet Scott, Centre for Green
Chemistry, Monash University,
Australia

Dr A Michael Warhurst,
University of Massachusetts,
USA
E-mail michael-warhurst@uml.edu

Professor Tom Welton,
Imperial College, UK
E-mail t.welton@ic.ac.uk

Professor Roshan Jachuck,
Clarkson University, USA
E-mail rjachuck@clarkson.edu

Dr Paul Anastas, Green Chemistry
Institute, USA
E-mail p_anastas@acs.org

Professor Buxing Han, Chinese
Academy of Sciences
E-mail hanbx@iccas.ac.cn

Associate editors

Professor C. J. Li, McGill
University, Canada
E-mail cj.li@mcgill.ca
Professor Kyoko Nozaki
Kyoto University, Japan
E-mail nozaki@chembio-tu-tokyo.ac.jp

INTERNATIONAL ADVISORY EDITORIAL BOARD

James Clark, York, UK
Avelino Corma, Universidad
Politécnica de Valencia, Spain
Mark Harmer, DuPont Central
R&D, USA

Herbert Hugl, Lanxess Fine
Chemicals, Germany
Makato Misono, Kogakuin
University, Japan
Colin Raston,
University of Western Australia,
Australia

Robin D. Rogers, Centre for Green
Manufacturing, USA
Kenneth Seddon, Queen's
University, Belfast, UK
Roger Sheldon, Delft University of
Technology, The Netherlands
Gary Sheldrake, Queen's
University, Belfast, UK
Pietro Tundo, Università ca
Foscari di Venezia, Italy
Tracy Williamson, Environmental
Protection Agency, USA

INFORMATION FOR AUTHORS

Full details of how to submit material for publication in Green Chemistry are given in the Instructions for Authors (available from <http://www.rsc.org/authors>). Submissions should be sent via ReSource: <http://www.rsc.org/resource>.

Authors may reproduce/republish portions of their published contribution without seeking permission from the RSC, provided that any such republication is accompanied by an acknowledgement in the form: (Original citation) – Reproduced by permission of the Royal Society of Chemistry.

© The Royal Society of Chemistry 2006. Apart from fair dealing for the purposes of research or private study for non-commercial purposes, or criticism or review, as permitted under the Copyright, Designs and Patents Act 1988 and the Copyright and Related Rights Regulations 2003, this publication may only be reproduced, stored or transmitted, in any form or by any means, with the prior permission in writing of the Publishers or in the case of reprographic reproduction in accordance with the terms of

licences issued by the Copyright Licensing Agency in the UK. US copyright law is applicable to users in the USA.

The Royal Society of Chemistry takes reasonable care in the preparation of this publication but does not accept liability for the consequences of any errors or omissions.

Ⓢ The paper used in this publication meets the requirements of ANSI/NISO Z39.48-1992 (Permanence of Paper).

Royal Society of Chemistry: Registered Charity No. 207890

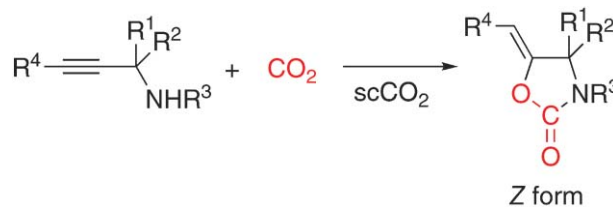
COMMUNICATION

1019

Carboxylative cyclization of propargylamines with supercritical carbon dioxide

Yoshihito Kayaki, Masafumi Yamamoto,
Tomoyuki Suzuki and Takao Ikariya*

The reaction of propargylamines in $scCO_2$ proceeds smoothly even in the absence of metal or strong base catalyst to give five-membered cyclic urethanes, (Z)-5-alkylidene-1,3-oxazolidin-2-ones, selectively.



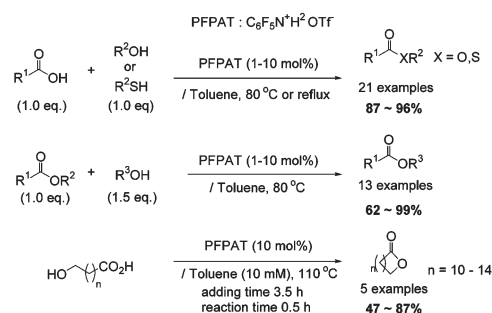
PAPERS

1022

Pentafluorophenylammonium triflate (PFPAT): an efficient, practical, and cost-effective catalyst for esterification, thioesterification, transesterification, and macrolactone formation

Takashi Funatomi, Kazunori Wakasugi, Tomonori Misaki and Yoo Tanabe*

PFPAT is air-stable, cost-effective, only mildly toxic, easy to handle, and easily removed from the reaction mixtures.

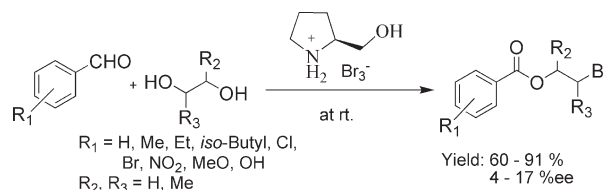


1028

An effective synthesis of bromoesters from aromatic aldehydes using tribromide ionic liquid based on L-prolinol as reagent and reaction medium under mild conditions

Weiliang Bao* and Zhiming Wang

Two kinds of ionic liquids have been synthesized in excellent yields, and used for the synthesis of 1,2- or 1,3-bromoesters at room temperature.

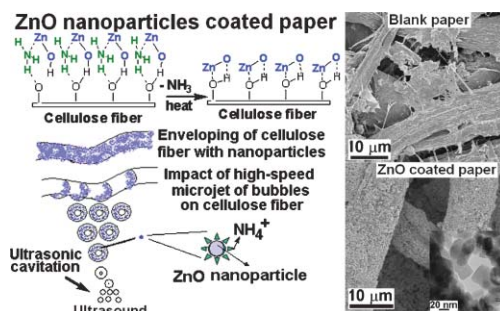


1034

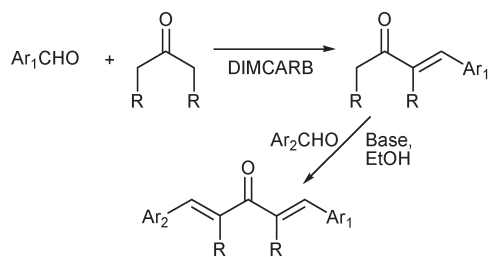
Preparation and characterization of ZnO nanoparticles coated paper and its antibacterial activity study

Kalyani Ghule, Anil Vithal Ghule, Bo-Jung Chen and Yong-Chien Ling*

A simple and economic green chemistry approach of ultrasound assisted coating of ZnO nanoparticles (~20 nm) on paper surface without the aid of binders.



1042



A direct, efficient synthesis of unsymmetrically substituted bis(arylidene)alkanones

Anthony E. Rosamilia, Marilena A. Giarrusso, Janet L. Scott* and Christopher R. Strauss*

An atom economical method to unsymmetrically substituted bis(arylidene)alkanones by sequential selective condensation reactions using DIMCARB and classical Claisen-Schmidt reaction conditions is reported.

1051

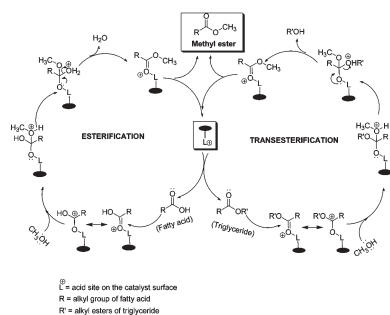


Low melting sugar–urea–salt mixtures as solvents for organic reactions—estimation of polarity and use in catalysis

Giovanni Imperato, Silke Höger, Dieter Lenoir and Burkhard König*

A polarity similar to DMSO or ethylene glycol was found for sugar–urea–salt melts, which are suitable solvents for catalytic organic reactions.

1056

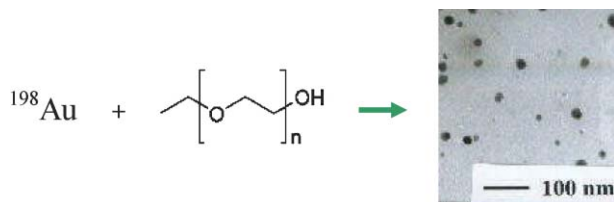


Solid acid catalyzed biodiesel production by simultaneous esterification and transesterification

Mangesh G. Kulkarni, Rajesh Gopinath, Lekha Charan Meher and Ajay Kumar Dalai*

12-Tungstophosphoric acid supported on hydrous zirconia is non-toxic, inexpensive, recyclable and promising eco-friendly catalyst for the biodiesel synthesis from low quality oils containing free fatty acids (FFAs). Simultaneous esterification and transesterification of oil containing large amounts of FFA takes place successfully on this catalyst *via* the proposed scheme given opposite.

1063



A green method for synthesis of radioactive gold nanoparticles

Kamalika Roy and Susanta Lahiri*

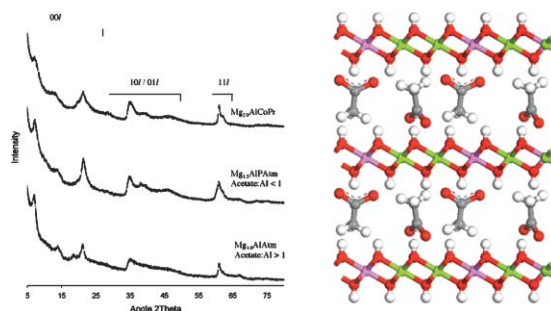
Radioactive gold-198 nanoparticles have been synthesized using a green and chemically safe solvent, PEG 4000.

1067

A one-pot synthesis of hybrid organo-layered double hydroxide catalyst precursors

H. Chris Greenwell,* William Jones,* Dennis N. Stamires, Paul O'Connor and Michael F. Brady

We describe the one-pot synthesis of layered double hydroxides containing organic (acetate) anions by a method that requires no excess of base, filtering or washing of the product.

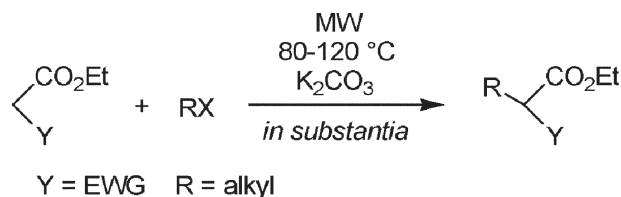


1073

Microwave irradiation as an alternative to phase transfer catalysis in the liquid-solid phase, solvent-free C-alkylation of active methylene containing substrates

György Keglevich,* Tibor Novák, László Vida and István Greiner

Solid/liquid phase C-alkylations were accomplished efficiently under MW irradiation in the absence of a phase transfer catalyst without the use of any solvent.

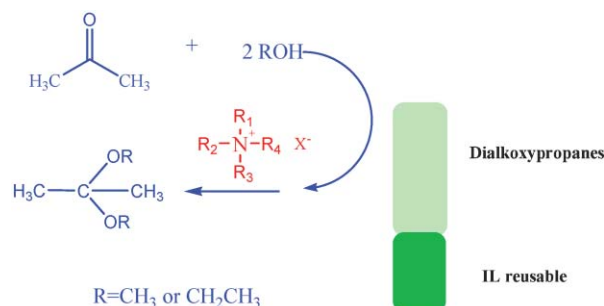


1076

Preparation of dialkoxypropanes in simple ammonium ionic liquids

Hui Jiang, Congmin Wang, Haoran Li* and Yong Wang

Simple ammonium ionic liquids are prepared and used as acidic catalysts for the synthesis of alkoxypropenes, eliminating the need for volatile organic solvents and poisonous catalysts. High conversion and selectivity are obtained in sulfate ionic liquids.

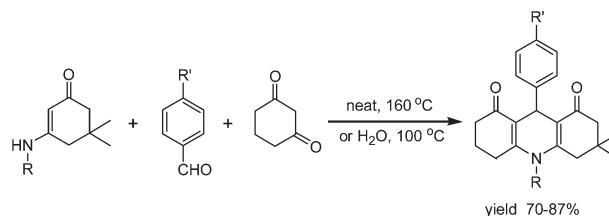


1080

Environmentally benign one-pot multi-component approaches to the synthesis of novel unsymmetrical 4-arylacridinediones

Guan-Wu Wang* and Chun-Bao Miao

The solvent-free and aqueous conditions give good yields that cannot be achieved in organic solvents.



AUTHOR INDEX

- | | | | |
|------------------------------|----------------------------|-----------------------------|-------------------------------|
| Bao, Weiliang, 1028 | Höger, Silke, 1051 | Li, Haoran, 1076 | Strauss, Christopher R., 1042 |
| Brady, Michael F., 1067 | Ikariya, Takao, 1019 | Ling, Yong-Chien, 1034 | Suzuki, Tomoyuki, 1019 |
| Chen, Bo-Jung, 1034 | Imperato, Giovanni, 1051 | Meher, Lekha Charan, 1056 | Tanabe, Yoo, 1022 |
| Dalai, Ajay Kumar, 1056 | Jiang, Hui, 1076 | Miao, Chun-Bao, 1080 | Vida, László, 1073 |
| Funatomi, Takashi, 1022 | Jones, William, 1067 | Misaki, Tomonori, 1022 | Wakasugi, Kazunori, 1022 |
| Ghule, Anil Vithal, 1034 | Kayaki, Yoshihito, 1019 | Novák, Tibor, 1073 | Wang, Congmin, 1076 |
| Ghule, Kalyani, 1034 | Keglevich, György, 1073 | O'Connor, Paul, 1067 | Wang, Guan-Wu, 1080 |
| Giarrusso, Marilena A., 1042 | König, Burkhard, 1051 | Rosamilia, Anthony E., 1042 | Wang, Yong, 1076 |
| Gopinath, Rajesh, 1056 | Kulkarni, Mangesh G., 1056 | Roy, Kamalika, 1063 | Wang, Zhiming, 1028 |
| Greenwell, H. Chris, 1067 | Lahiri, Susanta, 1063 | Scott, Janet L., 1042 | Yamamoto, Masafumi, 1019 |
| Greiner, István, 1073 | Lenoir, Dieter, 1051 | Stamires, Dennis N., 1067 | |

FREE E-MAIL ALERTS AND RSS FEEDS


Contents lists in advance of publication are available on the web *via* www.rsc.org/greenchem - or take advantage of our free e-mail alerting service (www.rsc.org/ej_alert) to receive notification each time a new list becomes available.

RSS Try our RSS feeds for up-to-the-minute news of the latest research. By setting up RSS feeds, preferably using feed reader software, you can be alerted to the latest Advance Articles published on the RSC web site. Visit www.rsc.org/publishing/technology/rss.asp for details.

ADVANCE ARTICLES AND ELECTRONIC JOURNAL

Free site-wide access to Advance Articles and the electronic form of this journal is provided with a full-rate institutional subscription. See www.rsc.org/ejs for more information.

* Indicates the author for correspondence: see article for details.

 Electronic supplementary information (ESI) is available *via* the online article (see <http://www.rsc.org/esi> for general information about ESI).

An Introduction to Pollution Science

By R M Harrison

A student textbook looking at pollution and its impact on human health and the environment. Topics include:

- pollution in the atmosphere
- the world's waters
- soil and land contamination
- institutional mechanisms for pollution management

Ideal for undergraduates studying environmental science and for those who have a general interest in the field.



Hardback | 2006 | ca xii+322 pages | £24.95 | RSC Member Price £16.50 | ISBN-10: 0 85404 829 4 | ISBN-13: 978 0 85404 829 8

Registered Charity No. 207890

26050690

RSC Publishing

www.rsc.org/books/8294

Highlights

DOI: 10.1039/b615594b

Markus Hölscher reviews some of the recent literature in green chemistry.

Reflections on the development of green chemistry topics over the last three years

During the last three years the interest in green chemistry topics has grown significantly, reflecting the increasing awareness of academic and industrial scientists to generate green and sustainable solutions for a variety of applications. If one simply compares the impact factors of this journal (2.5 in 2003 and 3.2 in 2006), it is impressive to see how fast researchers from nearly every place around the world are adopting the underlying idea of contributing to a safer, greener and more competitive future. Without neglecting the wealth of scientific contributions, certain fields emerged that constitute the prominent topics of current state of the art research. With regard to minimizing the energy consumption problem and to help reduce green house gas emissions in stationary and mobile energy generation processes, the application of fuel cells is one of the core developments that has attracted large interest. In the field of general chemistry, the avoidance of volatile organic solvents is one of the main fields contributing to a cleaner industrial production, and here the focus lies on the introduction of novel reaction media such as ionic liquids, supercritical fluids and novel non-volatile organic solvents. A whole new class of catalytic applications is very closely related to these developments, as researchers are constantly seeking ways to catalytically produce what conventionally would lead to a large amount of waste products. To strengthen the importance of this research, some of the most assessed publications in this journal are highlighted here. Another field which is attracting increasing interest is the mimicking of enzyme catalytic fundamentals in organocatalytic reactions, and one of the very recent examples is also included in this section.

Current status of fuel cell technology

In the March 2005 issue of Green Chemistry, Frank de Bruijn from the Energy Research Centre of the Netherlands reviewed the current status of fuel cell technology for mobile and stationary applications.¹ The basic principle of a fuel cell can be deduced from Fig. 1 below.

At the negative electrode (anode) a fuel such as hydrogen is oxidized, while at the cathode oxygen is reduced. The electrolyte between the two electrodes transports the ions, providing a closed cycle. Among the different types of fuel cells under investigation, two types have evolved to be the most promising technologies: the proton exchange membrane fuel cell (PEMFC) and the solid oxide fuel cell (SOFC). The PEMFC is the fuel cell of choice for mobile applications, while the SOFC is mainly in development for stationary applications. Current state of the art PEMFC performances by different manufactures are cell power densities of up to 0.84 W cm^{-2} at a cell voltage of 0.7 V. Also the stack technology has improved, and nowadays stack power densities of over 1.5 kW L^{-1} are realized by several firms, while powers go up to 85 kW. With regard to automotive applications, the storage and transport of hydrogen is a topic which has not yet reached satisfactory conditions. The U.S. Department of Energy targets are based on a driving range of 600 km for a passenger car. By 2015, the storage tank should have 56 kg of weight and a volume of 62 L, containing 5 kg of hydrogen at a cost of ca. \$333. Refuelling times of 2.5 minutes are anticipated. This leads to a volumetric density of ca. 3 kWh L^{-1} . Currently only values of up

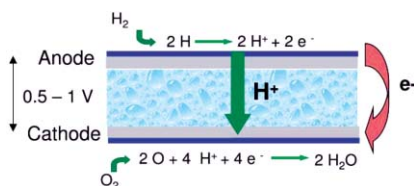


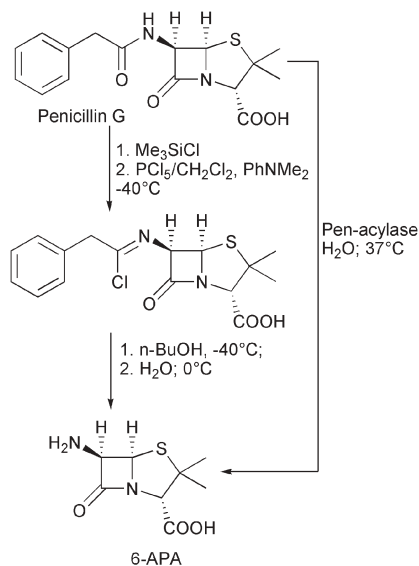
Fig. 1 Basic principle of a fuel cell.

to 1.6 can be achieved. The costs should be at \$2 per kWh, but currently they are ranging between 6 and 16, depending on the hydrogen storage technology used. As a result, the storage issue needs to be tackled very intensively. However, consequent progress would enable the use of fuel cells as a technology which reduces green house emissions drastically while making societies much less dependent on oil. Before commercial introduction can be envisaged, proof of reliability is needed as well as lower costs.

Green solvents in organic synthesis

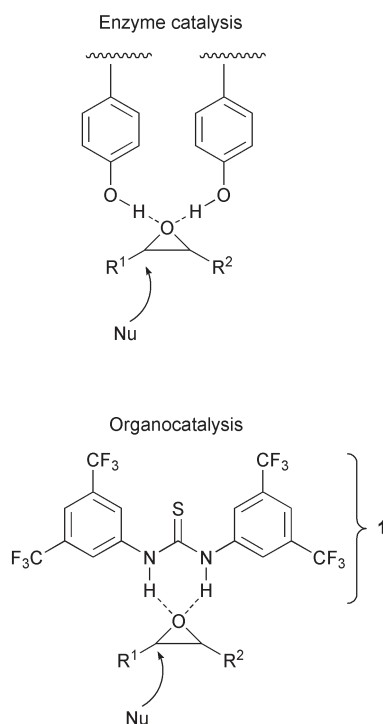
One of the main problems associated with conventional organic solvents is their energy consumptive recovery and/or polluting power due to their volatility. Accordingly, alternatives are desirable which are non-volatile (ideally also non-toxic and not inflammable/corrosive) and easy to recover and reuse. With regard to the design of sustainable industrial chemistry processes, both ionic liquids and supercritical fluids are at the core of the most promising developments of the last years. In most of the newly designed reactions these novel reaction media are used together with appropriate catalysts and catalyst technology. Roger A. Sheldon from the Delft University of Technology reviewed the current state of green solvent technology in Green Chemistry.² One of the approaches that has led to industrial realization is **aqueous biphasic catalysis**. The catalyst resides in the aqueous phase, while the product is contained in an organic solvent immiscible with water. The hydroformylation of propene to *n*-butanal in the Ruhrchemie/Rhone-Poulenc process is one of the successful industrial examples of this technology. Oxidation reactions also often suffer from the generation of undesired waste. However, by using hydrogen peroxide in conjunction with water as the solvent, the oxidation of alcohols to aldehydes or ketones and the epoxidation of olefins can be carried out

conveniently. Also, the use of molecular oxygen is possible, e.g. in the presence of appropriate Pd-catalysts. **Biocatalysis** has also made significant progress. The advantages of biocatalytic processes are mild reaction conditions, an environmentally compatible catalyst (an enzyme) and very often water as a green solvent. Also, the activities are very high in many cases, while chemo-, regio- and stereoselectivities are often outstanding. Approximately 130 processes are currently in industrial use. One illustrative example is the synthesis of 6-aminopenicillanic acid (6-APA), which is a key raw material for semi-synthetic penicillin and cephalosporin antibiotics. The chemical procedure, which is outlined below, resulted in the need for various chemicals (Me₃SiCl, 0.6 kg; PCl₅, 1.2 kg; PhNMe₂, 1.6 kg; NH₃, 0.2 kg; *n*-BuOH, 8.4 L; CH₂Cl₂, 8.4 L for the production of 1 kg of product). This process was replaced by an enzymatic process that is operated in water at 37 °C, and only NH₃ (0.09 kg) is needed to adjust the pH value.



Water amplifies hydrophobic interactions in non-covalent organocatalytic reactions

As biocatalytic syntheses often can be accomplished under very mild conditions with outstanding chemo-, regio- and



stereoselectivities in the greenest solvent one can think of—water—it is desirable to mimic enzyme catalysts, or at least transfer biocatalytic principles to the rapidly expanding field of organocatalysis. While water does not dissolve many organic molecules very well, it has repeatedly been proven that reactions with organic substrates in, or at least in close proximity to, water are possible. More important is the rate enhancement of chemical reactions often observed with water-insoluble or partially soluble compounds, which has been ascribed to the effects of hydrophobic hydration. Organocatalytic reactions mainly based on non-covalent interactions cannot be *a priori* considered to be amenable to aqueous chemistry, as water, being a very good hydrogen bond donor and/or acceptor, could easily destroy the necessary interactions for the catalytic reaction. In turn, water should still be able to act as a hydrophobic hydrator, as it forms strong hydrogen bonds with itself and thus might very well accelerate such reactions. Schreiner and Kleiner from the University of Giessen very recently investigated these questions and found a

promising answer.³ They transferred the underlying concept of epoxide hydrolases by using organocatalyst **1**, which mimics the key structural features of an epoxide hydrolase.

Upon coordination of the epoxide to the catalyst, an incoming nucleophile can easily attack one of the epoxide carbon atoms. The reactions were run in dichloromethane and in water. Interestingly the rate acceleration that was observed for the reactions in water was up to 200-fold. The postulated reaction mechanism could nicely be supported by DFT calculations, taking into consideration the effect of the different solvents, thus showing that hydrophobic amplification, which is a key element in enzyme catalysis, also applies for reactions with non-covalently acting organocatalysts.

Thank you!!!

Over the past three years it could clearly be deduced, from the increasing amount of assessments, that the Highlights section continuously grew in importance to the readers. For this interest and support, which has been a strong part of our motivation, I would personally like to express my gratefulness at this point. However, journals do reshape from time to time, which in this case makes it necessary to close the Highlights section with this issue of Green Chemistry. This by no means has an effect on the high quality scientific papers, which the journal will continue to publish as usual. I do hope that you will keep up your interest in this publication to stay tuned with the latest developments in one of the fundamental sciences that help shape a better future. Good luck to all of you!

Markus Hölscher

References

- 1 F. de Bruijn, *Green Chem.*, 2005, 7, 132–150.
- 2 R. A. Sheldon, *Green Chem.*, 2005, 7, 267–278.
- 3 C. M. Kleiner and P. R. Schreier, *Chem. Commun.*, 2006, 4315–4317.

Carboxylative cyclization of propargylamines with supercritical carbon dioxide†

Yoshihito Kayaki, Masafumi Yamamoto, Tomoyuki Suzuki and Takao Ikariya*

Received 13th March 2006, Accepted 11th September 2006

First published as an Advance Article on the web 26th September 2006

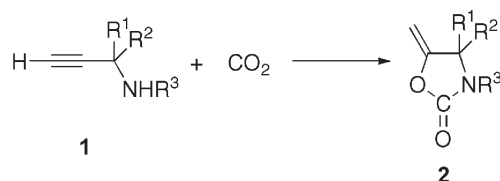
DOI: 10.1039/b603700c

Propargylic amines were found to react smoothly with carbon dioxide under supercritical conditions to give (*Z*)-5-alkylidene-1,3-oxazolidin-2-ones exclusively, even in the absence of any metal or base catalyst.

The chemical conversion of carbon dioxide (CO₂) is a viable approach to utilize an abundant and inexpensive C1 feedstock.¹ Based on the fact that CO₂, potentially acting as a Lewis acid, can react with primary and secondary amines to form carbamic acid and their ammonium salts, a variety of CO₂ fixation systems relevant to phosgene-free processes has been studied.² Recently, efficient syntheses of urethanes have been achieved by using supercritical CO₂ (scCO₂) as a reactant and a promising reaction medium.^{3,4} Considerable attention has been focused on scCO₂ owing to its tunable solvent properties as well as environmental advantages.⁵

We⁶ and Baiker's group⁷ have independently reported the positive effects of scCO₂ on the outcome of the reaction of terminal alkynes, diethylamine and CO₂ promoted by ruthenium catalysts. The dense CO₂ medium can facilitate the formation of the carbamic acid or intermediates, leading to a marked improvement in the selectivity of vinyl carbamate formation. In this study, we have extended the scope of the reaction to propargylic amines having both alkyne and amino moieties in the same molecules, and we have found that carboxylative cyclization can take place without any catalysts in scCO₂ to give the cyclic urethanes, 5-alkylidene-1,3-oxazolidin-2-ones (Scheme 1).⁸

We first examined the reaction of *N*-methylpropargylamine (R¹, R² = H, R³ = CH₃) **1a** with 8.0 MPa of CO₂ in a 50 mL stainless-steel autoclave at 60 °C, as shown in Table 1.†§ The reaction proceeded slowly to give a five-membered cyclic urethane, 3-methyl-5-methylene-1,3-oxazolidin-2-one **2a**, as the sole product in 10% yield after 18 h (entry 1). On raising the temperature to



Scheme 1 Carboxylative cyclization of propargylic amines.

PRESTO, Japan Science and Technology Agency and Graduate School of Science and Engineering, Tokyo Institute of Technology, O-okayama, Meguro-ku, Tokyo, 152-8552, Japan. E-mail: tikariya@apc.titech.ac.jp
 † Electronic supplementary information (ESI) available: Experimental section and analytical details of new compounds. See DOI: 10.1039/b603700c

Table 1 Transformation of **1a** and CO₂ into **2a**^a

Entry	Temp/°C	Pressure/MPa	Yield ^b (%)
1	60	8.0	10
2	80	3.0	31
3	80	6.0	43
4	80	8.0	64
5	80	10.0	39
6	100	9.0	88 (71) ^c

^a Reaction conditions: **1a** (20 mmol), 18 h. ^b Determined by ¹H NMR. ^c Isolated yield.

80 °C, the reaction accelerated (entries 2–5), and an increase in the pressure from 3.0 to 8.0 MPa caused a marked improvement (up to 64%) in the yield of **2a**. A further increase in the pressure above 8.0 MPa resulted in a drop in the yield. After optimization of the reaction conditions, a maximum yield of 88% was obtained at 100 °C and 9.0 MPa (entry 6). Notably, scCO₂ can promote the formation of the 5-exo-dig cyclization product without any additives, although it has been reported that a catalytic amount of transition metals⁹ or super bases, such as substituted guanidines,¹⁰ is essential for the reaction of propargylamines and CO₂ in an organic liquid solvent system.¹¹

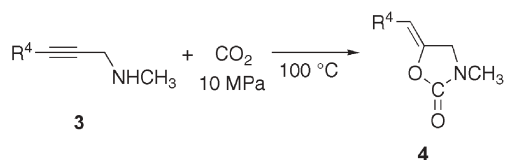
As shown in Table 2, other *N*-substituted propargylic amines **1b–1h** also afforded the corresponding exocyclic urethanes **2b–2h**. The reaction of sterically congested amines (**1d**, **1g** and **1h**) around the amino groups required a longer reaction time. In contrast, the reaction of the primary amine **1i** gave an unsatisfactory result, possibly due to formation of the corresponding ammonium carbamate as a less reactive CO₂-insoluble solid.

In order to gain insight into the cyclization mechanism, we examined reactions with internal propargylic amines **3** (Scheme 2). Although no transformation into the cyclic urethane was observed for the propargylic amine **3a** having a methyl substituent at R⁴, the reaction of 3-arylprop-2-ynylamines **3b–3f** gave 5-benzylidene-1,3-oxazolidin-2-one derivatives **4b–4f** in moderate to good yields, as

Table 2 Carboxylative cyclization of **1** and CO₂^a

Amine	R ¹ , R ²	R ³	Time/h	Yield of 2 ^b (%)
1b	H, H	CH ₂ CH ₃	18	60
1c	H, H	CH ₂ CH ₂ CH ₃	24	67
1d	H, H	CH(CH ₃) ₂	72	42
1e	H, CH ₃	CH ₃	18	68
1f	H, CH ₃	CH ₂ CH ₃	18	89
1g	H, CH ₃	CH ₂ C ₆ H ₅	72	84
1h	CH ₃ , CH ₃	CH ₃	72	79
1i	H, H	H	24	0

^a Reaction conditions: **1** (2.0 mmol), 10 MPa, 100 °C. ^b Determined by ¹H NMR.



Scheme 2

Table 3 Formation of *Z*-4-alkylidene-1,3-oxazolidin-2-one^a

Amine	R ⁴	Time/h	Yield of 4 ^b (%)
3a	CH ₃	15	0
3b	C ₆ H ₅	15	89
3c	4-CF ₃ C ₆ H ₄	15	77
3d	3,5-(CF ₃) ₂ C ₆ H ₃	24	51
3e	4-NCC ₆ H ₄	6	75
3f	4-CH ₃ COC ₆ H ₄	48	41

^a Reaction conditions: **3** (1.0 mmol), 10 MPa, 100 °C. ^b Isolated yield.

shown in Table 3. The ¹H NMR spectra of the crude products showed only a signal due to the olefinic proton, indicating that no isomeric compounds were formed through the cyclization. The C=C double bonds of the products were found to be in *Z* configuration by NMR spectroscopy and X-ray crystallography of **4c**.[¶] The structure of **4c** in solution is consistent with that found in the solid state by X-ray crystallography as depicted in Fig. 1. These results clearly indicate that the addition to alkynes proceeded predominantly in a *trans* fashion.

The selective formation of *Z*-5-alkylidene-1,3-oxazolidin-2-one implies that the reaction mechanism involves proton-assisted nucleophilic *trans* addition of carbamate anions to a C≡C triple bond (Fig. 2).¹² Under a CO₂ atmosphere, the reactant amines exist in equilibrium with the corresponding ammonium carbamates, which might provide a proton to activate the alkyne groups by approaching from the opposite side to the attacking carbamate anions. In the light of easy release of CO₂ upon heating,¹³ the positive CO₂ pressure effect on the carboxylative cyclization of **1a** observed in Table 1 could be explained by promotion of the carbamate salts formation from amines and CO₂.

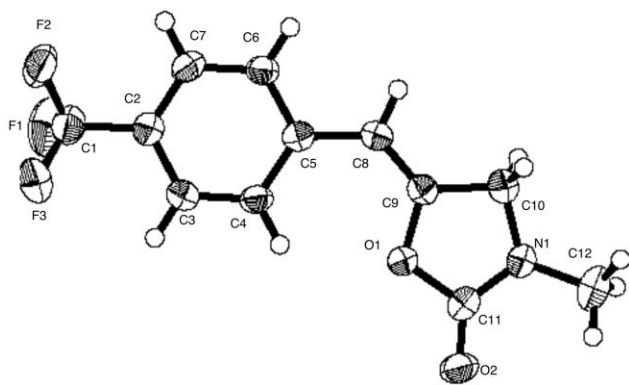


Fig. 1 Structure of **4c** determined by X-ray crystallography with 50% thermal ellipsoidal diagram. Selected bond distances (Å) and angles (°): C(8)–C(9) 1.323(2), C(9)–C(10) 1.504(2), C(10)–N(1) 1.442(2), C(11)–N(1) 1.336(2), C(11)–O(1) 1.393(1), C(11)–O(2) 1.205(1), C(11)–O(1) 1.379(1); C(8)–C(9)–O(1) 124.0(1), C(8)–C(9)–C(10) 128.3(1), C(10)–C(9)–O(1) 170.70(9), C(5)–C(8)–C(9)–O(1) –0.5(2).

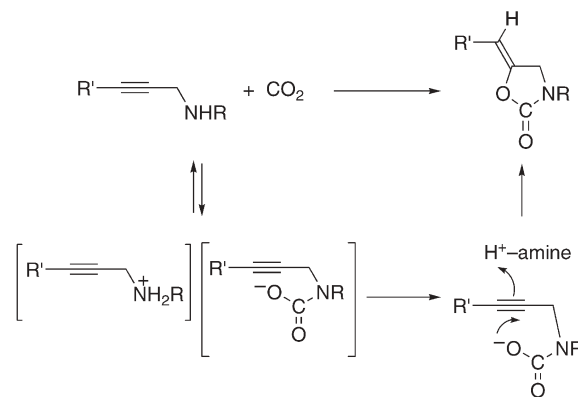


Fig. 2 A plausible proton-assisted addition mechanism.

Visual inspection using a high-pressure view cell under optimized reaction conditions revealed that phase separation from the scCO₂ phase occurred to form a liquid phase including ammonium carbamates derived from CO₂, where the neat reaction might proceed. The proposed ionic mechanism may be favorable in this polar reaction phase. Indeed, the urethane formation was significantly retarded by a large increase in the CO₂ pressure (Table 1, entry 6) that is possibly ascribed to reduction of the liquid reaction phase through enhancement of the solubility of reaction components in scCO₂.

In summary, we have demonstrated efficient and stereoselective synthesis of 5-alkylidene-1,3-oxazolidin-2-ones by carboxylative cyclization of propargylamines in scCO₂ with an atom economy of 100%. The use of scCO₂ causes a significant advantage for the CO₂ fixation *via* carbamate salt intermediates generated from the reactant amines. The present system provides an effective and straightforward method for the green synthesis of substituted five-membered cyclic urethanes without use of catalysts and organic solvents.

This work was financially supported by a Grant-in-Aid from the Ministry of Education, Culture, Sports, Science and Technology, Japan (No. 14078209 and 18065007) and partially supported by The 21st Century COE Program.

Notes and references

‡ CAUTION: highly compressed CO₂ must be used under appropriate safety conditions to minimize the risk of personal injury.

§ Reaction procedures: in a typical experiment, *N*-methylpropargylamine (**1a**, 1.70 mL, 20 mmol) was placed in a 50 mL stainless steel high-pressure reactor under argon atmosphere. The reactor was pressurized with CO₂ (Showa Tansan, 99.999%) at approximately 6.0 MPa by using a syringe pump (ISCO 260D) and heated to 100 °C. The final pressure of 9.0 MPa was reached by slow addition of the remaining CO₂ to the reactor. After 18 hours of stirring, the reactor was cooled in a bath of methanol with dry ice. CO₂ was slowly vented and the reactor was warmed to room temperature. The resulting mixture was extracted with diethyl ether. The residue obtained by evaporation of the ethereal solution was purified by column chromatography on silica gel (hexane–ethyl acetate) to yield the desired 3-methyl-5-methylene-1,3-oxazolidin-2-one (**2a**, 1.60 g, 14.2 mmol).

¶ Compound **4c**: C₁₂H₁₀F₃NO₂, *M* = 257.21, monoclinic, *a* = 7.925(5) Å, *b* = 10.643(6) Å, *c* = 13.886(8) Å, β = 99.478(8)°, *V* = 1155.2(12) Å³, 193 K, space group *P*2₁/*a*, *Z* = 4, μ (Mo–Kα) = 1.33 cm^{−1}, 8890 reflections measured, 8635 unique reflections (*R*_{int} = 0.045) which were used for all calculations, *R*₁ = 0.055 [*I* > 2.00σ(*I*)], *wR*₂ = 0.162 (all reflections). CCDC reference number 290587. For crystallographic data in CIF or other electronic format see DOI: 10.1039/b603700c.

- 1 (a) D. H. Gibson, *Chem. Rev.*, 1996, **96**, 2063; (b) *Carbon Dioxide Recovery and Utilization*, ed. M. Aresta, Kluwer Academic Publishers, Dordrecht, 2003.
- 2 (a) D. B. Dell'Amico, F. Calderazzo, L. Labella, F. Marchetti and G. Pampaloni, *Chem. Rev.*, 2003, **103**, 3857–3897; (b) F. Bigi, R. Maggi and G. Sartori, *Green Chem.*, 2000, **2**, 140–148.
- 3 (a) M. Yoshida, N. Hara and S. Okuyama, *Chem. Commun.*, 2000, 151–152; (b) M. Abla, J.-C. Choi and T. Sakakura, *Chem. Commun.*, 2001, 2238–2239; (c) M. Selva, P. Tundo and A. Perosa, *Tetrahedron Lett.*, 2002, **43**, 1217–1219; (d) H. Kawanami and Y. Ikushima, *Tetrahedron Lett.*, 2002, **43**, 3841–3844; (e) H. Kawanami, H. Matsumoto and Y. Ikushima, *Chem. Lett.*, 2005, **34**, 60–61.
- 4 (a) O. Ihata, Y. Kayaki and T. Ikariya, *Angew. Chem., Int. Ed.*, 2004, **43**, 717–719; (b) O. Ihata, Y. Kayaki and T. Ikariya, *Chem. Commun.*, 2005, 2268–2270; (c) O. Ihata, Y. Kayaki and T. Ikariya, *Macromolecules*, 2005, **38**, 6429–6434.
- 5 (a) P. G. Jessop, T. Ikariya and R. Noyori, *Chem. Rev.*, 1999, **99**, 475–494; (b) *Green Chemistry Using Liquid and Supercritical Carbon Dioxide*, ed. J. M. DeSimone and W. Tumas, Oxford University Press, New York, 2003; (c) *Chemical Synthesis Using Supercritical Fluids*, ed. P. G. Jessop and W. Leitner, Wiley-VCH, Weinheim, 1999; (d) W. Leitner, *Acc. Chem. Res.*, 2002, **35**, 746–756; (e) E. J. Beckman, *J. Supercrit. Fluids*, 2004, **28**, 121–191; (f) D. Prajapati and M. Gohain, *Tetrahedron*, 2004, **60**, 815–833.
- 6 Y. Kayaki, T. Suzuki, Y. Noguchi, S. Sakurai, M. Imanari and T. Ikariya, *Chem. Lett.*, 2002, 424–425.
- 7 M. Rohr, C. Geyer, R. Wandeler, M. S. Schneider, E. F. Murphy and A. B. Baiker, *Green Chem.*, 2001, **3**, 123–125.
- 8 Y. Kayaki and T. Ikariya, *JP Pat* 2004262830, 2004.
- 9 (a) P. Dimroth and H. Pasedach, *DE Pat* 1164411, 1964; P. Dimroth and H. Pasedach, *Chem. Abstr.*, 1964, **60**, 14510; (b) T. Mitsudo, Y. Hori, Y. Yamakawa and Y. Watanabe, *Tetrahedron Lett.*, 1987, **28**, 4417–4418; (c) M. Shi and Y.-M. Shen, *J. Org. Chem.*, 2002, **67**, 16–21.
- 10 (a) M. Costa, G. P. Chiusoli and M. Rizzardi, *Chem. Commun.*, 1996, 1699–1700; (b) M. Costa, G. P. Chiusoli, D. Taffurelli and G. Dalmonego, *J. Chem. Soc., Perkin Trans. 1*, 1998, 1541–1546.
- 11 Recently, the formation of 5-membered cyclic urethanes by stoichiometric reaction of propargylic amines with tetraethylammonium carbonate or tetraethylammonium hydrogen carbonate in DMSO was reported by Arcadi *et al.*: A. Arcadi, A. Inesi, F. Marinelli, L. Rossi and M. Verdecchia, *Synlett*, 2005, 67–70.
- 12 S. Fujiwara, Y. Shikano, T. Shin-ike, N. Kambe and N. Sonoda, *J. Org. Chem.*, 2002, **67**, 6275–6278.
- 13 D. M. Rudkevich and H. Xu, *Chem. Commun.*, 2005, 2651–2659 and references cited therein.

Find a SOLUTION

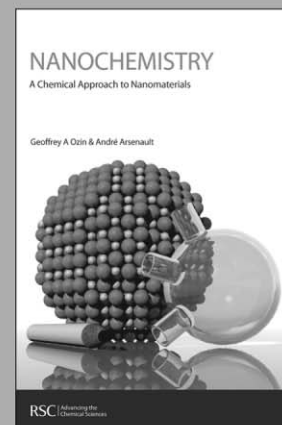
... with books from the RSC

Choose from exciting textbooks, research level books or reference books in a wide range of subject areas, including:

- Biological science
- Food and nutrition
- Materials and nanoscience
- Analytical and environmental sciences
- Organic, inorganic and physical chemistry

Look out for 3 new series coming soon ...

- RSC Nanoscience & Nanotechnology Series
- Issues in Toxicology
- RSC Biomolecular Sciences Series



RSC | Advancing the
Chemical Sciences

www.rsc.org/books

28040542

Pentafluorophenylammonium triflate (PFPAT): an efficient, practical, and cost-effective catalyst for esterification, thioesterification, transesterification, and macrolactone formation

Takashi Funatomi, Kazunori Wakasugi, Tomonori Misaki and Yoo Tanabe*

Received 28th June 2006, Accepted 18th August 2006

First published as an Advance Article on the web 7th September 2006

DOI: 10.1039/b609181b

A pentafluorophenylammonium triflate (PFPAT) catalyst (1–10 mol%) efficiently promoted esterification and thioesterification between a 1 : 1 mixture of carboxylic acids and alcohols or thiols in good to excellent yield under mild reaction conditions. Transesterification of carboxylic esters with a slight excess of alcohols (1.5 equiv.) also proceeded using the PFPAT catalyst. The PFPAT-catalyzed 13 to 17 membered macrolactone formation of ω -hydroxycarboxylic acids was successfully performed using 10 mol% of the catalyst (total 44 examples). These catalytic condensations have advantages from the viewpoint of green chemistry. PFPAT organocatalyst is air-stable, cost-effective, easy to handle, and easily removed from the reaction mixtures. The operation is quite simple, because a dehydrating system such as the Dean–Stark apparatus is not necessary.

Introduction

Esterifications are well recognized as fundamental processes in various fields of organic synthesis.¹ Direct esterification of carboxylic acids with alcohols using small amounts of catalyst is the most ideal method, but in most cases, large excess amounts of either carboxylic acids and/or alcohols are used for this purpose. From the standpoint of green chemistry, the reaction of a 1 : 1 mixture of carboxylic acids and alcohols is the ultimate goal. Several efficient methods have been exploited for esterification with catalysts such as (SCN)Bu₂SnOSnBu₂(OH),² TiCl₂(OTf)₂,³ Sc(OTf)₃,⁴ and HfCl₄·2THF.⁵ These methods have superior reactivity, but are not suitable in terms of the recent trends in process chemistry, due to the use of metallic catalysts. Therefore, a method using a nonmetallic catalyst is desirable.

Along with our continued interest in mild and effective condensation reactions,⁶ in a preceding letter,⁷ we reported that diphenylammonium triflate (DPAT), which is readily prepared from Ph₂NH and CF₃SO₃H, efficiently catalyzes the ester condensation of a 1 : 1 mixture of carboxylic acids and alcohols without azeotropic water removal. Recently, Ishihara and Sakakura's group developed bulky diarylammonium arenosulfonates,⁸ which are superior to DPAT in efficiency; the hydrophobic effect of the bulky ammonium triflates has remarkable catalytic esterification activity. We present herein an efficient method for esterification, thioesterification, transesterification, and lactone formation utilizing pentafluorophenylammonium triflate (C₆F₅N⁺H₃·OTf⁻; PFPAT), a new effective catalyst.

Department of Chemistry, School of Science and Technology, Kwansei Gakuin University, 2-1 Gakuen, Sanda, Hyogo, 669-1337, Japan.
E-mail: tanabe@kwansei.ac.jp; Fax: +81-795-65-9077;
Tel: +81-795-65-8394

Results and discussion

To develop the methodology utilizing ammonium triflate catalysts, we focused our attention on some practical issues from the recent green chemical standpoint; (i) high reactivity, (ii) total cost effectiveness,⁹ (iii) easy preparation, handling, stability, and moisture insensitivity of the catalyst, (iv) convenient removal of the catalyst from the reaction mixture, and (v) elimination of the azeotropic water removal procedure. To this end, we designed several ammonium triflates and chose a novel PFPAT catalyst. The catalytic activity of four catalysts [1 mol%; CSA (camphorsulfonic acid; C₁₀H₁₆O₄S), PTS (*p*-toluenesulfonic acid; C₇H₈O₃S), DPAT, and PFPAT) was compared using gas chromatographic (GC) monitoring during the reaction between a 1 : 1 mixture of Me₃CCO₂H and 1-octanol at 80 °C in toluene, without a requiring dehydration technique such as a Dean–Stark apparatus. (Fig. 1). Among them, PFPAT had the highest activity; >95% GC conversion within 5 to 6 h. The superiority of PFPAT to DPAT is ascribed to the lower basicity of the C₆F₅NH₂ counter amine compared to Ph₂NH.¹⁰

This promising result led us to investigate the PFPAT-catalyzed esterification (A), thioesterification (B), transesterification (C), macrolactone formation (D), no solvent method for the esterification (E), and chemoselective esterification (F).

(A) Esterification

Table 1 lists successful results of the esterification between a 1 : 1 mixture of various carboxylic acid and alcohols catalyzed by PFPAT (1 mol%) at 80 °C. The salient features are as follows. (i) Several primary and secondary alcohols underwent smooth esterification with PhCH₂CH₂CO₂H in good to excellent yield (entries 1–8). (ii) Several functionalities in alcohols such as a halogen, a double bond, a 4-nitrobenzyl, and a *gem*-dichlorocyclopropane were tolerated. (iii) The

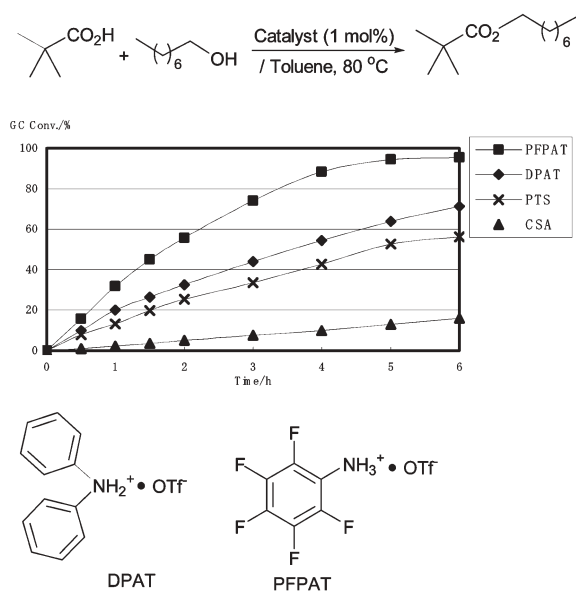


Fig. 1 GC conversion giving octyl pivaloate using two ammonium catalysts and two sulfonic acid catalysts.

Table 1 Esterification between a 1 : 1 mixture of carboxylic acids and alcohols using PFPAT catalyst

R^1CO_2H + R^2OH		$\xrightarrow[\text{/ Toluene, } 80^\circ\text{C}]{\text{PFPAT (1 mol\%)}}$		$R^1CO_2R^2$	
(1.0 eq.)		(1.0 eq.)			
Entry	R^1CO_2H	R^2OH	Time/h	Product	Yield (%)
1			2	1	94
2			2	2	96
3			2	3	87
4			3	4	96
5			4	5	92
6			6	6	92
7			24	7	90
8			48	8	90
9			4	9	91
10			6	10	90
11			2	11	90
12			2	12	96
13			3	13	92
14			24	14	87
15			24	15	90

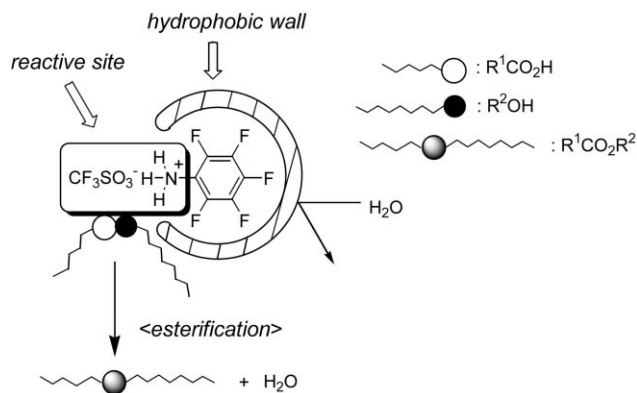


Fig. 2 Schematic representation of the esterification process.

reaction using sterically-congested carboxylic acids also produced satisfactory results (entries 9, 10). (iv) Levulinic and mandelic acids underwent the reaction without protection of the ketone or hydroxyl group (entries 12, 13). (v) The reaction using benzoic acid and α,β -unsaturated carboxylic acids was also successful (entries 14, 15), although it required a longer reaction period (24 h).

Note that the present method did not necessitate the use of a dehydration reagent and/or technique for azeotropic water removal. In addition, the PFPAT catalyst was easily separated from the reaction mixture after work-up; washing with NaOH aqueous solution removed CF_3SO_3H , followed by distillation under reduced pressure ($C_6F_5NH_2$: bp $153^\circ C$ at 760 mmHg).

The reason azeotropic removal of water is unnecessary is not very clear at present. We assume that the pentafluoro moiety of PFPAT contributes to the functionality in the organic phase, even in the presence of small amount of water: the highly hydrophobic wall of pentafluorophenyl moiety effectively repels H_2O produced by the esterification (Fig. 2). This contributes to the elimination of azeotropic water removal.

(B) Thioesterification

PFPAT-catalyzed thioesterification between a 1 : 1 mixture of $PhCH_2CH_2CO_2H$ and 1-octanthiol was performed, although the rate of conversion was somewhat slower than that of esterification (Table 2). Under conditions identical to those for the esterification [(A); 1 mol% of PFPAT, $80^\circ C$, 2 h, toluene], the desired thioesterification did not proceed. When 5 mol% of PFPAT was used under reflux conditions, however, the yield increased remarkably to 93% (entry 1). The reaction using two thiols ($PhCH_2SH$ and $cyclo-C_6H_{11}SH$) and three carboxylic acids [$Cl(CH_2)_4CO_2H$, $cyclo-C_6H_{11}CO_2H$, and $(CH_3)_3CO_2H$] produced good results (entries 2–6). These features coincide with an efficient method recently reported by Kobayashi's group, wherein CF_3SO_3H was used as the catalyst.¹¹

(C) Transesterification

There are some efficient methods for catalytic transesterification utilizing metallic catalysts (Ti-, Sn-, Zr-, Hf-, complexes, zeolite, etc.), and organic catalysts (I_2 , etc.).¹² We investigate the transesterification of methyl esters to the corresponding esters using primary alcohols (1.5 equiv.). Table 3 lists the

Table 2 Thioesterification between a 1 : 1 mixture of carboxylic acids and thiols using PFPAT catalyst

Entry	R ¹ CO ₂ H (1.0 eq.)	R ² SH (1.0 eq.)	Time/h	Product	Yield (%)
1			4	16	93 (trace) ^a
2			4	17	87
3			24	18	89
4			4	19	87
5			8	20	93
6			24	21	88 ^b

^a 1 mol% of PFPAT was used at 80 °C for 2 h. ^b 10 mol% of PFPAT was used.

successful results. The salient features are as follows. (i) Similar to the esterification (A), the transesterification of PhCH₂CH₂CO₂CH₃ with several alcohols proceeded smoothly to give the corresponding products (entries 1–4), although it required a rather longer reaction period (24 h). (ii) Not only

Table 3 Transesterification between 1 : 1.5 mixture of carboxylic esters and alcohols using PFPAT catalyst

Entry	R ¹ CO ₂ R ² (1.0 eq.)	R ³ OH (1.5 eq.)	Product	Yield (%)
1			1	98
2			2	96
3			3	91
4			4	94
5			7	62 ^a
6			1	90
7			1	97 ^a
8			1	99
9			9	96
10			12	98
11			10	64 ^a
12			13	96
13			22	68 ^a

^a 10 mol% of PFPAT was used.

methyl esters, but also Et, *i*-Pr, and *t*-Bu esters underwent smooth transesterification to give the corresponding products (entries 6–8). (iii) The reaction between bulky methyl pivalate and 2-octanol somewhat resisted the present transesterification (entries 5, 11). (iv) A β-keto ester, which is prone to decarboxylation, however, could be used. (entry 13).

Note that the present transesterification showed higher reactivity and a reverse relationship for reactivity compared with the Sn-complex-catalyzed method,² [See also (F)]; the esterification is smoother than the transesterification.

(D) Macrolactone formation

Preparation of macrolactones from ω-hydroxycarboxylic acids is an important topic in organic synthesis, because the macrolide structure is contained in a large number of natural products. Several efficient methods using condensing agents have been developed, but most of them use equimolar and expensive reagents. To the best of our knowledge, only two catalytic methods, using (SCN)Bu₂SnOSnBu₂(OH)¹³ and zeolite,¹⁴ have been reported for this purpose. In the present study, we extend the PFPAT-catalysed esterification to macrolactone formation. Thus, successful results were obtained (Table 4): the reaction of ω-hydroxycarboxylic acids using PFPAT (10 mol%) in toluene at 110 °C gave the corresponding 13- to 17-membered lactones in moderate to good yield (47–87%) with small amounts of diolides as the main by-product. Compared with the Sn-catalyzed method,¹³ the present method produced a better yield.

(E) No solvent method for the esterification

The present esterification was performed in the absence of toluene solvent. Table 5 lists several examples; this method was carried out even at 40 °C to give desired esters in good to excellent yield.

(F) Selective esterification

Finally, a couple of selective esterifications were investigated (Scheme 1). First is the esterification using a 1 : 1 mixture of

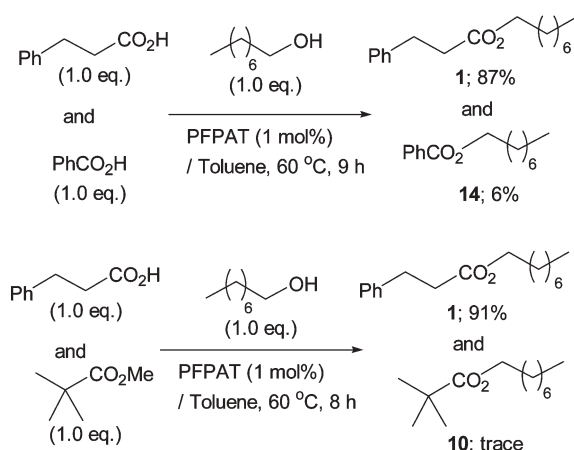
Table 4 Macrolactone formation of ω-hydroxycarboxylic acids using PFPAT catalyst

Entry	<i>n</i>	Product	Yield (%)	
			Lactone	Diolide
1	10	23a, 23b	47 (trace) ^a	31
2	11	24a, 24b	70	16
3	12	25a, 25b	70	16
4	13	26a, 26b	86 (78) ^a	13
5	14	27a, 27b	87	10

^a Reported method using catalyst (SCN)Bu₂SnOSnBu₂(OH) catalyst, 10 mM, 175 °C, 24 h

Table 5 Esterification in the absence of solvents using PFPAT catalyst

Entry	R ¹ CO ₂ H (1.0 eq.)	R ² OH (1.2 eq.)	Time/h	Product	Yield (%)
1		MeOH	12	28	93
2			12	1	95
3			18	29	95
4			24	9	92
5			8	30	87

**Scheme 1**

PhCH₂CH₂CO₂H and PhCO₂H with 1-octanol, which resulted in the formation of PhCH₂CH₂CO₂(1-Oct) (**1**) as a major product. The second is a comparison between the esterification of PhCH₂CH₂CO₂H and the transesterification of *t*-BuCO₂CH₃, that is, **1** was also obtained as the sole product.

Conclusions

We achieved PFPAT-catalyzed efficient and total cost-effective esterification, thioesterification, transesterification, and macrolactone formation (total 44 examples). The present practical method is a new candidate for synthetic chemists to use for these important reactions.

Experimental

Preparation of pentafluorophenylammonium triflate (PFPAT)

CF₃SO₃H (7.50 g, 50 mmol) was added to a stirred solution of 2,3,4,5,6-pentafluoroaniline (9.15 g, 50 mmol) in toluene (50.0 ml) at 0–5 °C, and the mixture was stirred at the same temperature for 30 min. Evaporation of the solvent gave the crude product, which was washed with hexane (50 ml × 5) to give a pure PFPAT (15.8 g, 95%) as colourless crystals.

¹H NMR (acetone-*d*₆, 300 MHz) δ: 7.43–7.66 (brs, 3H); IR (KBr) 3416, 2965, 1532, 1250, 1179 cm⁻¹.

The following esters, thioesters, and lactones obtained in the work are known compounds: 1-octyl 3-phenylpropionate (**1**),⁷ 2-phenylethyl 3-phenylpropionate (**2**),⁷ 6-chlorohexyl 3-phenylpropionate (**3**),⁷ 9-decene-1-yl 3-phenylpropionate (**4**),⁷ 2,2-dichloro-1-methylcyclopropylmethyl 3-phenylpropionate (**6**),⁷ 2-octyl 3-phenylpropionate (**7**),⁷ *l*-methyl-3-phenylpropionate (**8**),⁷ 1-octyl cyclohexanecarboxylate (**9**),⁷ 1-octyl 2,2-dimethylpropionate (**10**),⁷ 1-octyl 4-oxopentanoate (**12**),^{8b} 1-octyl benzoate (**14**),⁷ 1-octyl 3-phenylpropionate (**15**),^{8b} 1-octyl 3-phenylpropionthioate (**16**),^{6b} benzyl 3-phenylpropionthioate (**17**),^{6b} cyclohexyl 3-phenylpropionthioate (**18**),^{6b} 1-octyl cyclohexanecarboxthioate (**20**),^{6b} 1-octyl 2-methyl-3-oxobutanoate (**22**),^{6b} 12-dodecanolide (**23a**),¹⁵ 1,14-dioxacyclohexacosane-2,15-dione (**23b**),¹⁵ 13-tridecanolide (**24a**),¹⁵ 1,15-dioxacyclooctacosane-2,16-dione (**24b**),¹⁵ 14-tetradecanolide (**25a**),¹⁵ 1,16-dioxacyclotriacontane-2,17-dione (**25b**),¹⁵ 15-pentadecanolide (**26a**),¹⁵ 1,17-dioxacyclodotriacontane-2,18-dione (**26b**),¹⁵ 16-hexadecanolide (**27a**),¹⁵ 1,18-dioxacyclotetracontane-2,19-dione (**27b**),¹⁵ methyl-3-phenylpropionate (**28**) (commercially available), benzyl 3-phenylpropionate (**29**),^{6b} 1-octyl tetrahydrofuran-2-carboxylate (**30**).^{8b}

General procedure for esterification

(Either open or closed vessel can be used.) A carboxylic acid (1.0 mmol), an alcohol (1.0 mmol), and PFPAT (0.01 mmol) in toluene (2.0 ml) were heated at 80 °C for 2–48 h.

After cooling to room temperature, the organic phase was washed with 1 M NaOH aqueous solution (1 ml). The separated organic phase was evaporated under reduced pressure at *ca.* 40 °C (bath temperature) to give a crude product, which was purified by distillation or by column chromatography (hexane–ether = 50 : 1–10 : 1).

Typical scale-up procedure for esterification without column chromatographic purification

3-Phenylpropionic acid (7.51 g, 50.0 mmol), 1-octanol (6.51 g, 50.0 mmol), and PFPAT (0.17 g, 0.5 mmol) in toluene (100 ml) were heated at 80 °C for 2 h. After cooling to room temperature, the organic phase was washed with 1 M NaOH aqueous solution (20 ml). The separated organic phase was evaporated under reduced pressure to give crude 1-octyl 3-phenylpropionate (**1**), which was distilled to give pure product (bp 110–113 °C at 0.15 mmHg; 12.08 g, 92%).

4-Nitrobenzyl 3-phenylpropionate (**5**)

Orange oil; ¹H NMR (300 MHz, CDCl₃) δ 2.74 (2H, t, *J* = 7.6 Hz), 2.99 (2H, t, *J* = 7.6 Hz), 5.18 (2H, s), 7.17–7.32 (5H, m), 7.35–7.42 (2H, m), 8.14–8.21 (2H, m); ¹³C NMR (75 MHz, CDCl₃) δ 30.7, 35.5, 64.5, 123.5, 126.2, 128.1, 128.4, 140.0, 143.1, 147.4, 172.2; *v*_{max} (neat)/cm⁻¹ 3029, 2938, 1742, 1522, 1346, 1150. Anal. Calcd for C₁₆H₁₅NO₄: C, 67.36; H, 5.30, found: C, 67.1; H, 4.1.

1-Octyl 5-chloropentanoate (**11**)

Colorless oil; ¹H NMR (300 MHz, CDCl₃) δ 0.87 (3H, t, *J* = 6.9 Hz), 1.19–1.41 (10H, m), 1.55–1.69 (2H, m), 1.72–1.89 (4H, m), 2.34 (2H, t, *J* = 6.9 Hz), 3.55 (2H, t, *J* = 6.5 Hz), 4.07 (2H,

t, $J = 6.5$ Hz); ^{13}C NMR (75 MHz, CDCl_3) δ 14.0, 22.2, 22.6, 25.9, 28.6, 29.1, 31.7, 31.8, 33.4, 44.4, 64.6, 173.2; ν_{max} (neat)/ cm^{-1} 2928, 2857, 1736, 1460, 1179. Anal. Calcd for $\text{C}_{12}\text{H}_{23}\text{ClO}_2$: C, 61.39; H, 9.87, found: C, 61.1; H, 9.6.

1-Octyl (S)-2-hydroxy-2-phenylethanoate (13)

Colorless crystals; mp 29.5–30.0 °C; $[\alpha]_{\text{D}}^{24}$ 76.7 (c 1.38, CHCl_3); ^1H NMR (300 MHz, CDCl_3) δ 0.88 (3H, t, $J = 6.9$ Hz), 1.12–1.34 (10H, m), 1.48–1.64 (2H, m), 3.41–3.50 (1H, brs), 4.16 (2H, t, $J = 6.5$ Hz), 5.16 (1H, s), 7.28–7.46 (5H, m); ^{13}C NMR (75 MHz, CDCl_3) δ 13.9, 22.5, 25.6, 27.9, 28.5, 29.1, 29.7, 31.6, 37.8, 64.7, 172.7, 206.6; ν_{max} (KBr)/ cm^{-1} 3443, 2926, 1738, 1263, 1184. Anal. Calcd for $\text{C}_{16}\text{H}_{24}\text{O}_3$: C, 72.69; H, 9.15, found: C, 72.5; H, 8.9.

General procedure for thioesterification

A carboxylic acid (1.0 mmol), a thiol (1.0 mmol), and PFPAT (0.05–0.1 mmol) in toluene (2.0 ml) were refluxed for 4–24 h. After cooling to room temperature, the organic phase was washed with 1 M NaOH aqueous solution (1 ml). The separated organic phase was evaporated under reduced pressure at *ca.* 40 °C (bath temperature) to give a crude product, which was purified by distillation or by column chromatography (hexane–ether = 50 : 1–10 : 1).

1-Octyl 5-chloropentan-3-thioate (19)

Colorless oil; ^1H NMR (300 MHz, CDCl_3) δ 0.88 (3H, t, $J = 6.9$ Hz), 1.19–1.42 (10H, m), 1.50–1.62 (2H, m), 1.74–1.90 (4H, m), 2.52–2.64 (2H, m), 2.87 (2H, t, $J = 7.2$ Hz), 3.49–3.59 (2H, m); ^{13}C NMR (75 MHz, CDCl_3) δ 14.0, 22.5, 22.8, 28.7, 28.7, 29.0, 29.4, 31.5, 31.7, 42.9, 44.2, 198.8; ν_{max} (neat)/ cm^{-1} 2928, 2857, 1690, 1458. Anal. Calcd for $\text{C}_{12}\text{H}_{23}\text{ClOS}$: C, 57.46; H, 9.24, found: C, 57.3; H, 9.3.

1-Octyl 2,2-dimethylpropionthioate (21)

Colorless oil; ^1H NMR (300 MHz, CDCl_3) δ 0.88 (3H, t, $J = 7.2$ Hz), 1.23 (9H, s), 1.24–1.42 (10H, m), 1.48–1.61 (2H, m), 2.82 (2H, t, $J = 7.2$ Hz); ^{13}C NMR (75 MHz, CDCl_3) δ 14.1, 22.6, 27.4, 28.5, 28.9, 29.1, 29.5, 31.8, 46.3, 207.0; ν_{max} (neat)/ cm^{-1} 2928, 2857, 1680, 1458, 1366, 1036. Anal. Calcd for $\text{C}_{13}\text{H}_{26}\text{OS}$: C, 67.77; H, 11.37, found: C, 67.4; H, 11.2.

General procedure for transesterification

A carboxylic ester (1.0 mmol), an alcohol (1.5 mmol) and PFPAT (0.01–0.1 mmol) in toluene (2.0 ml), were heated at 80 °C for 24 h. After cooling to room temperature, the organic phase was washed with 1 M NaOH aqueous solution (1 ml). The separated organic phase was evaporated under reduced pressure at *ca.* 40 °C (bath temperature) to give a crude product, which was purified by distillation or by column chromatography (hexane–ether = 50 : 1–10 : 1).

General procedure for lactone formation

An ω -hydroxycarboxylic acid (0.5 mmol) was added to a stirred mixture of PFPAT (0.05 mmol) in toluene (50 ml) at 110 °C over 3.5 h, and the reaction mixture was stirred at the

same temperature for 0.5 h. Evaporation of toluene (*ca.* 40 °C) under reduced pressure gave the crude material, which was purified by column chromatography (hexane–ether = 30 : 1–10 : 1) to give desired lactone.

General procedure for esterification in the absence of solvent

A carboxylic acid (10.0 mmol), an alcohol (12.0 mmol), and PFPAT (0.1 mmol) were heated at 40 °C for 8–24 h. The mixture was washed with 1 M NaOH aqueous solution (5 ml). The organic phase was purified by distillation or by column chromatography (hexane–ether = 50 : 1–10 : 1).

Selective esterification

(i) 3-Phenylpropionic acid (1.0 mmol), benzoic acid (1.0 mmol), 1-octanol (1.0 mmol), and PFPAT (0.01 mmol) in toluene (2.0 ml) were heated at 60 °C for 9 h. Toluene (*ca.* 40 °C) was evaporated under reduced pressure to give the crude material, which was purified by column chromatography (hexane–ether = 10 : 1) to give the desired ester **1** (87%) and **14** (6%).

(ii) 3-Phenylpropionic acid (1.0 mmol), methyl 2,2-dimethylpropionate (1.0 mmol), 1-octanol (1.0 mmol), and PFPAT (0.01 mmol) in toluene (2.0 ml) were heated at 60 °C for 8 h. Toluene (*ca.* 40 °C) was evaporated under reduced pressure to give the crude material, which was purified by column chromatography (hexane–ether = 10 : 1) to give the desired ester **1** (91%) and **10** (trace).

Acknowledgements

This research was partially supported by Grant-in-Aids for Scientific Research on Basic Areas (B) “18350056”, Priority Areas (A) “17035087” and “18037068”, and Exploratory Research “17655045” from MEXT.

References

- (a) G. Benz, in *Comprehensive Organic Synthesis*, ed. B. M. Trost, I. Fleming, Pergamon, Oxford, 1991, vol. 6, p. 323; (b) A. S. Franklin, *J. Chem. Soc., Perkin Trans. 1*, 1998, 2451; A. S. Franklin, *J. Chem. Soc., Perkin Trans. 1*, 1999, 3537; (c) J. Otera, *Esterification Methods, Reactions and applications*, Wiley-VCH, Weinheim, Germany, 2003.
- J. Otera, N. Dan-oh and H. Nozaki, *J. Org. Chem.*, 1991, **56**, 5307.
- (a) I. Shiina, T. Mukaiyama, S. Miyoshi and M. Miyashita, *Chem. Lett.*, 1994, 515; (b) T. Mukaiyama and I. Shiina, *Chem. Lett.*, 1995, 141.
- (a) K. Ishihara, M. Kubota, H. Kurihara and H. Yamamoto, *J. Org. Chem.*, 1996, **61**, 4560.
- K. Ishihara, S. Ohara and H. Yamamoto, *Science*, 2000, **290**, 1140.
- (a) Y. Tanabe, T. Misaki, A. Iida and Y. Nishii, *J. Synth. Org. Chem., Jpn.*, 2004, **62**, 1248; (b) K. Wakasugi, A. Iida, T. Misaki, Y. Nishii and Y. Tanabe, *Adv. Synth. Catal.*, 2003, **345**, 1209; (c) J. Morita, H. Nakatsuji, T. Misaki and Y. Tanabe, *Green Chem.*, 2005, **7**, 711 and other recent references cited therein; (d) H. Nakatsuji, J. Morita, T. Misaki and Y. Tanabe, *Adv. Synth. Catal.*, 2006, **348**, in press.
- K. Wakasugi, T. Misaki, K. Yamada and Y. Tanabe, *Tetrahedron Lett.*, 2000, **41**, 5249.
- (a) K. Ishihara, S. Nakagawa and A. Sakakura, *J. Am. Chem. Soc.*, 2005, **127**, 4168; (b) A. Sakakura, S. Nakagawa and K. Ishihara, *Tetrahedron*, 2006, **62**, 422.
- Although $\text{C}_6\text{F}_5\text{NH}_2$ is more expensive than Ph_2NH , total efficiency of reactivity vs. cost of PFPAT is superior to DPAT.

- 10 pK_b value: *ca.* 9.4 (aniline), 13.2 (Ph_2NH), 14.2 ($\text{C}_6\text{F}_5\text{NH}_2$), calculated by SciFinder Scholar[®]. Calculated by Advanced Chemistry Development (ACD/Labs) Software V8.14 for Solaris[®] 1994–2006 ACD/Labs).
- 11 S. Iimura, K. Manabe and S. Kobayashi, *Chem. Commun.*, 2002, 94.
- 12 (a) J. Otera, *Chem. Rev.*, 1993, **93**, 1449; (b) B. S. Balaji, M. Sasidharan, R. Kumar and B. Chanada, *Chem. Commun.*, 1996, 707; (c) K. Ramalinga, P. Vijayalakshmi and T. N. B. Kaimal, *Tetrahedron Lett.*, 2002, **43**, 879; (d) X. Hao, A. Yoshida and J. Nishikido, *Tetrahedron Lett.*, 2004, **45**, 781.
- 13 (a) J. Otera, T. Yano, Y. Himeno and H. Nozaki, *Tetrahedron Lett.*, 1986, **27**, 4501.
- 14 (a) T. Tatsumi, H. Sakashita and K. Asano, *J. Chem. Soc., Chem. Commun.*, 1993, 1264; (b) T. Ookoshi and M. Onaka, *Tetrahedron Lett.*, 1998, **39**, 293.
- 15 I. Shiina and T. Mukaiyama, *Chem. Lett.*, 1994, 677.

STOP!

searching...

Save valuable time searching for that elusive piece of vital chemical information.

Let us do it for you at the Library and Information Centre of the RSC.

We are your chemical information support, providing:

- Chemical enquiry helpdesk
- Remote access chemical information resources
- Speedy response
- Expert chemical information specialist staff

Tap into the foremost source of chemical knowledge in Europe and send your enquiries to

library@rsc.org

RSCPublishing

www.rsc.org/library

12120515

An effective synthesis of bromoesters from aromatic aldehydes using tribromide ionic liquid based on L-prolinol as reagent and reaction medium under mild conditions†

Weiliang Bao* and Zhiming Wang

Received 20th March 2006, Accepted 23rd August 2006

First published as an Advance Article on the web 13th September 2006

DOI: 10.1039/b604096a

Two kinds of ionic liquids have been directly synthesized from L-prolinol by a simple and convenient method in excellent yields. The application of the ionic liquids as reagents and solvents for the chemoselective, regioselective, and stereoselective synthesis of 1,2- or 1,3-bromoesters from aromatic aldehydes and 1,2- or 1,3-diols at room temperature has been studied. Good to excellent yields and moderate enantiomeric excesses were obtained under these reaction conditions

Introduction

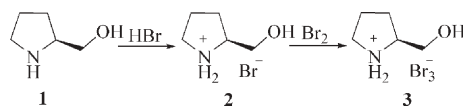
Bromoesters are valuable intermediates in organic synthesis. They could be employed as building blocks in organic, bioorganic, medicinal, and material chemistry.¹ A variety of the approaches to their preparation are available in the literature.² Traditionally, one of the most popular and convenient methods involves the conversion of cyclic acetals into the corresponding bromoesters by using the brominating reagents, such as NBS,^{2e,2h-i} bromine,^{2f} and bromoform.^{2c-d} Recently, one-pot synthesis of ω -bromoesters from aromatic aldehydes and diols using pyridinium hydrobromide perbromide (PHPB) has been developed by Aoyama and his co-workers.³ However, the use of toxic/corrosive materials or volatile organic solvents makes these processes cumbersome with respect to both industrial and environmental viewpoints. In addition, most of the work has concentrated on the control of regioselectivity of this process,^{2c-i} while there is very few example reported up to now of the study on stereoselectivity of this reaction under the chiral reaction conditions.^{2i,4}

At the same time, ionic liquids (ILs) as ionic solvents that combine the advantages of both traditional organic solvents and melting salts, have attracted increasing interest in the context of green chemistry in recent years.⁵ Although they were initially introduced as alternative green reaction media because of their unique chemical and physical properties of nonvolatility, nonflammability, thermal stability, and ease of recyclability, today ILs have marched far beyond this border, showing their significant roles in controlling the reaction as new reagents.^{6,7a} For example, tribromide ILs based on imidazolium or pyridinium as nonvolatile and regioselective brominating reagents have been developed by two different groups.^{6c-d} Furthermore, the studies of chiral ILs have provided chemists an opportunity leading to asymmetric synthesis in these novel chiral solvents.⁸ In continuation of

our studies on preparation of novel ILs from different sources, particularly from natural compounds, and their use as solvents or reagents for organic synthesis,⁷ we report here the synthesis of tribromide IL **3** based on L-prolinol (**1**) and its use as reagent and solvent for chemoselective, regioselective, and stereoselective synthesis of ω -bromoesters at room temperature (rt).

Results and discussion

Although ILs have been regarded as replacements for traditional organic solvents in synthesis because of their unique properties mentioned above, their preparations using renewable or inexpensive resources and their low toxic properties remain to be addressed.⁹ Several novel ILs derived from different natural sources such as amino acids,^{7d,10a-c} sugars,^{10d-e} and choline chloride^{10f-g} have been developed with their successful applications in Heck reactions and Diels–Alder reactions reported.^{10e,11} The neutralizing reaction is one of the most efficient and atom-economical methods for synthesis of these ILs.^{10a-b,10h-i} By using this meaningful protocol, IL **2** was obtained by mixing the correct molar ratio (1 : 1) of L-prolinol (**1**) and hydrobromide acid (40%) in water (Scheme 1). After the water was removed under vacuum at 60 °C, the reaction yielded a viscous IL **2**. Adding molecular bromine dropwise under mechanical stirring to **2**, the red liquid tribromide **3** was formed exothermically. The IL **3** could be stored for several weeks without change of structure and loss of activity. Even after prolonged heating at 60 °C under vacuum (<10 mmHg), **3** was recovered unaltered without loss of bromine. Interestingly, in comparison with the ILs based-on choline chloride,⁹ IL **3** could be stirred smoothly only using a magnetic stirrer at rt or even at –10 °C. This character provided a chance that this IL might be used as reaction reagent or solvent at rt. The IL **3** was miscible with water, ethanol, acetone,



Scheme 1 Synthesis of ILs **2** and **3**.

Department of Chemistry, Zhejiang University, Xi Xi Campus, Hangzhou, Zhejiang, 310028, P.R. China. E-mail: wbao@zhnc.com; Fax: +86 571 88911554; Tel: +86 571 88911554

† Electronic supplementary information (ESI) available: General experiment methods and characterization data of ILs and bromoesters. See DOI: 10.1039/b604096a

Table 1 Synthesis of bromoesters under various reaction conditions

Entry	IL	Temp/°C	Time/h	Yield (%) ^{a,c}
1	3	rt	28	90
2	3	rt	28	89 ^b
3	[Bmim]Br ₃ ^d	rt	28	50 ^f
4	[Bmim]Br ₃	50	40	82
5	[Bpy]Br ₃ ^e	50	40	80
6	3	rt	28	90–85 ^g

^a Reaction conditions: benzaldehyde (2 mmol), ethylene glycol (4 mmol), and IL (4 mmol) at rt. ^b Triethoxymethane (2.4 mmol) was used. ^c Isolated yield. ^d Bmim = 1-butyl-3-methylimidazolium. ^e Bpy = *N*-butylpyridinium. ^f The reaction was not completed. ^g The recovered IL was used and the process was repeated for 4 times.

DMSO, and other strong polar organic solvents and immiscible with ether, chloroform, and other weakly polar organic solvents. It is meaningful that the chiral centers of ILs **2** and **3** were retained in the synthetic precursors and no racemization was detected in the acidic conditions.^{7c}

Our experiment was first conducted by mixing IL **3**, benzaldehyde (**4**), and ethylene glycol (**5**) in a 10 mL capped flask at rt (Table 1). The 2-bromoethyl benzoate (**6**) was obtained after 28 h in 90% yield. Although the reaction yield was slightly lower and the reaction time was longer comparing with PHPB reaction system,³ the largely excessive amount of diol and additional reagent triethoxymethane were not needed (Table 1, entry 2). Furthermore, the reaction could take place smoothly at rt. Among the tribromide ILs, IL **3** is the best one. [Bmim]Br₃ also gave **6** in 50% under the same conditions with incomplete conversion of benzaldehyde (**4**) (Table 1, entry 3). When the temperature was raised to 50 °C, **6** was obtained by using [Bmim]Br₃ or [Bpy]Br₃ in 82% or 80% yields, respectively for 40 h (Table 1, entries 4–5). Another merit of the IL **3** was that its cation could be reused. After the reaction finished, the products were extracted with ether (3 × 2 mL) and then the recovered IL solvent was concentrated in vacuum (10 mmHg for 2 h at 50 °C). With further amount of molecular bromine added, the recovered IL **3** could be readily reused for the second run and the process was repeated up to 4 times. It seems that there is little decline in the rate or yield of the reaction during each cycle (Table 1, entry 6).

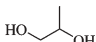
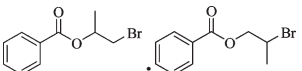
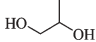
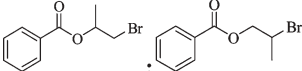
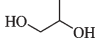
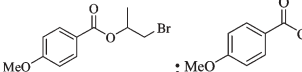
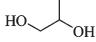
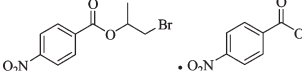
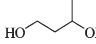
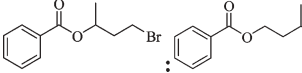
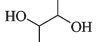
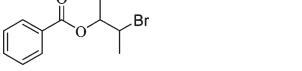
In a similar way, the reaction of ethylene glycol with a series of aromatic aldehydes containing different groups was investigated. The results were summarized in Table 2. It was found that both electron-rich and electron-deficient aromatic aldehydes were suitable for this reaction, giving the desired products in good to excellent yields. For the electron-donating group such as methyl, ethyl, *tert*-butyl, methoxy, and dimethoxy, the by-products of electrophilic aromatic bromination were not found (entries 1–3, 9–10). Unexpectedly, when **3**, 4, 5-trimethoxy benzaldehyde was used for this reaction, the brominated product was obtained as the main product (entry 11). Interestingly, 2-bromo-3,4,5-trimethoxy benzaldehyde was a very useful intermediate widely used in organic

Table 2 Synthesis of 1,2-bromoesters from ethylene glycol and various aldehydes

Entry	Aldehyde	Product	Yield (%) ^{a,b}
1			90
2			89
3			91
4			87
5			86
6			82
7			80
8			80 ^c
9			89
10			85
11			88
12			68 ^d
13			60 ^d

^a Reaction conditions: aromatic aldehyde (2 mmol), ethylene glycol (4 mmol), and IL **3** (4 mmol) at rt for 28–36 h. ^b Isolated yield. ^c Ethylene glycol (6 mmol) and IL **3** (6 mmol) was used. ^d IL **3** (7 mmol) was used.

Table 3 The study of regioselectivities of synthesis of ω -bromoesters from various diols

Entry	Diol	Product	Yield (%) ^{a,b}
1			90 19 : 1
2			89 ^c 4 : 1
3			88 14 : 1
4			83 17 : 1
5			91 3.7 : 1
6			86 ^d

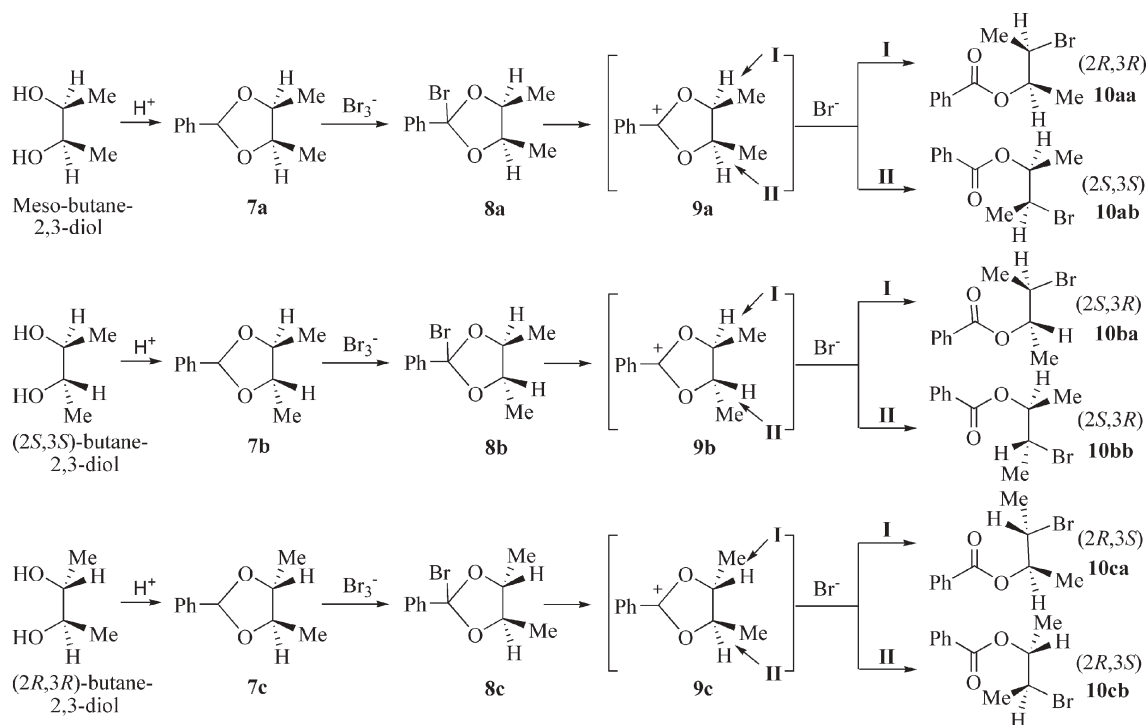
^a Reaction conditions: aromatic aldehyde (2 mmol), diol (4 mmol), and IL **3** (4 mmol) at rt for 36 h. ^b Isolated yield. The ratios of the isomers were based on ¹H NMR spectrum (–CH₃). ^c at 80 °C. ^d The ratio of *erythro* : *threo* isomers was 1.7 : 1.

synthesis and no similar tribromide reagent system for its preparation had been reported.¹² When the reaction was carried out in the presence of large excess of IL **3**, 2-bromoethyl 2-bromo-3,4,5-trimethoxybenzoate (**6l**) was obtained in 68%

yield (entry 12). Further, when the 2-hydroxybenzaldehyde was used as starting material, 2-bromoethyl 5-bromo-2-hydroxybenzoate (**6m**) was obtained as the main product in the similar reaction conditions (entry 13).

The observed regioselectivity of the brominating reactions of benzaldehyde and 1,2-propanediol in the reaction system ranged from 4 : 1 to 19 : 1 (Table 3, entries 1–2). These ratios are comparable to selectivities reported for other brominating reagents, such as NBS (at rt, 5 : 1 to 10 : 1),^{2h-i} *N,N*-bibromobenzene sulfonamide (at 77 °C, 9 : 1),^{2g} Br₂ (at 0 °C, 18 : 1)^{2f} or PHPB (at 50 °C, less than 6% of the regioisomer).³ And the favorable selectivity of regioisomers was also achieved when 4-nitrobenzaldehyde or 4-methoxybenzaldehyde was used as the reaction material (Table 3, entries 3–4). Unfortunately, when 1,3-butanediol was used as the starting material, only 3.7 : 1 ratio of the regioisomers was obtained (Table 3, entry 5). With 2,3-butanediol (*DL*/*meso* = 1 : 1)¹⁴ as a substrate, 1.7 : 1 ratio of the *erythro*/*threo* isomers was detected (Table 3, entry 6). According to the plausible mechanism based on reported literature (Scheme 2),^{2e-i,4} it seemed that the formation of the reaction intermediate **7b** or **7c** from D- or L- 2,3-butanediol was easier than the one (**7a**) from *meso*-2,3-butanediol in our reaction system.

As a variety of chiral ILs have been synthesized from different chiral sources, the study of their applications for asymmetric reactions are underway.⁸ There are a few examples reported of their applications in Diels–Alder reactions,^{10e,13a} Baylis–Hillman reactions,^{13b} photoisomerizations,^{13c} and Michael additions^{7c} with moderate enantiomeric excesses. According to the plausible mechanism displayed in Scheme 2, there are two new chiral centers created during the reaction of 2,3-butanediol with benzaldehyde. Since either D- or L- 2,3-butanediol would give the enantiomerically pure bromoester

**Scheme 2** Plausible mechanism for stereoselective synthesis of 3-bromobutan-2-yl benzoate.

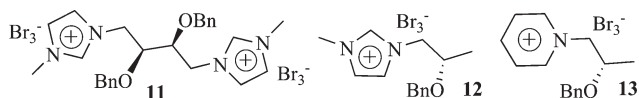


Fig. 1 The chiral ILs based on L-lactic acid or L-tartaric acid.

Table 4 Stereoselective synthesis of **6n** in the present of different chiral ILs

Entry ^a	Chiral IL	Temp/°C	Time/h	Yield (%) ^b	ee (%) ^c
1	3	rt	36	86	4
2	11	rt	48	75	0 ^d
3	12	rt	48	81	11
4	13	rt	48	80	11
5	12	rt	48	83	6 ^d
6	3	-10	48	80	5
7	12	-10	60	79	17

^a Reaction conditions: aromatic aldehyde (2 mmol), *meso*-2,3-butanediol (4 mmol), and chiral IL (4 mmol). ^b Isolated yield. ^c After the reaction was completed, the resultant product was extracted with Et₂O (3 × 2 mL) and dried with Na₂SO₄. The product was further purified by column chromatography (8 : 1 petroleum ether/ethyl acetate) and ee determined by chiral HPLC.¹⁵ ^d 8 mmol of *meso*-2,3-butanediol was used.

(**10ba** or **10ca**) while *meso*-2,3-butanediol would give the enantiomers **10aa** and **10ab** by the reaction routes **I** and **II**, respectively, we chose the reaction of *meso*-2,3-butanediol with benzaldehyde as the model reaction to investigate the chiral induction of IL **3** and other chiral ILs **11–13**¹⁶ (Fig. 1) as chiral reagents or solvents. As illustrated in Table 4, 0–17% ee were achieved using the different chiral ILs **3** and **11–13**. Comparison of entries 1 to 4 shows that the greatest part of chiral discrimination came from the construction of cations. The result of entry 5 implied that the enantioselectivity would be decreased by adding large excess of diol. When the reaction temperature changed from rt to -10 °C, the enantiomeric excesses rose from 11% to 17%. All these are consistent with the hypothesis that the ion-pairing interaction between chiral ILs anion and cation is the key to the reaction chiral induction. Although the reason for the enantioselectivity is not clear and the enantiomeric excesses are moderate at present, the results of this work could provide meaningful insights in the understanding of the use of chiral ILs in asymmetric induction.

Conclusions

In summary, we report an effective and mild method for 1,2- or 1,3-bromoester synthesis using ionic liquid **3** based on L-prolinol as a new reagent and reaction medium. To the best of our knowledge, it is the first example that protic ILs from secondary amines were used both as solvents and as reagents.^{5d,10b,20} While there is still a need to use organic solvents for the product extraction, this process provides an opportunity to reduce solvent consumption and the selection of less hazardous reagents compared to the reaction system of

traditional brominating reagents. The simplicity of the methodology, ease of the product isolation, mild conditions and possibility of IL recycling could make this process available in the future on the industrial scales.

Experimental

Synthesis of IL 2

To a solution of L-proline (**1**, 1.21 g, 12 mmol) in H₂O (30 mL) was dropwise added the aqueous solution of HBr (40%, 2.43 g, 12 mmol). After the reaction mixture was stirred over 0.5 h at rt, the water was evaporated under reduced pressure at 60 °C. Without any further purification, the IL **2** was obtained 2.18 g (100% yield) as a straw yellow viscous oil. $[\alpha]_{\text{D}}^{20} = +9.5$ (c 1.0, EtOH); ¹H NMR (400 MHz, DMSO-*d*₆): δ 9.09 (s, 1H), 8.42 (s, 1H), 5.19 (s, 1H), 3.64–3.61 (m, 1H), 3.55–3.47 (m, 2H), 3.15–3.09 (m, 2H), 1.98–1.80 (m, 3H), 1.64–1.56 (m, 1H); ¹³C NMR (100 MHz, DMSO-*d*₆): δ 65.27, 64.56, 49.32, 30.32, 27.80; IR (KBr): ν 3354, 2954, 2747, 1392, 1048 cm⁻¹; Anal. Calcd for C₅H₁₂BrNO: C, 32.99; H, 6.64; N, 7.69%. Found: C, 32.88; H, 6.78; N, 7.59%.

Synthesis of IL 3

In a fume cupboard, adding molecular bromine (2.16 g, 12 mmol) dropwise under mechanical stirring to ionic liquid **2** (2.18 g, 12 mmol) exothermically formed the red liquid IL **3**. Under reduced pressure over 5 h at 60 °C, the pure IL **3** was obtained 4.02 g (98% yield) as red oil. $[\alpha]_{\text{D}}^{20} = +10.6$ (c 1.0, EtOH); ¹H NMR (400 MHz, DMSO-*d*₆): δ 9.02 (s, 1H), 8.37 (s, 1H), 5.28–5.26 (br, 1H), 3.64–3.60 (m, 1H), 3.52–3.46 (m, 2H), 3.13–3.11 (m, 2H), 1.97–1.79 (m, 3H), 1.63–1.54 (m, 1H); ¹³C NMR (100 MHz, DMSO-*d*₆): δ 65.30, 64.55, 49.37, 30.29, 27.82; IR (KBr): ν 3379, 2925, 2744, 1388, 1044 cm⁻¹; Anal. Calcd for C₅H₁₂Br₃NO: C, 17.57; H, 3.54; N, 4.10. Found: C, 17.46; H, 3.68; N, 4.07.

General procedure for the synthesis of bromoesters

In a 10 mL capped flask, a mixture of *tert*-butyl benzaldehyde (0.57 g, 2 mmol), ethylene glycol (0.25 g, 4 mmol) and IL **3** (1.45 g, 4 mmol) was stirred at rt for 28 h. After the reaction was completed, the resultant product was extracted with Et₂O (3 × 2 mL) and dried with Na₂SO₄. The product 2-bromoethyl 4-*tert*-butylbenzoate (**6c**) was further purified by column chromatography (8 : 1 petroleum ether/ethyl acetate), yield: 91%, colorless oil. ¹H NMR (400 MHz, CDCl₃): δ 8.00 (d, *J* 8.8 Hz, 2H), 7.46 (d, *J* 8.8 Hz, 2H), 4.60 (t, *J* 6.0 Hz, 2H), 3.62 (t, *J* 6.0 Hz, 2H), 1.33 (s, 9H); ¹³C NMR (100 MHz, CDCl₃): δ 165.98, 156.83, 129.52, 126.69, 125.32, 63.87, 34.98, 30.97, 28.84; IR (KBr): ν 3061, 2962, 1722, 1117, 855 cm⁻¹; Anal. Calcd for C₁₃H₁₇BrO₂: C, 54.75; H, 6.01%. Found: C, 54.84; H, 6.11%.

Data of other bromoesters

6c: oil, ¹H NMR (CDCl₃, 400 MHz): δ 8.10 (d, *J* 8.0 Hz, 2H), 7.61 (t, *J* 7.0 Hz, 1H), 7.48 (q, *J*₁ 8.0 Hz, *J*₂ 7.0 Hz, 2H), 4.65 (t, *J* 6.0 Hz, 2H), 3.67 (t, *J* 6.0 Hz, 2H); IR (KBr): ν 3065, 2967, 1726, 1115, 712 cm⁻¹.

6a: oil, ^3H NMR (CDCl_3 , 400 MHz): δ 7.93 (d, J 8.2 Hz, 2H), 7.21 (d, J 8.2 Hz, 2H), 4.57 (t, J 6.0 Hz, 2H), 3.60 (t, J 6.0 Hz, 2H), 2.38 (s, 3H); IR (KBr): ν 3033, 2924, 1721, 1107, 753 cm^{-1} .

6b: oil, ^1H NMR (CDCl_3 , 400 MHz): δ 7.98 (d, J 8.4 Hz, 2H), 7.25 (d, J 8.4 Hz, 2H), 4.58 (t, J 6.0 Hz, 2H), 3.61 (t, J 6.0 Hz, 2H), 2.68 (q, J 7.6 Hz, 2H), 1.23 (t, J 7.6 Hz, 3H); ^{13}C NMR (100 MHz, CDCl_3): δ 165.80, 149.92, 129.65, 127.74, 126.84, 63.81, 28.77, 28.74, 15.01; IR (KBr): ν 3023, 2964, 1723, 1177, 853 cm^{-1} ; Anal. Calcd for $\text{C}_{11}\text{H}_{13}\text{BrO}_2$: C, 51.38; H, 5.10%. Found: C, 51.30; H, 5.26%.

6d: mp: 33–34 $^{\circ}\text{C}$, ^2c ^1H NMR (CDCl_3 , 400 MHz): δ 7.97 (d, J 8.0 Hz, 2H), 7.40 (d, J 8.0 Hz, 2H), 4.60 (t, J 6.0 Hz, 2H), 3.61 (t, J 6.0 Hz, 2H); IR (KBr): ν 3064, 2968, 1725, 1173, 850 cm^{-1} .

6e: mp: 57–58 $^{\circ}\text{C}$, ^3H NMR (CDCl_3 , 400 MHz): δ 7.89 (d, J 8.4 Hz, 2H), 7.56 (d, J 8.4 Hz, 2H), 4.59 (t, J 6.0 Hz, 2H), 3.60 (t, J 6.0 Hz, 2H); IR (KBr): ν 3053, 2950, 1718, 1108, 843 cm^{-1} .

6f: mp: 41–42 $^{\circ}\text{C}$, ^3H NMR (CDCl_3 , 400 MHz): δ 8.24 (d, J 9.2 Hz, 2H), 8.18 (d, J 9.2 Hz, 2H), 4.65 (t, J 6.0 Hz, 2H), 3.66 (t, J 6.0 Hz, 2H); IR (KBr): ν 3122, 2962, 1729, 1106, 719 cm^{-1} .

6g: oil, ^{17}H NMR (CDCl_3 , 400 MHz): δ 8.87 (t, J 2.0 Hz, 1H), 8.47–8.42 (m, 1H), 8.42–8.40 (m, 1H), 7.71 (t, J 8.0 Hz, 1H), 4.72 (t, J 6.0 Hz, 2H), 3.71 (t, J 6.0 Hz, 2H); ^{13}C NMR (100 MHz, CDCl_3): δ 163.85, 148.10, 135.31, 131.19, 129.68, 127.60, 124.55, 64.84, 28.39; IR (KBr): ν 3089, 2930, 1730, 1136, 822 cm^{-1} .

6h: mp: 96–97 $^{\circ}\text{C}$ (Lit, 2c 96–100 $^{\circ}\text{C}$), ^1H NMR (CDCl_3 , 400 MHz): δ 8.11 (s, 4H), 4.63 (t, J 6.0 Hz, 4H), 3.63 (t, J 6.0 Hz, 4H); IR (KBr): ν 3068, 2961, 1723, 1128, 728 cm^{-1} .

6i: oil, ^1H NMR (CDCl_3 , 400 MHz): δ 7.96 (d, J 8.4 Hz, 2H), 7.24 (d, J 8.4 Hz, 2H), 4.62 (t, J 6.0 Hz, 2H), 3.63 (t, J 6.0 Hz, 2H), 2.41 (s, 3H); IR (KBr): ν 3079, 2935, 1715, 1168, 848 cm^{-1} .

6j: mp: 75–76 $^{\circ}\text{C}$, ^{18}H NMR (CDCl_3 , 400 MHz): δ 7.72 (dd, J_1 8.4 Hz, J_2 1.8 Hz, 1H), 7.56 (d, J 1.8 Hz, 1H), 6.90 (d, J 8.4 Hz, 1H), 4.60 (t, J 6.0 Hz, 2H), 3.94 (s, 3H), 3.93 (s, 3H), 3.64 (t, J 6.0 Hz, 2H); ^{13}C NMR (100 MHz, CDCl_3): δ 165.71, 153.14, 148.54, 123.74, 121.92, 111.90, 110.18, 63.92, 55.92, 55.89, 28.87; IR (KBr): ν 3083, 2964, 1705, 1177, 822 cm^{-1} .

6k: mp: 70–71 $^{\circ}\text{C}$, (Lit, 19 70.5–71.5 $^{\circ}\text{C}$), ^1H NMR (CDCl_3 , 400 MHz): δ 10.30 (s, 1H), 7.31 (s, 1H), 3.99 (s, 3H), 3.92 (s, 6H); IR (KBr): ν 3078, 2940, 2866, 1689, 1575 cm^{-1} .

6l: oil, ^1H NMR (CDCl_3 , 400 MHz): δ 7.25 (s, 1H), 4.64 (t, J 6.0 Hz, 2H), 3.94 (s, 3H), 3.90 (s, 3H), 3.89 (s, 3H), 3.66 (t, J 6.0 Hz, 2H); ^{13}C NMR (100 MHz, CDCl_3): δ 165.31, 152.29, 151.54, 146.30, 126.60, 110.35, 109.81, 64.68, 61.15, 61.01, 56.18, 28.56; IR (KBr): ν 3077, 2939, 1734, 1170, 736 cm^{-1} ; Anal. Calcd for $\text{C}_{12}\text{H}_{14}\text{Br}_2\text{O}_5$: C, 36.21; H, 3.55%. Found: C, 36.12; H, 3.67%.

6m: oil, ^1H NMR (CDCl_3 , 400 MHz): δ 10.53 (s, 1H), 7.98 (d, J 2.4 Hz, 1H), 7.56 (dd, J_1 8.8 Hz, J_2 2.4 Hz, 1H), 6.94 (d, J 8.8 Hz, 1H), 4.66 (t, J 6.0 Hz, 2H), 3.66 (t, J 6.0 Hz, 2H); ^{13}C NMR (100 MHz, CDCl_3): δ 168.47, 160.71, 138.82, 132.19, 119.65, 113.33, 110.93, 64.75, 27.92; IR (KBr): ν 3220, 3088, 2920, 1199, 828 cm^{-1} ; Anal. Calcd for $\text{C}_9\text{H}_8\text{Br}_2\text{O}_3$: C, 33.37; H, 2.49%. Found: C, 33.26; H, 2.58%.

6n: oil, 4a $[\alpha]_{\text{D}}^{20} = +0.9$ (c 2.0, CH_2Cl_2); ^1H NMR (CDCl_3 , 400 MHz): δ 8.07 (d, J 7.2 Hz, 2H), 7.54 (t, J 7.2 Hz, 1H), 7.43 (t, J 7.2 Hz, 2H), 5.23–5.20 (m, 1H), 4.25–4.23 (m, 1H), 1.71 (d, J 7.2 Hz, 3H), 3.66 (d, J 7.2 Hz, 3H); IR (KBr): ν 3066, 2985, 1720, 1110, 712 cm^{-1} .

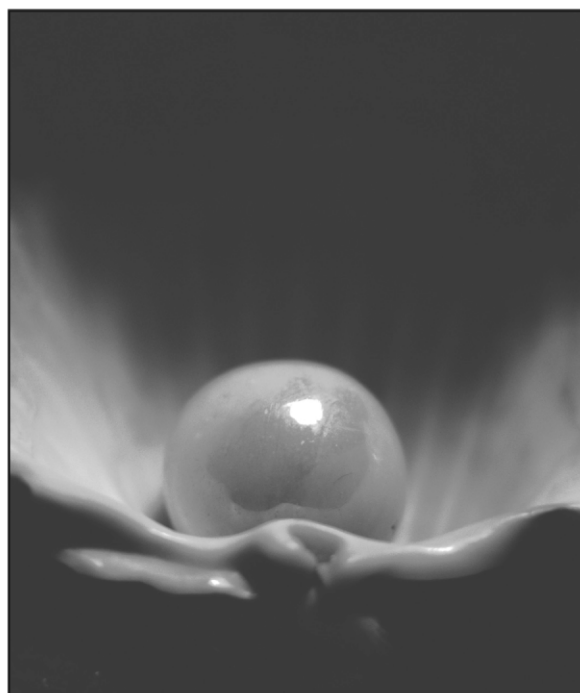
Acknowledgements

This work was financially supported by the Natural Science Foundation of China (no. 20372058).

References

- (a) C. Lherbet, R. Castonguay and J. W. Keillor, *Tetrahedron Lett.*, 2005, **46**, 3565; (b) R. L. Wiseman, S. M. Johnson, M. S. Kelker, T. Foss, L. A. Wilson and J. W. Kelly, *J. Am. Chem. Soc.*, 2005, **127**, 5540; (c) C. Cena, M. L. Lolli, L. Lazzarato, E. Gualta, G. Morini, G. Coruzzi, S. P. McElroy, I. L. Megson, R. Fruttero and A. Gasco, *J. Med. Chem.*, 2003, **46**, 747; (d) I. Berque-Bestel, J.-L. Soulier, M. Giner, L. Rivail, M. Langlois and S. Sicsic, *J. Med. Chem.*, 2003, **46**, 2606; (e) E. Teodori, S. Dei, A. Garnier-Suillerot, F. Cualtier, D. Manetti, C. Martelli, M. N. Romanelli, S. Scapecchi, P. Sudwan and M. Salerno, *J. Med. Chem.*, 2005, **48**, 7426; (f) R. Paulini, B. L. Frankamp and V. M. Rotello, *Langmuir*, 2002, **18**, 2368.
- (a) A. Iwata, H. Tang, A. Kunai, J. Ohshita, Y. Yamamoto and C. Matui, *J. Org. Chem.*, 2002, **67**, 5170; (b) D. Yang, J. C. Soulier, S. Sicsic, M. Mathé-Allainmat, B. Brémont, T. Croci, R. Cardamone, G. Aureggi and M. Langlois, *J. Med. Chem.*, 1997, **40**, 608; (c) H. X. Lin, L. H. Xu and N. J. Huang, *Synth. Commun.*, 1997, **27**, 303; (d) P. M. Collins, A. Manro, E. C. Oparamottah and M. H. Ali, *J. Chem. Soc., Chem. Commun.*, 1988, 272; (e) R. W. Binkley and M. R. Sivik, *J. Org. Chem.*, 1986, **51**, 2619; (f) S. D. Venkataramu, J. H. Cleveland and D. E. Pearson, *J. Org. Chem.*, 1979, **44**, 3082; (g) Y. Kamiya and S. Takemura, *Chem. Pharm. Bull.*, 1974, **22**, 201; (h) D. A. Seeley and J. McElwee, *J. Org. Chem.*, 1973, **38**, 1691; (i) J. D. Prugh and W. C. McCarthy, *Tetrahedron Lett.*, 1966, 1351.
- T. Aoyama, T. Takido and M. Kodomari, *Tetrahedron Lett.*, 2005, **46**, 1989.
- (a) R. K. Hill, S. W. Rhee, E. Leete and B. A. McGaw, *J. Am. Chem. Soc.*, 1980, **102**, 7344; (b) V. Schurig, B. Koppenhoefer and W. Buerkle, *J. Org. Chem.*, 1980, **45**, 538.
- For review, see: (a) T. Welton, *Chem. Rev.*, 1999, **99**, 2071; (b) P. Wasserscheid and W. Keim, *Angew. Chem., Int. Ed.*, 2000, **39**, 3772; (c) R. Sheldon, *Chem. Commun.*, 2001, 2399; (d) S. T. Handy, *Curr. Org. Chem.*, 2005, **9**, 959; (e) P. Wasserscheid and T. Welton, *Ionic liquids in Synthesis*, Wiley-VCH, Weinheim, Germany, 2003.
- (a) J. H. Davis, *Chem. Lett.*, 2004, **33**, 1072 and references cited therein; (b) M. J. Earle, S. P. Katdare and K. R. Seddon, *Org. Lett.*, 2004, **6**, 707; (c) Z. G. Le, Z. C. Chen, Y. Hu and Q. G. Zheng, *Synthesis*, 2004, 2809; (d) J. Salazar and R. Dorta, *Synlett*, 2004, 1318; (e) B. C. Ranu and S. J. Banerjee, *J. Org. Chem.*, 2005, **70**, 4517; (f) G. Noguera, J. Mostany, G. Agrifoglio and R. Dorta, *Adv. Synth. Catal.*, 2005, **347**, 231.
- (a) W. Qian, E. Jin, W. Bao and Y. Zhang, *Angew. Chem., Int. Ed.*, 2005, **44**, 952; (b) Z. Wang, W. Bao and Y. Jiang, *Chem. Commun.*, 2005, 2849; (c) Z. Wang, Q. Wang, Y. Zhang and W. Bao, *Tetrahedron Lett.*, 2005, **46**, 4657; (d) W. Bao, Z. Wang and Y. Li, *J. Org. Chem.*, 2003, **68**, 591; (e) W. Qian, E. Jin, W. Bao and Y. Zhang, *Tetrahedron*, 2006, **62**, 556; (f) Y. Zheng, X. Du and W. Bao, *Tetrahedron Lett.*, 2006, **47**, 1217.
- (a) C. Baudequin, D. Brégeon, J. Levillain, F. Guillen, J.-C. Plaquevent and A.-C. Gaumont, *Tetrahedron: Asymmetry*, 2005, **16**, 3921 and references cited therein; (b) J. Ding and D. W. Armstrong, *Chirality*, 2005, **17**, 281; (c) C. Baudequin, J. Baudoux, J. Levillain, D. Cahard, A.-C. Gaumont and J.-C. Plaquevent, *Tetrahedron: Asymmetry*, 2003, **14**, 3081.
- (a) B. Jastorff, K. Mölter, P. Behrend, U. Botein-Weber, J. Filser, A. Heimers, B. Ondruschka, J. Ranke, M. Schaefer, H. Schröder, A. Stark, P. Stepnowski, F. Stock, R. Störmann, S. Stolte, U. Welz-Biermann, S. Ziegert and T. Thöming, *Green Chem.*, 2005, **7**, 362;

- (b) B. Jastorff, R. Störmann, J. Ranke, J. Ranke, F. Stock, B. Oberheitmann, W. Hoffmann, J. Hoffmann, M. Nüchter, B. Ondruschka and J. Filser, *Green Chem.*, 2003, **5**, 136; (c) S. T. Handy, *Chem.-Eur. J.*, 2003, **9**, 2938 and references cited therein.
- 10 (a) K. Fukumoto, M. Yoshizawa and H. Ohno, *J. Am. Chem. Soc.*, 2005, **127**, 2398; (b) G. Tao, L. He, N. Sun and Y. Kou, *Chem. Commun.*, 2005, 3562; (c) B. Ni, A. D. Headley and G. Li, *J. Org. Chem.*, 2005, **70**, 10600; (d) E. B. Carter, S. L. Cilver, P. A. Fox, R. D. Goode, I. Ntai, M. D. Tickell, R. K. Traylor, N. W. Hoffman and J. H. Davis, Jr., *Chem. Commun.*, 2004, 630; (e) G. Imperato, E. Eibler, J. Niedermater and B. König, *Chem. Commun.*, 2005, 1170; (f) A. P. Abbott, G. Capper, D. L. Davies, R. K. Rasheed and V. Tambyrajah, *Chem. Commun.*, 2003, 70; (g) A. P. Abbott, G. Capper, D. L. Davies, H. Munro, R. K. Rasheed and V. Tambyrajah, *Chem. Commun.*, 2001, 2010; (h) H.-P. Zhu, F. Yang, T. Tang and M.-Y. He, *Green Chem.*, 2003, **5**, 38; (i) S. Guo, Z. Du, S. Zhang, D. Li, Z. Li and Y. Deng, *Green Chem.*, 2006, **8**, 296.
- 11 (a) S. T. Handy, M. Okello and G. Dickenson, *Org. Lett.*, 2003, **5**, 2513; (b) S. T. Handy and M. Okello, *Tetrahedron Lett.*, 2003, **44**, 8395; (c) S. T. Handy and M. Okello, *Tetrahedron Lett.*, 2003, **44**, 8399; (d) A. P. Abbott, G. Capper, D. L. Davies, R. K. Rasheed and V. Tambyrajah, *Green Chem.*, 2002, **4**, 24.
- 12 (a) S. H. Yu, M. J. Ferguson, R. McDonald and D. G. Hall, *J. Am. Chem. Soc.*, 2005, **127**, 12808; (b) R. S. Coleman, S. R. Gurralla, S. Mitra and A. Rao, *J. Org. Chem.*, 2005, **70**, 8932.
- 13 (a) M. J. Earle, P. B. McCormac and K. R. Sedden, *Green Chem.*, 1999, **1**, 23; (b) B. Pégot, G. Vo-Thanh, D. Gori and A. Loupy, *Tetrahedron Lett.*, 2004, **45**, 6425; (c) J. Ding, V. Desikan, X. Han, T. L. Xiao, R. Ding, W. S. Jenks and D. W. Armstrong, *Org. Lett.*, 2005, **7**, 335.
- 14 2,3-Butanediol (DL/*meso* = 1 : 1) was purchased from Acros Organic (107640050). The ratio of DL/*meso* isomers was based on ¹H NMR spectrum (–CH₃).
- 15 Separation conditions: OB-H column and elution with hexane/iso-propanol; flow rate 0.7 mL min⁻¹.
- 16 11–13 could be readily obtained from the known chiral ILs in ref. 7c.
- 17 R. H. Shapiro and K. B. Tomer, *Org. Mass Spectrom.*, 1970, **3**, 333.
- 18 S. G. Agbalyan and V. V. Darbinyan, *Arm. Khim. Zh.*, 1972, **25**, 693.
- 19 G. A. Monlander, K. M. George and L. G. Monovich, *J. Org. Chem.*, 2003, **68**, 9533.
- 20 G. Tao, L. He, W. Lin, L. Xu, W. Xiong, T. Wang and Y. Kou, *Green Chem.*, 2006, **8**, 639.



Looking for that **special** research paper from applied and technological aspects of the chemical sciences?

TRY this free news service:

Chemical Technology

- highlights of newsworthy and significant advances in chemical technology from across RSC journals
- free online access
- updated daily
- free access to the original research paper from every online article
- also available as a free print supplement in selected RSC journals.*

*A separately issued print subscription is also available.

Registered Charity Number: 207890

RSC Publishing

www.rsc.org/chemicaltechnology

Preparation and characterization of ZnO nanoparticles coated paper and its antibacterial activity study

Kalyani Ghule, Anil Vithal Ghule, Bo-Jung Chen and Yong-Chien Ling*

Received 20th April 2006, Accepted 31st August 2006

First published as an Advance Article on the web 15th September 2006

DOI: 10.1039/b605623g

Coating of ZnO nanoparticles on paper surface has potential technological applications. With this motivation, a simple approach of ultrasound assisted coating of paper with ZnO nanoparticles (~20 nm) without the aid of binder is reported for the first time in this work. The ultrasound assisted coating approach concurs with “green” chemistry as it is simple and environmentally friendly. Scanning electron microscope is used to characterize the surface morphology showing ZnO nanoparticles bound to cellulose fibers. Further characterization of coated surface is performed by attenuated total reflectance-Fourier transform infrared, X-ray diffraction, and time-of-flight secondary ion mass spectrometry in positive ion detection mode along with its imaging capability. The effect of ultrasound irradiation time on ZnO nanoparticles loading is estimated by thermogravimetric analysis. A plausible coating mechanism is proposed. The ZnO nanoparticles coated paper is found to possess antibacterial activity against *Escherichia coli* 11634.

Introduction

ZnO is considered as workhorse of technological development exhibiting excellent electrical, optical, and chemical properties with broad range of applications as semiconductors, in optical devices, piezoelectric devices, surface acoustic wave devices, sensors, transparent electrodes, solar cells, antibacterial activity *etc.*^{1–15} Extensive work on synthesis of ZnO nanoparticles and nanostructures using physical and wet chemical methods has been reported since last decade, with regards to controlling the morphology and properties based on the applications.^{1–9} Thin films or nanoscale coating of ZnO nanoparticles on suitable substrates is also important for its potential applications as substrates for functional coatings, printing, UV inks, e-print, optical communications (security-papers), protection, barriers, portable energy, sensors, photocatalytic wallpaper with antibacterial activity *etc.*^{8,10–12,14–24} Various methods like chemical, thermal, spin coating, spray pyrolysis, pulsed laser deposition *etc.* have been developed to coat ZnO nanoparticles in form of thin films on solid supports such as metal, metal oxides, glass or thermally stable substrates.^{17–19,23–26} However, coatings of ZnO nanoparticles on thermolabile surfaces are scarce²⁷ and coating on paper is yet to be reported. Coatings with biomolecules, oil, pigments (calcium carbonate, clay, talc, silicates, TiO₂, *etc.*), polymers, plastics *etc.* has been reported with the help of suitable binders and co-binders.²⁸ However, less attention is paid to ZnO nanomaterials as coatings, in spite of its known technological applications. To the best of our knowledge only one report on low temperature growth of ZnO nanorods on cotton fabric exists.²⁷

It is well known that purity of ZnO is important for its application,^{7–9} demanding extreme thermal treatment after its synthesis or coating.^{29,30} This is with the intension of reducing

or eliminating the organic species adsorbed on the surface of ZnO, which are inevitable irrespective of the methods (physical or chemical) used for synthesis of ZnO nanoparticles. Furthermore, employing extreme heat treatment process after coating of ZnO particles on the paper surface is detrimental. For this reason, use of preformed heat-treated ZnO nanoparticles for coating on thermolabile substrates is desirable, although ZnO nanoparticles could be formed/grown on the substrate.²⁷

On the other hand, choice of paper coating technique is an important consideration. Coating techniques (off-machine and machine) like dip, brush, mechanical blade or bench coater, rolling, air brush, curtain, spin coating, spray, extruded, print, cast, strip coaters *etc.*, have been used for coating the paper surfaces since decades.^{31–33} However, some of these techniques, especially contact mechanical techniques cause web break, surface defects, variable layer (thickness and composition), consume more material by filling fiber interstices, need excess solvent (water), energy *etc.* and affect surface properties, gloss and brightness.³¹ Non-impact spray based techniques are generally preferred as these avoid web breaks and streak defects, and have certain advantages in terms of durability and surface quality.³⁴ But, these are costly, require maintenance, consume more solvent medium to maintain viscosity and spray quality. Thus, improved techniques compatible with coating on nanoscale and consuming less material are required. Furthermore, with increased emphasis on “green” chemistry, interest has been developed towards adoption and implementation of sustainable processes by minimizing the use of toxic chemicals, solvents, energy *etc.*^{35–37} Thus, development of a nonimpact coating technique on the verge of “green” chemistry and nanoscience, revitalizing the progress through nanostructuring is crucial.

Recently, sonochemical processing has proven to be a useful technique in synthesis of nanomaterials and coating metal or metal oxide nanoparticles on suitable substrate. The chemical

Department of Chemistry, National Tsing Hua University, Hsinchu, 30013, Taiwan. E-mail: ycling@mx.nthu.edu.tw; Fax: +886-35711082; Tel: +886-35721484

effects of ultrasound arise from acoustic cavitation phenomena, that is, the formation, growth, and implosive collapse of bubbles in a liquid medium. These unusual chemical and physical environments are generally utilized in sonochemical processing. Although, sonochemistry has been exploited in industries³⁸ and in fabrication of nanomaterials,³⁹ its application in coating nanoparticles to paper surface is yet to be reported.

In this work, a simple, green, and cost-effective ultrasound assisted coating of ZnO nanoparticles on paper surface without the aid of binders is reported. The paper surface coated with ZnO nanoparticles is characterized using scanning electron microscope (SEM), X-ray diffraction (XRD), and attenuated total reflectance-Fourier transform infrared (ATR-FTIR). Loading of ZnO nanoparticles on the paper surface is estimated from the thermogravimetric analysis (TGA). Furthermore, time-of-flight secondary ion mass spectrometry (TOF-SIMS) is used to characterize the surface composition of the coated surface, binding sites of the nanoparticles, and distribution of the coated ZnO nanoparticles. A plausible coating mechanism is proposed. The ZnO nanoparticles coated paper was further tested for antibacterial activity using *Escherichia coli* 11634.

Experimental

ZnO nanoparticles (average diameter ~ 20 nm) were procured from Echo Chemicals, Taiwan. Prior to their use in experiments, the nanoparticles were heated to 450 °C to remove organic contaminants. Further, the ZnO nanoparticles were characterized using transmission electron microscope (TEM) (Philips, Tecnai 20, 200 kV) with inbuilt energy dispersive X-ray analysis (EDS).

In typical experiments for coating ZnO nanoparticles on the paper surface: 2 g of ZnO nanoparticles were dispersed in 200 mL of deionized (DI) water using a fixed power sonicator (L&R Ultrasonics, Quantrex 140, 150 W, 45 kHz) for 10 min. This was followed by drop wise addition of NH_4OH till a pH of 8 was achieved to be in accord with the alkalinity of the paper and sonicated for additional 10 min prior to the experiments. Use of NH_3 is also acceptable. The paper surface to be coated (white paper, YFY Papers, Taiwan) was attached face down to the substrate, and the position was set such that the paper surface just touched the dispersed solution. The sonication time (5, 10, 15, 20, 25, and 30 min) was varied in each experiment. Thereafter the coated paper was detached and dried at 80 °C prior to characterization.

Surface morphology and elemental composition was characterized using SEM (Hitachi-S4700) with inbuilt EDS. TGA analyzer (Perkin Elmer TGA6) was used to record the thermograms in the temperature range from 30 to 500 °C with a heating rate of 5 °C min^{-1} in a flow of air at 20 mL min^{-1} . XRD patterns were obtained using Material Analysis and Characterization (MAC) advanced powder X-ray diffractometer (using $\text{Cu K}\alpha = 1.54056 \text{ \AA}$ radiation). ATR-FTIR spectra of blank paper and ZnO nanoparticles coated paper were recorded using Perkin Elmer (System 2000 FTIR). Samples (ZnO nanoparticles before and after treating with NH_4OH) pressed into KBr pellets were used to record FT-IR spectra (Bomem Hartmann & Braun, MB-series).

Positive TOF-SIMS (ION-TOF; Munich, Germany) measurements were performed for the analysis of blank paper and ZnO nanoparticles coated paper. The paper samples were carefully cut into $1 \times 1 \text{ cm}^2$ pieces and pressed onto the carbon tape supported on a clean Si wafer. The primary ions source was a pulsed $^{69}\text{Ga}^+$ source (pulsing current 2.5 pA, and a pulse width of 30 ns) operated at 15 keV with post-acceleration of 10 kV. The analysis area of $150 \mu\text{m} \times 150 \mu\text{m}$, data acquisition time of 200 s, and charge compensation by applying low-energy electrons ($\sim 30 \text{ eV}$) from a pulsed flood gun were used for the measurements. The pressure of the main chamber was kept between 10^{-8} and 10^{-9} Torr. The best resolution obtained was $m/\Delta m = 5000$. Calibration of the mass spectra was based on the peaks such as H^+ (1.007 m/z), CH_3^+ (15.024 m/z), C_2H_5^+ (29.044 m/z), Na^+ (22.989 m/z), and Ca^+ (39.959 m/z). The peak areas were normalized to the most intense peak in the spectrum. The generated data was processed using IonSpec software and the ion images were obtained using inbuilt Ionimage software.

Antibacterial activity of the ZnO nanoparticles coated paper and the blank controls (white cotton and blank uncoated paper) were investigated using the Japanese Industrial Standard method (JIS L 1902–1998). The test was performed in Food Industry Research and Development Institute of Taiwan using the 11634 strain of *Escherichia coli* on sample specimens of $5 \times 5 \text{ cm}^2$ size. All the samples were pretreated for 30 min using 254 nm UV light prior to their use in the experiments. In one set of experiments, the samples were illuminated with light source of 365 nm (1 mW cm^{-2}) for 1 and 3 h, respectively. And in the other set, the samples were illuminated with light source of 543 nm ($1000 \text{ lux} \approx 0.1464 \text{ mW cm}^{-2}$ i.e. household fluorescent tube light) for 24 h. Control experiments were also performed in which the samples were treated in the same way except for the use of light sources. The viable bacteria were monitored using the standard protocol by counting the number of colony-forming units (CFU).

Results and discussion

SEM, XRD and TGA characterization

SEM image of the blank paper (Fig. 1a) shows dense network of entwined cellulose fibers with wide pores and damaged surface, probably formed during the paper making process. Representative SEM image of ZnO nanoparticles coated paper obtained after 10 min of sonication is shown in Fig. 1b. The ZnO nanoparticles were observed to be coated on the surface of the cellulose fibers and could be confirmed from the magnified images obtained from SEM. EDS analysis also showed the presence of Zn, Ca, Mg, C, and O confirming the deposition of ZnO nanoparticles (data not shown). The inset of Fig. 1b shows TEM image of the ZnO nanoparticles (~ 20 nm) used in these experiments. Fig. 2a and b show SEM images of the paper surface coated with ZnO nanoparticles obtained after 20 and 30 min of sonication, respectively. SEM images show increase in ZnO coating with increasing sonication time thereby reducing the interstitial voids between fibers. Inset in Fig. 2a is the magnified SEM image showing ZnO nanoparticles bound to the cellulose fibers. Magnified SEM images (Fig. 3a, b and c) were also recorded from the paper

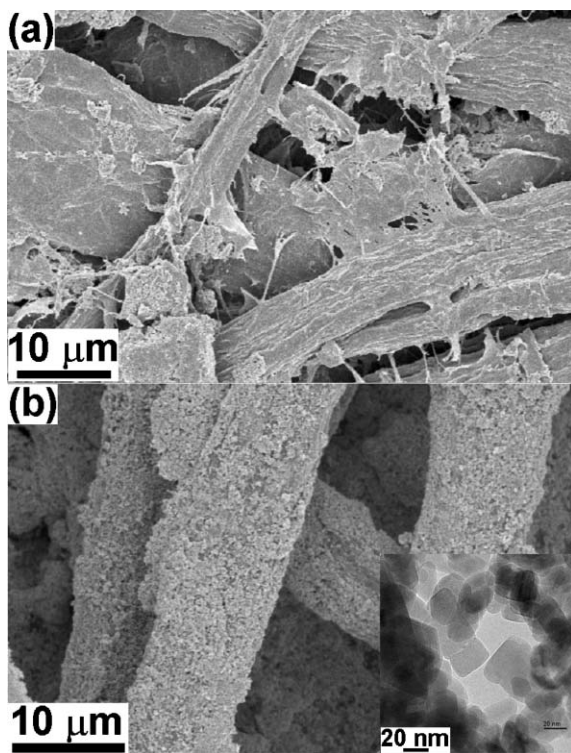


Fig. 1 SEM images of (a) blank paper and (b) ZnO nanoparticles coated paper obtained after 10 min of sonication. Inset is the TEM image of the ZnO nanoparticles used in this work.

surface coated with ZnO nanoparticles obtained after 10, 20, and 30 min of sonication, respectively, to compare the effect of sonication on the particle size. No notable difference in the particle size is observed except for the close packing of the ZnO nanoparticles after 30 min, presumably due to the subsequent collapse of the nanoparticles pushing them close together.

To further confirm the coating of ZnO nanoparticles on the paper surface and its crystallinity, XRD spectra were recorded. Representative XRD spectra recorded from blank paper and ZnO nanoparticles coated paper obtained after 20 min of sonication are shown in Fig. 4. The composition of paper in general is very complex. However, the major composition of paper includes cellulose, CaCO_3 , silicates, thickeners, and binders. For simplicity, we have focused on tracing major components like cellulose and CaCO_3 in the XRD spectra. The XRD spectra of blank paper showed characteristic peaks corresponding to cellulose (JCPDS 03-0289) and CaCO_3 (JCPDS 85-1108). The peaks without asterisk mark in Fig. 4a (blank paper) correspond to cellulose and those with asterisk (labeled as " CaCO_3 ") correspond to CaCO_3 . The XRD pattern recorded from ZnO nanoparticles coated paper (Fig. 4b) showed peaks at 2θ value of 31.7 (100), 34.4 (002), 36.2 (101), 47.5 (102), 56.6 (110), 62.8 (103), 66.4 (200), 67.9 (112) and 69.1 (201) characteristic of ZnO (marked with asterisk and labeled as " ZnO ") and were in good agreement with literature report (JCPDS 89-0510). The remaining peaks in the spectra are attributed to cellulose and CaCO_3 as denoted in Fig. 4a.

It was also noted that the coating of ZnO increased with the sonication time and the amount of ZnO loading on the paper surface was estimated using TGA. Representative TGA

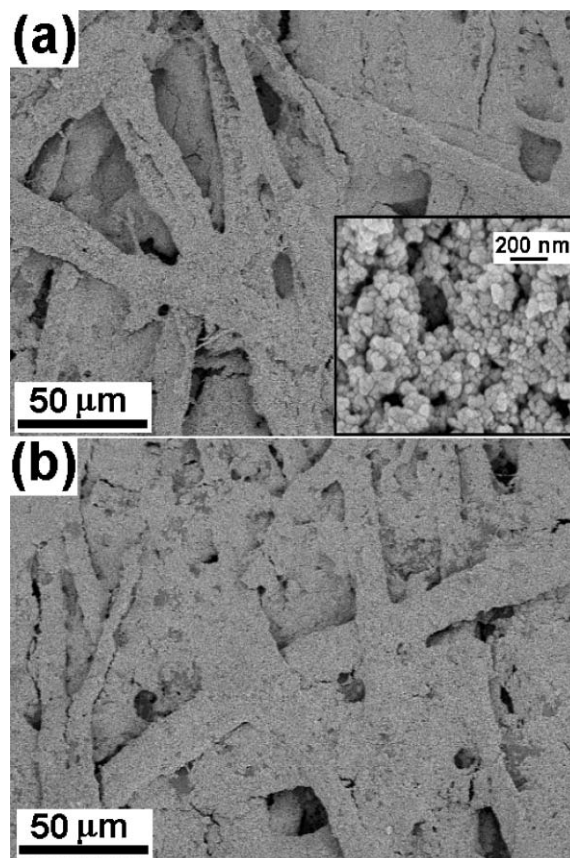


Fig. 2 SEM images of ZnO nanoparticles coated paper obtained after (a) 20 min and (b) 30 min of sonication. Inset shows magnified image of the ZnO nanoparticles bound to cellulose fibers.

thermograms (30–500 °C) obtained from blank paper (dash-dot line) and ZnO nanoparticles coated paper obtained after sonication time of 10 (thin line) and 30 min (bold line) are shown in Fig. 5. TGA thermogram obtained from blank paper showed first weight loss below 100 °C due to desorption of moisture and two consecutive weight losses around 325 and 425 °C extending to 450 °C as a result of decomposition of cellulose. No further weight loss was observed at higher temperature. Total weight loss was 90.8% and remaining 9.2% can be attributed to binders and pigments used during the paper making process. The ZnO coated paper sonicated for 10 and 30 min showed total weight losses of 76.5 and 73.1%, respectively. The differences in weight losses (14.3 and 17.7%) compared to blank paper correspond to the amount of ZnO nanoparticles deposited on the paper surface with sonication time of 10 and 30 min, respectively. ZnO loading as a function of sonication time (5, 10, 15, 20, 25, and 30 min) was also estimated from TGA and the corresponding graph is shown as inset in Fig. 5. It indicates that most of ZnO nanoparticles were bound within 5 min of sonication and showed little increase in ZnO loading with increase of sonication time. If ZnO nanoparticles had to fill the voids or form thick layers of coating, the graph would have shown substantial increase of ZnO loading with sonication time. This suggests that with increasing sonication time, the ZnO nanoparticles might tend to bind only to the available –OH functional groups and avoid

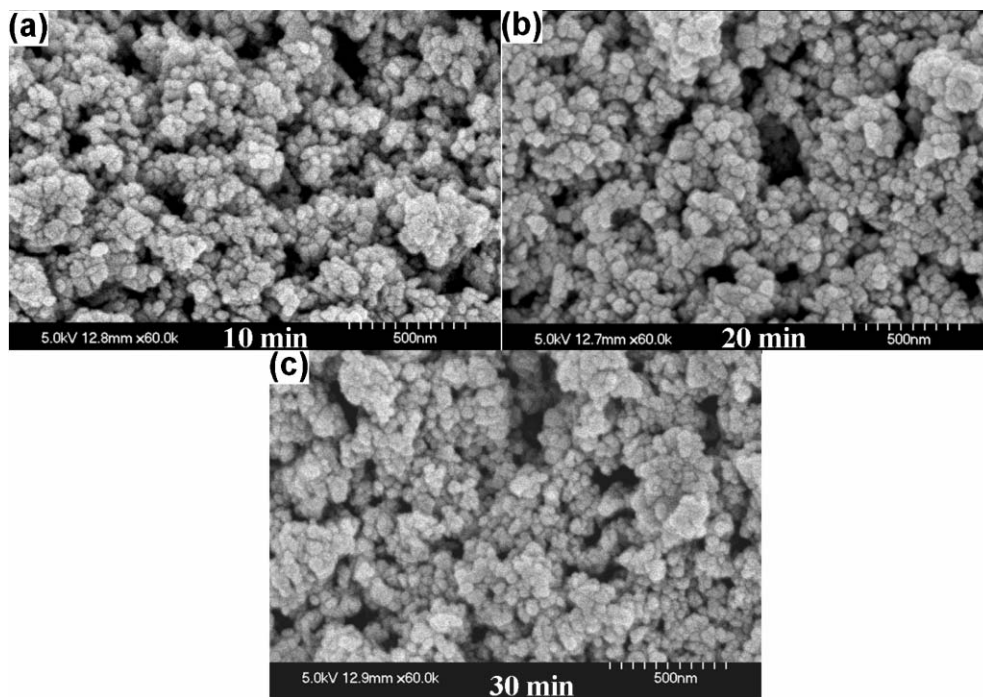


Fig. 3 Magnified SEM images of paper surface coated with ZnO nanoparticles obtained after (a) 10, (b) 20, and (c) 30 min of sonication.

thick multi-layer formation (see below). From these experiments it can be elucidated that 10–20 min of sonication is sufficient for efficient coating of ZnO nanoparticles and was in agreement with SEM results.

TOF-SIMS characterization

Knowing that the ZnO nanoparticles were coated on the surface of paper, it was important to investigate the nature of binding and also the distribution of the ZnO nanoparticles on the coated paper surface. To investigate this, TOF-SIMS spectra in positive ion detection mode were obtained from blank paper and ZnO nanoparticles coated paper obtained after varying sonication time. Representative TOF-SIMS

spectra in positive ion detection mode obtained from blank paper and that obtained from ZnO nanoparticles coated paper after 20 min of sonication are shown in Fig. 6a and b, respectively. The TOF-SIMS spectra of blank paper showed presence of hydrocarbon, oxyhydrocarbon, Ca^+ , Mg^+ , Na^+ etc peaks originating from the paper composition. However, in case of ZnO nanoparticles coated paper (Fig. 6b), additional ions corresponding to $^{64}\text{Zn}^+$ and its isotopes ($^{66}\text{Zn}^+$ and $^{68}\text{Zn}^+$) were clearly observed and agreed well with their natural isotopic abundance. Natural isotopic percentage abundance of ^{64}Zn , ^{66}Zn , and ^{68}Zn is 48.63, 27.9, and 18.75%, respectively.

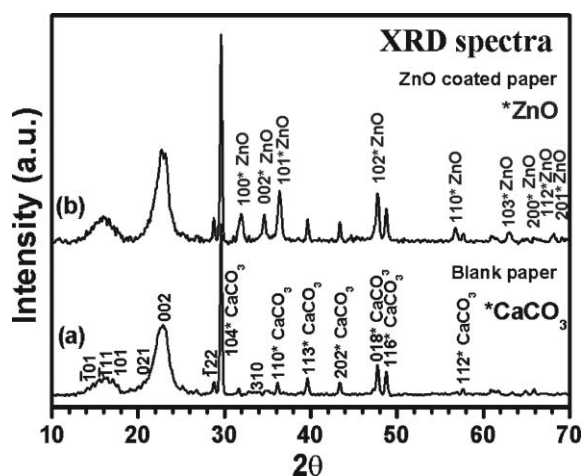


Fig. 4 Representative XRD spectra obtained from (a) blank paper and (b) ZnO nanoparticles coated paper obtained after 20 min of sonication.

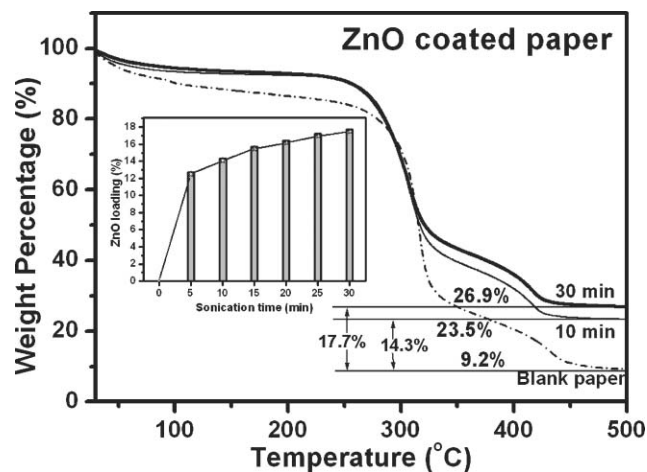


Fig. 5 TGA thermograms recorded from blank paper (dash-dot line) compared to that of ZnO nanoparticles coated paper obtained after 10 (thin line) and 30 min (bold line) of sonication. Inset shows histogram of ZnO loading on the paper with increasing sonication time. ZnO loading is the difference in weight loss when compared to the blank paper.

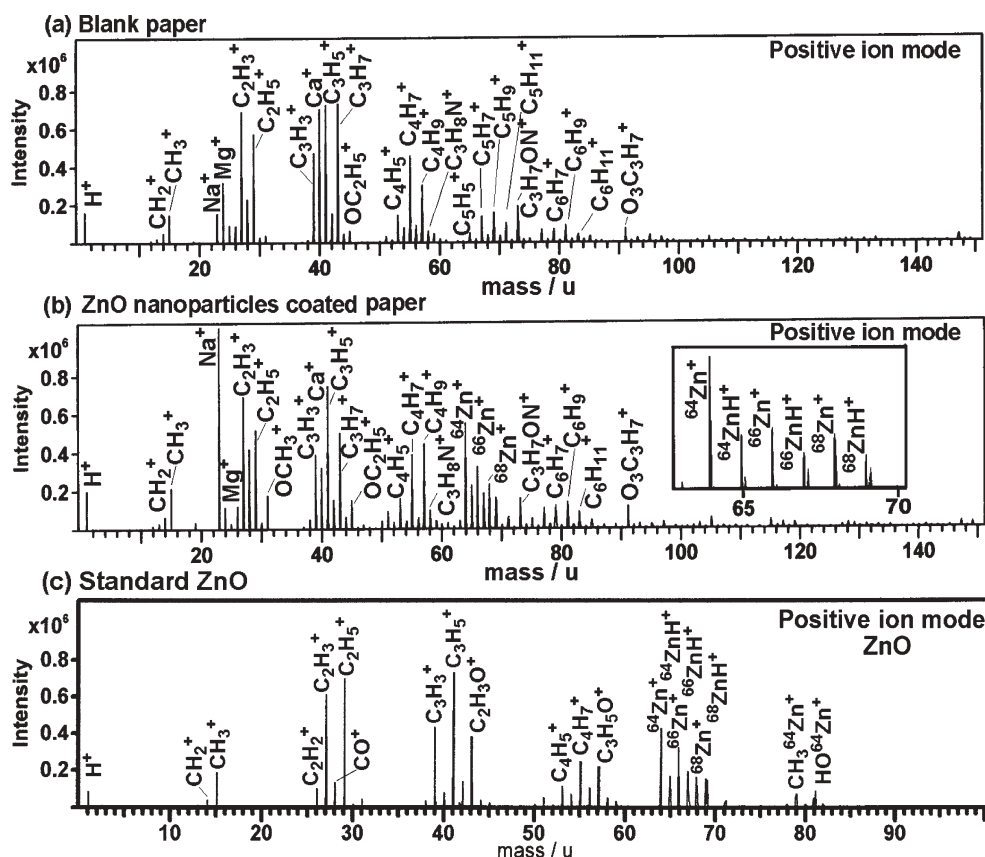


Fig. 6 Representative TOF-SIMS spectra in positive detection mode obtained from (a) blank paper, (b) ZnO nanoparticles coated paper obtained after 20 min of sonication and (c) standard ZnO.

Peaks corresponding to the presence of hydrocarbons, oxyhydrocarbon, Ca^+ , Mg^+ , Na^+ etc. were also observed similar to those in blank paper, confirming the coating of ZnO nanoparticles on paper. The intensity of Na^+ peak was observed to be higher in ZnO nanoparticles coated paper compared to the blank paper and is presumed to be the impurity during sample preparation. Presence of additional peaks corresponding to $^{64}\text{ZnH}^+$, $^{66}\text{ZnH}^+$, and $^{68}\text{ZnH}^+$ possibly indicate that the ZnO nanoparticles might be bound to the hydroxyl groups of cellulose fibers through hydrogen bonding.

To differentiate between the peaks originating from blank paper and those from ZnO nanoparticles, TOF-SIMS spectra in positive ion detection mode was obtained from standard ZnO (Merck) and ZnO nanoparticles used in these experiments. Similar TOF-SIMS spectra were obtained from both and only representative TOF-SIMS spectra obtained from standard ZnO is shown in Fig. 6c. It is important to note that the spectral peak pattern in the TOF-SIMS spectra of blank paper and ZnO nanoparticles coated paper was nearly similar with the exception of Zn^+ ions. However, the spectral peak pattern was different from that obtained from standard ZnO. The peaks other than those observed from standard ZnO can be attributed to those arising from cellulose and paper composition. In addition to $^{64}\text{Zn}^+$, $^{64}\text{ZnH}^+$, $^{66}\text{Zn}^+$, $^{66}\text{ZnH}^+$, $^{68}\text{Zn}^+$, and $^{68}\text{ZnH}^+$ ion peaks, the spectra obtained from standard ZnO showed relatively intense peaks corresponding to CH_2^+ , CH_3^+ , C_2H_2^+ , C_2H_3^+ , CO^+ , C_3H_3^+ , C_3H_5^+ and $\text{C}_2\text{H}_3\text{O}^+$. These peaks probably originate from the fragmentation of the

organic remnants left on the surface of standard ZnO. Additional peaks corresponding to C_4H_5^+ , C_4H_7^+ , and $\text{C}_3\text{H}_5\text{O}^+$ were also observed supporting our speculation and also the fact that organic species as remnants on the surface of ZnO are inevitable irrespective of the method used for its synthesis. TOF-SIMS spectra obtained from heat-treated ZnO nanoparticles also showed similar peak patterns, however, with relatively low intensities of hydrocarbon peaks (spectra not shown). Although $^{64}\text{ZnH}^+$, $^{66}\text{ZnH}^+$, and $^{68}\text{ZnH}^+$ peaks were observed in spectra obtained from standard ZnO nanoparticles, the $^{64}\text{ZnH}^+$: $^{64}\text{Zn}^+$ (0.43), $^{66}\text{ZnH}^+$: $^{66}\text{Zn}^+$ (0.57) and $^{68}\text{ZnH}^+$: $^{68}\text{Zn}^+$ (0.71) ion intensity ratios in ZnO nanoparticles coated paper was higher than that observed in spectra obtained from standard ZnO, i.e. 0.28, 0.42, 0.69, respectively. Furthermore, the ambiguity of C_5H_5^+ , C_5H_7^+ and C_5H_9^+ ions originating from paper composition and contributing to the observed increase in intensity of $^{64}\text{ZnH}^+$, $^{66}\text{ZnH}^+$, and $^{68}\text{ZnH}^+$ ions could be ruled out, as the peaks corresponding to C_5H_5^+ (65.033 *m/z*) and $^{64}\text{ZnH}^+$ (64.938 *m/z*), C_5H_7^+ (67.051 *m/z*) and $^{66}\text{ZnH}^+$ (66.934 *m/z*), and C_5H_9^+ (69.067 *m/z*) and $^{68}\text{ZnH}^+$ (68.932 *m/z*) could be clearly resolved as shown in inset of Fig. 6b. This supports our speculation of ZnO nanoparticles being bound to the cellulose through hydrogen bonding. This is further supported by the FTIR experiments (see below) and is in accord with the proposed mechanism.

The distribution of the ZnO nanoparticles on the paper surface was investigated by obtaining the ion images of individual Zn^+ , ZnH^+ and its isotopes as shown in Fig. 7. Ion

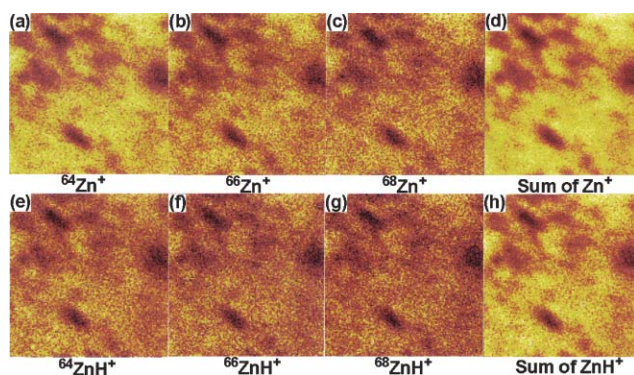


Fig. 7 Ion images of (a) $^{64}\text{Zn}^+$, (b) $^{66}\text{Zn}^+$, (c) $^{68}\text{Zn}^+$, (d) sum of all ($^{64}\text{Zn}^+ + ^{66}\text{Zn}^+ + ^{68}\text{Zn}^+$), (e) $^{64}\text{ZnH}^+$, (f) $^{66}\text{ZnH}^+$, (g) $^{68}\text{ZnH}^+$ and (h) sum of all ($^{64}\text{ZnH}^+ + ^{66}\text{ZnH}^+ + ^{68}\text{ZnH}^+$) from ZnO nanoparticles coated paper obtained after 20 min of sonication.

images of $^{64}\text{Zn}^+$, $^{66}\text{Zn}^+$, $^{68}\text{Zn}^+$ and sum of all ($^{64}\text{Zn}^+ + ^{66}\text{Zn}^+ + ^{68}\text{Zn}^+$) obtained from paper surface coated with ZnO nanoparticles (sonicated for 20 min) are shown in Fig. 7a–d, respectively. The ion images clearly indicate that the ZnO nanoparticles are uniformly distributed and coated on the paper surface. Ion images of $^{64}\text{ZnH}^+$, $^{66}\text{ZnH}^+$, $^{68}\text{ZnH}^+$ and sum of all ($^{64}\text{ZnH}^+ + ^{66}\text{ZnH}^+ + ^{68}\text{ZnH}^+$) are shown in Fig. 7e–h. The dark contrasts observed in the ion images possibly originate from the voids of the entwined cellulose fiber network, which affects the ion collection efficiency from the specific areas. It might also be due to less concentration of ZnO nanoparticles in voids. Further, it is understood that the coating of ZnO nanoparticles on the paper surface would depend on the density of the entwined cellulose fiber network as the nanoparticles are coated on the fibers.

Plausible coating mechanism

Typical coating setup and plausible proposed mechanism of coating ZnO nanoparticles on the paper surface is as shown in Fig. 8. The height adjustment in the setup is to adjust the paper substrate at the surface of the dispersed solution. This setup enables coating of ZnO nanoparticles only on one side of the paper thereby reducing the amount of ZnO nanoparticles

required. Furthermore, by this way only required amount of ZnO nanoparticles and little solvent medium is consumed and also prevents the ZnO nanoparticles being filled in the interstitial voids unlike mechanical blades, bench coaters or spray techniques. The use of NH_4OH was to maintain the basicity of the solution to be compatible with the alkalinity of the paper. Although, pH of 8 was set in all experiments, variation of pH even up to 10 did not show significant effect on the coating efficiency. The NH_4OH dissociates into NH_4^+ and OH^- ions and the NH_4^+ ions tend to get adsorbed on ZnO nanoparticles forming a monolayer. A similar phenomenon of NH_4^+ adsorption was reported by Sherif and Via⁴⁰ and Wang and Muhammed.⁴¹ It is expected that the nanoparticles dispersed ultrasonically in the medium create high-speed microjets in form of bubbles collapsing on the cellulose fibers and bind uniformly as depicted in the schematic representation of the mechanism. The coating might be due to high impact or *via* hydrogen bonding.⁴² Subsequent collapse of the nanoparticles might push the coated nanoparticles towards the fiber and strengthen the coated layer. Although, sonication time was varied from 5 min to 30 min, no significant increase in ZnO loading was observed. Thus, it is expected that the adsorption of NH_4^+ ions on the ZnO nanoparticles might prevent subsequent loading of ZnO nanoparticles as a result of charge repulsion avoiding multi-layer formation.

FTIR characterization

To further support the mechanism, ATR-FTIR spectra were recorded from the blank paper and the ZnO nanoparticles coated paper obtained after 10 and 30 min of sonication as shown in Fig. 9a. The spectra recorded from blank paper (i) shows a weak band at 460 cm^{-1} characteristic of metal–oxygen (M–O) vibrational band,⁴³ possibly arising from CaCO_3 , CaO , MgO or silicates usually used during paper making process. A weak broad band at 732 cm^{-1} might be due to the overlap of the bands at 710 and 750 cm^{-1} , which are characteristic of I_β and I_α phases of cellulose.⁴⁴ This possibly indicates their presence as a mixture in the composition of paper. The bands in the range from 900 – 1300 cm^{-1} and 1300 – 1500 cm^{-1} are associated with C–O and C–H vibrations of cellulose.⁴⁴ The band at 1640 cm^{-1} can be attributed to the absorbed water in

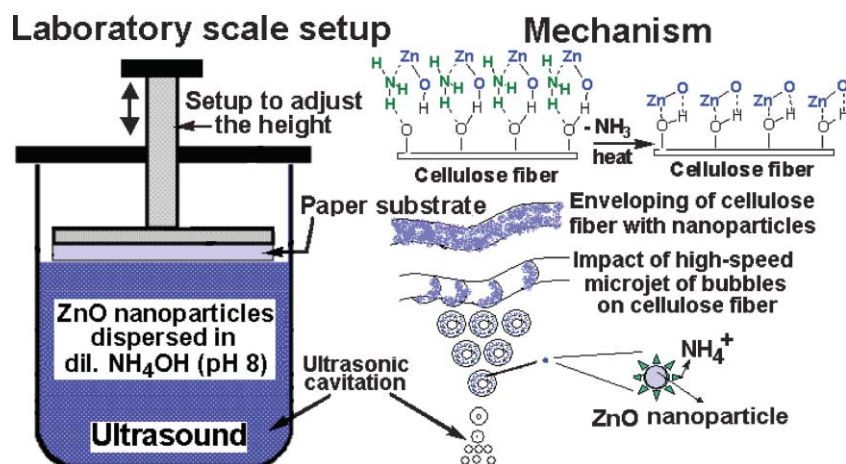


Fig. 8 Schematic diagram of the set-up used for coating ZnO nanoparticles on the paper surface and the proposed mechanism.

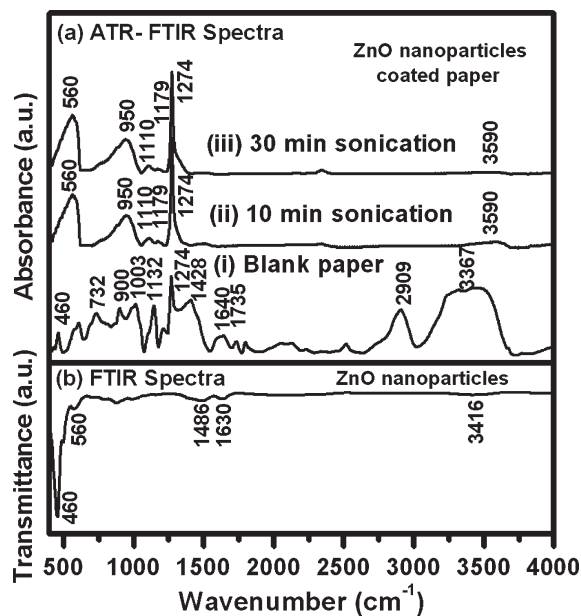


Fig. 9 (a) ATR-FTIR spectra obtained from (i) blank paper and ZnO nanoparticles coated paper obtained after (ii) 10 and (iii) 30 min of sonication. (b) Representative FTIR spectra of ZnO nanoparticles after 30 min of sonication in presence of NH_4OH .

the cellulose fibers^{44,45} and is in agreement with TGA data showing initial weight loss (below $100\text{ }^\circ\text{C}$) from blank paper as a result of desorption of water. The band at 1735 cm^{-1} is characteristic of hemicelluloses and the band at 2909 cm^{-1} can be attributed to the C–H stretching vibrations of cellulose. A broad band ($3100\text{--}3700\text{ cm}^{-1}$) centered around 3367 cm^{-1} characteristic of –OH functional group (free and H-bonded) is also observed.

Similarly, spectra were recorded from ZnO nanoparticles coated paper obtained after (ii) 10 and (iii) 30 min of sonication. Both of the spectra showed a broad band at 560 cm^{-1} and seemed to have an overlap of bands at 460 cm^{-1} characteristic of M–O vibrational band.⁴³ The bands at 950, 1110, 1179, 1274 and 3590 cm^{-1} are attributed to cellulose (paper composition).⁴⁴ The band at 3590 cm^{-1} representative of free –OH shows decrease in intensity with increase in sonication time, suggests that the hydroxyl functional groups are occupied with the ZnO nanoparticles. The band seems to disappear after sonication for 30 min, suggesting that almost all the –OH functional groups are occupied. FTIR spectra of standard ZnO nanoparticles and ZnO nanoparticles on sonication in presence of NH_4OH were also recorded to support the phenomenon of NH_4^+ adsorption. A representative FTIR

spectrum of ZnO nanoparticles obtained after sonication in presence of NH_4OH is shown in Fig. 9b. The spectrum showed bands at 460 and 560 cm^{-1} corresponding to metal–oxygen (M–O) and metal–nitrogen (M–N) vibrational bands, respectively.⁴³ The bands at 1486 and 1630 cm^{-1} correspond to N–H bending mode and the band at 3416 cm^{-1} can be attributed to free NH stretching vibrations.⁴³ On the other hand, the spectrum recorded from untreated ZnO nanoparticles showed a single band at 460 cm^{-1} attributed to M–O vibrational band.⁴³

Antibacterial activity study

The antibacterial activity of ZnO nanoparticles coated paper was tested using *Escherichia coli* 11634 in comparison with white cotton and blank paper as controls, the results of which are presented in Table 1. The best antibacterial activity could be obtained on illumination with 543 nm, 1000 lux ($\sim 0.1464\text{ mW cm}^{-2}$) light *i.e.* household fluorescent tube light for 24 h. Same result was obtained without illumination but treating for 24 h. This shows that ZnO nanoparticles coated paper shows antibacterial activity even in the absence of light supporting the fact that, antibacterial activity is induced by the hydrogen peroxide (H_2O_2) generated from ZnO.^{10,46} H_2O_2 is a powerful oxidizing agent and more reactive than oxygen molecules. It is well known that H_2O_2 is harmful to the cells of living organisms and is the major contributor of antibacterial activity.^{10,46} Thus, the natural tendency of cellulose fibers absorbing moisture and the ZnO nanoparticles generating H_2O_2 can be taken to the advantage of forming antibacterial wall papers. On the other hand, the white cotton and blank paper (controls) did not show antibacterial activity on illumination with or without 543 nm, 1000 lux light as expected. The samples illuminated with UV light of 365 nm, 1 mW cm^{-2} for 1 and 3 h, respectively, showed increased antibacterial activity with the increase in exposure time. Although, UV light is observed to contribute to the increased antibacterial activity, exposure time or time of interaction of bacteria with ZnO nanoparticles is also an important parameter. Interestingly, blank paper also showed some antibacterial activity when illuminated with UV light of 365 nm and can be attributed to the contribution from the CaO and MgO present as a part of paper composition and with known potential antibacterial activity.⁴⁶

It is to be noted that the simplicity, flexibility and adaptability of ultrasound assisted coating approach makes it suitable for this work. It was also observed that the ZnO nanoparticles could be formed on the paper surface on treating with aqueous solution of zinc acetate, either by dip coating or dipping followed by sonication. However, by the dip coating

Table 1 Anti-bacterial activity test using *E. coli* 11634. The viable bacteria were monitored by counting the number of colony-forming units (CFU)

	Bacteria count (CFU) after seeding and washing immediately	Bacteria count (CFU) on illumination with 365 nm light (1 mW cm^{-2} , 1 h)		Bacteria count (CFU) on illumination with 365 nm light (1 mW cm^{-2} , 3 h)		Bacteria count (CFU) on illumination with 543 nm, 1000 lux $\approx 0.1464\text{ mW cm}^{-2}$, 24 h	
		In light	No light	In light	No light	In light	No light
Blank (white cotton)	1.1×10^5	2.6×10^5	6.4×10^5	2.4×10^6	5.0×10^6	2.4×10^8	2.7×10^8
Blank paper	1.1×10^4	1.3×10^3	2.0×10^4	4.8×10^3	1.5×10^5	3.7×10^6	5.4×10^6
ZnO nanoparticles coated paper	1.0×10^4	1.6×10^2	3.2×10^2	1.3×10^2	1.2×10^4	<20	<20

approach, the nanoparticles are coated on either sides of the paper consuming more material. On the other hand, sonication on dipping adds to web defects destroying the paper quality. Additionally, the resultant ZnO nanoparticles coatings are bound to have organic species on the surface and removal of these organic species adsorbed on the surface of ZnO nanoparticles demands high temperature treatment, which is not feasible once coated on thermolabile substrates such as paper. Furthermore, these surface bound organic species are known to affect the optical and catalytic properties. Thus, ZnO nanoparticles used in these experiments were pretreated at 450 °C with the intention of eliminating or reducing the organic contaminants on the surface of the nanoparticles. By using ultrasound, the ZnO nanoparticles could be coated on the cellulose fibers through hydrogen bonding as explained earlier.

Conclusions

In conclusion, coating of ZnO nanoparticles on the cellulose fibers of the paper using an ultrasonic approach is reported for the first time. This coating approach is “green” chemistry because it is simple, inexpensive, consumes less material, avoids waste and minimizes the use of solvent medium, unlike mechanical bench coaters and spray techniques. The paper surface coated with ZnO has been characterized using SEM, EDS, TGA, XRD, ATR-FTIR, and TOF-SIMS. TOF-SIMS could provide information with regards to the surface composition of the coated paper, the binding site of ZnO nanoparticles and also their distribution on the surface. The antibacterial activity of the ZnO nanoparticle coated paper was also tested and the best activity could be obtained on treating for 24 h in the presence and in the absence of light (543 nm, 1000 lux \approx 0.1464 mW cm⁻², *i.e.* household fluorescent tube light) supporting the role of H₂O₂ in antibacterial activity. Furthermore, considering the potential implication of this coating technique, nanoparticles and coated layers can be varied using suitable chemistry for desired applications. For example, sonochemically coated nanoparticles of Al₂O₃ and SiO₂ on a paper surface would provide a good economic alternative for TLC plates in separation science. Research towards this goal is currently under work.

Acknowledgements

Financial support by National Science Council (NSC94-2218-E-007-052) and National Tsing Hua University is gratefully acknowledged.

References

- 1 E. A. Meulenkamp, *J. Phys. Chem. B*, 1998, **102**, 5566.
- 2 Y. N. Xia, P. D. Yang, Y. G. Sun, Y. Y. Wu, B. Mayers, B. Gates, Y. D. Yin, F. Kim and Y. Q. Yan, *Adv. Mater.*, 2003, **15**, 353.
- 3 X. S. Fang, C. H. Ye, L. D. Zhang, Y. Li and Z. D. Xiao, *Chem. Lett.*, 2005, **34**, 436.
- 4 M. H. Huang, S. Mao, H. Feick, H. Q. Yan, Y. Y. Wu, H. Kind, E. Weber, R. Russo and P. D. Yang, *Science*, 2001, **292**, 1897.
- 5 X. S. Fang and L. D. Zhang, *J. Mater. Sci. Technol.*, 2006, **22**, 1.
- 6 Z. W. Pan, Z. R. Dai and Z. L. Wang, *Science*, 2001, **291**, 1947.
- 7 Z. Y. Fan and J. G. Lu, *J. Nanosci. Nanotechnol.*, 2005, **5**, 1561.
- 8 U. Ozgur, Y. I. Alivov, C. Liu, A. Teke, M. A. Reshchikov, S. Dogan, V. Avrutin, S. J. Cho and H. Morkoc, *J. Appl. Phys.*, 2005, **98**, 041301.
- 9 G. C. Yi, C. R. Wang and W. I. Park, *Semicond. Sci. Technol.*, 2005, **20**, S22.
- 10 O. Yamamoto, *Int. J. Inorg. Mater.*, 2001, **3**, 643.
- 11 O. Yamamoto, M. Komatsu, J. Sawa and Z. E. Nakagawa, *J. Mater. Sci.: Mater. Med.*, 2004, **15**, 847.
- 12 J. Sawai, S. Shoji, H. Igarashi, A. Hashimoto, T. Kokugan, M. Shimizu and H. Kojima, *J. Ferment. Bioeng.*, 1998, **86**, 521.
- 13 B. Lo, J. Y. Chang, A. V. Ghule, S. H. Tzing and Y. C. Ling, *Scr. Mater.*, 2006, **54**, 411.
- 14 S. J. Pearton, D. P. Norton, K. Ip, Y. W. Heo and T. Steiner, *J. Vac. Sci. Technol., B*, 2004, **22**, 932.
- 15 R. Brayner, R. Ferrari-Iliou, N. Brivois, S. Djediat, M. F. Benedetti and F. Fievet, *Nano Lett.*, 2006, **6**, 866.
- 16 L. Q. Jing, X. J. Sun, J. Shang, W. M. Cai, Z. L. Xu, Y. G. Du and H. G. Fu, *Sol. Energy Mater. Sol. Cells*, 2003, **79**, 133.
- 17 W. F. Shen, Y. Zhao and C. B. Zhang, *Thin Solid Films*, 2005, **483**, 382.
- 18 S. H. Bae, S. Y. Lee, B. J. Jin and S. Im, *Appl. Surf. Sci.*, 2001, **169**, 525.
- 19 T. P. Niesen and M. R. De Guire, *J. Electroceram.*, 2001, **6**, 169.
- 20 E. M. Bachari, S. Ben Amor, G. Baud and M. Jacquet, *Mater. Sci. Eng., B*, 2001, **79**, 165.
- 21 R. U. Ibanez, J. R. R. Barrado, F. Martin, F. Brucker and D. Leinen, *Surf. Coat. Technol.*, 2004, **188–89**, 675.
- 22 N. Golego, S. A. Studenikin and M. Cocivera, *J. Electrochem. Soc.*, 2000, **147**, 1592.
- 23 S. Chaudhuri, D. Bhattacharyya, A. B. Maity and A. K. Pal, *Surf. Coat. Adv. Mater.*, 1997, **246**, 181.
- 24 D. Bahnemann, *Sol. Energy*, 2004, **77**, 445.
- 25 Y. Lee, H. Kim and Y. Roh, *J. Appl. Phys.*, 2001, **40**, 2423.
- 26 M. Berber, V. Bulto, R. Kliss and H. Hahn, *Scr. Mater.*, 2005, **53**, 547.
- 27 R. H. Wang, J. H. Xin, X. M. Tao and W. A. Daoud, *Chem. Phys. Lett.*, 2004, **398**, 250.
- 28 C. Kugge, V. S. J. Craig and J. Daicic, *Colloids Surf., A*, 2004, **238**, 1.
- 29 A. V. Ghule, B. Lo, S. H. Tzing, K. Ghule, H. Chang and Y. C. Ling, *Chem. Phys. Lett.*, 2003, **381**, 262.
- 30 A. V. Ghule, K. Ghule, C. Y. Chen, W. Y. Chen, S. H. Tzing, H. Chang and Y. C. Ling, *J. Mass Spectrom.*, 2004, **39**, 1202.
- 31 E. Lehtinen, in *Pigment coating and surface sizing of paper*, ed. J. Glulichsen and H. Paulapuro, TAPPI Press, Helsinki, 2000, 810 pp.
- 32 N. Ignjatovic, Z. Brankovic, M. Dramicanin, J. M. Nedeljkovic and D. P. Uskokovic, *Adv. Mater. Processes*, 1998, **282**, 147.
- 33 Y. Natsume and H. Sakata, *Thin Solid Films*, 2000, **372**, 30.
- 34 T. Gliese, *Wochenbl. Papierfabr.*, 2004, **132**, 540 (abstract).
- 35 A. S. Matlack, *Introduction to Green Chemistry*, Marcel Dekker, Inc., New York, 2001.
- 36 P. T. Anastas and J. C. Warner, *Green Chemistry: Theory and Practice*, Oxford University Press, Inc., New York, 1998.
- 37 P. T. Anastas and J. B. Zimmerman, *Environ. Sci. Technol.*, 2003, **95A**.
- 38 S. Vajnhandl and A. M. Le Marechal, *Dyes Pigm.*, 2005, **65**, 89.
- 39 A. Gedanken, *Ultrason. Sonochem.*, 2004, **11**, 47.
- 40 F. G. Sherif and F. A. Via, to Akzo America Inc., U.S. Pat., 4764357, 1988.
- 41 L. Wang and M. Muhammed, *J. Mater. Chem.*, 1999, **9**, 2871.
- 42 L. de Smet, G. A. Stork, G. H. F. Hurenkamp, Y. Q. Sun, H. Topal, P. J. E. Vronen, A. B. Sieval, A. Wright, G. M. Visser, H. Zuilhof and E. J. R. Sudholter, *J. Am. Chem. Soc.*, 2003, **125**, 13916.
- 43 K. Nakamoto, *Infrared and Raman Spectra of Inorganic and Co-ordination Compounds*, Wiley, Chichester, 1978.
- 44 R. G. Liu, H. Yu and Y. Huang, *Cellulose*, 2005, **12**, 25.
- 45 G. Gastaldi, G. Capretti, B. Focher and C. Cosentino, *Ind. Crops Prod.*, 1998, **8**, 205.
- 46 J. Sawai, *J. Microbiol. Methods*, 2003, **54**, 177.

A direct, efficient synthesis of unsymmetrically substituted bis(arylidene)alkanones†

Anthony E. Rosamilia,^a Marilena A. Giarrusso,^a Janet L. Scott^{*a} and Christopher R. Strauss^{*b}

Received 28th April 2006, Accepted 18th August 2006

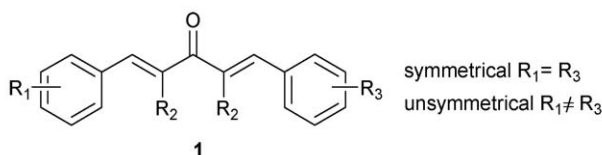
First published as an Advance Article on the web 6th September 2006

DOI: 10.1039/b606042k

A direct method to unsymmetrically substituted bis(arylidene)alkanones by sequential, selective condensation reactions is reported. Analytically pure compounds were obtained in high yield using atom-economical reactions and without the need for purification of the final products. Although a two-step process could be conducted in one pot by three different methods, recrystallisation was required.

Introduction

Bis(arylidene)alkanones **1** are useful chemical building blocks for the synthesis of biologically important heterocycles such as dihydropyrazoles,¹ substituted pyridines or pyran derivatives,² as well as for mixed systems containing pyrroles in combination with pyrazolines and isoxazolines.³ We have employed this motif in the construction of dienone macrocycles that may find uses themselves or that can be readily converted to new families such as Horning-crowns by simple chemical transformations.⁴



In addition, some examples of **1** have activity as enzyme inhibitors,⁵ cytotoxic agents,⁶ blood coagulators,⁷ antitumour⁸ and anticancer agents.⁹ Remarkably, most of the compounds tested in this regard have been symmetrical bis(arylidene)alkanones **1**. Few unsymmetrically substituted ($R_1 \neq R_3$) compounds have been described, presumably owing to difficulties with preparation. A direct, energy efficient, high yielding route to unsymmetrical bis(arylidene)alkanones, amenable to applications in combinatorial library synthesis, would provide ready access to libraries of such compounds.

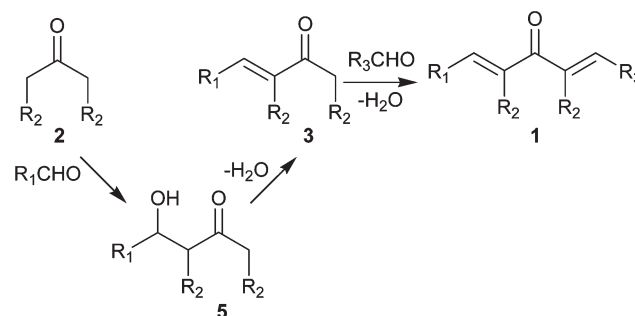
As α,β -unsaturated ketones are readily prepared by Claisen-Schmidt condensation of aldehydes and ketones, it is tempting to suggest that careful control of stoichiometry might allow preparation of unsymmetrical examples of **1**, using sequential

aldol condensation reactions with different aldehydes, Scheme 1. Unfortunately, even with a large molar excess of the ketone **2**, the intermediate α,β -unsaturated ketone **3**, preferentially reacts with a second mole of aldehyde providing symmetrical **1**.¹⁰

The α,β -unsaturated ketone **3** may be prepared by dehydration of the aldol addition product **5**,¹¹ which can be synthesised by a number of routes including a Mukaiyama type reaction utilising a silyl enol ether of the ketone,¹² with organocatalysts such as proline or 5,5-dimethyl thiazolidinium-4-carboxylate¹³ as well as with aqueous base.¹⁴ The first of these routes yields a stoichiometric quantity of waste, significantly lowering atom economy and the last is not always predictable or high yielding. Preformed enamines of ketones with cyclic amines have been used to form α,β -unsaturated ketones **3** in preference to symmetrical **1**, yielding a stoichiometric quantity of amine as waste.¹⁵

We have recently demonstrated that α,β -unsaturated ketones **3** are readily accessible by using the 'distillable ionic medium' DIMCARB.¹⁶ We chose this as the starting point for a simple, direct, low-waste route to a range of unsymmetrically substituted examples of **1**.

DIMCARB is the product of reaction between the gases carbon dioxide and dimethylamine, which react rapidly (and exothermically) yielding a free-flowing liquid: a mixture of *N,N*-dimethylcarbamic acid and the salt, *N,N*-dimethylammonium *N',N'*-dimethylcarbamate, Scheme 2.¹⁷ DIMCARB may be used as both solvent and catalyst, and is comparably similar to store and handle as organic solvents such as acetone. Herein



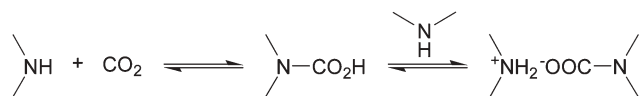
Scheme 1

^aARC Special Research Centre for Green Chemistry, Monash University, Clayton, Victoria, 3800, Australia.

E-mail: janet.scott@sci.monash.edu.au; Fax: +61 3 99054597; Tel: +61 3 99054600

^bCSIRO Molecular and Health Technologies, Private Bag 10, Clayton South, Victoria, 3169, Australia. E-mail: chris.strauss@csiro.au; Fax: +61-3-9545-2446; Tel: +61-3-9545-2183

† Electronic supplementary information (ESI) available: NMR spectra for selected compounds **1a–d**. Crystal structure data for compounds **1n**, **1o**, **1p** (CCDC 605464–605466), **8a**, **8b** and **9** (CCDC 605784–605786). See DOI: 10.1039/b606042k



Scheme 2

is reported a simple synthesis of unsymmetrically substituted bis(arylidene)alkanones **1** by condensation of **3** (prepared in DIMCARB) with a range of aryl aldehydes. Analytically pure products are provided directly in good to excellent yields, and DIMCARB may be readily recovered and recycled in a process analogous to distillation.¹⁸ Examination of reaction by-products obtained under certain conditions sheds light on the mechanism of action of DIMCARB.

Results and discussion

Pure samples of α,β -unsaturated ketones **3a–d** (Scheme 4) were prepared by DIMCARB-mediated reactions of *p*-anisaldehyde or *p*-diethylaminobenzaldehyde with cyclohexanone, cyclopentanone or acetone as previously described.¹⁶ These were, in turn, reacted with a second arylaldehyde in a classical Claisen-Schmidt type reaction to provide analytically pure **1a–w** directly in good to excellent yields (see Table 1). Claisen-Schmidt condensation is particularly favoured as it is predictable, generally proceeds to completion at ambient temperature, is simple to execute and yields only water as a

by-product. Thus the overall reaction is atom economical, energy efficient and low in hazard, with little attendant waste.

To develop convenient means for condensation and product isolation, Amberlite[®] IRA-400(OH) resin and (*n*-Bu)₄NOH (as well as more common NaOH and KOH) were explored as catalytic bases. Use of the resin allows for separation of soluble products by filtration and the converse applies with the soluble base and poorly soluble **1**. The latter approach proved to be more effective for recovering pure products directly as crystallisation of poorly soluble **1** (compared with **2**) from solution is a purification step. Occasionally, the use of less than stoichiometric quantities of base at room temperature afforded minor amounts of aldol adducts among products **1**. Microwave heating was useful in shortening reaction times and lowered the requirements of base to catalytic quantities.¹⁹ A diverse range of non-enolisable, mostly aromatic aldehydes were condensed with **3** in this manner, yielding arylidenes containing carbocycles, furfural and pyridyl groups. Cinnamaldehydes were similarly employed to afford 2-arylidene-5-(3-phenylallylidene)cyclopentanones.

Previously, in the DIMCARB-mediated reaction of aldehyde and ketone to yield **3**, the intervention of an enamine, formed by reaction of the ketone with *N,N*-dimethylamine, was postulated, but not demonstrated.¹⁶ Here also, no enamine formation was detected spectroscopically. Nonetheless, in some cases the formation of by-products indicated that enamines were involved. In the reaction between benzaldehyde

Table 1 Summary of reaction conditions and isolated yields of unsymmetrical bis(arylidene)alkanones **1**, Scheme 4

Ketone	Aldehyde		Catalyst	Mol. eq. cat.	<i>T</i> / ^o C	<i>t</i> /h	Product	Yield (%)
	R ₃	R ₄						
3a	H	H	NaOH	1.0	22	3	1a	82
3a	furfural	H	(<i>n</i> -Bu) ₄ NOH	0.1	78 ^a	25 min	1a	87
			NaOH	1.0	22	2	1b	90
3a	1-naphthaldehyde	H	Amberlite	1.7	78	1	1b	92
			(<i>n</i> -Bu) ₄ NOH	0.1	78 ^a	10 min	1b	92
3a	3-NO ₂	H	NaOH	1.0	22	2	1c	87
			NaOH	0.2	78 ^a	30 min	1c	80
3a	4-Br	H	NaOH	1.0	22	6	1d	91
			(<i>n</i> -Bu) ₄ NOH	0.1	78 ^a	10 min	1d	91
3a	4-Br	H	NaOH	1.0	22	4	1e	88
			(<i>n</i> -Bu) ₄ NOH	0.1	78 ^a	10 min	1e	88
3a	pyridine-3-carbaldehyde	H	NaOH	1.0	22	2	1f	77
			(<i>n</i> -Bu) ₄ NOH	0.2	22	30 min	1f	82
3a	2-MeO	5-Br	NaOH	1.0	22	24	1g	81
			(<i>n</i> -Bu) ₄ NOH	0.2	22 (78) ^b	30 (+10) min ^b	1g	90
3a	2-MeO	H	NaOH	1.0	22	3	1h	86
			(<i>n</i> -Bu) ₄ NOH	0.1	78 ^a	10 min	1h	80
3a	3-MeO	4-MeO	Amberlite	1.14	78	3	1i	97
3a	4-Me	H	Amberlite	0.7	78	3	1j	97
3a	cinnamaldehyde	H	Amberlite	0.6	78	1.5	1k	73
3a	2-nitrocinnamaldehyde	H	(<i>n</i> -Bu) ₄ NOH	1.0	22	3	1l	74
3b	4-Br	H	(<i>n</i> -Bu) ₄ NOH	0.16	22	13	1m	87
3b	3-MeO	4-EtO	(<i>n</i> -Bu) ₄ NOH	0.16	22	10	1n	78
3b	4-NO ₂	H	(<i>n</i> -Bu) ₄ NOH	0.16	22	10 min	1o	97
3b	6-bromopyridine-2-carbaldehyde	H	(<i>n</i> -Bu) ₄ NOH	0.16	22	1	1p	78
3b	3-NO ₂	H	(<i>n</i> -Bu) ₄ NOH	0.16	22	15	1q	85
3b	furfural	H	(<i>n</i> -Bu) ₄ NOH	0.16	22	10 min	1r	76
3b	pyridine-3-carbaldehyde	H	(<i>n</i> -Bu) ₄ NOH	0.16	22	10 min	1s	79
3c	4-NO ₂	H	NaOH	0.2	22 (78) ^b	1 (+10) min ^b	1t	90
3c	furfural	H	NaOH	0.2	22 (78) ^b	1.25 (+10) min ^b	1u	92
3d	4-Br	H	KOH	0.2	22 (78) ^b	10 (+10) min ^b	1v	83
3d	4-NO ₂	H	KOH	0.2	22 (78) ^b	10 (+10) min ^b	1w	75

^a microwave heating ^b +10 min at reflux.

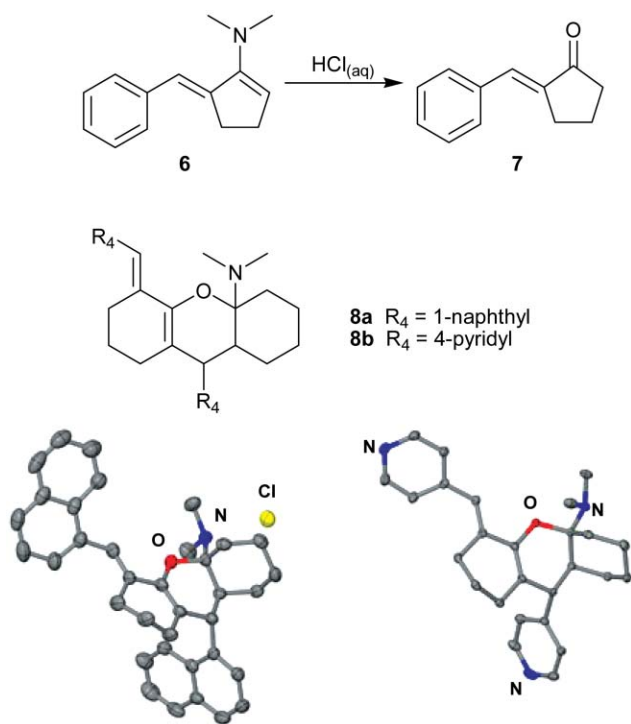
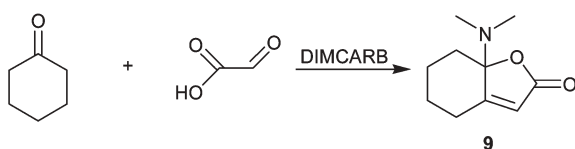


Fig. 1 Molecular diagrams from single crystal structures of **8a** (as the HCl salt) (top) and **8b**. Ellipsoids are at the 50% probability level and data were collected at 293 K and 123 K for **8a**·HCl and **8b** respectively.



Scheme 3

and cyclopentanone in DIMCARB–diethyl ether (1 : 1), 5-benzylidene-1-(*N,N*-dimethylamino)cyclopent-1-ene **6** was detected. This product could be hydrolysed to the α,β -unsaturated ketone **7** by treatment with dilute aqueous acid (the method of choice for clean workup of reaction mixtures from DIMCARB). Conversely, treatment of **7** with DIMCARB did not yield appreciable quantities of **6**, indicating participation of the enamine of cyclopentanone in the reaction rather than through attack on **7**.

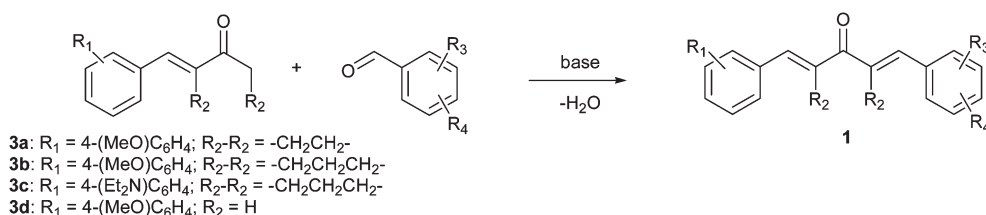
Myers *et al.* have previously discussed the importance of the rate of hydrolysis of analogues of **7** in controlling further reaction.²⁰ In two instances here, products analogous to these xanthenyl derivatives were isolated as the major components

of DIMCARB-mediated reactions. They involved 1-naphthaldehyde and cyclohexanone to afford **8a**, and isonicotinaldehyde and cyclohexanone to give **8b**. Single crystal structures of these products were obtained (see Fig. 1). Further evidence for the presence of enamine intermediates formed between the ketone and dimethylamine was obtained through the isolation of the stable lactone **9** in the DIMCARB mediated reaction of cyclohexanone and glyoxylic acid, Scheme 3 (again verified by single crystal structure analysis).

The work described above established a convenient, direct and high-yielding method to unsymmetrically substituted bis(arylidene)alkanes in two steps. Attention was next directed toward obtaining the products in one pot, without isolation of crude intermediates **3**. Three different approaches were pursued. *p*-Anisaldehyde and cyclopentanone were allowed to react in DIMCARB at ambient temperature for 4.75 h in each case, this was followed by the introduction of *m*-nitrobenzaldehyde under the conditions outlined below. In the first case, the second aldehyde was added in DIMCARB and the temperature elevated to 50 °C and held for 12 h. This process afforded a crude mixture of **1d**, accompanied by symmetrical **1** [($R_1 = R_3 = p\text{-MeO}$) and ($R_1 = R_3 = m\text{-NO}_2$)]. Recrystallisation from toluene afforded the desired pure product **1d** in 61% yield. In the second case, in a procedure that was repeated once, EtOH was added to the crude reaction mixture, which was heated to 60 °C *in vacuo*. These manipulations concentrated the crude intermediate **3a** in EtOH and were followed by addition of NaOH and *m*-nitrobenzaldehyde. During the course of reaction at room temperature for 3 h, the crude product **1d** (in greater than 90% purity) crystallised out and was purified by recrystallisation to afford an 80% yield. In the final variant, the DIMCARB was removed by heating *in vacuo* at 60 °C, before the addition of EtOH, NaOH and *m*-nitrobenzaldehyde. The outcome was comparable with that of the second procedure outlined immediately above. These experiments confirmed that the sequential process could be conducted in one pot and in good yields, but necessitated recrystallisation of the product **1**.

Conclusions

A direct, two-step route to unsymmetrically substituted bis(arylidene)alkanes by DIMCARB-mediated condensation of aldehyde and ketone to form a mono(arylidene)alkane (by *in situ* formation and reaction of an enamine) followed by a Claisen-Schmidt condensation is reported. Thus, eighteen new products were prepared using three simple symmetrical ketones, illustrating the scope of this procedure. Pure crystalline products were isolated directly



Scheme 4

from the reaction mixture. An example of the two step process was conducted successfully in one pot, by three different methods.

Experimental

Most reagents were used as obtained from suppliers (97% purity or better). Benzaldehyde, cinnamaldehyde and *p*-tolualdehyde were dissolved in ether, washed with aqueous NaOH solution to remove any carboxylic acid formed during storage, dried with MgSO₄, filtered and distilled at reduced pressure.

Elemental analyses were performed by Chemical & Micro Analytical Services Pty. Ltd., Victoria, Australia or by the University of Otago, Dunedin, New Zealand. ¹H and ¹³C NMR spectra were recorded on a Bruker AC-200 spectrometer, DPX-300 spectrometer or Bruker Avance DRX 400 spectrometer in CDCl₃ using TMS as the internal standard. Infrared (IR) spectra were recorded on a Perkin-Elmer 1600 Series Fourier Transform spectrophotometer (cm⁻¹ scale) and refer to KBr pellets (KBr) or nujol mulls (nujol). High-resolution mass spectra (HRMS) were recorded on a Bruker BioApex 47e FTMS fitted with an Analytical electrospray source, using NaI for accurate mass calibration (accuracy ± 3 ppm). Low-resolution mass spectra were recorded on a Micromass Platform II (now Waters) QMS quadrupole fitted with Waters Alliance autosampler. Melting points were recorded on a Stuart Scientific melting point apparatus, SMP3. UV-vis spectra were recorded using a Varian Cary 100 UV-visible spectrophotometer as solutions in ethanol (96%). Microwave heating was performed in a Milestone HPR3600 reactor equipped with a thermocouple.

Crystals suitable for single crystal X-ray diffraction experiments were grown by slow evaporation of solutions in suitable solvents (usually hexane or hexane/MeOH) and data were collected on an Enraf-Nonius Kappa CCD or Bruker Kappa Apex CCD diffractometer at 123 K (or 293 K for **8a**) using graphite monochromated Mo-Kα radiation (λ = 0.71073 Å, φ and ω scans in 1° or 0.5° steps as appropriate). Structures were solved by direct methods using the program SHELXS-97²¹ and refined by full matrix least squares refinement on *F*² using the programs SHELXL-97²² and XSeed.²³ Non-hydrogen atoms were refined anisotropically and hydrogen atoms inserted in geometrically determined positions with temperature factors fixed at 1.2 that of the parent atom.

Synthesis of **3b** and **3c**

3b; 1-(4-Methoxybenzylidene)acetone. *p*-Anisaldehyde (1.36 g, 10 mmol) and acetone (0.70 g, 12.0 mmol) were added to DIMCARB (5 mL) at ambient temperature with stirring. After reaction at room temperature (22 °C) for 22 h, the solvent was removed *in vacuo* providing an oil, which yielded, post flash chromatography on silica with Et₂O/hexane (70 : 30) eluent, 1-(4-methoxybenzylidene)acetone (1.20 g, 70%) as a yellow solid; mp 70.7–73.6 °C (lit.²⁴ mp 72–72.5 °C). δ_H(300 MHz, CDCl₃, Me₄Si) 2.36 (3H, s, Me), 3.85 (3H, s, OMe), 6.60 (1H, d, *J* 16.2, CH=C), 6.92 (2H, d, *J* 8.9, Ar), 7.48 (1H, d, *J* 16.5, CH=C), 7.50 (2H, d, *J* 8.5, Ar).

3c; 2-(4-Diethylaminobenzylidene)cyclohexanone. 4-Diethylaminobenzaldehyde (1.77 g, 10.0 mmol) and cyclohexanone (0.98 g, 10.0 mmol) were added to DIMCARB (5 mL) at ambient temperature with stirring. No gas was evolved. After reaction at room temperature (22 °C) for 22 h, the solvent was removed *in vacuo* providing a dark orange oil, which yielded, post flash chromatography on silica with hexane eluent, 2-(4-diethylaminobenzylidene)cyclohexanone (1.74 g, 68%) as a yellow solid; mp 89.0–90.5 °C (Found: C, 79.50; H, 8.99; N, 5.44. C₁₇H₂₃NO requires C, 79.33; H, 9.01; N, 5.44%); λ_{max}(EtOH)/nm 389, 259 (ε/dm³ mol⁻¹ cm⁻¹ 13262, 7347); ν_{max}(KBr)/cm⁻¹ 2967 w, 2937 w, 2902 w, 2806 w, 1662 m, 1612 m, 1570 s, 1556 s, 1518 s, 1410 m, 1312 m, 1275 m, 1192 s, 1143 m, 1068 w; δ_H(200 MHz, CDCl₃, Me₄Si) 1.19 (6H, t, *J* 7.1, CH₃), 1.72–1.96 (4H, m, CH₂CH₂CH₂CH₂), 2.50 (2H, t, *J* 6.6, C=OCH₂), 2.87 (2H, td, *J* 6.3, 1.7, C=CCH₂), 3.39 (4H, q, *J* 7.1, NCH₂), 6.65 (2H, d, *J* 9.0, Ar), 7.39 (2H, d, *J* 8.9, Ar), 7.53 (1H, t, *J* 1.9, CH=C); δ_C(50 MHz, CDCl₃, Me₄Si) 12.8 (2C), 23.5, 24.1, 29.3, 40.2, 44.6 (2C), 111.2 (2C), 122.9, 131.3, 133.2 (2C), 137.6, 148.3, 201.3; *m/z* (ESI) 258.2 ([M + H]⁺ C₁₇H₂₄NO⁺ requires 258.2).

Representative procedure for NaOH method at 22 °C

1t; 2-(4-Diethylaminobenzylidene)-6-(4-nitrobenzylidene)cyclohexanone. To a solution of 2-(4-diethylaminobenzylidene)cyclohexanone (0.321 g, 1.25 mmol) and 4-nitrobenzaldehyde (0.189 g, 1.25 mmol) in 7.5 mL ethanol (96%) was added 2.5% (w/v) aqueous NaOH solution (0.400 mL, 0.25 mmol). The mixture was stirred at room temperature for 1 h, during which time a precipitate formed. If required, the reaction mixture was heated to reflux for 10 min, cooled and the crystalline product recovered by filtration, yielding 2-(4-diethylaminobenzylidene)-6-(4-nitrobenzaldehyde)cyclohexanone (0.424 g, 90%) as a deep red solid, mp 184.0–186.5 °C (Found: C, 73.73; H, 6.77; N, 7.05. C₂₄H₂₆N₂O₃ requires C, 73.82; H, 6.71; N, 7.17%); λ_{max}(EtOH)/nm 219, 323, 460 (ε/dm³ mol⁻¹ cm⁻¹ 15521, 19914, 23526); ν_{max}(KBr)/cm⁻¹ 2974 w, 2927 w, 2862 w, 1654 m, 1601 m, 1589 m, 1546 m, 1520 s, 1509 s, 1340 s, 1275 m, 1197 w, 1167 m, 1154 s, 1133 m, 1078 w, 1012 w, 966 w; δ_H(200 MHz, CDCl₃, Me₄Si) 1.20 (6H, t, *J* 7.1, CH₂CH₃), 1.83 (2H, app p, *J* 6.2, CH₂CH₂CH₂), 2.87 (2H, t, *J* 5.8, CH₂CH₂CH₂), 2.97 (2H, t, *J* 6.0, CH₂CH₂CH₂), 3.41 (4H, q, *J* 7.1, NCH₂), 6.68 (2H, d, *J* 8.8, Ar), 7.45 (2H, d, *J* 8.7, Ar), 7.56 (2H, d, *J* 8.9, Ar), 7.76 (1H, s, CH=C), 7.80 (1H, s, CH=C), 8.29 (2H, d, *J* 8.8, Ar); δ_C(50 MHz, CDCl₃, Me₄Si) 12.8 (2C), 23.1, 28.6, 29.0, 44.7 (2C), 111.3 (2C), 123.0, 123.8 (2C), 130.6, 130.8 (2C), 132.7, 133.6 (2C), 140.0, 140.2, 143.3, 147.2, 148.7, 189.4; *m/z* (ESI) 391.2 ([M + H]⁺ C₂₄H₂₇N₂O₃⁺ requires 391.2).

Representative procedure for Amberlite resin method

1i; 2-(3,4-Dimethoxybenzylidene)-5-(4-methoxybenzylidene)cyclopentanone. To a solution of 2-(4-methoxybenzylidene)cyclopentanone (0.505 g, 2.50 mmol) and 3,4-dimethoxybenzaldehyde (0.415 g, 2.50 mmol) in 20 mL absolute ethanol was added Amberlite-400(OH) resin (1.0 g, 2.85 mmol). The mixture was stirred and refluxed for 3 h. During this period a yellow precipitate formed and post cooling the product and resin were collected by filtration.

Product was recovered from the Amberlite resin by dissolution in hot toluene and solvent was removed *in vacuo* to afford pure 2-(3,4-dimethoxybenzylidene)-5-(4-methoxybenzylidene)cyclopentanone (0.85 g, 97%) as a yellow solid, mp 180–182 °C (lit.²⁵ mp 182–183 °C) (Found: C, 75.30; H, 6.30. C₂₂H₂₂O₄ requires C, 75.41; H, 6.33%); $\lambda_{\max}(\text{EtOH})/\text{nm}$ 245, 397 ($\epsilon/\text{dm}^3 \text{ mol}^{-1} \text{ cm}^{-1}$ 8661, 18197); $\nu_{\max}(\text{KBr})/\text{cm}^{-1}$ 2913 w, 1686 w, 1619 m, 1600 s, 1560 m, 1509 s, 1421 w, 1310 w, 1256 s, 1171 s, 1117 s, 1032 w, 985 w, 816 w; $\delta_{\text{H}}(300 \text{ MHz}, \text{CDCl}_3, \text{Me}_4\text{Si})$ 3.10 (4H, m, CH₂CH₂), 3.86 (3H, s, OMe), 3.93 (6H, m, OMe), 6.94 (2H, d, *J* 8.3, Ar), 6.98 (1H, s, Ar), 7.13 (1H, d, *J* 2.0, Ar), 7.23 (1H, d, *J* 8.4, Ar), 7.54–7.58 (4H, m, CH=C, Ar); $\delta_{\text{C}}(75 \text{ MHz}, \text{CDCl}_3, \text{Me}_4\text{Si})$ 26.7 (2 ×), 55.6, 56.2, 56.2, 111.5, 113.8, 114.6 (2C), 124.7, 129.0, 129.3, 132.7 (2C), 133.5, 133.8, 135.4, 135.8, 149.2, 150.3, 160.6; 196.1; *m/z* (ESI) 351.4 ([M + H]⁺ C₂₂H₂₃O₄⁺ requires 351.2).

Representative procedure for (n-Bu)₄NOH at 22 °C

1f; 2-(4-Methoxybenzylidene)-5-(pyridin-3-ylmethylidene)cyclopentanone. To a solution of 2-(4-methoxybenzylidene)cyclopentanone (0.253 g, 1.25 mmol) and 3-pyridylcarboxaldehyde (0.134 g, 1.25 mmol) in 10.0 mL ethanol (96%) was added 20% (w/v) (n-Bu)₄NOH in water (0.162 mL, 0.125 mmol). The mixture was stirred at room temperature (22 °C) for 30 min, during which time a precipitate formed.

Filtration of the precipitate afforded pure (*E,E*)-2-(4-methoxybenzylidene)-5-(pyridin-3-ylmethylidene)cyclopentanone (0.424 g, 90%) as a yellow solid; mp 162.0–163.5 °C (Found: C, 78.40; H, 5.91; N, 4.84. C₁₉H₁₇NO₂ requires C, 78.33; H, 5.88; N, 4.81%); $\lambda_{\max}(\text{EtOH})/\text{nm}$ 235, 380 ($\epsilon/\text{dm}^3 \text{ mol}^{-1} \text{ cm}^{-1}$ 15746, 30442); $\nu_{\max}(\text{KBr})/\text{cm}^{-1}$ 3054 w, 3023 w, 2970 w, 2840 w, 1684 s, 1628 m, 1610 s, 1591 s, 1566 s, 1560 s, 1546 w, 1512 s, 1466 w, 1418 m, 1313 w, 1418 m, 1313 w, 1265 s, 1202 s, 1182 s, 1116 w, 1027 m; $\delta_{\text{H}}(400 \text{ MHz}, \text{CDCl}_3, \text{Me}_4\text{Si})$ 3.09 (4H, s, CH₂CH₂), 3.85 (3H, s, OMe), 6.96 (2H, d, *J* 8.8, Ar), 7.35 (1H, ddd, *J* 7.9, 4.8, 0.4, Ar), 7.50 (1H, s, CH=C), 7.56 (2H, d, *J* 8.8, Ar), 7.58 (1H, s, CH=C), 7.85 (1H, td, *J* 8.0, 1.8, Ar), 8.57 (1H, dd, *J* 4.8, 1.6, Ar), 8.83 (1H, d, *J* 2.0, Ar); $\delta_{\text{C}}(100 \text{ MHz}, \text{CDCl}_3, \text{Me}_4\text{Si})$ 26.6, 26.7, 55.6, 114.6 (2C), 123.7, 128.6, 129.4, 132.0, 132.9 (2C), 134.5, 134.8, 137.0, 140.0, 149.7, 151.8, 161.1, 195.8; *m/z* (ESI) 292.2 ([M + H]⁺ C₁₉H₁₈NO₂⁺ requires 292.1).

Representative procedure for reaction under MW heating

1d; 2-(4-Methoxybenzylidene)-5-(3-nitrobenzylidene)cyclopentanone. To a solution of 2-(4-methoxybenzylidene)cyclopentanone (0.253 g, 1.25 mmol) and 3-nitrobenzaldehyde (0.189 g, 1.25 mmol) in 10 mL ethanol (96%) was added 20% (w/v) (n-Bu)₄NOH in water (0.162 mL, 0.125 mmol). The mixture was heated steadily for 3 min from 22 to 78 °C, using MW energy, and maintained at 78 °C for 10 min. Upon cooling, a precipitate formed, which was recovered by filtration to afford pure 2-(4-methoxybenzylidene)-5-(3-nitrobenzylidene)cyclopentanone (0.382 g, 91%) as a yellow solid, mp 215.5–216.5 °C (Found: C, 71.37; H, 5.00; N, 4.17. C₂₀H₁₇NO₄ requires C, 71.63; H, 5.11; 4.18%); $\lambda_{\max}(\text{EtOH})/\text{nm}$ 380 ($\epsilon/\text{dm}^3 \text{ mol}^{-1} \text{ cm}^{-1}$ 28840); $\nu_{\max}(\text{nujol})/\text{cm}^{-1}$ 1672 w, 1589 s, 1517 s, 1344 m, 1244 s, 1178 s, 1028 w; $\delta_{\text{H}}(200 \text{ MHz},$

CDCl₃, Me₄Si) 3.15 (4H, m, CH₂CH₂), 3.87 (3H, s, OMe), 6.98 (2H, d, *J* 8.8, Ar), 7.57–7.63 (5H, m, CH=C, Ar), 7.86 (1H, d, *J* 7.8, CH=C), 8.21 (1H, dd, *J* 8.04, 1.23, Ar), 8.45 (1H, s, Ar); $\delta_{\text{C}}(50 \text{ MHz}, \text{CDCl}_3, \text{Me}_4\text{Si})$ 26.6, 26.7, 55.6, 114.7 (2C), 123.7, 124.5, 128.5, 130.0, 130.3, 133.1 (2C), 134.4, 135.3, 136.6, 137.8, 140.7, 148.7, 161.2, 195.9; *m/z* (ESI) 336.1240 ([M + H]⁺ C₂₀H₁₈NO₄⁺ requires 336.1236).

Characterisation of compounds 1a–c, 1e, 1g–h, 1j–s & 1u–w.

1a; 2-(4-Methoxybenzylidene)-5-benzylidenecyclopentanone. Yellow solid (0.440 g, 87%); mp 170–171 °C (lit.²⁵ 171–172 °C) (Found: C, 82.49; H, 6.37. C₂₀H₁₈O₂ requires C, 82.73; H, 6.25%); $\lambda_{\max}(\text{EtOH})/\text{nm}$ 377 ($\epsilon/\text{dm}^3 \text{ mol}^{-1} \text{ cm}^{-1}$ 24498); $\nu_{\max}(\text{nujol})/\text{cm}^{-1}$ 1689 w, 1626 w, 1589 s, 1510 m, 1377 s, 1317 w, 1256 m, 1172 m, 1127 w, 1035 w; $\delta_{\text{H}}(200 \text{ MHz}, \text{CDCl}_3, \text{Me}_4\text{Si})$ 3.08 (4H, m, CH₂CH₂), 3.85 (3H, s, OMe), 6.95 (2H, d, *J* 8.8, Ar), 7.35–7.47 (3H, m, Ar), 7.53–7.58 (6H, m, CH=C, Ar). $\delta_{\text{C}}(50 \text{ MHz}, \text{CDCl}_3, \text{Me}_4\text{Si})$ 26.7 (2 ×), 55.6, 114.5 (2C), 128.9, 128.9 (2C), 129.4, 130.9 (2C), 132.8 (2C), 133.5, 134.0, 135.2, 136.2, 137.9, 160.9, 196.5; *m/z* (ESI) 291.1385 ([M + H]⁺ C₂₀H₁₉O₂⁺ requires 291.1380).

1b; 2-Furfurylidene-5-(4-methoxybenzylidene)cyclopentanone. Yellow solid (0.322 g, 92%); mp 181–183 °C (lit.²⁵ mp 178–179 °C) (Found: C, 77.23; H, 5.61. C₁₈H₁₆O₃ requires C, 77.12; H, 5.75%); $\lambda_{\max}(\text{EtOH})/\text{nm}$ 397 ($\epsilon/\text{dm}^3 \text{ mol}^{-1} \text{ cm}^{-1}$ 14875); $\nu_{\max}(\text{KBr})/\text{cm}^{-1}$ 1681 w, 1623 s, 1606 s, 1588 s, 1568 m, 1512 m, 1474 w, 1425 w, 1252 s, 1180 m, 1024 w; $\delta_{\text{H}}(200 \text{ MHz}, \text{CDCl}_3, \text{Me}_4\text{Si})$ 3.05–3.15 (4H, m, CH₂CH₂), 3.83 (3H, s, OMe), 6.52 (1H, t, *J* 3.4, Ar), 6.66 (1H, d, *J* 3.4, Ar), 6.94 (2H, dd, *J* 6.8, 1.9, Ar), 7.36–7.40 (1H, m, CH=C), 7.52–7.60 (4H, m, CH=C, Ar); $\delta_{\text{C}}(50 \text{ MHz}, \text{CDCl}_3, \text{Me}_4\text{Si})$ 26.1 (2 ×), 55.3, 112.5, 114.3 (2C), 115.7, 119.7, 128.7, 132.5 (2C), 133.4, 135.4, 135.6, 144.8, 152.8, 160.6, 195.6; *m/z* (ESI) 281.1168 ([M + H]⁺ C₁₈H₁₇O₃⁺ requires 281.1172).

1c; 2-(4-Methoxybenzylidene)-5-(naphth-1-ylmethylidene)cyclopentanone. Yellow solid (0.340 g, 80%); mp 157.5–159 °C (Found: C, 84.85; H, 5.84. C₂₄H₂₀O₂ requires C, 84.68; H, 5.92%); $\lambda_{\max}(\text{EtOH})/\text{nm}$ 378 ($\epsilon/\text{dm}^3 \text{ mol}^{-1} \text{ cm}^{-1}$ 17689); $\nu_{\max}(\text{KBr})/\text{cm}^{-1}$ 1680 m, 1610 s, 1587 s, 1513 s, 1309 w, 1258 s, 1198 m, 1170 s, 1035 m; $\delta_{\text{H}}(200 \text{ MHz}, \text{CDCl}_3, \text{Me}_4\text{Si})$ 3.06 (4H, s, CH₂CH₂), 3.86 (3H, s, OMe), 6.97 (2H, d, *J* 8.8, Ar), 7.49–7.55 (5H, m, Ar), 7.63 (1H, s, Ar), 7.67 (1H, d, *J* 7.1, Ar), 7.68–7.89 (2H, m, Ar), 8.05 (1H, d, *J* 8.0, Ar), 8.31 (1H, s, CH=C); $\delta_{\text{C}}(50 \text{ MHz}, \text{CDCl}_3, \text{Me}_4\text{Si})$ 26.8, 26.9, 55.6, 114.5 (2C), 124.3, 125.3, 126.4, 126.9, 127.3, 128.8, 128.9, 129.8, 129.9, 132.5, 132.8 (2C), 132.8, 133.8, 134.2, 135.4, 140.1, 160.9, 196.2; *m/z* (ESI) 341.1526 ([M + H]⁺ C₂₄H₂₁O₂⁺ requires 341.1536).

1e; 2-(4-Bromobenzylidene)-5-(4-methoxybenzylidene)cyclopentanone. Green/yellow solid (0.407 g, 88%); mp 235.5–236.5 °C (Found: C, 65.14; H, 4.68. C₂₀H₁₇BrO₂ requires C, 65.05; H, 4.64%); $\lambda_{\max}(\text{EtOH})/\text{nm}$ 240, 380 ($\epsilon/\text{dm}^3 \text{ mol}^{-1} \text{ cm}^{-1}$ 12185, 20235); $\nu_{\max}(\text{KBr})/\text{cm}^{-1}$ 1696 m, 1594 s, 1510 s, 1486 m, 1460 w, 1401 w, 1308 w, 1257 s, 1172 s; $\delta_{\text{H}}(200 \text{ MHz}, \text{CDCl}_3, \text{Me}_4\text{Si})$ 3.07 (4H, m, CH₂CH₂), 3.85 (3H, s, OMe), 6.96 (2H, d,

J 8.9, Ar), 7.44 (2H, d, *J* 8.5, Ar), 7.48 (1H, s, CH=C), 7.53–7.58 (5H, m, 4 × Ar, 1 × CH=C); δ_{C} (75 MHz, CDCl₃, Me₄Si) 26.7 (2 ×), 55.6, 114.6 (2C), 123.7, 128.8, 132.1, 132.2 (2C), 132.2 (2C), 132.9 (2C), 134.4, 134.9, 135.1, 138.6, 161.0, 196.2; *m/z* (ESI) 369.0492 ([M + H]⁺ + C₂₀H₁₈⁷⁹BrO₂⁺ requires 369.0485) and 371.0470 ([M + H]⁺ + C₂₀H₁₈⁸¹BrO₂⁺ requires 371.0464).

1g; 2-(5-Bromo-2-methoxybenzylidene)-5-(4-methoxybenzylidene)cyclopentanone. Yellow solid (0.451 g, 90%); mp 200–202 °C (Found: C, 63.47; H, 4.71. C₂₁H₁₉BrO₃ requires C, 63.17; H, 4.80%); λ_{max} (EtOH)/nm 386 ($\epsilon/\text{dm}^3 \text{ mol}^{-1} \text{ cm}^{-1}$ 47337); ν_{max} (KBr)/cm⁻¹ 1697 m, 1612 s, 1595 s, 1510 m, 1258 s, 1173 s, 1119 w, 1076 m; δ_{H} (200 MHz, CDCl₃, Me₄Si) 3.02 (4H, m, CH₂CH₂), 3.84 (3H, s, OMe); 3.85 (3H, s, OMe), 6.79 (1H, d, *J* 8.8, Ar), 6.95 (2H, d, *J* 8.8, Ar), 7.40 (1H, dd, *J* 8.8, 2.4, Ar), 7.52–7.60 (4H, m, CH=C, Ar), 7.84 (1H, s, CH=C); δ_{C} (50 MHz, CDCl₃, Me₄Si) 26.4, 26.6, 55.4, 55.9, 112.6, 112.7, 114.4 (2C), 126.2, 127.2, 128.7, 132.1, 132.6 (2C), 132.9, 133.9, 135.0, 138.8, 158.0, 160.7, 195.9; *m/z* (ESI) 399.0603 ([M + H]⁺ + C₂₀H₂₀⁷⁹BrO₃⁺ requires 399.0590) and 401.0571 ([M + H]⁺ + C₂₀H₂₀⁸¹BrO₃⁺ requires 401.0570).

1h; 2-(2-Methoxybenzylidene)-5-(4-methoxybenzylidene)cyclopentanone. Yellow solid (0.322 g, 80%); mp 147–148 °C (Found: C, 78.59, H, 6.11. C₂₁H₂₀O₃ requires C, 78.73; H, 6.29%); λ_{max} (EtOH)/nm 383 ($\epsilon/\text{dm}^3 \text{ mol}^{-1} \text{ cm}^{-1}$ 23776); ν_{max} (nujol)/cm⁻¹ 1698 m, 1626 s, 1595 s, 1569 m, 1511 s, 1485 m, 1422 m, 1305 w, 1246 s, 1204 w, 1174 s, 1163 s, 1121 w, 1032 w; δ_{H} (300 MHz, CDCl₃, Me₄Si) 3.05 (4H, m, CH₂CH₂), 3.86 (3H, s, OMe), 3.89 (3H, s, OMe), 6.92–7.02 (4H, m, Ar), 7.32–7.37 (1H, m, Ar), 7.53–7.58 (4H, m, CH=C, Ar), 7.99 (1H, s, CH=C); δ_{C} (50 MHz, CDCl₃, Me₄Si) 26.8, 26.9, 55.6, 55.7, 105.2, 111.0 (2C), 114.5, 120.5, 125.2, 128.1, 129.0, 130.9, 132.7 (2C), 133.6, 135.5, 137.8, 159.1, 160.7, 196.5; *m/z* (ESI) 321.1477 ([M + H]⁺ + C₂₁H₂₁O₃⁺ requires 321.1485).

1j; 2-(4-Methoxybenzylidene)-5-(4-methylbenzylidene)cyclopentanone. Yellow solid (0.740 g, 97%); mp 196–197 °C (lit.²⁵ 197–198 °C) (Found: C, 82.66; H, 6.62. C₂₁H₂₀O₂ requires C, 82.86; H, 6.62%); λ_{max} (EtOH)/nm 239, 379 ($\epsilon/\text{dm}^3 \text{ mol}^{-1} \text{ cm}^{-1}$ 19088, 34877); ν_{max} (KBr)/cm⁻¹ 2913 w, 1686 w, 1619 m, 1600 s, 1560 m, 1509 s, 1421 w, 1310 w, 1256 s, 1171 s, 1117 w, 1032 w, 985 w, 816 w; δ_{H} (400 MHz, CDCl₃, Me₄Si) 2.39 (3H, s, ArMe), 3.08 (4H, m, CH₂CH₂), 3.85 (3H, s, OMe), 6.96 (2H, d, *J* 8.5, Ar), 7.24 (2H, d, *J* 8.5, Ar), 7.50 (2H, d, *J* 8.1, Ar), 7.56 (2H, d, *J* 8.5, Ar), 7.55–7.57 (2H, m, CH=C); δ_{C} (100 MHz, CDCl₃, Me₄Si) 21.7, 26.7, 26.8, 55.6, 114.6 (2C), 129.7 (2C), 131.0 (2C), 132.8 (2C), 133.6, 133.8, 129.1, 133.5, 135.4, 136.9, 139.9, 160.8, 196.5; *m/z* (ESI) 305.3 ([M + H]⁺ + C₂₁H₂₁O₂⁺ requires 305.2).

1k; 2-(4-Methoxybenzylidene)-5-cinnamylidenecyclopentanone. Yellow solid (0.290 g, 73%); mp 179–180 °C (lit.²⁵ 180–181 °C) (Found: C, 83.49; H, 6.40. C₂₂H₂₀O₂ requires C, 83.52; H, 6.37%); ν_{max} (KBr)/cm⁻¹ 1682 m, 1628 m, 1598 s, 1509 m, 1442 w, 1304 w, 1281 m, 1034 m, 970 m, 828 m, 756 m, 696 w; δ_{H} (400 MHz, CDCl₃, Me₄Si) 2.89–2.94 (2H, m, CH₂CH₂),

3.00–3.05 (2H, m, CH₂CH₂), 3.84 (3H, s, OMe), 6.91–6.99 (4H, m, Ar, CH=C), 7.28–7.40 (4H, m, Ar, CH=C), 7.47–7.50 (3H, m, Ar), 7.53 (2H, d, *J* 8.8, Ar); δ_{C} (100 MHz, CDCl₃, Me₄Si) 24.5, 26.2, 55.5, 114.5 (2C), 125.0, 127.4 (2C), 128.9, 129.0 (2C), 129.1, 132.7 (2C), 132.9, 133.5, 136.5, 136.8, 139.0, 141.4, 160.8, 195.8; *m/z* (EI) 316 (M⁺, 100%), 239 (29), 207 (26), 165 (11), 141 (36), 115 (35), 103 (22), 91 (32), 77 (35), 55 (34).

1l; 2-(4-Methoxybenzylidene)-5-(2-nitrocinnamylidene)cyclopentanone. Yellow solid (0.335 g, 74%); mp 171–173 °C (Found: C, 73.20; H, 5.31; N, 3.74. C₂₂H₁₉NO₄ requires C, 73.12; H, 5.30; N, 3.88%); λ_{max} (EtOH)/nm 244, 396 ($\epsilon/\text{dm}^3 \text{ mol}^{-1} \text{ cm}^{-1}$ 18955, 39549); ν_{max} (KBr)/cm⁻¹ 2913 w, 1677 s, 1621 s, 1600 s, 1580 m, 1523 s, 1426 m, 1364 m, 1262 s, 1195 m, 1164 m, 1026 m; δ_{H} (300 MHz, CDCl₃, Me₄Si) 2.92–2.97 (2H, m, CH₂CH₂), 3.04–3.09 (2H, m, CH₂CH₂), 3.86 (3H, s, OMe), 6.96 (2H, d, *J* 8.9, Ar), 6.90–6.99 (1H, m, CH=CH), 7.30 (1H, dt, *J* 11.7, 2.4, CH=CH), 7.4–7.49 (2H, m, Ar, CH=C), 7.52–7.59 (2H, m, CH=C), 7.55 (2H, d, *J* 8.8, Ar), 7.61 (1H, td, *J* 7.7, 1.1, Ar), 7.73 (1H, dd, *J* 7.9, 1.4, Ar), 7.97 (1H, dd, *J* 8.2, 1.2, Ar); δ_{C} (75 MHz, CDCl₃, Me₄Si) 24.6, 26.3, 55.6, 114.6 (2C), 125.1, 128.6, 128.8, 129.2, 129.8, 131.6, 132.4, 132.9 (2C), 133.3, 134.2, 135.1, 136.0, 141.3, 148.2, 161.0, 195.6; *m/z* (EI) 361 (M⁺, 100%), 344 (68), 316 (18), 226 (22), 199 (43), 183 (36), 145 (34), 128 (33), 115 (62), 103 (48), 91 (27), 77 (50), 63 (17).

1m; 2-(4-Bromobenzylidene)-6-(4-methoxybenzylidene)cyclohexanone. Yellow solid (0.417 g, 87%); mp 154–158 °C (Found: C, 65.97; H, 5.11. C₂₁H₁₉BrO₂ requires C, 65.81; H, 5.00%); λ_{max} (EtOH)/nm 238, 347 ($\epsilon/\text{dm}^3 \text{ mol}^{-1} \text{ cm}^{-1}$ 20737, 18678); ν_{max} /cm⁻¹ 1658 w, 1600 s, 1599 m, 1560 m, 1509 m, 1399 m, 1312 m, 1253 s, 1162 s, 1141 s; δ_{H} (200 MHz, CDCl₃, Me₄Si) 1.74–1.86 (2H, m, CH₂CH₂CH₂), 2.83–2.97 (4H, m, CH₂CH₂CH₂), 3.85 (3H, s, OMe), 6.94 (2H, d, *J* 8.9, Ar), 7.31 (2H, d, *J* 8.5, Ar), 7.46 (2H, d, *J* 8.8, Ar), 7.53 (2H, d, *J* 8.6, Ar), 7.69 (1H, t, *J* 2.0, CH=C), 7.76 (1H, t, *J* 2.0, CH=C); δ_{C} (75 MHz, CDCl₃, Me₄Si) 23.2, 28.6, 28.8, 55.6, 114.2 (2C), 122.9, 128.8, 131.8 (2C), 132.0 (2C), 132.6 (2C), 134.2, 135.2, 135.3, 137.2, 137.6, 160.4, 190.2; *m/z* (ESI) 383.2 (100%) ([M + H]⁺ + C₂₁H₂₀⁷⁹BrO₂⁺ requires 383.1) and 385.2 (98) ([M + H]⁺ + C₂₁H₂₀⁸¹BrO₂⁺ requires 385.1).

1n; 2-(4-Ethoxy-3-methoxybenzylidene)-6-(4-methoxybenzylidene)cyclohexanone. Yellow solid (0.368 g, 78%); mp 131–133 °C (Found: C, 76.35; H, 7.01. C₂₄H₂₆O₄ requires C, 76.17; H, 6.92%); λ_{max} (EtOH)/nm 246, 368 ($\epsilon/\text{dm}^3 \text{ mol}^{-1} \text{ cm}^{-1}$ 23464, 35070); ν_{max} /cm⁻¹ 1660 w, 1597 m, 1510 m, 1256 s, 1159 m, 1136 m, 1027 m, 811 w; δ_{H} (200 MHz, CDCl₃, Me₄Si) 1.48 (3H, t, *J* 7.0, CH₂CH₃) 1.75–1.88 (2H, m, CH₂CH₂CH₂), 2.90–2.97 (4H, m, CH₂CH₂CH₂), 3.85 (3H, s, OMe), 3.90 (3H, s, OMe), 4.14 (2H, q, *J* 7.0, CH₂CH₃), 6.88–6.97 (3H, m, Ar), 7.02 (1H, d, *J* 1.9, 1H), 7.09 (1H, dd, *J* 8.3, 1.9, Ar), 7.45 (2H, d, *J* 8.8, Ar), 7.74–7.78 (2H, m, CH=C); δ_{C} (75 MHz, CDCl₃, Me₄Si) 15.0, 23.3, 28.7, 28.8, 55.6, 56.3, 64.6, 112.4, 114.2 (2C), 114.4, 124.2, 129.0, 129.2, 132.5 (2C), 134.6, 134.7, 136.8, 137.0, 149.2 (2 ×), 160.2, 190.4; *m/z* (ESI) 379.2 ([M + H]⁺ + C₂₄H₂₇O₄⁺ requires 379.2).

Crystal data for In. C₂₄H₂₆O₄, *M_r* = 378.45, triclinic, space group *P*1̄, *a* = 11.2190(3), *b* = 12.8515(3), *c* = 14.1651(4) Å, α = 82.272(1), β = 88.467(1), γ = 75.715(1)°, *V* = 1961.17(9) Å³, *Z* = 4 (2 molecules with distinctly different conformations in the ASU), *D_{calc}* = 1.282 g cm⁻³, μ (MoK α) = 0.086 mm⁻¹. Of 112188 reflections measured, 11417 were unique (*R_{int}* = 0.0381), with 8758 *I* > 2 σ (*I*), *R* indices [*I* > 2 σ (*I*)] *R*₁ = 0.0450, *wR*₂ = 0.1069, GoF on *F*² = 1.024 for 511 refined parameters and 0 restraints.

CCDC reference number 605464. For crystallographic data in CIF or other electronic format see DOI: 10.1039/b606042k

1o; 2-(4-Methoxybenzylidene)-6-(4-nitrobenzylidene)cyclohexanone. Yellow solid (0.425 g, 97%); mp 197–198 °C, (Found: C, 72.29; H, 5.58; N, 3.95. C₂₁H₁₉NO₄ requires C, 72.19; H, 5.48; N, 4.01%); λ_{\max} (EtOH)/nm 348 (ε/dm³ mol⁻¹ cm⁻¹ 19448); ν_{\max} /cm⁻¹ 1658 w, 1600 s, 1557 m, 1164 m, 1149 m, 1024 m; δ_{H} (300 MHz, CDCl₃, Me₄Si) 1.79–1.87 (2H, m, CH₂CH₂CH₂), 2.87–2.98 (4H, m, CH₂CH₂CH₂), 3.85 (3H, s, OMe), 6.95 (2H, d, *J* 8.9, Ar), 7.47 (2H, d, *J* 8.6, Ar), 7.57 (2H, d, *J* 8.4, Ar), 7.77 (1H, t, *J* 2.0, CH=C), 7.79 (1H, t, *J* 2.1, CH=C), 8.25 (2H, d, *J* 8.7, Ar); δ_{C} (100 MHz, CDCl₃, Me₄Si) 23.0, 28.6, 28.7, 55.6, 114.3 (2C), 123.8 (2C), 128.6, 130.9 (2C), 132.7 (2C), 133.6, 133.7, 138.4, 139.8, 143.0, 147.4, 160.6, 189.8; *m/z* (ESI) 350.2 ([M + H]⁺ C₂₁H₂₀NO₄⁺ requires 350.1).

Crystal data for 1o. C₂₁H₁₉NO₄, *M_r* = 349.37, triclinic, space group *P*1̄, *a* = 7.8646(3), *b* = 9.6830(3), *c* = 11.3746(5) Å, α = 95.587(1), β = 102.801(1), γ = 91.992(2)°, *V* = 839.25(6) Å³, *Z* = 2, *D_{calc}* = 1.383 g cm⁻³, μ (MoK α) = 0.096 mm⁻¹. Of 6955 reflections measured, 3102 were unique (*R_{int}* = 0.0390), with 2280 *I* > 2 σ (*I*), *R* indices [*I* > 2 σ (*I*)] *R*₁ = 0.0400, *wR*₂ = 0.0904, GoF on *F*² = 1.044 for 236 refined parameters and 0 restraints.

CCDC reference number 605465. For crystallographic data in CIF or other electronic format see DOI: 10.1039/b606042k

1p; 2-(6-Bromopyridin-2-ylmethylidene)-6-(4-methoxybenzylidene)cyclohexanone. Yellow solid (0.344 g, 78%); mp 119 °C, (Found: C, 62.49; H, 4.87; N, 3.64. C₂₀H₁₈BrNO₂ requires C, 62.51; H, 4.72; N, 3.65%); λ_{\max} (EtOH)/nm 341 (ε/dm³ mol⁻¹ cm⁻¹ 14026); ν_{\max} /cm⁻¹ 1662 m, 1600 m, 1572 m, 1546 m, 1508 m, 1434 m, 1310 m, 1298 m, 1248 m, 1161 m, 1144 m, 411 s; δ_{H} (400 MHz, CDCl₃, Me₄Si) 1.80–1.87 (2H, m, CH₂CH₂CH₂), 2.93 (2H, td, *J* 7.2, 2.0, CH₂CH₂CH₂), 3.29 (2H, td, *J* 7.4, 2.2, CH₂CH₂CH₂), 3.85 (3H, s, OMe), 6.94 (2H, d, *J* 8.9, Ar), 7.36–7.38 (2H, m, Ar), 7.46 (2H, d, *J* 8.7, Ar), 7.52–7.75 (2H, m, CH=C, Ar), 7.76 (1H, s, CH=C); δ_{C} (100 MHz, CDCl₃, Me₄Si) 22.7, 28.5, 28.7, 55.6, 114.3 (2C), 126.0, 126.9, 128.8, 131.5, 132.7 (2C), 134.4, 137.7, 138.7, 141.8, 142.0, 156.8, 160.4, 190.8; *m/z* (ESI) 384.2 (100%) ([M + H]⁺ C₂₀H₁₉⁷⁹BrNO₂⁺ requires 384.1) and 386.2 (98%) ([M + H]⁺ C₂₀H₁₉⁸¹BrNO₂⁺ requires 386.1).

Crystal data for 1p. C₂₀H₁₈BrNO₂, *M_r* = 384.26, monoclinic, space group *P*2₁/*c*, *a* = 18.5748(1) Å, *b* = 6.2641(1) Å, *c* = 15.9337(1) Å, β = 115.194(1)°, *V* = 1677.59 (3) Å³, *Z* = 4, *D_{calc}* = 1.521 g cm⁻³, μ (MoK α) = 2.462 mm⁻¹. Of 6923 reflections measured, 3878 were unique (*R_{int}* = 0.0409), with

2825 *I* > 2 σ (*I*), *R* indices [*I* > 2 σ (*I*)] *R*₁ = 0.0371, *wR*₂ = 0.0697, GoF on *F*² = 1.027 for 218 refined parameters and 0 restraints.

CCDC reference number 605466. For crystallographic data in CIF or other electronic format see DOI: 10.1039/b606042k

1q; 2-(4-Methoxybenzylidene)-6-(3-nitrobenzylidene)cyclohexanone. Yellow solid (0.370 g, 85%); mp 118–119 °C, (Found: C, 72.38; H, 5.54; N, 4.11. C₂₁H₁₉NO₄ requires C, 72.19; H, 5.48; N, 4.01%); λ_{\max} (EtOH)/nm 348 (ε/dm³ mol⁻¹ cm⁻¹ 18430); ν_{\max} /cm⁻¹ 1716 w, 1660 w, 1634 w, 1600 m, 1559 m, 1522 m, 1377 m, 1347 m, 1301 m, 1275 m, 1258 m, 1165 m, 1144 s, 1033 m; δ_{H} (300 MHz, CDCl₃, Me₄Si) 1.81–2.16 (2H, m, CH₂CH₂CH₂), 2.17–2.99 (4H, m, CH₂CH₂CH₂), 3.86 (3H, s, OMe), 6.95 (2H, d, *J* 8.8, Ar), 7.47 (2H, d, *J* 8.6, Ar), 7.55–7.61 (1H, m, Ar), 7.73 (1H, d, *J* 7.7, Ar), 7.77 (1H, t, *J* 2.1, CH=C), 7.80 (1H, *J* 2.1, CH=C), 8.16–8.20 (1H, m, Ar), 8.30 (1H, t, *J* 2.0, Ar); δ_{C} (75 Hz, CDCl₃, Me₄Si) 23.1, 28.5, 28.7, 55.6, 114.3 (2C), 123.2, 124.6, 128.7, 129.6, 132.7 (2C), 133.5, 133.8, 136.3, 138.0, 138.2, 138.0, 148.6, 160.5, 189.8; *m/z* (ESI) 350.2 ([M + H]⁺ C₂₁H₂₀NO₄⁺ requires 350.1).

1r; 2-(Furfurylidene)-6-(4-methoxybenzylidene)cyclohexanone. Yellow solid (0.280 g, 76%); mp 105–106 °C (lit.²⁶ mp 99–100 °C) (Found: C, 77.51; H, 6.28. C₁₉H₁₈O₃ requires C, 77.53; H, 6.16%); λ_{\max} (EtOH)/nm 243, 368 (ε/dm³ mol⁻¹ cm⁻¹, 14558, 25368); ν_{\max} /cm⁻¹ 1656 w, 1596 w, 1508 w, 1301 w, 1259 w, 1182 w, 1162 w, 1140 w, 1029 w, 981 w; δ_{H} (200 MHz, CDCl₃, Me₄Si) 1.78–1.90 (2H, m, CH₂CH₂CH₂), 2.87–3.04 (4H, m, CH₂CH₂CH₂), 3.84 (3H, s, OMe), 6.49–6.53 (1H, m, Ar), 6.65–6.67 (1H, m, Ar), 6.93 (2H, d, *J* 8.8, Ar), 7.44 (2H, d, *J* 8.7, Ar), 7.55–7.58 (2H, m, CH=C), 7.75–7.76 (1H, m, Ar); δ_{C} (50 MHz, CDCl₃, Me₄Si) 22.6, 28.4, 28.6, 55.6, 112.5, 114.2 (2C), 116.1, 123.7, 129.0, 132.5 (2C), 133.5, 134.5, 136.8, 144.7, 153.2, 160.2, 189.8; *m/z* (ESI) 295.2 ([M + H]⁺ C₁₉H₁₉O₃⁺ requires 295.1).

1s; 2-(4-Methoxybenzylidene)-6-(pyrid-3-ylmethylidene)cyclohexanone. Yellow solid (0.301 g, 79%); mp 146–148 °C, (Found: C, 78.78; H, 6.34; N, 4.66. C₂₀H₁₉NO₂ requires C, 78.66; H, 6.27; N, 4.59%); ν_{\max} /cm⁻¹ 1663 m, 1607 m, 1562 m, 1507 m, 1416 m, 1308 w, 1276 m, 1248 s, 1155 s, 1022 m, 837 m, 710 m; δ_{H} (200 MHz, CDCl₃, Me₄Si) 1.82 (2H, app p, *J* 6.2, CH₂CH₂CH₂), 2.88–2.98 (4H, m, CH₂CH₂CH₂), 3.85 (3H, s, OMe), 6.94 (2H, d, *J* 8.8, Ar), 7.40–7.49 (3H, m, Ar), 7.70–7.87 (3H, m, 2 × CH=C, Ar), 8.58 (1H, d, *J* 3.89, Ar), 8.72 (1H, s, Ar); δ_{C} (100 MHz, CDCl₃, Me₄Si) 23.1, 28.6, 28.7, 55.6, 114.2 (2C), 123.5, 128.7, 132.2, 132.6 (2C), 132.7, 134.0, 137.2, 137.9, 138.6, 149.3, 151.3, 160.4, 189.9; *m/z* (ESI) 306.2 ([M + H]⁺ C₂₀H₂₀NO₂⁺ requires 306.2).

1u; 2-(4-Diethylaminobenzylidene)-6-(furfurylidene)cyclohexanone. Orange solid (0.386 g, 92%); mp 107.5–109.5 °C (Found: C, 78.77; H, 7.54; N, 4.20. C₂₂H₂₅NO₂ requires C, 78.77; H, 7.51; N, 4.18%); λ_{\max} (EtOH)/nm 269, 348, 449 (ε/dm³ mol⁻¹ cm⁻¹ 14599, 16204, 34672); ν_{\max} (KBr)/cm⁻¹ 2967 w, 2932 w, 2898 w, 2872 w, 1637 m, 1599 s, 1586 s, 1570 w, 1560 s, 1540 m, 1518 s, 1466 w, 1405 w, 1358 m, 1308 w, 1282 m, 1272 m, 1196 m, 1168 s, 1132 s, 1074 m, 1030 w; δ_{H} (300 MHz, CDCl₃, Me₄Si) 1.19 (6H, t, *J* 7.1, Me), 1.84 (2H, app p, *J* 6.3,

CH₂CH₂CH₂), 2.93 (2H, td, *J* 6.2, 1.9, CH₂CH₂CH₂), 2.99 (2H, td, *J* 6.3, 2.0, CH₂CH₂CH₂), 3.40 (4H, q, *J* 7.1, NCH₂), 6.50 (1H, dd, *J* 3.3, 1.7, Ar); 6.63 (1H, d, *J* 3.5, Ar), 6.67 (2H, d, *J* 9.0, Ar), 7.42 (2H, d, *J* 8.9, Ar); 7.53–7.56 (2H, m, CH=C, Ar), 7.76 (1H, s, CH=C); δ_{C} (75 MHz, CDCl₃, Me₄Si) 12.9 (2C), 22.7, 28.4, 28.8, 44.6 (2C), 111.3 (2C), 112.4, 115.5, 122.8, 123.3, 131.5, 133.2 (2C), 134.0, 138.3, 144.3, 148.3, 153.3, 189.6; *m/z* (ESI) 336.3 ([M + H]⁺ C₂₂H₂₆NO₂⁺ requires 336.2).

1v; 1-(4-Bromobenzylidene)-3-(4-methoxybenzylidene)acetone. Pale green solid (0.295 g, 90%); mp 182–183 °C (Found: C, 62.86; H, 4.41. C₁₈H₁₅BrO₂ requires C, 62.99; H, 4.41, %); λ_{max} (EtOH)/nm 237, 348 ($\epsilon/\text{dm}^3 \text{ mol}^{-1} \text{ cm}^{-1}$ 23089, 30031); $\nu_{\text{max}}/\text{cm}^{-1}$ 1647 m, 1591 m, 1560 m, 1511 m, 1460 s, 1420 w, 1400 w, 1340 w, 1300 w, 1265 w, 1249 m, 1194 w, 1174 m, 1111 w, 1070 w, 1032 m, 1008 w, 980 m, 886 w, 864 w, 829 m, 809 w; δ_{H} (300 MHz, CDCl₃, Me₄Si) 3.86 (3H, s, OMe), 6.94 (1H, d, *J* 15.9, CH=C), 6.94 (2H, d, *J* 8.8, Ar), 7.06 (1H, d, *J* 15.9, CH=C), 7.65 (1H, d, *J* 15.9, CH=C), 7.71 (1H, d, *J* 15.9, CH=C), 7.47 (2H, d, *J* 8.5, Ar), 7.55 (2H, d, *J* 8.3, Ar), 7.57 (2H, d, *J* 8.4, Ar); δ_{C} (75 Hz, CDCl₃, Me₄Si) 55.7, 114.8 (2C), 123.6, 124.8, 126.3, 127.7, 129.9 (2C), 130.5 (2C), 132.5 (2C), 134.2, 141.6, 143.7, 162.1, 188.8, *m/z* (ESI) 365.1 ([M + Na]⁺ C₁₈H₁₅⁷⁹BrO₂Na⁺ requires 365.0) and 367.1 ([M + Na]⁺ C₁₈H₁₅⁸¹BrO₂Na⁺ requires 367.0).

1w; 1-(4-Methoxybenzylidene)-3-(4-nitrobenzylidene)acetone. Yellow solid (0.355 g, 83%); mp 181–183 °C, (Found: C, 69.76; H, 5.10; N, 4.55. C₁₈H₁₅NO₄ requires C, 69.89; H, 4.89; N, 4.53%); λ_{max} (EtOH)/nm 347 ($\epsilon/\text{dm}^3 \text{ mol}^{-1} \text{ cm}^{-1}$ 21420); $\nu_{\text{max}}/\text{cm}^{-1}$ 1651 s, 1600 s, 1588 s, 1519 s, 1463 s, 1410 w, 1377 m, 1340 s, 1309 w, 1258 m, 1198 m, 1173 m, 1105 w, 1024 w, 988 w; δ_{H} (200 MHz, CDCl₃, Me₄Si) 3.87 (3H, s, OMe), 6.94 (1H, d, *J* 15.9, CH=C), 6.95 (2H, d, *J* 6.8, Ar), 7.18 (1H, d, *J* 15.9, CH=C), 7.59 (2H, d, *J* 6.7, Ar), 7.70–7.77 (4H, m, Ar, CH=C), 8.27 (2H, d, *J* 6.9, Ar); δ_{C} (75 Hz, CDCl₃, Me₄Si); 55.7, 114.8 (2C), 123.4, 124.4 (2C), 127.5, 129.1 (2C), 129.3, 130.6 (2C), 139.8, 141.5, 144.5, 148.7, 162.3, 188.3; *m/z* (ESI) 332.09 ([M + Na]⁺ C₁₈H₁₅NO₄Na⁺ requires 332.09).

8a. *Crystal data for 8a.* C₃₆H₃₈NOCl, *M_r* = 536.12, triclinic, space group *P1*(bar), *a* = 11.5683(4), *b* = 12.3023(4), *c* = 13.6088(5) Å, α = 98.825(1), β = 110.125(2), γ = 111.483(2)°, *V* = 1603.3(1) Å³, *Z* = 2, *D*_{calc} = 1.111 g cm⁻³, $\mu(\text{MoK}\alpha)$ = 0.146 mm⁻¹. Of 27554 reflections measured, 7612 were unique (*R*_{int} = 0.087), with 3336 *I* > 2σ(*I*), *R* indices [*I* > 2σ(*I*)] *R*₁ = 0.0644, *wR*₂ = 0.1623, GoF on *F*² = 0.988 for 355 refined parameters and 0 restraints

CCDC reference number 605784. For crystallographic data in CIF or other electronic format see DOI: 10.1039/b606042k

8b. *Crystal data for 8b.* C₂₆H₃₁N₃O, *M_r* = 401.54, monoclinic, space group *P2₁/n*, *a* = 10.0896(1), *b* = 13.2900(2), *c* = 16.6649(3) Å, β = 103.981(1)°, *V* = 2168.41(6) Å³, *Z* = 4, *D*_{calc} = 1.230 g cm⁻³, $\mu(\text{MoK}\alpha)$ = 0.076 mm⁻¹. Of 30375 reflections measured, 5297 were unique (*R*_{int} = 0.050), with 3772 *I* > 2σ(*I*), *R* indices [*I* > 2σ(*I*)] *R*₁ = 0.0498, *wR*₂ = 0.0985, GoF on *F*² = 1.059 for 273 refined parameters and 0 restraints.

CCDC reference number 605785. For crystallographic data in CIF or other electronic format see DOI: 10.1039/b606042k

9; 7a-Dimethylamino-5,6,7,7a-tetrahydro-4H-benzofuran-2-one. Glyoxylic acid monohydrate (0.98 g, 10 mmol) was added to DIMCARB (5 mL) at ambient temperature while stirring, resulting in the evolution of gas. The solution was heated to 50 °C, followed by addition of cyclohexanone (1.035 mL, 10.0 mmol) and stirring for a further 3 h at 50 °C.

DIMCARB was removed *in vacuo* and the residual mixture washed with water (10 mL) and extracted with dichloromethane (3 × 20 mL). The combined organic fractions were collected, dried with anhydrous MgSO₄, filtered and the solvent removed *in vacuo* to afford an orange oil, which post silica gel chromatography (eluent 1 : 1 hexane–ethyl acetate) yielded 7a-dimethylamino-5,6,7,7a-tetrahydro-4H-benzofuran-2-one (1.09 g, 60%) which was crystallised as clear crystals from ethyl acetate, mp 62–64 °C (Found: C, 66.27; H, 8.31; N, 7.76. C₁₀H₁₅NO₂ requires C, 66.27; H, 8.34; N, 7.73%); δ_{H} (200 MHz, CDCl₃, Me₄Si) 1.26–1.42 (2H, m, –CH₂–), 1.58–1.70 (2H, m, –CH₂–), 1.94–2.08 (1H, m, –CH₂–), 2.15–2.29 (1H, m, –CH₂–), 2.32 (6H, s, N(CH₃)₂), 2.70–2.75 (2H, m, –CH₂CO(N)), 5.71 (1H, t, *J* 1.8, CH=C); δ_{C} (50 MHz, CDCl₃, Me₄Si) 21.9, 27.6, 27.9, 37.0, 37.4 (2C), 103.0, 114.2, 172.0, 172.1; *m/z* (ESI) 181.8 ([M + H]⁺ C₁₀H₁₆NO₂⁺ requires 182.1).

Crystal data for 9. C₁₀H₁₅NO₂, *M_r* = 181.23, orthorhombic, space group *Pbca*, *a* = 8.7630(2), *b* = 10.9240(2), *c* = 20.1019(5) Å, *V* = 1924.29(7) Å³, *Z* = 8, *D*_{calc} = 1.251 g cm⁻³, $\mu(\text{MoK}\alpha)$ = 0.087 mm⁻¹. Of 2322 unique reflections measured with 1545 *I* > 2σ(*I*), *R* indices [*I* > 2σ(*I*)] *R*₁ = 0.0496, *wR*₂ = 0.1182, GoF on *F*² = 1.083 for 120 refined parameters and 0 restraints.

CCDC reference number 605786. For crystallographic data in CIF or other electronic format see DOI: 10.1039/b606042k.

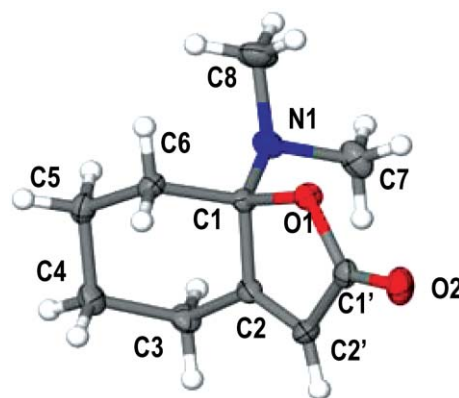


Fig. 2 Molecular diagram of **9** derived from single crystal structure analysis.

6; (E)-5-Benzylidene-1-(*N,N*-dimethylamino)cyclopent-1-ene. To an RBF containing a 1 : 1 DIMCARB/ether mixture (10 mL) was added benzaldehyde (1.06 g, 10.0 mmol) and cyclopentanone (1.01 g, 12.0 mmol) and stirred at room

temperature. After 24 h the volatile components, including cyclopentanone, were removed under high vacuum without heating. NMR analysis indicated two products present: 2-Benzylidenecyclopentanone; partial δ_{H} (200 MHz, CDCl_3 , Me_4Si) indicative peaks; 2.01 (2H, app p, J 7.4, $\text{CH}_2\text{CH}_2\text{CH}_2$), 2.96 (2H, td, J 7.2, 2.8, $\text{C}=\text{CCH}_2$); δ_{C} (50 MHz, CDCl_3 , Me_4Si) 20.4, 29.5, 38.0, 128.9 (2C), 129.5, 130.7 (2C), 132.5, 135.7, 136.3, 208.20 and 5-benzylidene-1-(*N,N*-dimethylamino)cyclopent-1-ene; δ_{H} (200 MHz, CDCl_3 , Me_4Si) indicative peaks; 2.86 (2H, td, J 5.3, 2.6, $\text{C}=\text{CCH}_2$), 5.29 (1H, t, J 2.8, $\text{NC}=\text{CH}$), 6.44 (1H, t, J 2.6, $\text{ArCH}=\text{C}$); δ_{C} (50 MHz, CDCl_3) 29.5, 32.1, 43.3 (2C), 115.1, 118.3, 125.9, 128.4 (2C), 128.5 (2C), 138.8, 144.2, 155.9.

Acknowledgements

We thank Milestone (Italy) for the loan of microwave reactors and ancillary equipment, Andrew Battle for the crystal structure analysis of compound **8a** and the Australian Research Council (ARC) for funding this research through the ARC Special Research Centre for Green Chemistry. One of the referees is thanked for helpful suggestions regarding the one pot process.

References

- (a) M. G. Martinez, T. Klimova-Berestneva, K. Damian-Zea, N. N. Meleshonkova and E. I. Klimova, *Russ. J. Gen. Chem.*, 2002, **72**, 1132–1140; (b) T. Lóránd, D. Szabó, A. Földesi, L. Párkányi, A. Kálmán and A. Neszmélyi, *J. Chem. Soc., Perkin Trans. 1*, 1985, 481–486.
- (a) D. V. Tyndall, T. Al Nakib and M. J. Meegan, *Tetrahedron Lett.*, 1988, **29**, 2703–2706; (b) J.-F. Zhou, *Synth. Commun.*, 2003, **33**, 99–103.
- V. Padmavathi, B. J. M. Reddy and D. R. C. V. Subbaiah, *New J. Chem.*, 2004, **28**, 1479–1483.
- (a) L. T. Higham, U. P. Kreher, C. L. Raston, J. L. Scott and C. R. Strauss, *Org. Lett.*, 2004, **6**, 3257–3259; (b) L. T. Higham, U. P. Kreher, C. L. Raston, J. L. Scott and C. R. Strauss, *Org. Lett.*, 2004, **6**, 3261–3264.
- R. Costi, R. Di Santo, M. Artico, S. Massa, R. Ragno, R. Loddo, M. La Colla, E. Tramontano, P. La Colla and A. Pani, *Bioorg. Med. Chem.*, 2004, **12**, 199–215.
- (a) J. R. Dimmock, U. Das, H. I. Gul, M. Kawase, H. Sakagami, Z. Baráth, I. Ocsovsky and J. Molnár, *Bioorg. Med. Chem. Lett.*, 2005, **15**, 1633–1636; (b) J.-Y. Chang, H.-P. Hsieh, W.-Y. Pan, J.-P. Liou, S.-J. Bey, L.-T. Chen, J.-F. Liu and J.-S. Song, *Biochem. Pharmacol.*, 2003, **65**, 2009–2019.
- W. J. Guilford, K. J. Shaw, J. L. Dallas, S. Koovakkat, W. Lee, A. Liang, D. R. Light, M. A. McCarrick, M. Whitlow, B. Ye and M. M. Morrissey, *J. Med. Chem.*, 1999, **42**, 5415–5425.
- S.-H. Juang, W.-Y. Pan, C.-C. Kuo, J.-P. Liou, Y.-M. Hung, L.-T. Chen, H.-P. Hsieh and J.-Y. Chang, *Biochem. Pharmacol.*, 2004, **68**, 293–303.
- R. J. Anto, K. Sukumaran, G. Kuttan, M. N. A. Rao, V. Subbaraju and R. Kutton, *Cancer Lett.*, 1995, **97**, 33–37.
- (a) H. M. Walton, *J. Org. Chem.*, 1957, **22**, 1161–1165; (b) M. Zheng, L. Wang, J. Shao and Q. Zhong, *Synth. Commun.*, 1997, **27**, 351–354.
- J. D. Billimoria, *J. Chem. Soc.*, 1955, 1126–1129.
- (a) T. Mukaiyama, K. Banno and K. Narasaka, *J. Am. Chem. Soc.*, 1974, **96**, 7503–7509; (b) S. E. Denmark, K.-T. Wong and R. A. Stavenger, *J. Am. Chem. Soc.*, 1997, **119**, 2333–2334; (c) S. E. Denmark, R. A. Stavenger, K.-T. Wong and X. Su, *J. Am. Chem. Soc.*, 1999, **121**, 4982–4991.
- (a) B. List, R. A. Lerner and C. F. Barbas, III, *J. Am. Chem. Soc.*, 2000, **122**, 2395–2396; (b) K. Sakthivel, W. Notz, T. Bui and C. F. Barbas, III, *J. Am. Chem. Soc.*, 2001, **123**, 5260–5267.
- Y.-S. Wu, W.-Y. Shao, C.-Q. Zheng, Z.-L. Huang, J. Cai and Q.-Y. Deng, *Helv. Chim. Acta*, 2004, **87**, 1377–1384.
- L. Birkhofer, S. M. Kim and H. D. Engels, *Chem. Ber.*, 1962, **95**, 1495–1504.
- U. P. Kreher, A. E. Rosamilia, C. L. Raston, J. L. Scott and C. R. Strauss, *Org. Lett.*, 2003, **5**, 3107–3110.
- V. W. Schroth, J. Andersch, H.-D. Schadler and R. Spitzner, *Chem. Zeit.*, 1989, **113**, 261–271.
- U. P. Kreher, A. E. Rosamilia, C. L. Raston, J. L. Scott and C. R. Strauss, *Molecules*, 2004, **9**, 387–393.
- B. A. Roberts and C. R. Strauss, *Acc. Chem. Res.*, 2005, **38**, 653–661.
- J. W. Lewis, P. L. Myers and M. J. Readhead, *J. Chem. Soc. C*, 1970, 1549–1553.
- G. M. Sheldrick, *SHELXS-97, Program for solution of crystal structures*, University of Göttingen, Germany, 1997.
- G. M. Sheldrick, *SHELXS-97, Program for solution of crystal structures*, University of Göttingen, Germany, 1997.
- L. J. Barbour, *J. Supramol. Chem.*, 2001, **1**, 189.
- M. L. Edwards, H. W. Ritter, D. M. Stemerick and K. T. Stewart, *J. Med. Chem.*, 1983, **26**, 431–436.
- A. Maccioni and E. Marongiu, *Ann. Chim. (Rome)*, 1959, **49**, 1283–1287.
- A. P. Kriven'ko, A. A. Bugaev and A. G. Golikov, *Chem. Heterocycl. Compd.*, 2005, **41**, 163–167.

Low melting sugar–urea–salt mixtures as solvents for organic reactions—estimation of polarity and use in catalysis

Giovanni Imperato,^a Silke Höger,^a Dieter Lenoir^b and Burkhard König^{*a}

Received 10th March 2006, Accepted 10th August 2006

First published as an Advance Article on the web 12th September 2006

DOI: 10.1039/b603660k

Mixtures of sugars, sugar alcohols or citric acid with urea and inorganic salts form stable melts if heated to 70 °C. The polarity of the melts was estimated using solvatochromic dyes and found to be in the range of DMF or water, depending on the sensitivity of the dye for hydrogen bonds. To explore the use of the melts as solvents in catalysis, Rh-catalyzed hydrogenations and Pd-catalyzed Suzuki reactions were performed. The hydrogenation of a double bond is sensitive to the composition of the melt, and no effect of the chiral melts on the stereochemical outcome of the reaction was observed. The Suzuki coupling proceeds rapidly, cleanly and quantitatively in all examined melts. The results recommend the non-toxic sugar–urea–salt melts as more sustainable reaction media for chemical transformations.

Introduction

The majority of chemical transformations are done in solution to more efficiently control the heat flow of exothermic and endothermic reactions. In addition, polar reactions which proceed *via* polar or ionic intermediates or transition states are promoted by polar solvents due to a strong stabilization by solvation of the polar intermediates. A small number of organic reactions can be performed in the solid state¹ and solventless reactions have been developed for organic synthesis,² but both approaches are limited.³ Several solvents used for reactions in the laboratory and in industry belong to the group of volatile organic compounds (VOC). Solvents like chlorinated hydrocarbons derived from methane, ethane, and propane are volatile and chemically relatively stable; they are harmful to the environment. Due to their persistence they accumulate in the atmosphere and contribute to ozone depletion and to smog in urban areas.⁴ To overcome this concern of synthetic organic chemistry, new “green solvents” have been developed, which are slowly finding their way into laboratories and chemical production. The new “green” solvents include supercritical carbon dioxide, ionic liquids, water, and fluorous biphasic mixtures.⁵ We have contributed to this field by using low melting mixtures consisting of sugars, urea, and inorganic salts as a solvent for organic transformations.⁶ The stable melts of the mixtures are environmentally benign, because they are easily biodegradable, non-toxic and they are available from bulk renewable resources without modification steps. Melting points are in the range of 65 to 85 °C, and Diels–Alder reactions, which were performed in the solvent system, illustrate their use in organic synthesis.⁷ To

characterize the solvent properties of the sugar–urea–salt melts more closely, we have investigated their polarities using two solvatochromic aromatic dyes, Reichardt’s dye⁸ and Nile red.⁹ In addition, the use of the melts for catalytic transformations was explored exemplarily by Rh-catalyzed hydrogenation reactions and Pd-catalyzed biaryl formation (Suzuki reaction).

Results and discussion

Determination of solvent polarities of sugar melts by solvatochromic dyes

Solvents can be classified into different types according to their behavior as media for chemical reactions,¹⁰ and they are typically divided into three main categories: non-polar solvents (hydrocarbons), polar protic solvents (*e.g.* water, alcohols) and polar aprotic solvents (*e.g.* DMSO, acetone). The dielectric constant of a solvent, a macroscopic property, describes polarity. The use of solvatochromic dyes allows a direct probe of the polarity of a solvent affecting the absorption properties of the dissolved dye molecule. Melted sugar–urea–salt mixtures were investigated by this method and the results are compared to the polarity of typical conventional solvents used in synthesis.

Solvatochromic behavior of Reichardt’s dye

Reichardt’s betaine dye, 2,6-diphenyl-4-(2,4,6-triphenyl-*N*-pyridino)phenolate (Fig. 1, right), is the most solvatochromic compound reported to date, showing a range of transition energies for the $\pi \rightarrow \pi^*$ adsorption band from 37.7 kcal mol⁻¹ (810 nm) in diphenyl ether to 67.7 kcal mol⁻¹ (453 nm) in water. This exceptional behaviour makes this dye a useful indicator for solvent polarity. It can be observed, that the absorption range is almost entirely within the visible region, and more quantitatively, by use of UV/Vis spectroscopy, as shown the Fig. 2: the dye is red in sorbitol–dimethylurea (DMU)–NH₄Cl (**2**), orange in mannitol–dimethylurea–NH₄Cl (**5**) and yellow in citric acid–dimethylurea (**1**) melts.

^aInstitut für Organische Chemie, Universität Regensburg, D-93040, Regensburg, Germany. E-mail: burkhard.koenig@chemi.uni-regensburg.de; Fax: +49 941 9431717; Tel: +49 941 9434576

^bGSF National Research Centre for Environment and Health, Institute of Ecological Chemistry, Ingolstadter Landstrasse 1, D-85764, Neuherberg, Germany. E-mail: Lenoir@gfsf.de; Fax: +49 89 31873371; Tel: +49 89 31872960

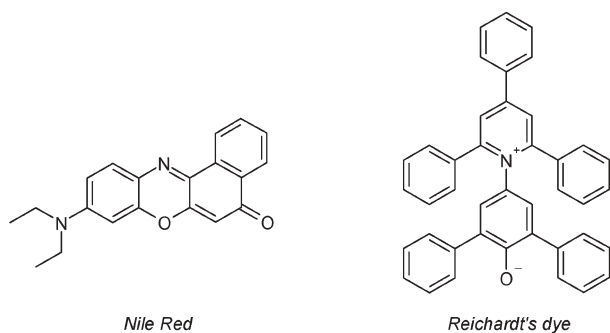


Fig. 1 Solvatochromic dyes used to estimate the polarity of sugar-urea-salt melts.



Fig. 2 From left to right: mannose-DMU (30 : 70) (8), sorbitol-DMU-NH₄Cl (70 : 20 : 10) (2), mannitol-DMU-NH₄Cl (50 : 40 : 10) (5), citric acid-DMU (40 : 60) (1).

The original solvent polarity scale, known as the $E_T(30)$ scale, is defined as the molar transition energy of the dye measured in solvents of different polarity at 30 °C and atmospheric pressure according to the following equation:

$$E_T(30) \text{ kcal mol}^{-1} = hc\nu_{\max}N_A = 28\,591/\lambda_{\max}$$

$$h = \text{Planck's constant; } c = \text{speed of the light; } \nu_{\max} = \text{wave number; } N_A = \text{Avogadro's constant}$$

The $E_T(30)$ values are defined for a temperature of 30 °C, but sugar-urea-salt melts are liquid above 70 °C only. To show that an estimation of polarity from solvatochromic measurements is still possible at higher temperatures, the

absorption maxima of Reichardt's dye in several solvents (water, ethylene glycol, 2-propanol, dimethylsulfoxide, dimethylformamide) were determined at 90 °C and compared to the value at 30 °C. The changes in the maximum absorption wavelength are small, and we conclude that an estimation of the relative order of polarity is possible from absorption values at 90 °C.

Table 1 shows the longest wavelength adsorption band from intramolecular charge-transfer $\pi \rightarrow \pi^*$ excitation of Reichardt's dye in several sugar-urea-salt melts, water and selected solvents at 90 °C. An examination of the results in Table 1 reveals that the $E_T(30)$ polarity values obtained for most sugar-urea-salt melts are much larger compared to water. $E_T(30)$ polarity values exceeding the water value are known for aqueous salt solutions⁸ and some ionic liquids.⁸ The $E_T(30)$ values of the lactose-DMU-NH₄Cl (7) and the mannose-DMU (8) melt are smaller and in the range of ethylene glycol and 2-propanol.

Solvatochromic behavior of Nile red

Although the exact molecular structure of the sugar-urea-salt melts remains speculative, a tight hydrogen bond network might be expected. It was reported that $E_T(30)$ values are very sensitive to solvents with acidic hydrogen bonds, which may adulterate the relative polarity ranking with organic solvents. Nile red (Fig. 1, left) is another dye, which shows a solvatochromic effect, but the absorbance maximum shift is less sensitive to acidic solvents due to its low basicity ($pK_a = 1$).¹¹ The dye dissolves in very polar liquids and is used to measure the polarity of acids and other very polar solvents. Its color remains unchanged for several months even in neat, strong acids, such as trifluoroacetic acid.

Depending on the solvents polarity, Nile red shows a bathochromic wavelength shift¹² consistent with stabilization of the excited state in $p \rightarrow \pi^*$ or $\pi \rightarrow \pi^*$ electronic transition, and comparable with the π^* scale of Kamlet and Taft.¹³ An empirical value, $E_T(\text{NR})$, can be defined for the polarity of solvents and provides an alternative useful scale to estimate the relative polarity of organic solvents and ionic liquids. Large shifts in the wavelength of maximum absorbance are observed with the dye in sugar-urea-salt melts. A pink solution is obtained in sorbitol-dimethylurea-NH₄Cl (2), fuchsia in mannitol-dimethylurea-NH₄Cl (5), dark violet in

Table 1 Intramolecular charge-transfer absorption bands (λ_{\max}) and corresponding $E_T(30)$ solvent polarity values for melting sugar mixtures and other solvents at 90 °C (Reichardt's dye)

Solvent	Melting point	λ_{\max}/nm (30 °C)	λ_{\max}/nm (90 °C)	$E_T(30)/\text{kcal mol}^{-1}$
Citric acid-DMU ^a (1) 40:60	65 °C	—	404	70.8
Sorbitol-DMU ^a -NH ₄ Cl (2) 70:20:10	67 °C	—	420	68.1
Maltose-DMU ^a -NH ₄ Cl (3) 50:40:10	84 °C	—	422	67.8
Fructose-urea-NaCl (4) 70:20:10	73 °C	—	430	66.5
Mannitol-DMU ^a -NH ₄ Cl (5) 50:40:10	89 °C	—	436	65.8
Glucose-urea-NaCl (6) 60:30:10	78 °C	—	444	64.4
Water	—	453	453	63.1
Ethylene glycol	—	507	510	56.1
Lactose-DMU ^a -NH ₄ Cl (7) 50:40:10	88 °C	—	530	53.9
Mannose-DMU ^a (8) 30:70	75 °C	—	530	53.9
2-Propanol	—	588	589 ^b	48.5
Dimethylsulfoxide	—	635	635	45.0
Dimethylformamide	—	652	655	43.6

^a DMU = *sym* dimethyl urea. ^b Determined at 83 °C.



Fig. 3 From left to right: mannose–DMU (**8**); sorbitol–DMU–NH₄Cl (**2**); mannitol–DMU–NH₄Cl (**5**); citric acid–DMU (**1**).

mannose–DMU (**8**), and a violet-blue color in citric acid–dimethylurea (**1**) (Fig. 3).

In Table 2 the λ_{\max} values for Nile red at 90 °C dissolved in sugar–urea–salt melts and five solvents are summarized. The Nile red λ_{\max} data reclassify the melts to be less polar than water. From the $E_T(\text{NR})$ values, a relative polarity of maltose–dimethylurea–NH₄Cl (**3**), sorbitol–dimethylurea–NH₄Cl (**2**) and citric acid–dimethylurea (**5**) similar to ethylene glycol is estimated, whereas mannose–dimethylurea (**8**) is similar to dimethyl sulfoxide, and mannitol–dimethylurea–NH₄Cl (**5**) close to dimethylformamide.

In Fig. 4 the measured $E_T(\text{NR})$ values are plotted against Reichardt's, $E_T(30)$ values. The relative order is consistent, but absolute values differ. The Nile red response is less sensitive to hydrogen bonding solvents and proton donor/acceptor solvents than E_T values of Reichardt's dye, which leaves all values in a much more narrow range.

It should be mentioned, that E_T values for both series have been developed mostly for pure solvents. The sugar–urea–salt melts are binary or tertiary mixtures, for which no additive behavior of its components can be expected. Synergistic (non-additive) behavior of physical properties of solvent mixtures have been found in special cases: *e.g.* some Rh(III) complexes are neither soluble in pure water nor in neat pyridine, but in a 1 : 1 mixture of the two solvents.¹⁴ Addition of inorganic salts like sodium chloride to various solvents can lead to a strong increase of the polarity of the mixture.¹⁵

Nile red is uniquely stable in acidic media and is not susceptible to loss of molar absorptivity in the presence of acids like Reichardt's dye. The absorbance maximum of

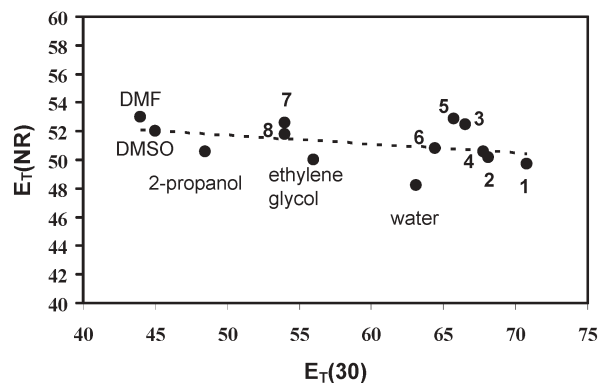


Fig. 4 Comparison of transition energies calculated from the absorption wavelength of Nile red, $E_T(\text{NR})$ and Reichardt's dye, E_T in sugar–urea–salt melts and some polar solvents.

$E_T(30)$ is extremely sensitive to hydrogen bonding solvents, while Nile red does not appear to shift significantly when subject to hydrogen bonding. Thus, we judge the estimates based on the Nile red absorption shifts as the more realistic ones for the sugar–urea–salt melts. The values place their polarity in a range comparable to DMSO and ethylene glycol, and show significant polarity differences depending on the composition of the melt. The citric acid–dimethylurea (**1**) melt is the most polar one, while mannose and lactose based melts **7** and **8** are least polar.

Reactions in sugar melts

Hydrogenation in melting sugar mixtures

Low melting mixtures of sugars, urea and salt have been successfully used as solvents for typical organic reactions, *e.g.* Diels–Alder⁷ or aldol reactions.⁶ To extend the scope of application, hydrogenation reactions were performed in the melts. Catalytic hydrogenation is a key synthetic method for the reduction of organic compounds. The reaction can be performed in various organic solvents,¹⁶ water¹⁷ or ionic liquids¹⁸ and supercritical carbon dioxide.¹⁹ The methyl ester of α -cinnamic acid (**9**) was used as the substrate for catalytic hydrogenation with Wilkinson's catalyst at 90 °C and 1 atm of dihydrogen (Fig. 5).

Table 2 Intramolecular charge-transfer absorption band (λ_{\max}) and corresponding $E_T(\text{NR})$ solvent polarity value for Nile red dye in sugar–urea–salt melts and other solvents for comparison at 90 °C

Solvent	Melting point	λ_{\max}/nm (25 °C)	λ_{\max}/nm (90 °C)	$E_T(\text{NR})/\text{kcal mol}^{-1}$
Water	—	593	593	48.21
Citric acid–DMU ^a (1) 40 : 60	65 °C	—	575	49.72
Sorbitol–DMU ^a –NH ₄ Cl (2) 70 : 20 : 10	67 °C	—	570	50.16
Ethylene glycol	—	565	565	50.60
Maltose–DMU ^a –NH ₄ Cl (3) 50 : 40 : 10	84 °C	—	565	50.60
Glucose–urea–NaCl (6) 60 : 30 : 10	78 °C	—	562	50.78
Mannose–DMU ^a (8) 30 : 70	75 °C	—	551	51.79
Dimethyl sulfoxide	—	549	549	52.07
Fructose–urea–NaCl (4) 70 : 20 : 10	73 °C	—	544	52.55
Lactose–DMU ^a –NH ₄ Cl (7) 50 : 40 : 10	88 °C	—	544	52.55
Dimethylformamide	—	541	541	52.84
Mannitol–DMU ^a –NH ₄ Cl (5) 50 : 40 : 10	89 °C	—	540	52.94
2-Propanol	—	540	540 ^b	52.94

^a DMU = *sym* dimethyl urea. ^b Determined at 83 °C.

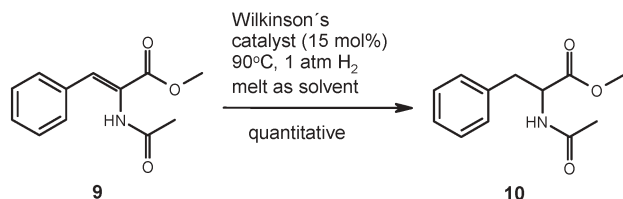


Fig. 5 Catalytic hydrogenation of methyl α -cinnamate (**9**) in a melt using Wilkinson's catalyst.

The reaction proceeds rapidly, cleanly and quantitatively in a citric acid–dimethylurea melt (**1**) and less efficiently (50% conversion) in melts **2** and **5**. In the other sugar–urea–salt melts, the catalytic systems show only low reactivity. Product **10** contains a chiral center and its configuration was investigated by chiral HPLC. Melts **2** and **5** contain chiral compounds and may affect the orientation of the hydrogenation reaction. However, the analysis revealed racemate formation, which shows that the chiral melts are not able to bias the stereochemical outcome of the reaction.

Suzuki reaction

The palladium-catalyzed cross coupling of aryl halides with boronic acids (Suzuki reaction) is one of the most versatile and widely utilized reactions for the selective construction of carbon–carbon bonds, in particular for the formation of biaryls. The biaryl motif is found in pharmaceuticals, herbicides, natural products, conducting polymers and liquid crystalline materials.²⁰ Suzuki reactions have been described in organic solvents,^{21,22} in water,²³ in supercritical carbon dioxide²⁴ and in ionic liquids.²⁵ We extend the scope by using sugar–urea–salt melts as the solvent. Phenyl boronic acid (**11**) was coupled with three aryl bromides (**12**) in the melts **2–8** at 90 °C using 10 mol% of Pd(OAc)₂ as catalyst and 1.2 equiv. of Na₂CO₃ as base (Fig. 6). All reactions show quantitative conversion of the starting materials after 6 h. Hydrodeboronation as a competing process was not observed under these conditions.

Work up of the reaction mixture is very easy. After cooling to room temperature, water was added and the aqueous phase was extracted with pentane. Product analysis by NMR and GC shows clean formation of the expected product. The isolated yields range from 78 to 97%, which is mainly caused by different efficacy of product extraction in work up (Table 3).

Conclusions

Stable melts are obtained at around 75 °C from several mixtures of sugars, sugar alcohols or citric acid with urea and

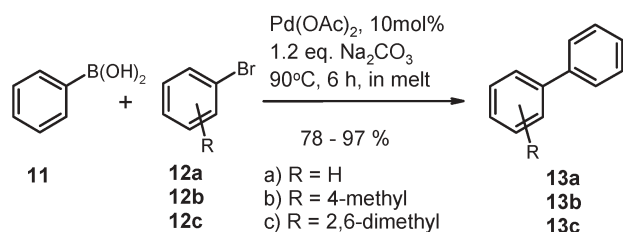


Fig. 6 Suzuki coupling in sugar–urea–salt melts.

Table 3 Suzuki coupling in sugar–urea–salt melts

Composition of melt	Isolated yield (%)		
	13a	13b	13c
Fructose–urea–NaCl (4) 70 : 20 : 10	82	81	78
Maltose–DMU–NH ₄ Cl (3) 50 : 40 : 10	84	83	81
Mannose–DMU ^a (8) 30 : 70	98	93	88
Lactose–DMU ^a –NH ₄ Cl (7) 60 : 30 : 10	89	86	91
Mannitol–DMU ^a –NH ₄ Cl (5) 50 : 40 : 10	97	96	97
Sorbitol–DMU ^a –NH ₄ Cl (2) 70 : 20 : 10	98	95	94
Glucose–urea–NH ₄ Cl (6) 60 : 30 : 10	86	80	83

^a Sym dimethylurea.

inorganic salts. As an important solvent parameter, the polarity of the melts was estimated using solvatochromic dyes. While Reichardt's dye rates all melts more polar than water, the more suitable estimation using Nile red places their polarity in the range of DMSO and ethylene glycol. While previous experiments demonstrated the use of sugar–urea–salt melts as solvents for typical organic transformations, we have now extended the application to transition metal catalyzed reactions. Hydrogenation with Wilkinson's catalyst proceeds very well in a citric acid–dimethylurea melt. The reaction is sensitive to the composition of the melt and results vary with the sugar or sugar alcohol used. No stereochemical bias of the hydrogenation reaction in chiral melts was observed. The palladium-catalyzed Suzuki reaction proceeds equally well in all investigated melts as solvents and variations in isolated yields are caused by different product extraction efficacy.

In summary, the reported sugar–urea–salt melts represent a suitable replacement for polar organic solvents, like DMF, DMSO or ethylene glycol in organic synthesis. The non-toxic melts are available from bulk renewable resources and simple inorganic salts without prior steps by simple mixing of the components. With these properties they may contribute to the development of more sustainable chemical transformations and processes.

Experimental

Solvatochromic measurements of solvents and melts

Reichardt's dye and Nile red were obtained from Aldrich Chemical Co. and were used as received. All sugars were commercially available with D-configuration. Samples for spectroscopic studies were prepared as follows: an appropriate aliquot of the solvatochromic dye was added at 90 °C to the analyzed solvent and allowed to equilibrate for a sufficient time. Then a 1 ml aliquot was placed into a cuvette, which was beforehand filled with argon.

Hydrogenation reaction

All reactions were carried out in a dihydrogen atmosphere and all chemicals were used as purchased. In a typical experiment 0.1 mmol of methyl α -cinnamate and Wilkinson's catalyst (15 mol%) were added under argon to 10 ml of a sugar–urea–salt melt at 90 °C. The mixture was degassed and flushed with dihydrogen three times. The reaction was stopped when no more dihydrogen was consumed. After cooling to room temp. the product was extracted with ethyl acetate, dried over

MgSO₄ and chromatographed on silica gel using hexane–ethyl acetate, 2 : 1, as eluent. The product was analyzed by ¹H and ¹³C NMR.

Suzuki reaction

All reactions were carried out in air and all chemicals were used as purchased. In a typical experiment 2.2 mmol of boronic acid, 2 mmol of the aryl bromide, 2.5 mmol of Na₂CO₃ and 0.4 mmol of Pd(OAc)₂ were added to 5 ml of a sugar–urea–salt melt at 90 °C. The reaction tube (10 ml) was sealed (caution: all necessary precaution should be taken when such experiments are performed, pressure may develop inside). The reaction was stirred for 6 h, and then cooled to room temperature. The product was extracted with pentane (6 × 2 ml); the solvent was evaporated and the product analyzed by ¹H and ¹³C NMR. All spectroscopic data match the values reported in the literature.²⁶

References

- 1 K. Tanaka and F. Toda, *Chem. Rev.*, 2000, **100**, 1025–1074.
- 2 R. S. Varma and Y. Ju, Solventless Reactions (SLR), in *Green Separation Processes*, ed. C. A. M Alfonso, J. G. Crespo, Wiley-VCH, Weinheim, 2005.
- 3 Limitations may arise from small reaction rates and the control of heat flow.
- 4 J. G. Watson, J. C. Chow and E. M. Fujita, *Atmos. Environ.*, 2001, **35**, 1567–1584.
- 5 R. A. Sheldon, *Green Chem.*, 2005, **7**, 267–278.
- 6 G. Imperato, *PhD Thesis*, University of Regensburg, 2006.
- 7 E. Eibler, J. Niedermaier and B. König, *Chem. Commun.*, 2005, 1170–1172.
- 8 C. Reichardt, *Chem. Rev.*, 1994, **94**, 2319.
- 9 A. J. Carmichael and K. R. Seddon, *J. Phys. Org. Chem.*, 2000, **13**, 591–595.
- 10 C. Reichardt, *Solvents and Solvent Effects in Organic Chemistry*, 3rd edn, Wiley-VCH, Weinheim, 2003.
- 11 J. B. Deye and T. A. Berger, *Anal. Chem.*, 1990, 615–622.
- 12 This in contrast to a hypsochromic shift of Reichardt's dye.
- 13 (a) M. J. Kamlet and R. W. Taft, *J. Am. Chem. Soc.*, 1976, **98**, 377–383; (b) M. J. Kamlet and R. W. Taft, *J. Am. Chem. Soc.*, 1976, **98**, 2886–2894; (c) M. J. Kamlet, J. L. Abboud and R. W. Taft, *J. Am. Chem. Soc.*, 1977, **99**, 6027–6038.
- 14 R. D. Gillard, E. D. McKenzie and M. D. Ross, *J. Inorg. Nucl. Chem.*, 1966, **28**, 1429.
- 15 H. Langhals, *Tetrahedron*, 1987, **43**, 1771–1773.
- 16 P. N. Nylander, Solvents in Catalytic Hydrogenations, in *Catalysis in Organic Synthesis*, ed. W. J. Jones, Academic Press, New York, 1980.
- 17 J. B. Arterburn, M. Pannala, A. M. Gonzales and R. M. Chamberlin, *Tetrahedron Lett.*, 2000, 7847–7849.
- 18 (a) R. Sheldon, *Chem. Commun.*, 2001, 2399–2407; (b) K. Anderson, P. Goodrich, C. Hardacre and D. W. Rooney, *Green Chem.*, 2003, 448–453; (c) P. G. Jessop, R. R. Stanley, R. A. Brown, C. A. Eckert, C. L. Liotta, T. T. Ngo and P. Pollet, *Green Chem.*, 2003, 123–128; (d) P. A. Z. Suarez, J. E. L. Dullius, S. Einloft, R. F. De Souza and J. Dupont, *Polyhedron*, 1996, 1227–1229; (e) P. A. Z. Suarez, J. E. L. Dullius, S. Einloft, R. F. De Souza and J. Dupont, *Inorg. Chim. Acta*, 1997, 207–209; (f) P. J. Dyson, D. J. Ellis, W. Henderson and G. Laurency, *Adv. Synth. Catal.*, 2003, 216–221; (g) Z. Baán, Z. Finta, G. Keglevich and I. Hermeicz, *Tetrahedron Lett.*, 2005, 6203–6204; (h) R. A. Brown, C. A. Eckert, C. L. Liotta, P. Pollet, E. McKoon and P. G. Jessop, *J. Am. Chem. Soc.*, 2001, **123**, 1254–1255.
- 19 (a) R. A. Brown, C. A. Eckert, C. L. Liotta, P. Pollet, E. McKoon and P. G. Jessop, *J. Am. Chem. Soc.*, 2001, **123**, 1254–1255; (b) P. G. Jessop, R. R. Stanley, R. A. Brown, C. A. Eckert, C. L. Liotta, T. T. Ngo and P. Pollet, *Green Chem.*, 2003, 123–128; (c) P. Stephenson, P. Licence, S. K. Ross and M. Poliakov, *Green Chem.*, 2004, 521–523; (d) J. Huang, T. Jiang, B. Han, T. Mu, Y. Wang, X. Li and H. Chen, *Catal. Lett.*, 2004, 225–228.
- 20 (a) J. Hassan, M. Sévignon, C. Gozz, E. Schulz and M. Lemaire, *Chem. Rev.*, 2002, **102**, 1359–1470; (b) A. Suzuki, *J. Organomet. Chem.*, 1999, **576**, 147–168.
- 21 N. Miyaura and A. Suzuki, *Chem. Rev.*, 1995, **95**, 2457–2483.
- 22 R. K. Arvela, N. E. Leadbeater, M. S. Sangi, V. A. Williams, P. Granados and R. D. Singer, *J. Org. Chem.*, 2005, **70**, 161–168.
- 23 (a) N. E. Leadbeater and M. Marco, *J. Org. Chem.*, 2003, **68**, 888–892; (b) L. Bai, J. Wang and Y. Zhang, *Green Chem.*, 2003, 615–617.
- 24 (a) L. Bai and J. X. Wang, *Curr. Org. Chem.*, 2005, 535–553; (b) D. Prajapati and M. Gohain, *Tetrahedron*, 2004, 815–833; (c) T. R. Early, R. S. Gordon, M. A. Carroll, A. B. Holmes, R. E. Shute and I. F. McCovey, *Chem. Commun.*, 2001, 1966–1967.
- 25 (a) R. Rajagopal, D. V. Jarikote and K. V. Srinivansan, *Chem. Commun.*, 2002, 616–617; (b) C. J. Mathews, P. J. Smith and T. Welton, *Chem. Commun.*, 2005, 1249–1250; (c) J. McNulty, A. Carpetta, J. Wilson, J. Dyck, G. Adjabeng and A. Robertson, *Chem. Commun.*, 2002, 1986–1987; (d) G. Zou, Z. Wang, J. Zhu, J. Tang and M. Y. He, *J. Mol. Catal. A*, 2003, 193–198; (e) F. McLachlan, C. J. Mathews, P. J. Smith and T. Welton, *Organometallics*, 2003, 5350–5357.
- 26 *Biphenyl*: (a) R. Leardini, D. Nanni, I. Nicolson and D. Reed, *J. Chem. Soc., Perkin Trans. 1*, 2001, 1079–1085; *4-methylbiphenyl*: (b) A. Zapf, A. Ehrentraut and M. Beller, *Angew. Chem., Int. Ed.*, 2000, **39**, 4153–4155; *2,6-dimethylbiphenyl*: (c) J. P. Wolfe, R. A. Singer, B. H. Yang and S. L. Buchwald, *J. Am. Chem. Soc.*, 1999, **121**, 9550–9561.

Solid acid catalyzed biodiesel production by simultaneous esterification and transesterification

Mangesh G. Kulkarni, Rajesh Gopinath, Lekha Charan Meher and Ajay Kumar Dalai*

Received 21st April 2006, Accepted 25th August 2006

First published as an Advance Article on the web 15th September 2006

DOI: 10.1039/b605713f

12-Tungstophosphoric acid (TPA) impregnated on four different supports such as hydrous zirconia, silica, alumina and activated carbon was evaluated as solid acid catalysts for the biodiesel production from low quality canola oil containing upto 20 wt% free fatty acids. The hydrous zirconia supported TPA was found to be the most promising catalyst exhibiting the highest ester yield (~77%). The FTIR, XRD and nitrogen adsorption analysis revealed that the Lewis acid sites generated by the strong interaction of TPA and surface hydroxyl groups of zirconia are responsible for their higher activity. Further, the optimization of reaction parameters was carried out with the most active catalysts *i.e.* TPA supported hydrous zirconia and it was found that at 200 °C, 1 : 9 oil to alcohol molar ratio and 3 wt% catalysts loading a maximum ester yield of 90 wt% could be obtained. The catalysts were recycled and reused with negligible loss in activity.

Introduction

Alternative fuels developed from renewable feedstocks are gaining market share recently. Biodiesel which is recognized as 'green fuel' is one of such alternative fuel produced from vegetable oils. In spite of all the advantages such as low emissions, biodegradable, non-toxic, and better lubricity, biodiesel is not yet commercialized all over the world. The major hurdle in commercialization of biodiesel is higher cost of biodiesel than petro-diesel due to higher cost of virgin oil.¹ Use of low quality feedstocks such as waste cooking oils which are available cheaply, instead of neat vegetable oil will help in improving the economical feasibility of biodiesel. The amount of waste cooking oil generated in each country varies, depending on the use of vegetable oil. An estimate of the potential amount of waste cooking oil from the collection in European Union (EU) is approximately 0.7 to 1.0 Mt per year. In United States and Canada on an average 9 and 8 pounds per person of yellow grease are produced, respectively.^{1,2} Thus, substantial amount of biodiesel can be produced from this economical feedstock which would partly decrease the dependency on petroleum-based fuel.

The production of biodiesel from low quality oils is challenging due to the presence of undesirable components especially free fatty acids (FFAs) and water. Usage of homogeneous base catalyst for transesterification of such feedstock suffers from serious limitation of formation of undesirable side reaction such as saponification which creates serious problem of product separation and ultimately lowers the ester yield substantially.³ Homogeneous acid catalysts have the potential to replace base catalysts since they do not show measurable susceptibility to FFAs and can catalyze esterification and

transesterification simultaneously. However, requirement of high temperature, high molar ratio of oil and alcohol, separation of the catalyst, serious environmental and corrosion related problems make their use non-practical for biodiesel production.⁴

Solid acid catalysts have the strong potential to replace liquid acids, eliminating separation, corrosion and environmental problems. Recently a review is published that elaborates the importance of solid acids for biodiesel production.⁴ Solid acids having interconnected system of large pores, a moderate to strong acid sites and a hydrophobic surface would be ideal for biodiesel preparation.⁴

Heteropolyacids (HPA) and their salts are a class of highly acidic polyoxometalates compounds made up of heteropolyanions having metal-oxygen octahedral as the basic structural unit.⁵ The HPA having Keggin structure is thermally stable and easy to synthesize than other HPAs. The major disadvantages of keggins-type HPA such as low specific surface areas and solubility in polar media can be overcome by dispersing it on high surface area supports.

To date, most of the studies on biodiesel synthesis have been focussed on either base-catalyzed or homogenous acid catalyst system employing refined vegetable oils. Apart from few reports^{6,7} on solid acid catalyzed esterification and transesterification of model compounds, to our knowledge utilization of solid acids for biodiesel production from low quality real feedstocks has not been explored. Therefore in an attempt to develop a strong solid acid catalyst that can simultaneously catalyze esterification as well as transesterification reactions, 12-tungstophosphoric acid (TPA), one of the highest acidic Keggin-type HPAs were impregnated on various supports such as hydrous zirconia (HZ), silica (Si), alumina (Al) and activated carbon (AC).

In the present work, the activity of supported TPA was evaluated for the biodiesel preparation from canola oil containing 10 and 20 wt% FFA. Influence of various reaction

Catalysis and Chemical Reaction Engineering Laboratories, Department of Chemical Engineering, University of Saskatchewan, Saskatoon, SK, Canada S7N 5C5. E-mail: ajay.dalai@usask.ca; Fax: +1 306-966-4777; Tel: +1 306-966-4771

parameters such as reaction temperature, molar ratio of oil to alcohol, catalyst loading and amount of FFA on activity of most efficient catalyst was also studied.

Experimental

Reagents

Canola oil was obtained from local grocery shop. Methanol (99.8%), oleic acid (90%), methyl oleate, tri-olein, di-olein, mono-olein, glycerol were obtained from Sigma–Aldrich, MO, USA. 12-Tungstophosphoric acid (TPA) of AR grade was purchased from BDH chemicals Ltd, England. All the supports, except zirconia were obtained from commercial sources. γ -Alumina was obtained from Sud-chemie India Ltd., Delhi, India. Silica and activated carbon were obtained from Engelhard and Envirotrol, NJ, USA, respectively.

Catalyst preparation

HZ was prepared by the hydrolysis of $ZrOCl_2 \cdot 8H_2O$ by adding aqueous ammonia to a pH of up to 9. The gel was washed with deionized water until no chloride ion was detected by silver nitrate solution. The zirconium oxyhydroxide was then dried at 120 °C for 12 h, powdered well and dried for another 12 h. Silica, alumina, activated carbon and hydrous zirconia supported 12-tungstophosphoric acid of 10 and 20 wt% were prepared by impregnation method. The material thus obtained was dried at 110 °C overnight and finally calcined at 300 °C for 5 h.

Catalyst characterization

Specific surface area and pore size measurements of the catalysts were performed using Micrometrics adsorption equipment (Model ASAP 2000) at 78 K using liquid nitrogen. Prior to the analysis the catalyst was evacuated at 200 °C in a vacuum of 5×10^{-4} atm to remove all adsorbed moisture from the catalyst surface and pores. XRD analysis was performed using Rigaku diffractometer (Rigaku, Tokyo, Japan) using Cu K α radiation at 40 kV and 130 mA in the scanning angle (2θ) of 5–70° at a scanning speed of 10° min⁻¹. The FTIR spectra of the catalysts were obtained using Perkin Elmer FTIR spectrum GX. Samples for the FTIR analysis were prepared by compressing a well mixed 3 mg of catalyst powder with 200 mg of KBr. The nature of acid sites (Brønsted and Lewis) of the catalysts was distinguished by *in situ* infrared (FTIR) spectroscopy with chemisorbed pyridine. The catalyst sample was placed in a designed cell and heated *in situ* from room temperature to 400 °C in a flowing stream of pure N₂. The sample was kept at 400 °C for 3 h and then cooled to 100 °C. Pyridine vapour was introduced in flowing nitrogen and the spectra were recorded from 1400–1700 cm⁻¹. The elemental composition of W and P in the catalysts was determined by inductivity coupled plasma-mass spectrometer (ICP-MS).

Transesterification of canola oil and analysis of the products

Canola oil containing 10% free fatty acids (FFAs) was prepared manually by mixing 90 parts of canola oil and

10 parts of oleic acid. Transesterification of canola oil having 10% FFAs using supported TPA as a catalyst was carried out in a 500 cc Parr reactor (Parr Instrument Co.) equipped with a temperature controller. Initially the reactor was charged with 100 g of canola oil and heated to the desired temperature with optimized stirring at 600 rpm. Methanol and catalyst were added to the reaction vessel. Depending on reaction temperature, the reactor was pressurized to ensure that at the desired reaction temperature the reactants are in the liquid phase. For example, at reaction temperature of 200 °C, pressure of 600 psi was chosen. All the reactions were carried out for a reaction time of 10 h unless otherwise stated. Samples taken at regular time interval were analyzed using gel permeation chromatography (GPC) equipped with a RI detector and two 300 × 7.8 mm phenogel columns connected in series. HPLC grade tetrahydrofuran (THF) was used as a mobile phase. Triglycerides, diglycerides, monoglycerides and methyl esters in transesterified product were quantified by comparing the peak areas of their corresponding standards.

Results and discussion

The textural properties of the catalysts are summarized in Table 1. Pure TPA, hydrous zirconia, silica, alumina and activated carbon showed a surface area of 8, 221, 218, 223, and 1003 m² g⁻¹, respectively. The total pore volume and their average pore diameter also varied in the wide range of 14 to 118 Å. TPA loading of 10 and 20 wt% produced a decrease in the accessible area and pore diameter of all the supports except activated carbon. The effect was significant in the case of silica, hydrous zirconia and alumina which were attributed to pore plugging of the supports. In the case of activated carbon the micropores are in majority and were too narrow to accommodate a big TPA molecule. These results indicate that TPA were immobilized in the channels of alumina, zirconia and silica and dispersed in a monolayer on the surface.^{8,9}

The XRD patterns of pure TPA and supported TPA catalysts are as shown in Fig. 1. The XRD spectrum of pure TPA exhibited characteristic crystalline peaks of TPA (intense peak at $2\theta = 10^\circ$) and coincided with those previously reported.¹⁰ In the case of supported TPA only the XRD patterns of silica supported TPA catalysts displayed peaks

Table 1 Textural properties of various catalysts

Catalysts	TPA wt%	Surface area m ² g ⁻¹	Average pore volume cc g ⁻¹	Average pore diameter Å
Pure TPA	—	8	—	20.7
Hydrous zirconia (HZ)	—	221	0.12	23.0
TPA/HZ	10	146	0.08	21.8
	20	143	0.07	21.8
SiO ₂	—	218	0.21	29.0
TPA/SiO ₂	10	177	0.17	28.0
	20	137	0.12	27.4
Alumina	—	223	0.72	118.0
TPA/Al ₂ O ₃	10	207	0.59	107.0
	20	193	0.46	95.7
Activated carbon (AC)	—	1003	0.46	14
TPA/AC	10	990	0.53	14.3
	20	997	0.59	14.0

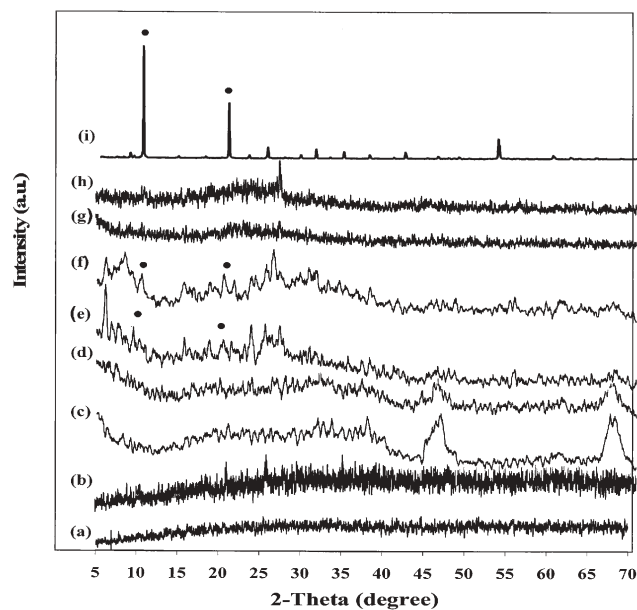


Fig. 1 XRD diffraction patterns of pure and supported TPA catalyst. (a) 10% TPA/HZ, (b) 20% TPA/HZ, (c) 10% TPA/Al₂O₃, (d) 20% TPA/Al₂O₃, (e) 10% TPA/SiO₂, (f) 20% TPA/SiO₂, (g) 10% TPA/AC, (h) 20% TPA/AC, (i) Pure TPA.

corresponding to TPA. However, hydrous zirconia, alumina and activated carbon supported TPA displayed no indication of any crystalline phases related to TPA indicating that the particles are too small or well dispersed to be detected by XRD technique. These results are indicative of a stronger interaction between TPA and alumina, activated carbon and hydrous zirconia. Lopez-Salinas also made similar observation from XRD analysis of TPA supported on silica and zirconia and reported that the interaction between TPA and zirconia surface is stronger than those in silica.¹⁰

The FTIR spectrum of supported TPA catalysts is shown in Fig. 2. Pure TPA exhibited typically three major IR bands located at 1080, 985 and 890 cm⁻¹ attributed to absorption modes of Keggin ion [PW₁₂O₄₀]³⁻. The bands at 1080, 985 and 890 cm⁻¹ are associated to the stretching modes of oxygen atom bonded to tungsten and phosphorus assigned to γ (W=O); γ (P-O) and γ (W-O-W) edge, respectively.^{11,12} In supported TPA catalysts no clear absorption bands of Keggin structure were visible even with 20 wt% TPA loading. These results clearly indicated that TPA is highly dispersed on the surface of supports. It should also be noted that the peaks of support HZ and Al overlap with those of TPA. Jin *et al.*⁸ also noticed no clear peaks of TPA even with 60 wt% loading when supported on silica and MCM-41.

The FTIR spectra of adsorbed pyridine were recorded from 1400 to 1700 cm⁻¹ to distinguish the type of acid sites (Lewis or Brønsted) on the catalyst (Fig. 3). The FTIR spectra of adsorbed pyridine on pure TPA showed typically intense bands at 1533, 1638 and 1545 cm⁻¹ characterized by Brønsted type acidity.¹³ The intense band at 1485 cm⁻¹ is ascribed to both Lewis and Brønsted acid sites.¹³ Also, very weak bands can be seen at 1441 cm⁻¹ related to Lewis acidity. The FTIR spectra of adsorbed pyridine on supported catalysts showed

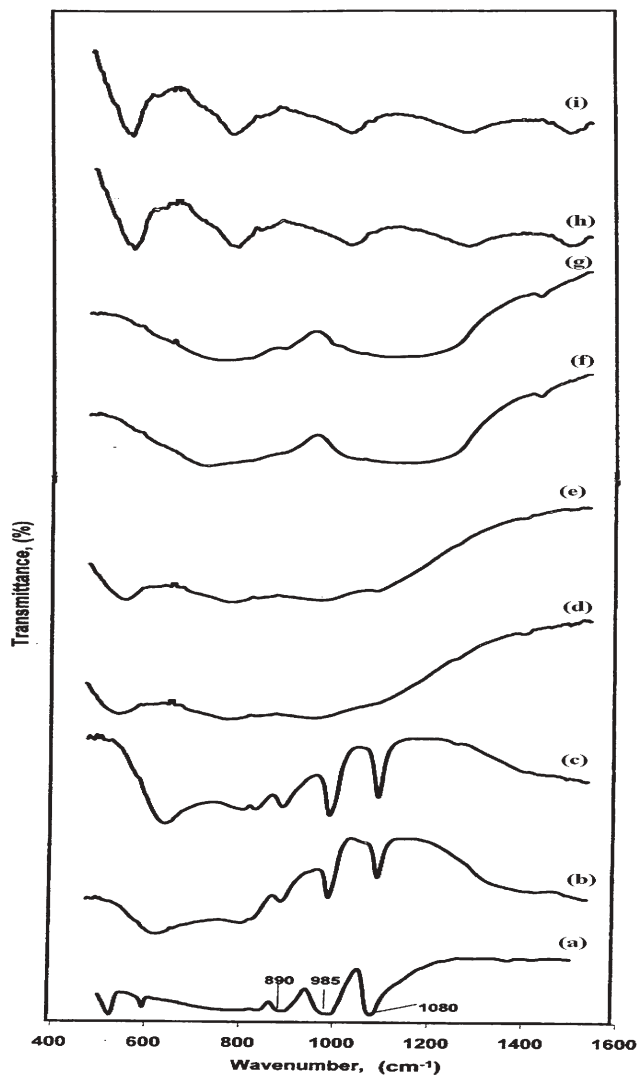


Fig. 2 FTIR spectra of supported and pure TPA catalysts. (a) Pure TPA, (b) 10% TPA/HZ, (c) 20% TPA/HZ, (d) 10% TPA/Al₂O₃, (e) 20% TPA/Al₂O₃, (f) 10% TPA/SiO₂, (g) 20% TPA/SiO₂, (h) 10% TPA/AC, (i) 20% TPA/AC.

predominantly intense bands around 1441 cm⁻¹ ascribed to strong Lewis acidity and very weak bands at 1533, 1545 cm⁻¹ due to Brønsted sites. Also the band at 1485 cm⁻¹ is visible. It appears that during the process of impregnation of TPA on alumina, silica, hydrous zirconia and activated carbon and calcinations, the hydroxyl groups (OH) of support react with TPA protons to form water thereby decreasing the Brønsted acid sites in the catalysts.¹⁰

The XRD, FTIR and nitrogen adsorptions measurements indicate the existence of a strong interaction particularly between TPA and -OH groups in hydrated zirconia. The stronger interaction of ≡ZrOH groups with Keggin units lead to the formation of (≡Zr-OH₂)_n⁺[H_{3-n}W₁₂PO₄₀]ⁿ⁻³ or (≡Zr-O)_n⁻{H_{3-n}W₁₂PO_{40-n}} as reported by Lopez-Salinas *et al.*¹⁰ These TPA species form bonds of type Zr-O-W after the process of calcination and would exert an electron withdrawing effect on surface Zr⁴⁺ cations making them to behave as strong Lewis acid sites.

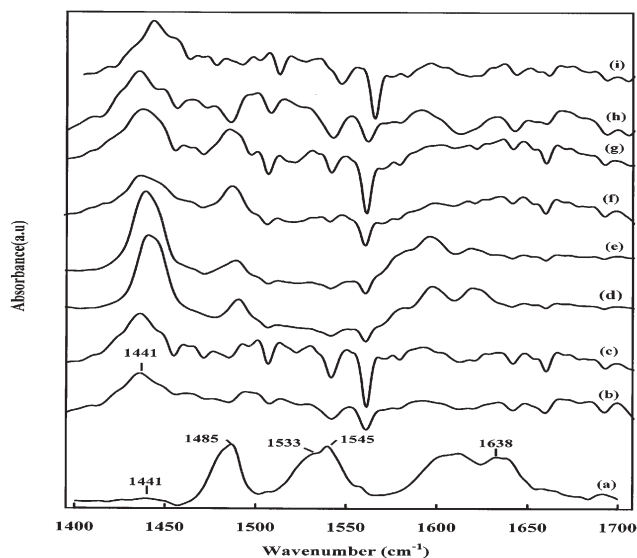


Fig. 3 FTIR spectra of pyridine adsorbed on pure and supported TPA catalysts. (a) Pure TPA, (b) 10% TPA/HZ, (c) 20% TPA/HZ, (d) 10% TPA/Al₂O₃, (e) 20% TPA/Al₂O₃, (f) 10% TPA/SiO₂, (g) 20% TPA/SiO₂, (h) 10% TPA/AC, (i) 20% TPA/AC.

The prepared catalysts *i.e.* 10 and 20 wt% TPA supported on alumina, silica, hydrous zirconia and activated carbon were screened for the transesterification of canola oil containing 10% FFA under identical reaction conditions such as reaction temperature of 200 °C, molar ratio of oil to alcohol 1 : 6 and 3% w/w catalyst loading. The best catalysts were selected on the basis of maximum ester yield. The TPA supported on alumina, silica and activated carbon exhibited almost similar ester yield of about ~65 wt%. TPA supported on hydrous zirconia (TPA/HZ) was the most active catalyst showing ~77 wt% ester yield irrespective of the TPA loading (Fig. 4).

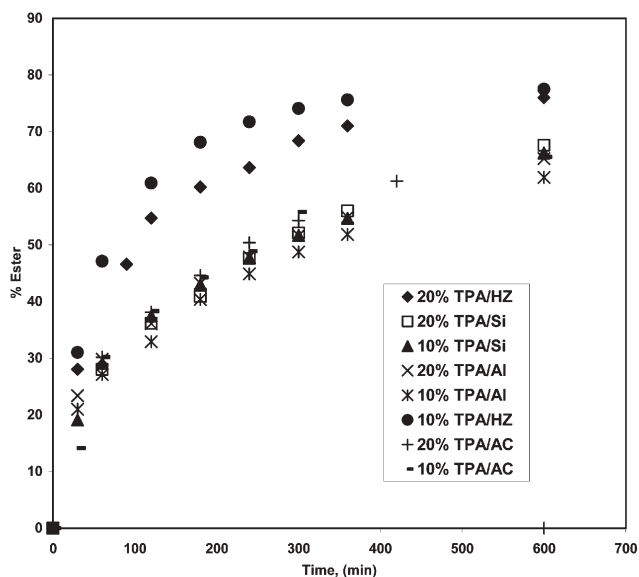
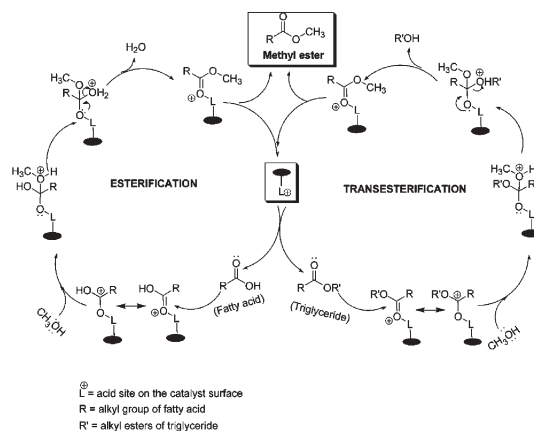


Fig. 4 Screening of supported TPA for biodiesel production from canola oil. Reaction conditions: reaction temperature 200 °C, molar ratio of oil to alcohol 1 : 6, stirring speed 600 rpm, catalyst loading 3% w/w.

The higher activity of zirconia supported TPA catalysts compared to other supports could be due to the Lewis acidity arising due to the stronger interactions between TPA and -OH groups of zirconia. It is believed that the Lewis acidity arising due to electron withdrawing effects on the surface Zr⁴⁺ is similar to that existing in the sulfated zirconia. The comparatively lower ester yields in alumina supported TPA could be due to its surface basicity. Even though alumina is an interacting support, it is assumed that the surface basicity could bring about the decomposition of TPA.^{14,15} The intense Lewis acidic peaks observed in alumina supported TPA catalysts in Fig. 3 could be mainly related to the Lewis acidity of the alumina itself. In the case of silica supported TPA, the interaction of TPA and silica surface is much weaker than that of ZrO₂ decreasing the possible formation of stronger Lewis acidic sites as observed in hydrous zirconia. The lower ester yield observed in activated carbon supported TPA catalysts could be related to a larger molecular size of the oil compared to the pore diameter of the catalyst. It can be observed from Table 1 that the TPA/AC has the smallest pore diameter compared to other supported catalysts. Literature studies also support this observation; as reactant molecule size was found to exert a marked influence on the heterogeneous reactions catalyzed by heteropolyacids supported on activated carbon.¹⁶

The reaction mechanism of simultaneous esterification and transesterification using Lewis acid is as shown in Scheme 1. The esterification takes place between free fatty acids (RCOOH) and methanol (CH₃OH) whereas transesterification takes place between monoglyceride (RCOOR') (taken as representative of triglycerides in this case) and methanol adsorbed on acidic site (L⁺) of catalyst surface. The interaction of the carbonyl oxygen of free fatty acid or monoglyceride with acidic site of the catalyst forms carbocation. The nucleophilic attack of alcohol to the carbocation produces a tetrahedral intermediate (Scheme 1). During esterification the tetrahedral intermediate eliminates water molecule to form one mole of ester (RCOOCH₃). The transesterification mechanism can be extended to tri- and di-glyceride. It is well known that transesterification is a stepwise reaction. In the reaction sequence the triglyceride is converted stepwise to di- and monoglyceride and finally glycerol. The tetrahedral intermediate formed during reaction eliminates di-, monoglyceride and



Scheme 1

glycerol when tri-, di- and monoglyceride come in contact with the acidic sites, respectively, to give one mole of ester (RCOOCH_3) in each step. In both cases, esterification and transesterification, the final product, methyl ester is the same. Also, as shown in Scheme 1, the catalyst is regenerated after the simultaneous esterification and transesterification reactions. Use of excess alcohol favours forward reaction and thus maximizes the ester yield.

Thus, based on highest activity towards both esterification and transesterification 10% TPA/HZ catalyst was selected further to study in detail the effect of various reaction parameters on ester yield.

Influence of reaction parameters

Reaction temperature. The reaction was carried out at 150, 200 and 225 °C to evaluate the influence of reaction temperature. Reaction pressure was adjusted accordingly to ensure that, at this reaction temperature the reactants were in the liquid phase. Other reaction parameters were molar ratio of oil to alcohol 1 : 6, stirring rate 600 rpm, and 3% w/w catalyst loading. As expected, the ester yield increased with the temperature (Fig. 5). However, when the reaction was carried out above 200 °C, the GPC analysis showed an additional peak before the methyl ester. This additional peak was related to the polymeric products formed by the degradation of triglycerides and unsaturated fatty acids due to exposure of oil to high temperature (225 °C) for 10 h. This additional peak was not observed when the reaction was carried out at lower temperature of 150 and 200 °C. As formation of polymeric compounds is not desirable during biodiesel production, the optimum reaction temperature was fixed at 200 °C for further studies.

Catalyst loading. The effect of TPA/HZ loading (1, 3 and 5% w/w) on ester yield during the transesterification of canola oil containing 10% FFA with methanol is studied. The molar

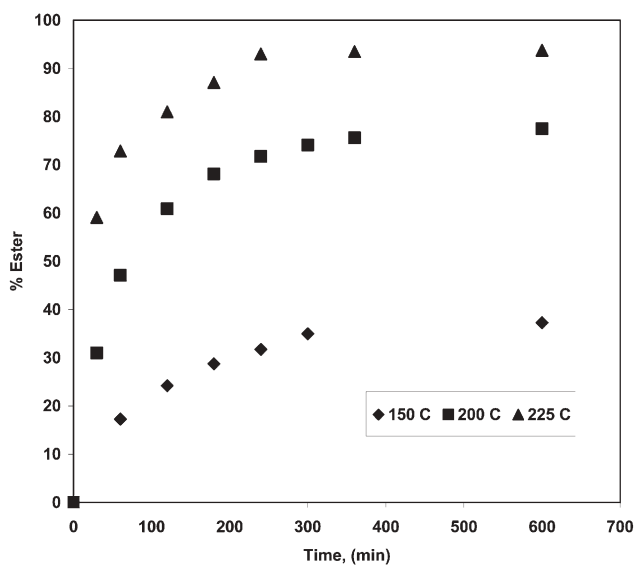


Fig. 5 Effect of temperature on ester yield using 10% TPA/HZ as a catalyst. Reaction conditions: molar ratio of oil to alcohol 1 : 6, stirring speed 600 rpm, catalyst loading 3% w/w.

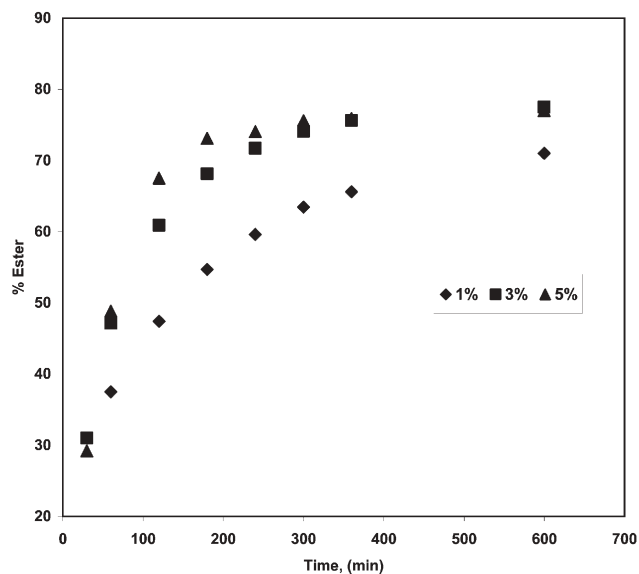


Fig. 6 Effect of catalyst loading on ester yield using 10% TPA/HZ as a catalyst. Reaction conditions: reaction temperature 200 °C, molar ratio of oil to alcohol 1 : 6, stirring speed 600 rpm.

ratio of oil to alcohol of 1 : 6 was used for the reaction. Increase in catalyst loading from 1 to 3% w/w showed substantial effect on conversion of triglycerides and fatty acids as the ester yield increased from 71 to 77 wt% (Fig. 6). However, when the catalyst loading was further increased to 5% w/w, the initial rate of the reaction increased but the final yield of the ester was similar to that obtained with 3% w/w catalyst loading. Thus, it is clear that increase in catalyst loading above 3% w/w did not help to improve the ester yield. The reaction was studied with 3% w/w of catalyst loading for further optimization of the reaction parameters.

Molar ratio of alcohol to oil. The methanol to oil molar ratio is one of the important parameters that affect the yield of methyl esters. Theoretically, the transesterification of vegetable oil requires 3 moles of methanol per mole of triglyceride. Since transesterification of triglyceride is a reversible reaction, the excess of methanol shifts the equilibrium towards the direction of ester formation. Freedman *et al.*³ suggested that 6 : 1 molar ratio of alcohol to oil is necessary to get the maximum ester yield thus minimizing the concentration of tri- di- and monoglycerides.

Transesterification reaction catalyzed by heterogeneous catalysts is well known for their slow reaction rates. In order to improve the rate of this reaction, usage of excess alcohol is one of the better options. Literature studies reveal that use of higher molar ratios of oil to alcohol such as 1 : 15, 1 : 40, and even 1 : 275 can improve the rate of transesterification reaction catalyzed by heterogeneous catalyst.¹⁷⁻¹⁹

In the present work, increase in the oil to alcohol molar ratio from 1 : 6 to 1 : 9 resulted a significant effect on the ester yield. The yield increased from 77 to 90 wt% after 10 h, however further increase in oil to alcohol ratio to 1 : 15 did not show any significant effect on the ester yield (Fig. 7). The excess methanol used in the reaction can be collected and reused.

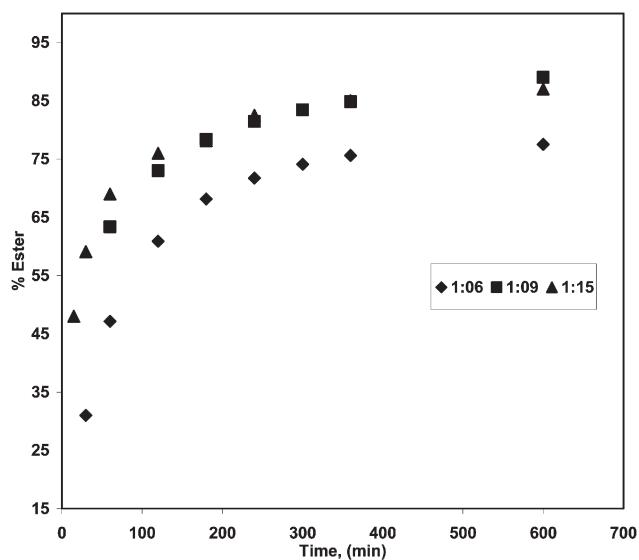


Fig. 7 Effect of oil to alcohol molar ratio on ester yield using 10% TPA/HZ as a catalyst. Reaction conditions: reaction temperature 200 °C, stirring speed 600 rpm, catalyst loading 3% w/w.

Free fatty acid content of oil. The presence of higher amounts of free fatty acids may have adverse effects on the catalyst activity or the ester yield. The effect of free fatty acids level on the ester yield was studied by adding 10 and 20 wt% of oleic acid to pure canola oil. The reaction was performed using the optimized reaction conditions such as reaction temperature of 200 °C, molar ratio of oil to alcohol 1 : 9, and 3% w/w catalyst loading.

It is quite interesting to note that the yield of ester increased with increase in free fatty acids to 20%, clearly indicating the simultaneous occurrence of esterification and transesterification reaction. Fig. 8 shows that after 10 h of reaction, the yield of esters reached 92 wt% when FFA content of canola oil was

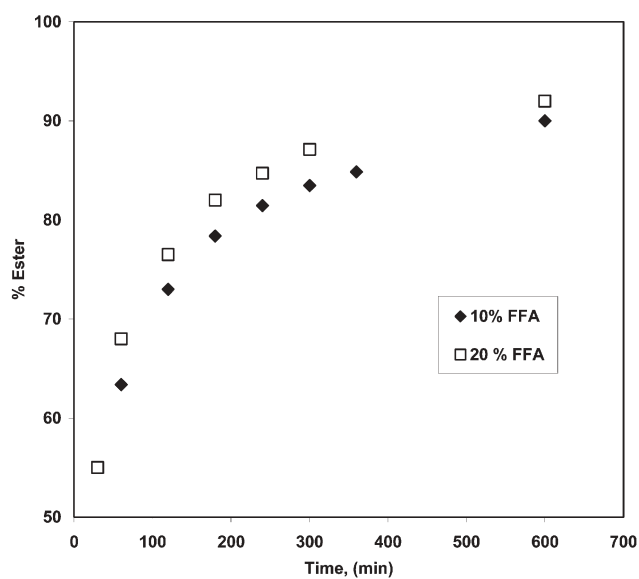


Fig. 8 Effect of free fatty acids on ester yield using 10% TPA/HZ as a catalyst. Reaction conditions: reaction temperature 200 °C, molar ratio of oil to alcohol 1 : 9, stirring speed 600 rpm, catalyst loading 3% w/w.

20 wt%. The increase in the ester yield in the presence of 20% oleic acid was due to the higher esterification rate of oleic acid compared to transesterification of triglycerides. This might be due to two possible reasons. First, fatty acids, particularly unsaturated ones, are more soluble in alcohol than triglycerides, therefore the reaction proceeded faster. The second reason is probably related to the reaction mechanism of esterification and transesterification. Methanolysis of FFAs proceeds *via* simple esterification while triglycerides proceed *via* transesterification which consists of number of consecutive, reversible reactions. Due to these reasons, the rate of transesterification of triglycerides is slower than esterification of fatty acids. Similar observation about the lower rate of transesterification than esterification was also made by Warabi *et al.*²⁰ Thus, it can be concluded from these results that the activity of TPA supported on hydrous zirconia (HZ) was not affected by the presence of higher amounts of free fatty acids even up to 20%. Nor was the activity of the catalyst affected by the water produced during the esterification of free fatty acids and alcohol. This finding has commercial importance as yellow grease, which is a potential feedstock for biodiesel production, contains free fatty acids up to 15% and synthesis of biodiesel from this feedstock using conventional catalysts is quite difficult.

Catalyst recycling. The catalyst recycling is an important step as it reduces the cost of the process. The efficiency of the catalysts also depends on its reusability. In order to prove the reusability, the TPA/HZ catalyst was filtered from the reaction mixture and then was initially soaked in hexane overnight to remove any non-polar compounds such as methyl esters present on the surface. Further, the catalyst was soaked in methanol to remove the polar compounds such as glycerol. Finally, the catalyst was dried overnight and used for transesterification. Reaction of canola oil containing 10% FFA with methanol was carried out using 3% w/w fresh and spent catalyst, 1 : 6 molar ratio of oil to alcohol and reaction temperature of 200 °C. Fig. 9 shows the ester yield obtained using 3% w/w fresh and spent catalyst. The reusability results revealed that the activity of the spent and fresh catalyst was almost the same clearly demonstrating the efficiency of the catalysts. The activity of the spent catalyst could be regenerated as there is a negligible loss in TPA after the reaction. This was confirmed by ICP-MS analysis of W and P content of fresh and regenerated catalyst as shown in Table 2.

Based on our studies on synthetic feedstock (canola oil containing ~20% FFA), it can be concluded that TPA/HZ catalyst can also be used for the synthesis of biodiesel from high free fatty acid containing feedstocks such as karanja (*Pongamia Pinnata*) (~7–8% FFA), rice bran (~15–20% FFA) and tall oil (~70% FFA). However, waste cooking oil is a complex mixture of many compounds including FFA and water. The nature of impurities present in waste cooking oil is not well known as its quality is not consistent and changes from one source to another depending on the degree of heating, type of oil and food used during cooking. The activity of the catalysts in the presence of various impurities present in waste cooking oil is quite important and needs to be investigated.

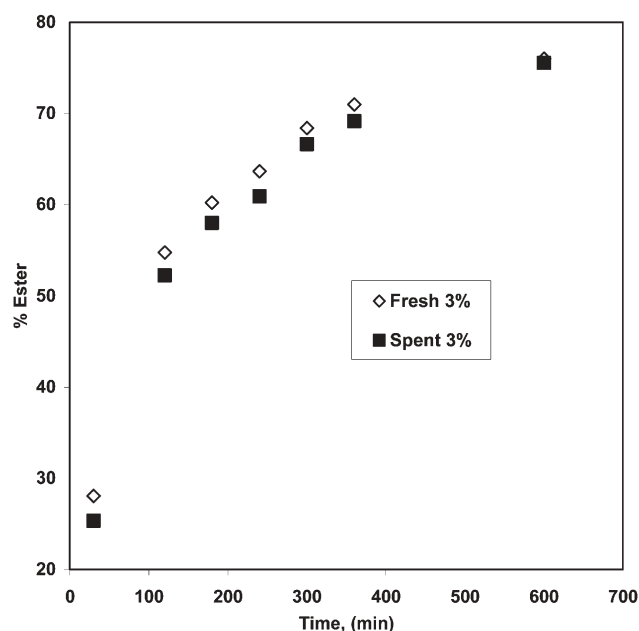


Fig. 9 Reusability of the spent catalyst 10% TPA/HZ. Reaction conditions: reaction temperature 200 °C, molar ratio of oil to alcohol 1 : 6, stirring speed 600 rpm, catalyst loading 3% w/w.

Table 2 Metal content in fresh and spent catalyst

Catalyst type	Metal content/ppm	
	Phosphorus	Tungsten
TPA/HZ (Fresh)	1385	119471
TPA/HZ (Spent)	1374	119448

^a Condition: Both catalysts are with 20% TPA loading.

In summary, the present study showed that hydrous zirconia supported 12-tungstophosphoric acid is a non-toxic, inexpensive, recyclable and a promising eco-friendly catalyst for the production of biodiesel from low quality oils containing high free fatty acids. This catalyst has potential for widespread applications in academic and industrial scale production of biodiesel from oils containing high FFA.

Acknowledgements

The financial support for this project from BIOCAP, Canada and Natural Sciences and Engineering Research Council of Canada (NSERC) and Canada Research Chair (CRC) funding to Dr A. K. Dalai is gratefully acknowledged.

References

- 1 M. G. Kulkarni and A. K. Dalai, *Ind. Eng. Chem. Res.*, 2006, **45**, 2901.
- 2 B. E. Holbein, J. D. Stephen and D. B. Latzell, Canadian Biodiesel Initiative, Final Report by Biocap Canada, Kingston, Ontario, 2004.
- 3 B. Freedman, E. H. Pryde and T. L. Mounts, *J. Am. Oil Chem. Soc.*, 1984, **61**(10), 1638.
- 4 E. Lotero, Y. Liu, D. E. Lopez, K. Suwannakarn, D. A. Bruce and J. G. Goodwin, *Ind. Eng. Chem. Res.*, 2005, **44**, 5353.
- 5 Biju M. Devassy and S. B. Halligudi, *J. Catal.*, 2005, **236**, 313.
- 6 Anton A. Kiss, Alexandre C. Dimian and Gadi Rothenberg, *Adv. Synth. Catal.*, 2006, **348**, 75.
- 7 Dora E. Lopez, James G. Goodwin Jr., David A. Bruce and Edgar Lotero, *Appl. Catal., A*, 2005, **295**, 97.
- 8 Dingfeng Jin, Zhaoyin Hou, Yongming Luo and Xiaoming Zheng, *J. Mol. Catal. A: Chem.*, 2006, **243**, 233.
- 9 A. D. Newman, A. F. Lee, K. Wilson and N. A. Young, *Catal. Lett.*, 2005, **102**, 45.
- 10 E. Lopez-Salinas, J. G. Hernandez-Cortez, I. Schifter, E. Torres-Garcia, J. Navarrete, A. Gutierrez-Carrillo, T. Lopez, P. P. Lottici and D. Bersani, *Appl. Catal., A*, 2000, **193**, 215.
- 11 M. Misono, *Catal. Rev. Sci. Eng.*, 1987, **29**, 269.
- 12 J. H. Sepulveda, J. C. Yori and C. R. Vera, *Appl. Catal.*, 2005, **288**, 18.
- 13 E. P. Parry, *J. Catal.*, 1963, **2**, 374.
- 14 S. Igarashi, T. Matsuda and Y. Ogino, *J. Jpn. Petrol. Ins.*, 1979, **22**, 331.
- 15 S. Igarashi, T. Matsuda and Y. Ogino, *J. Jpn. Petrol. Ins.*, 1980, **23**, 30.
- 16 L. R. Pizzio, P. G. Vazquez, C. V. Caceres, M. N. Blanco, E. N. Alesso, M. I. Erlich, R. Torviso, L. Finkielstein, B. Lantano, G. Y. Moltrasio and J. M. Aguirre, *Catal. Lett.*, 2004, **93**, 67.
- 17 W. Xie, H. Peng and L. Chen, *J. Mol. Catal. A: Chem.*, 2005, **246**, 24.
- 18 S. Furuta, H. Matsuhashi and K. Arata, *Catal. Commun.*, 2004, **5**, 721.
- 19 E. Leclercq, A. Finiels and C. Moreau, *J. Am. Oil Chem. Soc.*, 2001, **11**, 1161.
- 20 Y. Warabi, D. Kusdiana and S. Saka, *Bioresour. Technol.*, 2004, **91**, 283.

A green method for synthesis of radioactive gold nanoparticles

Kamalika Roy and Susanta Lahiri*

Received 20th April 2006, Accepted 25th August 2006

First published as an Advance Article on the web 15th September 2006

DOI: 10.1039/b605625c

Radioactive gold-198 nanoparticles have been synthesized using a green and chemically safe solvent, PEG 4000. In the present investigation, $^{198}\text{Au}(\text{III})$ has been quantitatively extracted by the PEG-rich phase without addition of any other extractant. Extraction is quantitative even at very high gold concentration (50 mM) and after extraction Au(III) is reduced to Au(0) forming radioactive gold nanoparticles. The PEG-rich phase containing radioactive gold nanoparticles has been characterized by UV-visible spectroscopy and the actual size has been determined using transmission electron microscopy (TEM).

Introduction

To date the most widely studied nanoparticles have been those made of metals, semiconductors and magnetic materials. Gold exhibits a unique catalytic nature and action when it is present as nanoparticles. A variety of methods including chemical, thermal, electrochemical and sonochemical pathways have so far been developed for the synthesis of gold nanoparticles.^{1–3} Radiolysis by γ -irradiation has also been used to synthesize nanoparticles in some cases. For example, gold nanoparticles were prepared in a quaternary ammonium-based ionic liquid under γ -irradiation using a total dose of 10.0 kGy (dose rate: 19.6 Gy min^{-1} for 8.5 h).⁴ However, to the best of our knowledge, the use of a radioactive isotope of a metal for synthesizing radioactive nanoparticles has not yet been explored.

In this work our aim is to study the distribution of ^{198}Au or bulk gold spiked with ^{198}Au in an aqueous biphasic system (ABS) consisting of PEG 4000 solution (50% w/w) and a suitable salt-rich phase keeping in mind that radiolytic products of water and glycol may have some reducing property towards the Au(III) cation.

The aqueous biphasic system is a liquid–liquid system which is obtained either by mixing the aqueous solutions of two polymers, or a polymer and a salt. Generally, the former is comprised of polyethylene glycol (PEG) and polymers like dextran,⁵ starch,⁶ polyvinyl alcohol, *etc.* In contrast, the latter is composed of PEG and phosphate, sulfate or carbonate salts. PEG/dextran systems appear to involve certain economical and operational limitations, which can be overcome by the use of PEG/salt phase systems. The basis of partitioning in these two phases depends on the surface properties of the particles, which include size, charge and hydrophobicity. A number of different chemical and physical interactions are involved, for example hydrogen bonds, charge interactions, van der Waals' forces, hydrophobic interactions, steric effects, *etc.*⁷ Polyethylene glycol (PEG) based aqueous biphasic systems (ABS) represent a benign method for selective extraction of metal ions. The ABS system has multifold advantages over the

traditional liquid–liquid extraction systems as the PEGs are nontoxic, nonvolatile, nonflammable and biodegradable in nature, also the use of a carcinogenic organic solvent is not required in an ABS system.

The only study of gold extraction using aqueous biphasic extraction was carried out by Zhang *et al.*, using the Au(I) cation.⁸ Again, to the best of our knowledge to date no extraction method of gold (III) has been developed using ABS.

In this paper we report the extraction of $\text{H}^{198}\text{AuCl}_4$ and ^{198}Au spiked stable HAuCl_4 into the PEG-rich phase of an aqueous biphasic system keeping in mind that the high intensity 411 keV γ -energy (95.5%) of ^{198}Au might cause radiolysis of PEG and H_2O , resulting in the formation of radioactive ^{198}Au nanoparticles, followed by stabilization of nanoparticles by PEG itself. The process may be designated as a green method for the extraction and synthesis of radioactive gold nanoparticles as it uses a low cost technique and the least amount of chemicals.

Materials and methods

Polyethylene glycol: PEG 4000 ($M = 3500\text{--}4000 \text{ g mol}^{-1}$) was procured from MERCK. ^{198}Au radiotracer as HAuCl_4 was procured from the Board of Radiation and Isotope Technology (BRIT), Mumbai, India. All other analytical grade chemicals were used without further purification. UV-visible absorption spectra were recorded with a Thermo Spectronic spectrophotometer model UNICAM UV500. Baseline correction was done with a blank solution of 50% (w/w) PEG 4000 before recording each set of data. The transmission electron microscopy (TEM) studies were carried out with a Hitachi electron microscope model 600 operating at 75 kV with a resolution of 5 Å. The samples were spread over the copper grid coated with carbon, and lyophilized using SICO (IIC) Lyophilab, Model M at $-38 \text{ }^\circ\text{C}$ for 24 hours before taking the pictures so as to remove the syrupy solvent which might cause an unclear image of the gold nanoparticles.

The aqueous two-phase system was prepared by mixing 3 mL of 50% (w/w) PEG 4000 solution and 3 mL of 2 M Na_2SO_4 . 100 μL ($\sim 0.01 \text{ mCi}$) of Au(III) solution was added to the system as $\text{H}^{198}\text{AuCl}_4$ and was shaken mechanically for 10 minutes. The system was centrifuged for 5 minutes and a

Chemical Sciences Division, Saha Institute of Nuclear Physics, 1/AF Bidhannagar, Kolkata, 700 064, India.
E-mail: susanta.lahiri@saha.ac.in; Fax: +91-33-2337-4637

1 mL aliquot from each of the two phases was removed for γ -spectrometric studies. Gamma spectroscopic analysis was carried out with the help of an HPGe (ORTEC) detector with a resolution of 2.0 keV at 1.33 MeV. The detector was coupled with a PC based multichannel analyzer PCA2 (Oxford). The counts corresponding to the area under the ^{198}Au photo peak at 411.8 keV were measured for 600 s for both the phases at a fixed source to detector geometry. The count of the salt-rich phase (C_1) was compared with the count of the PEG rich phase (C_2). The extraction (E) of ^{198}Au into the PEG-rich phase was calculated using the following formula:

$$E = \frac{C_2}{C_1 + C_2} \times 100\%$$

Appropriate decay corrections were made for each set of data.

Experiments were also carried out with bulk Au(III) solutions spiked with ^{198}Au . Different macro concentrations of Au(III) solution were prepared by dissolving weighed amounts of metallic gold in aqua regia. To get uniform properties between radioactive and stable gold the solution was spiked with ^{198}Au at this stage. The solution was then evaporated to dryness and the mass was dissolved in 1 M HCl.

The transparent PEG-rich phase slowly turned violet upon extraction of ^{198}Au which gave a visual indication of the formation of radioactive gold nanoparticles (both for trace and macro-scale). This phase was separated from the salt-rich phase and allowed to cool. In order to use the instrumental facilities designated for non-radioactive uses, the PEG phase containing ^{198}Au was stored for about three months to allow complete decay of the radioactivity. In fact, the cooling period is not required at all if the required instrumental facilities *e.g.*, UV-vis spectrometer, TEM, *etc.*, are available for use with radioactive samples. The violet colour formed in the PEG-rich phase is persistent for several months indicating that the radioactive ^{198}Au nanoparticles in PEG are stable at room temperature even when the radioactivity is decayed out. Therefore PEG is a good stabilizing matrix for gold nanoparticles. After decaying out the radioactivity, the PEG solution was taken for UV-visible spectrophotometry to determine the wavelength of maximum absorption and transmission electron microscopy (TEM) was used to determine size of gold nanoparticles in solution. To examine the effect of ^{198}Au , UV-vis and TEM studies were repeated with the PEG solution where stable Au(III) solution was injected initially.

ABS systems using different molecular weights of PEG, like PEG 400, PEG 600 and PEG 20 000 (25% w/w) and Na_2SO_4 (2 M) were also prepared. However, the two-phase system was destroyed in all the above cases on addition of a metal ion in the form of $\text{H}^{198}\text{AuCl}_4$ solution. Therefore all the biphasic extraction experiments were carried out only with PEG 4000. $\text{H}^{198}\text{AuCl}_4$ solution was also spiked directly into solutions of PEG 400, PEG 600, PE 4000 and PEG 20 000 without extraction in the biphasic system.

The pH of the salt-rich phase was adjusted using a dilute HCl solution and the effect that varying the pH from 1 to 6 had on the partition of Au(III) was studied. Extraction of gold into the PEG-rich phase was also studied by using 2 M solutions of three other salts, K_2CO_3 , $\text{Na}_2\text{S}_2\text{O}_3$ and Na_2HPO_4 .

Similarly, to find the best condition for maximum extraction of the Au(III) ions, first the concentration of the salt-rich phase was varied keeping the concentration (50% w/w) of the PEG phase fixed. Again, the concentration of the PEG phase was varied keeping the concentration of the Na_2SO_4 fixed at 2 M.

Results and discussions

When $\text{H}^{198}\text{AuCl}_4$ was injected into an aqueous biphasic system containing 2 M Na_2SO_4 and a 50%(w/w) solution of PEG 4000, two important observations were made: (i) The PEG phase quantitatively extracted ^{198}Au at both trace scale and in bulk amount (up to 50 mM) (Fig. 1); (ii) The PEG phase slowly turned violet in colour visually indicating the formation of ^{198}Au nanoparticles.

The extraction behaviour remained unchanged with variation in the pH of the salt-rich phase but was greatly influenced by the composition of the salt-rich phase. It was found that among the four salts, Na_2SO_4 , K_2CO_3 , $\text{Na}_2\text{S}_2\text{O}_3$ and Na_2HPO_4 , sodium sulfate offered the best condition for gold extraction (Fig. 2). The relative salting out ability follows the order $\text{Na}_2\text{SO}_4 > \text{Na}_2\text{HPO}_4 > \text{K}_2\text{CO}_3 > \text{Na}_2\text{S}_2\text{O}_3$. The minimum concentration of Na_2SO_4 required for quantitative extraction of gold was 2 M (Fig. 3). Similarly it was observed that 50% w/w was the minimum concentration of PEG-rich phase required for quantitative extraction of Au(III).

The ability of a salt to form an ABS can be related to the salt anion's Gibbs free energy of hydration. Although both cation and anion contribute to the salting out phenomenon, the contribution of the anion dominates. Metal ions with relatively small magnitudes of ΔG_{hyd} are chaotropic and tend to destabilize the hydrogen bonding structure of water and partition to the PEG-rich phase.⁹

The UV-vis absorption spectra of the violet coloured polyethylene glycol solution showed a maximum absorption peak at a wavelength of 550 nm, confirming the formation of ^{198}Au nanoparticles. The same method was repeated with stable gold solution in PEG phase without spiked ^{198}Au . The

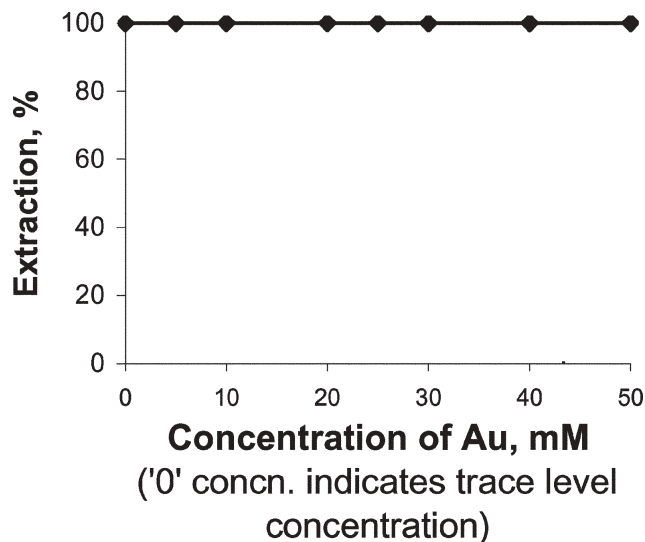


Fig. 1 Extraction profile of Au(III) ions in PEG phase with varying concentration of gold.

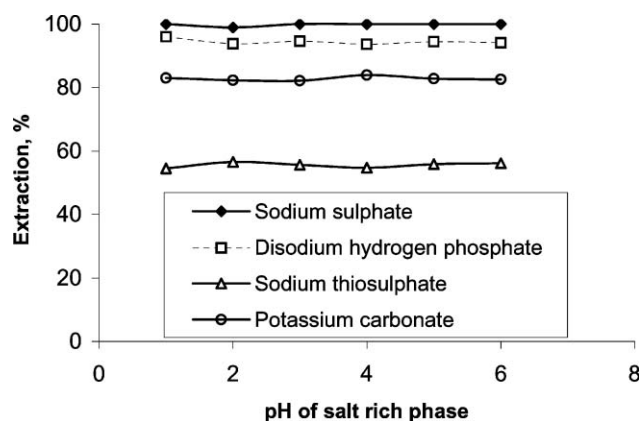
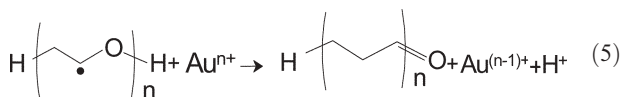
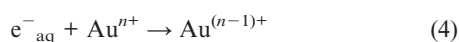
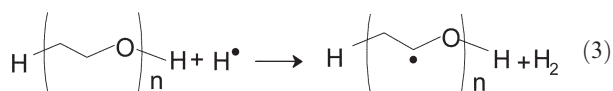
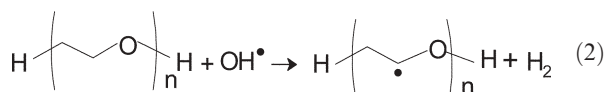


Fig. 2 Extraction profile of trace amount of Au(III) with varying pH of the salt-rich phase.

absorption was found in visible region only, confirming that the radioactivity due to ^{198}Au plays important role in the formation of radioactive ^{198}Au nanoparticles under the experimental condition (Fig. 4).

The transmission electron microscopy (TEM) studies also corroborate the same observation which clearly showed a particle size of 15–20 nm for the ^{198}Au spiked solution while particle size was much larger (a few μm) when the experiment was carried out without spiking with ^{198}Au (Fig. 5a and 5b).

The expected formation process of the radioactive nanoparticles may be due to the γ -ray energy of ^{198}Au at 411 keV, which transfers its energy into polyethylene glycol and water. The secondary electrons reduce the Au(III) ions. Elemental processes for the reduction of gold ions by the formation of monolithic noble metal particles may be as follows.¹⁰



Where eqn (1) represents the radiolysis of water and eqn (2) and (3) represent the radiolysis of polyethylene glycol. Generated hydrogen atoms H^\cdot and hydrated electrons e_{aq}^- are strong reducing agents and capable of reducing gold ions Au^{n+} to lower valencies and finally to the metallic state. The secondarily generated radical of $\text{HO}-(\text{CH}_2-\text{CH}_2-\text{O})_n-\text{H}$ can also reduce gold ions *in situ* to transform Au^{n+} to $\text{Au}^{(n-1)+}$ leading to the formation of radioactive gold nanoparticles. The PEG matrix also serves as an insulating medium. The possibility for the progression of nanostructural changes are mainly determined by the matrix material (insulator).¹¹ If there

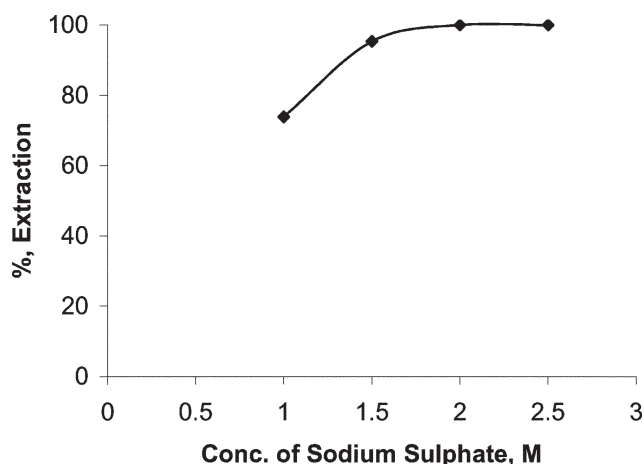


Fig. 3 Extraction profile of trace amount of Au(III) with varying concentration of salt-rich phase.

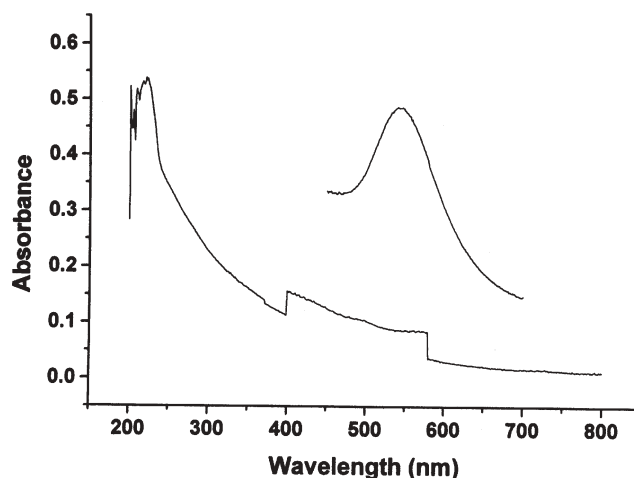


Fig. 4 UV-vis spectra of stable gold extracted in PEG-rich phase (lower curve) and ^{198}Au extracted in PEG-rich phase (upper curve).

is no matrix, diffusion of metal particles occurs in the substrate and thereby structural deformation occurs. PEG being a polymer acts as a good insulating medium and stabilizes the nanoparticles for the long term.

When ^{198}Au is directly injected into various PEG solutions, violet coloration was observed only in case of PEG 20 000 and PEG 4000. No violet colour was observed upon the direct addition of ^{198}Au (III) to PEG 400 or PEG 600 solutions.

Conclusion

The developed procedure using an ABS system is an environmentally benign tool for producing radioactive gold nanoparticles. The method involves no organic solvent and smaller amounts of chemicals. The method is simple and fast. ^{198}Au is short lived ($t_{1/2} = 2.69$ d) and has high intensity gamma energy at 411 keV; thus the synthesized radioactive gold nanoparticles may be useful for *in vivo* and *in vitro* applications where both the properties of this nanomaterial and the high energy gamma radiation could be useful. This experiment was performed with only ~ 0.01 mCi ^{198}Au , but for

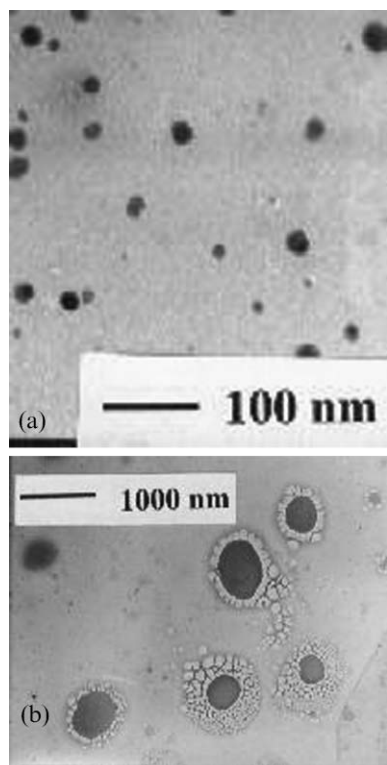


Fig. 5 TEM images of gold spiked with ^{198}Au (a) and stable gold (b).

in vivo or *in vitro* applications, the activity required is 2 mCi or more. The experiments with a bulk amount of gold spiked with ^{198}Au suggest that gold nanoparticles can be formed in concentrations up to 50 mM by the described method. Therefore the method can be extrapolated to a much higher

radioactivity in order to perform imaging based *in vivo* tracking and organ specific delivery using antibodies on the gold nanoparticle surface, which may be useful for simultaneous detection of the organs and destruction of the abnormal cells.

Acknowledgements

The authors gratefully acknowledge Mr Pulak Roy, Saha Institute of Nuclear Physics for extending help in obtaining TEM pictures. One of the authors (K. Roy) expresses sincere thanks to the Council of Scientific and Industrial Research (CSIR) for providing the necessary fellowship.

References

- 1 F. Porta and M. Rossi, *J. Mol. Catal.*, 2003, **204**, 553–559.
- 2 Y. Y. Yu, S. S. Chang, C. L. Lee and C. R. C. Wang, *J. Phys. Chem. B*, 1997, **101**, 6661–6664.
- 3 M. Nakanishi, H. H. Takatani, Y. Kobayashi, F. Hori, R. Taniguchi, A. Iwase and R. Oshima, *Appl. Surf. Sci.*, 2005, **241**, 209–212.
- 4 S. Chen, Y. Liu and G. Wu, *Nanotechnology*, 2005, **16**, 2360–2364.
- 5 H. Walter, D. E. Brooks and D. Fisher, in *Partitioning in Aqueous two phase systems: Theory, Methods, Uses and Applications to Biotechnology*, Academic Press, London, 1985.
- 6 P. A. Albertsson, G. Johansson and F. Tjerneld, *Separation Processes in Biotechnology*, Marcel Dekker, New York, 1990.
- 7 R. D. Rogers, A. H. Bond and C. B. Bauer, *Sep. Sci. Technol.*, 1993, **28**, 1091–1126.
- 8 T. Zhang, W. Li, W. Zhou, H. Gao, J. Wu, G. Xu, J. Chen, H. Liu and J. Chen, *Hydrometallurgy*, 2001, **62**, 41–46.
- 9 R. D. Rogers and J. Zhang, *Ion Exchange and Solvent Extraction*, Marcel Dekker, New York, 1997, vol. 13.
- 10 S. Seino, T. Kinoshita, Y. Otome, T. Nakagawa, K. Okitsu, Y. Mizukoshi, T. Nakayama, T. Sekino, K. Niihara and T. A. Yamamoto, *J. Magn. Magn. Mater.*, 2005, **293**, 144–150.
- 11 A. Heilmann, *Polymer Films with Embedded Metal Nano Particles*, Springer, Heidelberg, 2002.

A one-pot synthesis of hybrid organo-layered double hydroxide catalyst precursors†

H. Chris Greenwell,^{*a} William Jones,^{*b} Dennis N. Stamires,^c Paul O'Connor^d and Michael F. Brady^d

Received 25th April 2006, Accepted 23rd August 2006

First published as an Advance Article on the web 15th September 2006

DOI: 10.1039/b605851e

Organo-layered double hydroxides (LDHs) have attracted much attention recently for their utility as solid base catalysts, providing an environmentally friendly heterogeneous phase alternative to conventional stoichiometric liquid bases. Here we describe a synthetic approach for the production of layered double hydroxides containing organic (acetate) anions by a method that requires no excess of base, filtering or washing of the product. A mixture of a slurry of aluminium trihydroxide (or its thermally treated form), magnesium oxide, and magnesium acetate are reacted under atmospheric or autogenous conditions to prepare MgAl-acetate LDHs of general formula $Mg_{1-x}Al_x(OH)_2(CH_3CO_2)_x \cdot yH_2O$. Using this synthetic procedure it has been found that MgAl-acetate LDHs with either a full or partial acetate loading may be prepared for a range of Mg/Al stoichiometries. The LDHs formed have been characterised by X-ray diffraction, infra-red spectroscopy, solid state nmr and thermal methods. Depending on the synthesis method, the acetate LDHs had an interlayer spacing of between *ca.* 8.4 and 14.8 Å indicating the formation of monolayers and bilayers of acetate anions, respectively, in the LDH host.

1. Introduction

Layered double hydroxides (LDHs) are a diverse group of mixed metal hydroxide compounds with applications ranging from catalysis to drug delivery.^{1,2} They have a structure analogous to that of brucite, where M^{2+} cations ($M = Mg$ for brucite) are octahedrally co-ordinated by hydroxide. These octahedra share edges to form sheet-like structures of formula $Mg(OH)_2$. The sheets then stack (in the crystallographic *c* direction) to give a characteristic layered material. In the case of LDHs some of the M^{2+} species are substituted by M^{3+} species, resulting in the layers carrying a residual positive charge. This charge is balanced by the incorporation of anions between the layers. The anions may be organic or inorganic, and invariably have water molecules associated with them.³ Morphologically, crystals of LDHs usually consist of micron-sized stacks of hexagonal platelets. However, fibrous and extended sheet-like morphologies have also been described, depending on the conditions of synthesis.^{4,5}

Recently, the solid base catalytic properties of LDHs have received much attention as environmentally attractive replacements for stoichiometric liquid bases for a wide range of reactions.⁶ By way of example, organo-LDHs have been used

for epoxidation,⁷ Aldol condensations,⁸ cyanoethylation,⁹ Michael additions,¹⁰ and *trans*-esterifications.¹¹ However, as a chemical technology, these catalysts are not “truly” green since little attention has been given to the actual synthesis of the LDH catalysts. For example, a common method of preparation is co-precipitation, where two metal salt solutions of an appropriate M^{2+}/M^{3+} ratio are precipitated using a basic solution containing the anion of interest.^{12,13} This method requires substantial excess quantities of a base which the catalyst is itself intended to replace at a later stage in its life-cycle. (Typically substantial quantities of sodium hydroxide base are required for precipitation at the optimum pH of 10.) The resultant gel is then aged (hydrothermally, or at atmospheric pressure, at room or elevated temperature) for a period of time to increase the crystallinity of the product. More recent advances in the synthesis of LDHs have included the application of hydrothermal methods using relatively insoluble metal salts,¹⁴ microwave radiation,¹⁵ grinding¹⁶ and a variety of direct synthesis approaches where a range of M^{2+} and M^{3+} sources have been used.^{17–20} In addition a large variety of methods for the preparation of LDHs specifically with organic anions have been described.²¹ For example, the organic anion may be introduced by exchange of the anion for an inorganic species already present in a pre-prepared LDH.²² Other approaches include introducing the organic acid from the melt,²³ or utilising the so-called “memory effect” of calcined LDHs to incorporate organic acids during a rehydration cycle.²⁴

Pausch *et al.* first introduced the concept of incorporating the organic anion of interest into an LDH during synthesis by using an organic metal salt as both the anion source and the source of one of the metal cations in the LDH.¹⁸ Others methods have been utilized to prepare specifically acetate

^aCentre for Applied Marine Sciences, School of Ocean Sciences, University of Wales Bangor, Menai Bridge, Anglesey, UK LL59 5AB

^bDepartment of Chemistry, University of Cambridge, Lensfield Road, Cambridge, UK CB2 1EW

^cConsultant, Newport Beach, California, CA 92629, USA

^dAkzo Nobel Chemicals bv, Stationsplein 4, P. O. Box 247 3800 AE, Amersfoort, The Netherlands

† Electronic supplementary information (ESI) available: Variation in the relative intensity of X-ray diffraction reflections of selected impurity and LDH phases with starting Mg/Al ratio. See DOI: 10.1039/b605851e

LDHs. Martin *et al.* reported interlayer spacings for a hydroxalcalite-like material containing acetate, formed *via* exchange of a meixnerite intermediate, of 10.67 Å.²⁵ Schutz *et al.* synthesized a Mg/Al = 2 hydroxalcalite-like compound with acetate by peptising pseudoboehmite with acetic acid in an aqueous slurry followed by addition of a magnesium source giving interlayer spacings of approximately 12.5 Å.²⁶ Using a similar method, Kelkar and Schutz further report interlayer spacings of 11.28 Å and 10.71 Å for an MgAl-acetate LDH and a CoAl-acetate LDH respectively and spacings of 10.52, 10.81, and 10.62 Å for NiAl-acetate LDHs of Ni/Al ratio values of 2, 3, and 4 respectively.⁵ Using a non-conventional soft chemistry approach, Prevot *et al.* prepared the NiAl- and CoAl-acetate LDHs by hydrolysing the corresponding metal acetate salts in a polyol solution.²⁷ Applications of LDHs involving acetate containing species include the incorporation of ethylenediaminetetraacetate within LiAl LDHs to prepare solid-state chelating agents for removing transition metal cations from aqueous solution,²⁸ and carboxylate alkylation reactions to give long chain acetate esters.²⁹ Acetate has also been reported intercalated in a related group of compounds, the hydroxy (layered) double salts. Morioka *et al.* give an interlayer spacing of 13.4 Å for the acetate containing zinc double salt,³⁰ whilst Poul *et al.* reported spacings of 14.75, 12.90, and 10.64 Å for the Zn, Co, and Ni double salts respectively.³¹ More recently, Kandare and Hossenlopp have examined the kinetics of exchange reactions in acetate containing hydroxy double salts.³² In a further work, Prevot *et al.* used the Cu hydroxy (layered) double salts as precursors for grafting a range of functionalised organic molecules to the inorganic sheets.³³

A frequent problem associated with LDH synthesis is that many of the known methods involve filtering and washing of the LDH product. This results in added complexity, especially when considering large-scale synthesis. For example, washing will generate large amounts of a supernatant of high pH often containing excess organic anions and/or metal ions. Such solutions present significant disposal problems.

In this paper we consider the synthesis of MgAl-acetate LDHs by an environmentally attractive route.³⁴ Acetic acid is utilized within industry for the peptisation of alumina prior to extrusion. The acetate containing LDH may be a versatile precursor allowing exchange by bulkier anions such as *t*-butoxide. In particular we describe a one-pot synthesis, using economical reagents and without the need for filtering of the product, which yields LDHs with no, or very little, carbonate contamination.

2. Experimental

The metal nitrate salts, sodium hydroxide, sodium acetate, magnesium oxide, and magnesium acetate were obtained from Aldrich and used without further purification. The CP1.5 and gibbsite were ex-Alcoa and were also used as supplied. CP1.5 is a catalyst precursor grade calcined alumina with an average particle size of 1.5 µm. The purity of the alumina was ascertained to be 94% pure (5.8% loss on ignition). MgAl acetate LDHs were prepared by the various methods described below, with $R = 1, 1.5, 2,$ and 3 , where R is the ratio of Mg/Al in the reaction mixture. A schematic illustrating the different synthesis procedures is given in Fig. 1.

2.1 One-step method

As an illustration of the experimental procedure, a MgAl acetate LDH with a target Mg/Al ratio (R value) = 1 was prepared by the following method (Fig. 1(a)): $\text{Mg}(\text{CH}_3\text{CO}_2)_2 \cdot 2\text{H}_2\text{O}$ (4.28 g, 0.02 mol) was dissolved in 100 ml of deionised water. To this was added MgO (0.80 g, 0.02 mol) and CP1.5 (2.24 g, 0.02 mol, 95% Al_2O_3). The mixture was stirred for approximately 12 h at 65 °C. The resulting white slurry was dried directly in an oven at 80 °C and the resulting powder allowed to equilibrate under atmospheric conditions. The procedure was repeated except that the 65 °C treatment was replaced by a hydrothermal treatment at 165 °C for 4 h (in a Parr apparatus with overhead stirring, see Fig. 1(b)). For samples with greater R values the $\text{Mg}(\text{CH}_3\text{CO}_2)_2 \cdot 2\text{H}_2\text{O}$ content was increased accordingly. For comparison a further

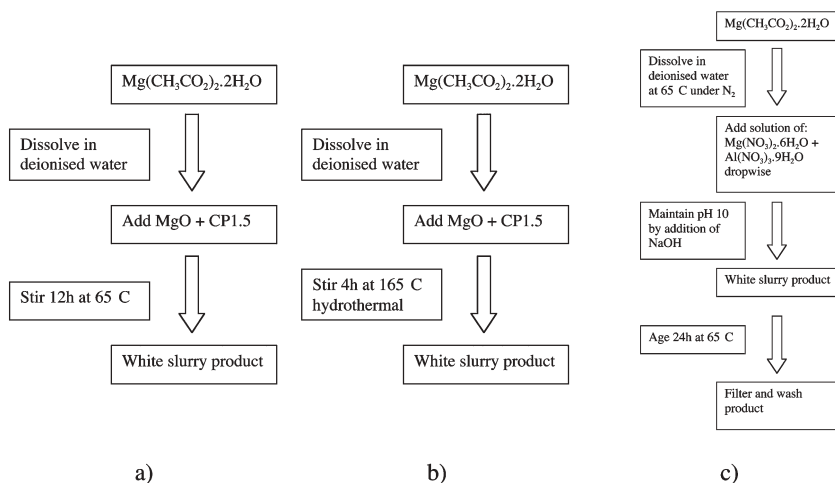


Fig. 1 Schematics to show the different methods of preparation employed: (a) one-pot synthesis under atmospheric conditions; (b) one-pot synthesis under hydrothermal conditions; (c) conventional co-precipitation method for comparison.

set of samples was prepared using the same procedures where there was insufficient acetate present to satisfy the anion exchange capacity of the LDH. In these samples the R value was increased by altering the amount of MgO present.

2.2 Co-precipitation method

For comparative purposes samples were prepared *via* a conventional co-precipitation method (Fig. 1(c)). For example, a $MgAl$ acetate LDH where $Mg/Al = 1$ was prepared as follows: a solution containing sodium acetate (11.48 g, 0.014 mol) was prepared in 90 ml of deionised water and heated to 65 °C. Nitrogen gas was passed through the solution at all times. $Mg(NO_3)_2 \cdot 6H_2O$ (2.57 g, 0.01 mol) and $Al(NO_3)_3 \cdot 9H_2O$ (3.75 g, 0.01 mol) were dissolved in 50 ml of deionised water and added with continuous stirring of the acetate solution. The pH of the mixture was maintained at pH 10 by the simultaneous drop-wise addition of a solution of NaOH (12 g) and sodium acetate (6.2 g) in 100 ml deionised water. Upon completion of addition of the metal salts the solution was aged for 24 h at 65 °C under a nitrogen gas atmosphere. The resulting white slurry was filtered, washed and dried in an oven at 80 °C, and allowed to equilibrate under atmospheric conditions.

2.3 Characterisation of samples

All products were analysed by reflection powder X-ray diffraction (PXRD) using a Phillips PW1710 instrument with $Cu K\alpha$ radiation ($\lambda = 1.5418 \text{ \AA}$). Patterns were obtained within a 2θ range of 2.00 to 80.00 degrees in increments of 0.04 degrees. Each step was scanned for 0.8 s. Indexing and refinement was not possible for any of the samples due to the limited number of reflections of adequate quality. The interlayer distance (d -spacing) was calculated using the position of the lowest angle basal reflection. The Mg/Al ratio was determined from the position of the d_{110} reflection.^{35,36} Thermogravimetric analysis (TGA) was obtained using a Polymer Laboratories PL1500 TGA with samples analysed under nitrogen gas flow. Fourier transform infra-red (FTIR) spectroscopy was carried out on a Perkin Elmer Paragon 1000 instrument using the KBr disk method, with approximately 1 part sample to 7 parts KBr. Each sample was scanned 16 times at 1 cm^{-1} resolution. The inductively coupled plasma optical emission spectroscopy (ICP-OES) was carried out at the Institute of Environmental Sciences, University of Wales, Bangor. Electron micrographs were obtained using a Jeol JSM-5800LV scanning electron microscope (SEM) with an accelerating voltage of 15 kV. Quantitative elemental analysis using EDS was calibrated using virtual standards. Solid-state ^{27}Al magic angle spinning (MAS) nuclear magnetic resonance (NMR) experiments were carried out at 9.4 T using a Chemagnetics CMX-400 spectrometer. Spectra were acquired at 104.20 MHz with pulses of less than $\pi/10$ (0.3 μs pulse length) using zirconia rotors, which were 4 mm diameter, spun in dry nitrogen at 8 kHz. For each sample 1000 scans were acquired with a recycle time of 0.5 s. The shift of the observed ^{27}Al resonance is reported with respect to external $Al(H_2O)_6^{3+}$ standard. Elemental analysis was performed using an Exeter Analytical Inc. CE440 instrument.

The samples are denoted using the following scheme:

- $Mg_RAlCoPr$ Samples prepared by the co-precipitation method.
 Mg_RAlAtm Samples prepared by the one-step synthesis carried out under atmospheric conditions. Acetate:Al > 1.
 Mg_RAlHT Samples prepared by the one-step synthesis carried out under hydrothermal conditions. Acetate:Al > 1.
 $Mg_RAlPATm$ Samples prepared by the one-step synthesis carried out under atmospheric conditions. Acetate:Al < 1.
 Mg_RAlPHT Samples prepared by the one-step synthesis carried out under hydrothermal conditions. Acetate:Al < 1.
 where: R is the target Mg/Al ratio and P indicates partial charge balance by acetate.

3. Results

In general, the powder X-ray diffraction patterns obtained were typical of LDH materials; many of the samples prepared contained varying types and amounts of aluminium hydroxide/oxyhydroxide or magnesium phases which had simultaneously formed. The amount of by-product varied depending on the R value and the synthesis procedure. Obtaining samples of high phase purity (as indicated by XRD) was difficult, and only achieved for certain R values and reaction conditions (see Fig. 2).

3.1 Sample composition

The FTIR spectra of the samples prepared by the one-step synthesis method where there was sufficient acetate in the reaction mixture (section 2.1) confirm that all the acetate present in the LDH sample was in anion form through the appearance of only symmetric and asymmetric carboxylate stretching absorption bands at approximately 1570 and 1409 cm^{-1} , respectively (Fig. 3).³¹ In the one-step synthesis procedure where there was insufficient acetate present to

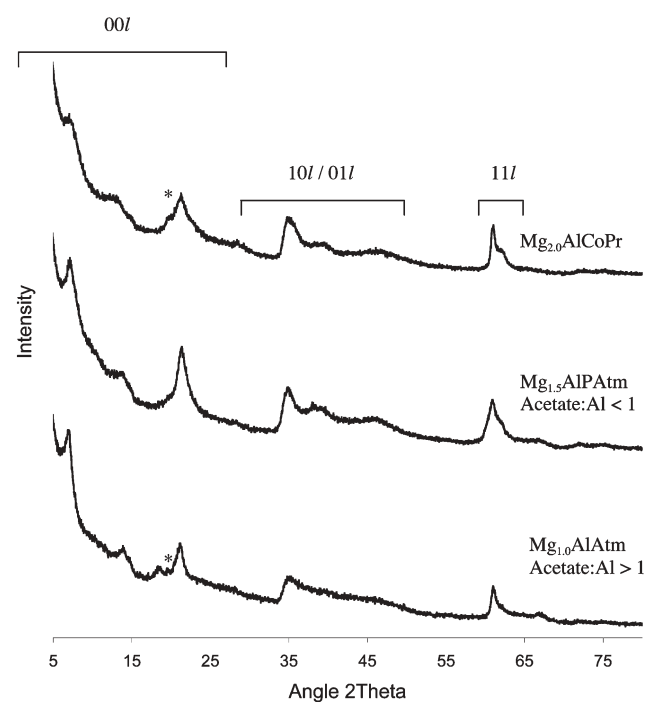


Fig. 2 PXRD patterns for LDH samples with highest purity. *indicates possible gibbsite reflection.

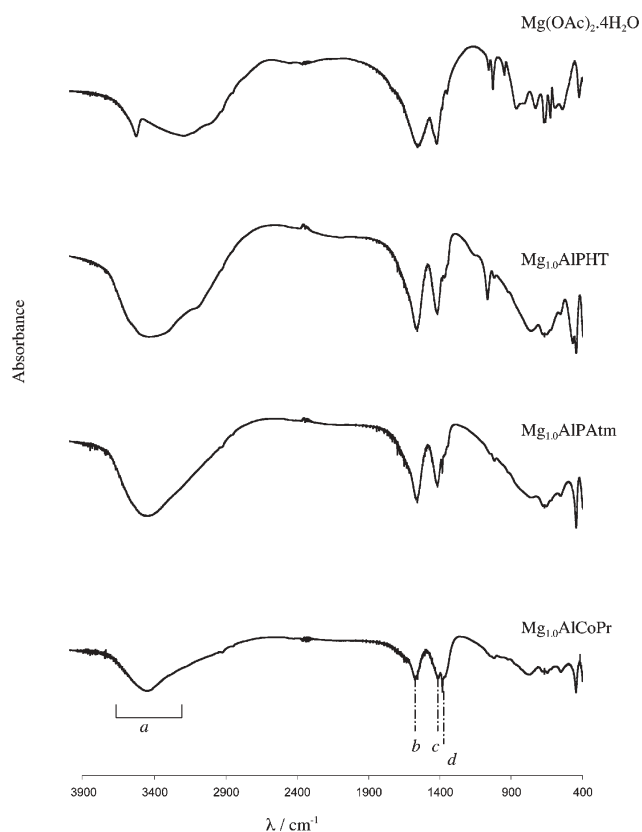


Fig. 3 FTIR spectra of selected LDH products. Principal bands are: *a* hydroxyl/water H-bonded; *b* C=O carboxylate asymmetric; *c* C=O carboxylate symmetric; *d* NO₃⁻.

completely charge balance the Al, with an acetate/Al ratio of approximately 0.39, it was expected that hydroxide anions would provide the remaining charge compensation. The broad bands observed at high frequency, approximately 3100–3500 cm⁻¹, indicate the presence of hydroxyl groups and water. The broad nature of these bands reflects the extensive hydrogen bonding found in these materials. FTIR analysis of the samples prepared by co-precipitation (Fig. 3) showed that, as with the one-step method, the acetate anion has been incorporated in all cases with the carboxylate C=O giving asymmetric and symmetric stretches at approximately 1570 and 1409 cm⁻¹ respectively.³¹ Additionally, in the sample prepared by co-precipitation there is a sharp absorbance at 1382 cm⁻¹ characteristic of the presence of NO₃⁻ with *D*_{3h} symmetry.³⁷

Thermogravimetric analysis (TGA) was used to deduce the amount of interlayer water present in the sample, with the weight loss up to 250 °C being attributed to the interlayer water.³⁸ It is appreciated that the lack of high crystallinity and possible presence of impurities makes the interpretation of TGA data difficult. Microanalysis further confirmed the presence of nitrate in the co-precipitated samples. ²⁷Al MAS NMR spectra shows one resonance, with no shoulder, suggesting the presence of only octahedrally coordinated Al (Fig. 4). The presence of AlO₂⁻ ions would have been indicated by a further resonance corresponding to the tetrahedral Al environment.

The Mg/Al ratio of the product was calculated using the *a* crystallographic parameter, obtained from the PXRD patterns

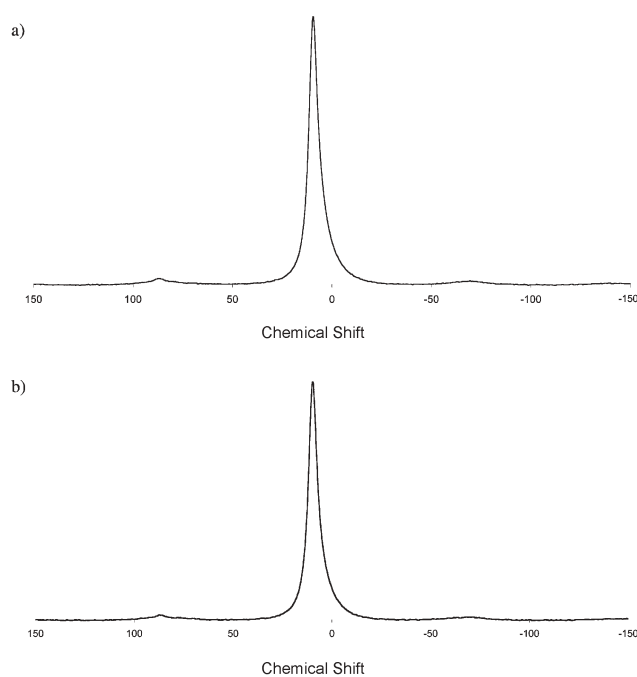


Fig. 4 Solid-state ²⁷Al MAS NMR spectra of co-precipitated samples, with (a) *R* = 1, and (b) *R* = 1.5.

(*d*₁₁₀) and is reported in Table 1 and Table 2 for the one-step reaction, and in Table 3 for the co-precipitated reaction. In nearly all cases the Mg/Al ratio within the LDH matrix was determined to be close to 2, irrespective of the reactant Mg/Al ratio. The co-precipitated products, which had been washed as part of the synthesis, were also tested by ICP-OES analysis (Table 3). The bulk composition of the co-precipitated samples, by ICP analysis, was in agreement with the initial ratio of reactants. This suggests that alternative, amorphous phases must be present to account for the discrepancy in product Mg/Al ratio. The preference of LDHs towards certain Mg/Al ratios is well documented, with co-precipitation methods giving best control over Mg/Al within certain limits. Other synthetic techniques, for example dialysis³⁹ or hydrothermal routes,⁴⁰ tend towards a highly crystalline nature but poor control of product Mg/Al with respect to

Table 1 Experimental parameters and composition of one-step synthesised samples with sufficient acetate

Sample	<i>d</i> ₁₁₀ /Å	Mg/Al ratio in LDH layer	OAc/Al ratio in reaction mixture	Interlayer spacing/Å
Mg _{1.0} AlAtm	1.519	1.81 ^a /1.97 ^b	1.0	12.64
Mg _{1.5} AlAtm	1.521	1.96 ^a /2.10 ^b	1.5	14.83
Mg _{2.0} AlAtm	1.520	1.92 ^a /2.06 ^b	2.0	12.55
Mg _{3.0} AlAtm	1.520	1.93 ^a /2.07 ^b	3.0	12.61
Mg _{1.0} AlIHT	1.522	2.03 ^a /2.15 ^b	1.0	14.75
Mg _{1.5} AlIHT	1.523	2.14 ^a /2.24 ^b	1.5	14.61
Mg _{2.0} AlIHT	1.523	2.14 ^a /2.24 ^b	2.0	15.11
Mg _{3.0} AlIHT	1.522	2.10 ^a /2.21 ^b	3.0	14.86

^a Mg/Al based on *d*₁₁₀ and using data from Kaneyoshi and Jones.³⁶

^b Mg/Al based on *d*₁₁₀ and using data from Kukkadapu *et al.*³⁵

Table 2 Experimental parameters and composition of one-step synthesised samples with insufficient acetate for complete charge balance

Sample	$d_{110}/\text{\AA}$	Mg/Al ratio in LDH layer	OAc/Al ratio in reaction mixture	Interlayer spacing/ \AA
Mg _{1.0} AlPAtm	1.519	1.86 ^a /2.01 ^b	0.39	12.42
Mg _{1.5} AlPAtm	1.521	2.02 ^a /2.14 ^b	0.39	12.78
Mg _{2.0} AlPAtm	1.522	2.08 ^a /2.19 ^b	0.39	8.46
Mg _{3.0} AlPAtm	1.522	2.08 ^a /2.19 ^b	0.39	8.39
Mg _{1.0} AlPHT	1.521	2.03 ^a /2.15 ^b	0.39	12.46
Mg _{1.5} AlPHT	1.521	1.98 ^a /2.11 ^b	0.39	12.41
Mg _{2.0} AlPHT	1.524	2.21 ^a /2.30 ^b	0.39	12.43
Mg _{3.0} AlPHT	1.527	2.56 ^a /2.57 ^b	0.39	12.23

^a Mg/Al based on d_{110} and using data from Kaneyoshi and Jones.³⁶
^b Mg/Al based on d_{110} and using data from Kukkadapu *et al.*³⁵

Table 3 Experimental parameters and composition of co-precipitated samples

Sample	Mg/Al ratio in LDH layer d_{110}	Mg/Al ratio (ICP) bulk value	OAc/Al ratio in reaction mixture	Interlayer spacing/ \AA
Mg _{1.0} AlCoPr	1.89	1.08	9	7.34
Mg _{1.5} AlCoPr	2.02	1.64	9	6.91
Mg _{2.0} AlCoPr	1.96	2.15	9	12.21

starting material Mg/Al ratio resulting in the formation of aluminium hydroxide and oxyhydroxide phases at values of Mg/Al less than 2 and magnesium oxide and hydroxide phases at Mg/Al greater than 3. Misra and Perrotta investigated the structure of 21 hydrotalcite-like compounds formed by reacting aluminate liquor with activated magnesia in different reactant ratios and found a significant preference for a Mg/Al of approximately 1.9.¹⁷

In the samples prepared here we also observe a strong tendency to form phases with similar Mg/Al ratio regardless of the starting Mg/Al ratio. The aluminium polymorph formed at low Mg/Al ratio varies according to the method of synthesis. The variation of impurity relative intensity in the XRD patterns is shown in Fig. S1 (see electronic supplementary information†). Under hydrothermal conditions boehmite is formed in the one-step method, whilst under atmospheric conditions gibbsite is formed. In the co-precipitation prepared samples only bayerite is observed. It may be that this is due to the inert atmosphere present during synthesis of the co-precipitation samples. In the one-step approach, at Mg/Al values greater than 2, the Mg phase formed depends on whether the acetate : Al ratio is greater, or less, than unity. In the samples with partial acetate loading brucite is formed, whilst in the samples prepared in the presence of an excess of acetate MgO is created.

3.2 Interlayer arrangement of acetate LDHs

Those preparations where there was an excess acetate balance resulted in the formation of MgAl acetate LDHs with basal d -spacings in the range 12.55 \AA to 15.11 \AA (Table 1), depending on the R value and whether hydrothermal treatment had been applied. These values, in general, show agreement with those of Schutz *et al.*²⁶ An interlayer spacing of 12.60 \AA gives a gallery height of 7.80 \AA , which is slightly

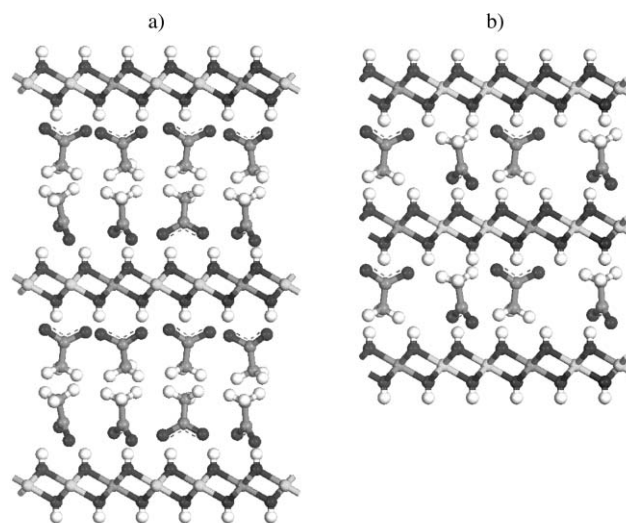


Fig. 5 Schematic to show the possible interlayer arrangement for (a) 12.6 \AA interlayer spacing, where the acetate are arranged in a bi-layer, and (b) 8.4 \AA interlayer spacing where the acetate are arranged in a monolayer perpendicular to the LDH sheet. Carbon atoms are in mid-grey, oxygen atoms in black, hydrogen in white, aluminium in dark grey, and magnesium in light grey.

more than twice the length of an acetate molecule (which is *ca.* 3.6 \AA), suggesting a bilayer interlayer arrangement—as depicted in Fig. 5(a). The hydrothermally treated samples were of more crystalline nature, with much sharper basal (00l) reflections in the PXRD pattern.

Kelkar and Schutz suggest that the presence of acetate is a requirement for the formation of extended sheet-like structures,⁵ and there was some reduction in crystallinity in the samples prepared here with partial acetate content as determined by the peak width of the basal reflection in the PXRD patterns. It might be expected that in samples with only a partial acetate loading the lower packing density of the bulky acetate anions would result in a smaller interlayer spacing, such as shown in Fig. 5(b). The observed interlayer spacings were indeed lower than those of the samples prepared with a full acetate balance (Table 2), however a bi-layer arrangement is still found in the hydrothermally treated samples, rather than an inter-penetrating bi-layer or monolayer with hydroxide. This may suggest that the acetate aggregates together within the LDH interlayer in hydrophobic clusters, and the periphery of the LDH crystal forms with hydroxyl anions. In the samples prepared under atmospheric conditions, at $R = 2$ or 3, interlayer spacings of *ca.* 8.4 are observed (Table 2). This corresponds to a gallery height of *ca.* 3.8 \AA , suggesting a monolayer arrangement of acetate molecules with their longest axes perpendicular to the LDH sheets in the interlayer (Fig. 5(b)). For comparison, the LDH crystal parameters of the co-precipitated samples are given in Table 3.

4. Conclusions

We have shown that in order for a catalytic process to truly conform to green chemistry principles the synthesis of the catalyst must also be considered. We have used a case study,

the synthesis of MgAl acetate LDHs (in a one-pot synthesis with high Al content in an economical and environmentally favourable manner), to illustrate this. By careful choice of synthetic method, and Mg/Al ratio, products can be prepared which are largely free of by-products, which is desirable for the manufacture of catalysts, pharmaceuticals, and cosmetics. A wide range of *d*-spacings is encountered, depending upon synthesis conditions and drying regime. In general, it may be said that the characteristics of organo-LDHs vary significantly depending upon water content and synthesis conditions. Further work will focus on using different organic-metal salts for the preparation of these interesting materials; the thermal evolution of these materials along with associated catalytic properties; the synthetic process for non-MgAl LDHs.

Acknowledgements

We acknowledge the EPSRC, and the Isaac Newton Trust, Cambridge (part funded by Akzo Nobel), for funding of HCG. We also acknowledge the help of Dr P. Holliman at University of Wales, Bangor for ICP-OES analysis, Dr F. Kooli at the Institute of Chemical and Engineering Sciences, Singapore, the Department of Material Science and Metallurgy, University of Cambridge for SEM and Dr Y. Khimyak for running the solid-state NMR experiments.

References

- 1 S. P. Newman and W. Jones, *New J. Chem.*, 1998, **22**, 105–115.
- 2 F. Cavani, F. Trifiro and A. Vaccari, *Catal. Today*, 1991, **11**, 173–301.
- 3 R. Allman, *Chimia*, 1970, **24**, 99.
- 4 S. Miyata and A. Okada, *US Pat.*, 4 351 814, 1982.
- 5 C. P. Kelkar and A. A. Schutz, *Microporous Mater.*, 1997, **10**, 163–172.
- 6 Y. Ono, *J. Catal.*, 2003, **216**, 406–415.
- 7 B. M. Choudary, M. L. Kantam, B. Bharathi and C. V. Reddy, *Synlett*, 1998, 1203–1204.
- 8 B. M. Choudary, M. L. Kantam, B. Kavita, C. V. Reddy, K. K. Rao and F. Figueras, *Tetrahedron Lett.*, 1998, **39**, 3555–3558.
- 9 B. M. Choudary, M. L. Kantam and B. Kavita, *Green Chem.*, 1999, **1**, 289–292.
- 10 B. M. Choudary, M. L. Kantam, B. Kavita, C. V. Reddy and F. Figueras, *Tetrahedron*, 2000, **56**, 9357–9364.
- 11 B. M. Choudary, M. L. Kantam, C. V. Reddy, S. Aranganathan, P. L. Santhi and F. Figueras, *J. Mol. Catal. A: Chem.*, 2000, **159**, 411–416.
- 12 E. L. Crepaldi, P. C. Pavan and J. B. Valim, *J. Braz. Chem. Soc.*, 2000, **11**, 64–70.
- 13 M. A. Drezdon, *US Pat.*, 4 774 212, 1988.
- 14 M. Ogawa and S. Asai, *Chem. Mater.*, 2000, **12**, 3253–3255.
- 15 S. Kannan and R. V. Jasra, *J. Mater. Chem.*, 2000, **10**, 2311–2314.
- 16 V. P. Isupov, L. E. Chupakhina and R. P. Mitrofanova, *J. Mater. Synth. Process.*, 2000, **8**, 251–253.
- 17 C. Misra and A. J. Perrotta, *Clays Clay Miner.*, 1992, **40**, 145–150.
- 18 I. Pausch, H. H. Lohse, K. Schurmann and R. Allmann, *Clays Clay Miner.*, 1986, **34**, 507–510.
- 19 P. Bar-On and S. Nadiv, *Thermochim. Acta*, 1988, **133**, 119–124.
- 20 M. Rajamathi and P. V. Kamath, *Bull. Mater. Sci.*, 2000, **23**, 355–359.
- 21 S. Carlino, *Solid State Ionics*, 1997, **98**, 73–84.
- 22 K. Takagi, T. Shichi, H. Usami and Y. Sawaki, *J. Am. Chem. Soc.*, 1993, **115**, 4339–4344.
- 23 S. Carlino and M. J. Hudson, *J. Mater. Chem.*, 1994, **4**, 99–104.
- 24 K. Chibwe and W. Jones, *Chem. Mater.*, 1989, **1**, 489–490.
- 25 E. S. Martin, J. M. Stinson, V. Cedro, III and W. E. Horn, Jr., *US Pat.*, 5 728 366, 1998.
- 26 A. Schutz, L. A. Cullo and C. P. Kelkar, *US Pat.*, 5 399 329, 1995.
- 27 V. Prevot, C. Forano and J. P. Besse, *Chem. Mater.*, 2005, **17**, 6695–6701.
- 28 K. A. Tarasov, D. O'Hare and V. P. Isupov, *Inorg. Chem.*, 2003, **42**, 1919–1927.
- 29 A. Luis Garcia-Ponce, V. Prevot, B. Casal and E. Ruiz-Hitzky, *New J. Chem.*, 2000, **24**, 119–121.
- 30 H. Morioka, H. Tagaya, M. Karasu, J. Kadokawa and K. Chiba, *J. Mater. Res.*, 1998, **13**, 848–851.
- 31 L. Poul, N. Jouini and F. Fievet, *Chem. Mater.*, 2000, **12**, 3123–3132.
- 32 E. Kandare and J. M. Hossenlopp, *J. Phys. Chem. B*, 2005, **109**, 8469–8475.
- 33 V. Prevot, C. Forano and J. P. Besse, *Appl. Clay Sci.*, 2001, **18**, 3–15.
- 34 D. N. Stamires, M. F. Brady, W. Jones and F. Kooli, *US Pat.*, 6 333 290, 2001.
- 35 R. K. Kukkadapu, M. S. Witkowski and J. E. Amonette, *Chem. Mater.*, 1997, **9**, 417–419.
- 36 M. Kaneyoshi and W. Jones, *J. Mater. Chem.*, 1999, **9**, 805–811.
- 37 Z. P. Xu and H. C. Zeng, *J. Phys. Chem. B*, 2001, **105**, 1743–1749.
- 38 G. Mascolo and O. Marino, *Mineral. Mag.*, 1980, **43**, 619–621.
- 39 M. C. Gastuche, G. Brown and M. M. Mortland, *Clay Miner.*, 1967, **7**, 177–192.
- 40 M. Ogawa and S. Asai, *Chem. Mater.*, 2000, **12**, 3253.

Microwave irradiation as an alternative to phase transfer catalysis in the liquid-solid phase, solvent-free C-alkylation of active methylene containing substrates

György Keglevich,^{*a} Tibor Novák,^b László Vida^c and István Greiner^d

Received 20th July 2006, Accepted 25th August 2006

First published as an Advance Article on the web 15th September 2006

DOI: 10.1039/b610481a

Simple CH-acidic compounds can be easily monoalkylated in solid-liquid phase in the absence of a phase transfer catalyst applying microwave under solvent-free conditions.

Introduction

Phase transfer catalysis (PTC) is a powerful technique accomplishing a variety of reactions including C-alkylations under mild conditions, in a selective and efficient way.¹ A logical combination is when phase transfer catalysed reactions are further promoted by microwave irradiation.² In the field of C-alkylations, the monosubstitution of diethyl malonate,³ ethyl phenylsulfonylacetate⁴ and ethyl phenylmercaptoacetate⁵ was realized under combined PTC-MW techniques in a solvent-free way. Dialkylation of active methylene containing substrates by one equivalent of 1,2-dibromoethane under similar conditions led to cyclopropane derivatives.⁶ There is, however, one main drawback regarding the environmentally-friendly aspects of the PTC-MW technique, that is the waste of phase transfer catalysts. On an industrial scale, the amount of the catalyst used cannot be ignored. A good solution that has not yet been generally spread is binding the catalysts to solid supports making regeneration possible by simple filtration. We decided to investigate how solid-liquid phase C-alkylations can be modified to be ecofriendlier.

Results and discussion

The alkylation of diethyl malonate (DEM) by ethyliodide served as the basic reaction model. Ethyliodide, due to its lower volatility, seemed to be more suitable as compared to ethylbromide, as we wished to work under certain pressure in the MW-reactor. The alkylation of DEM using ethylbromide was described in a variety of solvents applying the phase transfer catalytic technique.⁷ In DMF at 60 °C, the alkylation was completed after 4 h and the yield was 90%. Performing the reaction in boiling acetone the product was obtained in 66% yield after 11 h (Table 1).

To have a control experiment in hand, the model reaction was accomplished using triethylbenzylammonium chloride

(TEBAC), K₂CO₃ in boiling acetone. Monoethylmalonate was obtained in 78% yield after a 20 h reaction time. Carrying out the alkylation at 120 °C under solvent-free conditions in a MW reactor equipped with a pressure controller, the reaction became much faster (30 min) and remained efficient (88% yield). The effect of other catalysts, such as ethyltriphenylphosphonium bromide and 18-crown-6 was also tested, but their chemical substance did not have much impact on the course of the reaction. K₂CO₃ could be successfully replaced by KOH. The results are shown in Table 1.

The most interesting experience was, however, that omitting the phase transfer catalyst, the alkylation proceeded as well as in the presence of catalyst. The only difference was that completion of the reaction required 40 min instead of 30 min. The yield of the product was 94%. It is a quite surprising observation that although somewhat slower, a solid-liquid two phase alkylation could proceed in the absence of a phase transfer catalyst at 120 °C, under 13 bar applying MW. This must be due to the beneficial effect of MW irradiation and the pressure itself. It is noted that 120 °C seemed to be the optimum reaction temperature and the pressure of 13 bar was only a consequence of using a sealed tube. It was observed that the conversion of the monoalkylation of diethyl malonate was almost 80% after 20 min, but the last stage of the reaction was somewhat sluggish possibly due to the strong heterogeneity. For the same reason and to compensate for the absence of catalyst it was necessary to apply an irradiation of 40 W.

The optimum conditions (120 °C, MW) were then applied to the substitution of DEM by other alkylating agents, such as butylbromide and benzylbromide. As can be seen in Scheme 1, these reactions were also successful, although completion of the reaction required a somewhat longer period of time (*ca.* 2.5 h with BuBr and 1.5 h with BnBr). The yield in the alkylation with benzylbromide was lower (52%) than in the other cases (94 and 83%). The poorer yield is due to side reactions resulting in the formation of compounds with higher boiling points that were not investigated in the present stage of the project. The by-products did not include geminal dibenzylated species. The above data are shown in Scheme 1.

Finally, other CH acidic compounds, such as ethyl acetate and ethyl cyanoacetate were also tested in alkylations with ethyliodide. Scheme 2 shows that the monoalkylations

^aDepartment of Organic Chemical Technology, Budapest University of Technology and Economics, H-1521, Budapest, Hungary. E-mail: keglevich@mail.bme.hu; Fax: +36 (1) 463 3648

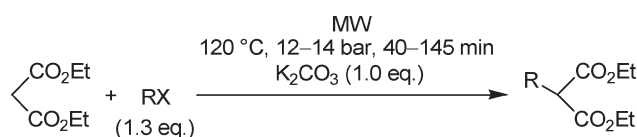
^bResearch Group of the Hungarian Academy of Sciences at the Department of Organic Chemical Technology, Budapest University of Technology and Economics, H-1521, Budapest, Hungary

^cDepartment of Chemical Technology, Budapest University of Technology and Economics, H-1521, Budapest, Hungary

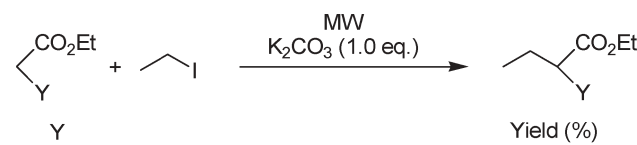
^dRichter Gedeon Rt., H-1475, Budapest 10, PO Box 27, Hungary

Table 1 Solid-liquid phase alkylation of DEM under different conditions

Base	EtX	Catalyst	Solvent	Method of heating	Conditions	Reaction time	Yield (%)	Ref.
K ₂ CO ₃ (1.5 eq.)	EtBr (1.5 eq.)	TEBAC (10%)	DMF	Oil bath	60 °C	4 h	90	7
K ₂ CO ₃ (1.5 eq.)	EtBr (1.5 eq.)	TEBAC (10%)	Acetone	Oil bath	56 °C	11 h	66	7
K ₂ CO ₃ (1.0 eq.)	EtI (1.3 eq.)	TEBAC (10%)	Acetone	Oil bath	56 °C	20 h	78	
K ₂ CO ₃ (1.0 eq.)	EtI (1.3 eq.)	TEBAC	—	MW	120 °C/13 bar	30 min	88	
K ₂ CO ₃ (1.0 eq.)	EtI (1.3 eq.)	Ethyltriphenyl-phosphonium bromide	—	MW	120 °C/13 bar	30 min	91	
K ₂ CO ₃ (1.0 eq.)	EtI (1.3 eq.)	18-Crown-6	—	MW	120 °C/13 bar	30 min	92	
KOH (1.0 eq.)	EtI (1.3 eq.)	TEBAC	—	MW	120 °C/13 bar	30 min	85	
K ₂ CO ₃ (1.0 eq.)	EtI (1.3 eq.)	—	—	MW	120 °C/13 bar	40 min	94	



RX	Reaction time (min)	Yield (%)
EtI	40	94
BuBr	145	83
BnBr	90	52

Scheme 1

Y	Yield (%)
CO ₂ Et	94
CH ₃ C(O)	86
CN	78

Scheme 2

could be successfully applied to these model compounds as well, as the isolated yields fall in the range of 78–94%. Due to the higher activity of these substrates minor modifications had to be made. Ethylating ethyl acetoacetate only one equivalent of ethyl iodide was used and the reaction was run at 100 °C for 30 min. The alkylation of ethyl cyanoacetate was carried out at as low a temperature as 80 °C, using again only one equivalent of the alkylating agent. Using more of the alkylating agent and performing the reaction at a higher temperature led to a considerable amount of the diethyl product. Monoalkylation of ethyl acetoacetate was entirely selective under the milder conditions, but the similar reaction of ethyl cyanoacetate led inevitably to *ca.* 10% of the disubstituted product. Nevertheless, the monoalkylated product could be separated efficiently from the dialkylated species by distillation.

It can be concluded that an environmentally friendly method was developed for the two phase alkylation of active methylene containing substrates simply by eliminating the phase transfer catalyst and applying MW under solvent-free conditions.

Experimental

General procedure

A mixture of 0.76 ml (5 mmol) of diethyl malonate, 6.5 mmol of the alkyl halogenide and 0.69 g (5 mmol) of potassium carbonate was heated at 120 °C (applying 40 W) in a vial in a CEM Discover microwave reactor equipped with a pressure controller for the corresponding time. The crude product was taken up in 25 ml of ethyl acetate and the suspension was filtered. The filtrate was extracted three times with 10 ml of water. The organic phase was dried (Na₂SO₄) and concentrated to afford the crude product. The resulting oil of two experiments was combined and purified by distillation in vacuum. Purity of the products was *ca.* 98%.

A similar procedure was used when a phase transfer catalyst was applied.

The following products were thus prepared:

Diethyl ethylmalonate. Yield: 94%; bp: 88–92 °C (15 mmHg); bp:⁸ 75–77 °C (5 mmHg); [M + H]⁺ = 189.

Diethyl butylmalonate. Yield: 83%; bp: 105–107 °C (14 mmHg); bp:⁹ 102–103 (11 mmHg), bp[8]: 235–240 °C; [M + H]⁺ = 217.

Diethyl benzylmalonate. Yield: 52%; bp: 103–105 °C (0.15 mmHg); bp:⁸ 162–163 °C (10 mmHg); [M + H]⁺ = 251.

Two other derivatives were prepared with minor modifications of the general procedure (see Scheme 2).

Ethyl 2-ethylacetoacetate. Yield: 86%; bp: 78–80 °C (11 mmHg); bp:⁸ 187–189 °C (743 mmHg); [M + H]⁺ = 159.

Ethyl 2-ethylcyanoacetate. Yield: 78%; bp: 89–90 °C (14 mmHg); bp:¹⁰ 104–108 °C (21 mmHg); [M + H]⁺ = 142.

Acknowledgements

The above project was supported by the joint funds from the European Union and the Hungarian State (GVOP-3.2.2.-2004-07-0006/3.1). G. K. is indebted to Dr. Ibolya Prauda for participating in the first part of the project. T. N. is grateful for the Bolyai fellowship.

References

- 1 C. M. Starks, C. L. Liotta and M. Halpern, *Phase Transfer Catalysis – Fundamentals, Applications and Industrial Perspectives*, Chapman & Hall, New York, London, 1994.
- 2 S. Deshayes, M. Liagre, A. Loupy, J.-L. Luche and A. Petit, *Tetrahedron*, 1999, **55**, 10851.
- 3 Y. Wang, R. Deng, A. Mi and Y. Jiang, *Synth. Commun.*, 1995, **25**, 1761.
- 4 Y. Wang and Y. Jiang, *Synth. Commun.*, 1992, **22**, 2287.
- 5 R. Deng, Y. Wang and Y. Jiang, *Synth. Commun.*, 1994, **24**, 1917.
- 6 V. K. Gumaste, A. J. Khan, B. M. Bhawal and A. R. A. S. Deshmukh, *Indian J. Chem.*, 2004, **43B**, 420.
- 7 N. N. Sukhanov, L. N. Trappel, V. P. Chetverikov and L. A. Yanovskaya, *Zh. Org. Khim.*, 1985, **21**, 2503.
- 8 *Aldrich Catalogue*, 2005–2006.
- 9 J. I. G. Cadogan, D. H. Hey and J. T. Sharp, *J. Chem. Soc. B*, 1966, 933.
- 10 H. F. Hadley, *J. Am. Chem. Soc.*, 1912, **34**, 923.

		<p>Comments received from just a few of the thousands of satisfied RSC authors and referees who have used ReSource - the online portal helping you through every step of the publication process.</p> <p>authors benefit from a user-friendly electronic submission process, manuscript tracking facilities, online proof collection, free pdf reprints, and can review all aspects of their publishing history</p> <p>referees can download articles, submit reports, monitor the outcome of reviewed manuscripts, and check and update their personal profile</p> <p>NEW!! We have added a number of enhancements to ReSource, to improve your publishing experience even further.</p> <p>New features include:</p> <ul style="list-style-type: none"> ● the facility for authors to save manuscript submissions at key stages in the process (handy for those juggling a hectic research schedule) ● checklists and support notes (with useful hints, tips and reminders) ● and a fresh new look (so that you can more easily see what you have done and need to do next) <p>Go online today and find out more.</p> <p style="text-align: right;"><small>Registered Charity No. 207890</small></p>
	<p>'I wish the others were as easy to use.'</p>	
<p>'ReSource is the best online submission system of any publisher.'</p>		

RSC Publishing
www.rsc.org/resource

Preparation of dialkoxypropanes in simple ammonium ionic liquids

Hui Jiang, Congmin Wang, Haoran Li* and Yong Wang

Received 12th June 2006, Accepted 25th August 2006

First published as an Advance Article on the web 18th September 2006

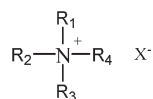
DOI: 10.1039/b608249a

Simple ammonium ionic liquids have been used as a dual catalyst and environmentally benign reaction medium for preparation of dialkoxypropanes, eliminating the need for volatile organic solvents and poisonous hydrogen chloride catalysts. These simple ammonium ionic liquids are air and water stable, easy to synthesise from amine and acid, and relatively cheap, which makes them suitable for industrial application. The results clearly demonstrate that these ionic liquids can be easily separated and reused without losing activity. These ionic liquids provide a good alternative for industrial preparation of dialkoxypropanes.

Introduction

Ionic liquids as new reaction media and catalysts have been experimentally and theoretically recognized and accepted.¹ They are environmentally friendly or “greener” alternatives to organic solvents² because they have very low vapor pressure and are non-explosive and thermally stable over a wide temperature range. They can be employed as solvents for a number of chemical processes, such as separation,³ reactions,⁴ two-phase catalysis,⁵ extractions⁶ and polymerizations.⁷ The application of ionic liquids as novel media may provide convenient solutions to both the solvent emission and catalyst reuse problem.⁸

Despite the unique advantages of ionic liquids, so far they have not been widely applied in industry. Seddon *et al.*⁹ cooperated with many chemical companies, such as BP, and manufactured the linear alkyl benzene based ionic liquids as reaction media. In 2003, the first industrial process involving ionic liquids by BASIL¹⁰ was reported. From then on, the potential of ionic liquids for novel chemical processes and technologies began to be popularly recognized. Recently, a series of simple ammonium ionic liquids¹¹ was studied in detail and successful industrial preparation of cinnamic acid using sulfate ionic liquids as solvent and catalysts was achieved. Furthermore, cracking reactions¹² have been investigated in simple ammonium ionic liquids. As part of our systematic research on simple ammonium ionic liquids and continuing our new findings in industrial applications, herein we report the industrial application of simple ammonium ionic liquids in the preparation of dialkoxypropanes from acetone and alcohols, Fig. 1.



R_{1,2,3}=H, Me, Et, Pr, Bu; X=H₂PO₄, HSO₄, BF₄

Fig. 1 The structures of simple ammonium ionic liquids.

Department of Chemistry, Zhejiang University, Hangzhou 310027, P. R. China. E-mail: lihr@zju.edu.cn; Fax: +86-571-8795-1895; Tel: +86-571-8795-2424

Dialkoxypropanes^{13–15} are a highly valuable class of fine chemicals. They are widely used in polymer preparation, surfactants, pharmaceutical synthesis, and natural product extraction as well as general organic synthesis. They are important intermediates in the manufacture of clarithromycin, β-ionone, vitamin A, vitamin E, alkoxypropene and so on. Acid-catalyzed formation of dialkoxypropanes^{16–18} derived from ketones and alcohols is the most practical method. Lorette *et al.*¹⁶ reported a method describing the synthesis of dialkoxypropanes catalyzed by strong acid ion exchangers at a rather low temperature (−28 °C). Helmut *et al.*¹⁷ disclosed a detailed method of industrial manufacture of dialkoxypropanes by reacting acetone and methanol in the presence of hydrogen chloride as an acidic catalyst and hydrocarbon compounds, such as decane, as solvent. Anhydrous calcium sulfate was added to the reaction system to remove the water from the ketalization equilibrium by forming a hydrate in favor of dialkoxypropanes formation. The shortcomings of these currently used methods are obvious: calls for the use of volatile organic solvents and toxic catalysts, corrosion problems, poor chemical selectivity and the use of a large excess of alcohols. On account of the large demand for dialkoxypropanes in recent years, the search for environmentally friendly catalysts and reaction media are still being actively motivated due to the problems and difficulties of the preparation process. Recently, Wu *et al.*¹⁹ reported the formation of ketals and acetals in Brønsted acidic ionic liquids [Hmim]BF₄. However, how to synthesize the dialkoxypropanes, such as 2,2-dimethoxypropane and 2,2-diethoxypropane was not involved. Despite numerous attempts to overcome these drawbacks, no benign methods have appeared for the synthesis of dialkoxypropanes so far.

We describe here the preparation of dialkoxypropanes in simple ionic liquids, Fig. 2.

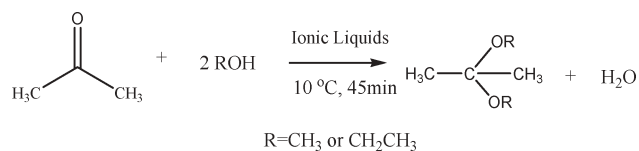


Fig. 2 The preparation of dialkoxypropanes in the ionic liquids.

Experimental

Materials

Acetone, methanol, ethanol, acetic acid, sulfuric acid, phosphoric acid, tetrafluoroboric acid, diethylamine, ethylamine, triethylamine, *n*-tripropylamine, isopropylamine, *n*-tributylamine, *n*-butylamine, *n*-butyl bromide, calcium sulfate dihydrate, imidazole and 1-methylimidazole were all used as received unless otherwise stated.

Instruments

The NMR spectra of the ionic liquids and dialkoxypropanes were recorded with a 500 MHz Bruker spectrometer in DMSO, CDCl₃ and calibrated with tetramethylsilane (TMS) as the internal reference. The purity of raw materials and alkoxypropanes was analysed using a Shang Feng GC112A gas chromatograph fitted with a SE-54 column (50 m, 0.25 mm diameter) and a flame ionisation detector. The structure and the purity of the products were further identified using a HP6890 GC/MS spectrometer by comparing retention times and fragmentation patterns with authentic samples. The melting point was recorded on digital melting point apparatus

Typical reaction procedures in ionic liquids

Simple ammonium ionic liquids of general type [amine][acid] were synthesized according to our former papers.^{11,12} The NMR data and other physical constants of the simple ammonium ionic liquids in this paper are in good agreement with our early reports.^{11,12} Other ionic liquids used in this paper were synthesized according to standard literature methods.²⁰ The reaction of acetone and methanol or ethanol was investigated in several simple ammonium ionic liquids. These reactions were carried out in a 100 ml volumetric flask set in a recirculating freeze-heat bath with a magnetic stir bar. In a typical reaction, acetone (0.05 mol), methanol (0.1 mol) and anhydrous calcium sulfate (0.1 mol), which was prepared from CaSO₄·2H₂O, were added to the simple ammonium ionic liquids, then the mixtures were stirred at 10 °C for 45 min. The calcium sulfate was separated from the reaction mixture by filtration under reduced pressure conditions. The calcium sulfate was subsequently washed with 20 ml ionic liquids three times to ensure no organic compounds were absorbed by the calcium sulfate. The products were concentrated in the solution phase. Because dialkoxypropanes are immiscible with these ionic liquids, the dialkoxypropanes could be isolated with high purity in many cases. The unreacted reactants were evaporated from the ionic liquids by heating. The calcium sulfate was eventually re-dehydrated by heating at 170 °C under reduced pressure in the ionic liquids until the weight remained unchanged.

Results and discussion

Table 1 summarises the results of the ketalization of acetone with methanol in different simple ammonium ionic liquids. The results appeared to be dependent on what kind of ionic liquids were used for a given reaction temperature and time. It

Table 1 The results of preparation of 2,2-dimethoxypropane in ionic liquids

Entry	Solvents	<i>T</i> /°C	Conversion ^a (%)	Selectivity (%)
1	[Et ₃ NH][H ₂ PO ₄]	10	46	98
2	[Me ₃ NH][H ₂ PO ₄]	10	51	97
3	[EtNH ₃][HSO ₄]	10	81	97
4	[Et ₃ NH][BF ₄]	10	15	92
5	[Et ₃ NH][CH ₃ COO]	10	24	98
6	[Hmim][BF ₄]	10	60	97
7	[Bmim][BF ₄]	10	11	96
8	Halohydrocarbon + ^b	10	76	79

^a Conversions after 45 min. ^b Hydrogen chloride. ^c Reaction temperature.

was clear that the catalytic activity was heavily influenced by the anion of the ionic liquids. The best results could be obtained in the case of the sulfate ionic liquids. However, when the tetrafluoroborate anion and acetic anion, such as [Et₃NH][BF₄] and [Et₃NH][CH₃COO] were used, the reaction was much slower and thus the conversion was lower than those obtained using the [HSO₄] anion. When the phosphate anion was employed, the conversion was also lower than those obtained using the [HSO₄] anion, although selectivity for 2,2-dimethoxypropane was much higher. Probably, this is due to the lower acidity of the dihydrogen phosphate counter-anion. A higher selectivity is observed with these ionic liquids in comparison to hydrogen chloride as catalyst and hydrocarbon compounds as solvent.

An important virtue of these reactions in simple ammonium ionic liquids is no evidence for significant formation of by-products. However, when reactions are carried out using a hydrocarbon as solvent and hydrogen chloride as catalyst, side products, such as di-acetone alcohol, would be formed.

In order to obtain reasonable results, different kinds of sulfate ionic liquids were employed in reactions. The results of the effect of the cation of these ionic liquids can be seen in Table 2. Changing the cation can impact the polarity and the solvent properties of the simple ammonium ionic liquids. These results indicated the small impact of the cation on the catalytic performance. It is possible that the immiscibility of the resulting dialkoxypropanes in simple ammonium ionic liquids may facilitate the reaction equilibrium in favor of dialkoxypropanes formation.

The reaction is preferably carried out at room temperature because the ketalization of dialkoxypropanes is exothermic. A lower temperature (−10 °C) favored dialkoxypropanes formation, however, it also led to poor conversion. Too much higher temperatures are less advisable, since in the case of higher temperatures, the water is no longer as effectively bound by the

Table 2 The results of preparation of 2,2-dimethoxypropane in sulfate ionic liquids

Entry	Solvents	<i>T</i> /°C	Conversion ^a (%)	Selectivity (%)
1	[EtNH ₃][HSO ₄]	10	81	97
2	[Et ₃ NH][HSO ₄]	10	82	98
3	[iso-Pr ₃ NH][HSO ₄]	10	78	96
4	[Pr ₃ NH][HSO ₄]	10	77	96
5	[Bu ₃ NH][HSO ₄]	10	76	95

^a Conversions after 45 min.

Table 3 Effect of the temperature and the quantity of [Et₃NH][HSO₄] ionic liquid^a

Entry	Quantity/mol	T/°C	Conversion ^b (%)	Selectivity (%)
1	0.15	10	62	97
2	0.25	10	70	98
3	0.60	10	82	97
4	0.80	10	82	96
5	1.00	10	81	97
6	0.60	0	76	97
7	0.60	25	70	82
8	0.60	50	42	63
9 ^c	0.60	10	85	93

^a The quantity of reactants were 0.05 mol. ^b Conversions after 45 min. ^c 2,2-Diethoxypropane was prepared.

Table 4 Effect of reused [Et₃NH][HSO₄] ionic liquid for preparation of 2,2-dimethoxypropane

Entry	Recycling	T/°C	Conversion ^a (%)	Selectivity (%)
1	0	10	82	98
2	1	10	80	97
3	2	10	82	96
4	3	10	81	95
5	4	10	78	97
6	5	10	82	95
7	6	10	80	96
8	7	10	82	95

^a Conversions after 45 min.

calcium sulfate and the selectivity for dialkoxypropanes would decreased due to the formation of by-products. Another important factor is the quantity of ionic liquids. The influence of the quantity of [Et₃NH][HSO₄] ionic liquids was investigated from 0.2 to 1.0 mol. As can be seen in Table 3, the desired dialkoxypropanes were obtained with good results at 0.6 mol. However, the yields did not continue improving when the quantity was higher than 0.6 mol.

Although we can not yet afford a reasonable explanation for the reaction mechanism of ketalization, these experimental results showed that the change of counteranion increases the reaction rate, while the change of cation has little impact on the catalytic performance.

Once the reaction was complete, the products could be isolated in high yields with high purity in many cases after the calcium sulfate was separated from the reaction mixture and the unreactive reactants were subsequently evaporated from the ionic liquids by heating. Due to the advantages of the highly thermal and chemical stability of the simple ammonium ionic liquids, the calcium sulfate could eventually be regenerated by heating at 170 °C in the ionic liquids prior to use. The simple ammonium ionic liquids were readily separated and reused after the calcium sulfate re-dehydrated. Table 4 shows that the conversion and the selectivity did not significantly decrease after eight uses. It seemed that [Et₃NH][HSO₄] could have the potential to be used for more than eight times.

Conclusion

For the purpose of practical application, imidazolium and other kinds of ionic liquids are expensive. In this paper, simple

ammonium ionic liquids are versatile catalysts/reaction media for the preparation of dialkoxypropanes. These simple ammonium ionic liquids provide good product selectivities as well as a balance between the yield achievable and the ease of catalyst/substrate separation provided by heterogeneous catalysts. These simple ammonium ionic liquids are air and water stable, easy to synthesis from amine and acid, and relatively cheap. During the preparation process, no volatile solvents are needed. These ionic liquids can be easily separated and reused. The dialkoxypropanes can be conveniently isolated with high purity. Even so, improvements in these systems would be welcome. These ionic liquids provide a good alternative for industrial synthesis of dialkoxypropanes.

Acknowledgements

This work was supported by the Natural Science Foundation of China (NO.20434020).

References

- R. D. Rogers and K. R. Seddon, *Science*, 2003, **302**, 792; R. Sheldon, *Green Chem.*, 2005, **7**, 267; C. C. Amanda, J. L. Jessica, N. Loanna, L. Kim, J. K. Trans, W. J. Kristin, F. C. David and J. H. Davis, Jr., *J. Am. Chem. Soc.*, 2002, **124**, 5962; P. Wasserscheid and W. Keim, *Angew. Chem., Int. Ed.*, 2000, **39**, 3773; C. G. Hanke, N. A. Afamas and R. M. Lynden-Bell, *Green Chem.*, 2002, **4**, 107; Y. Wang, H. Li and S. Han, *J. Chem. Phys.*, 2005, **123**, 174501; Y. Wang, H. Li and S. Han, *J. Chem. Phys.*, 2006, **124**, 044504.
- J. S. Wilkes, J. A. Levisky, R. A. Wilson and C. L. Hussey, *Inorg. Chem.*, 1982, **21**, 1263; J. S. Wilkes and M. J. Zaworotko, *Chem. Commun.*, 1992, 965.
- T. Welton, *Chem. Rev.*, 1999, **99**, 2071; J. Dupont, R. F. de Souza and P. A. Z. Suarez, *Chem. Rev.*, 2002, **102**, 3667.
- J. G. Huddleston, H. D. Willauer, R. P. Swatloski, A. E. Visser and R. D. Rogers, *Chem. Commun.*, 1998, 1765; J. Esser, P. Wasserscheid and A. Jess, *Green Chem.*, 2004, **6**, 316.
- R. Sheldon, *Chem. Commun.*, 2001, 2399; C. J. Adams, M. J. Earle, G. Roberts and K. R. Seddon, *Chem. Commun.*, 1998, 2097.
- A. J. Carmichael, M. J. Earle, J. D. Holbrey, P. B. McCormac and K. R. Seddon, *Org. Lett.*, 1999, **1**, 997.
- R. T. Carlin and J. S. Wilkes, *J. Mol. Catal. A: Chem.*, 1990, **63**, 125.
- F. C. Liu, M. B. Abrams, R. T. Baker and W. Tumas, *Chem. Commun.*, 2001, 433; E. D. Bates, R. D. Mayton, I. Ntai and J. H. Davis, *J. Am. Chem. Soc.*, 2002, **124**, 926; M. J. Earle, P. B. McCormac and K. R. Seddon, *Green Chem.*, 2000, **2**, 261; G. A. Olah, T. Mathew, A. Goeppert, B. Torok, I. Bucs, X. Y. Li, Q. Wang, E. R. Marinez, P. Batamack, R. Aniszfeld and G. K. S. Prakash, *J. Am. Chem. Soc.*, 2005, **127**, 5964.
- M. J. Earle, P. B. McCormac and K. R. Seddon, *Chem. Commun.*, 1998, 2245.
- M. Maase, K. Massonne, K. Halbritter, R. Noe, M. Bartsch, W. Siegel, V. Stegmann, M. Flores, O. Huttenloch and M. Becher, *EP Pat.*, EP 1 472 201, 2004.
- J. Weng, C. Wang, H. Li and Y. Wang, *Green Chem.*, 2006, **8**, 96.
- C. Wang, L. Guo, H. Li, Y. Wang, J. Weng and L. Wu, *Green Chem.*, 2006, **8**, 603.
- H. Jiang, H. Li, C. Wang, T. Tan and S. Han, *J. Chem. Thermodyn.*, 2003, **35**, 1567; V. R. Choudhary, V. H. Rane and A. M. Rajput, *Ind. Eng. Chem. Res.*, 2000, **39**, 904.
- W. G. S. Reyntjens and E. Goethals, *Polym. Adv. Technol.*, 2001, **12**, 107; E. M. Carreira, W. Lee and R. A. Singer, *J. Am. Chem. Soc.*, 1995, **117**, 3649.
- S. Frauchiger and A. Baiker, *Appl. Catal., A*, 2003, **253**, 33; J. R. Behling, P. Farid, I. Khanna, J. R. Medich, M. Prunier, M. G. Scaros and R. M. Weier, *US Pat.*, US 5 151 519, 1999.

- 16 N. B. Lorette, W. L. Howard and J. H. Brown, *J. Org. Chem.*, 1959, **24**, 1731.
- 17 Z. A. Helmut, D. Bad and S. Walter, *US Pat.*, US 4 136 124, 1979.
- 18 J. H. Brown, Jr. and N. B. Lorette, *US Pat.*, US 2 827 494, 1958.
- 19 H. Wu, F. Yang, P. Cui, J. Tang and Y. He, *Tetrahedron Lett.*, 2004, **45**, 4963.
- 20 G. Y. Zhao, T. Jiang, H. X. Gao, B. X. Han, J. Huang and D. H. Sun, *Green Chem.*, 2004, **6**, 75; L. Ropel, S. B. Lionel, N. V. K. A. Sudhir, A. S. Mark and J. F. Brennecke, *Green Chem.*, 2005, **7**, 83.

Textbooks from the RSC

The RSC publishes a wide selection of textbooks for chemical science students. From the bestselling *Crime Scene to Court*, 2nd edition to groundbreaking books such as *Nanochemistry: A Chemical Approach to Nanomaterials*, to primers on individual topics from our successful *Tutorial Chemistry Texts series*, we can cater for all of your study needs.

Find out more at www.rsc.org/books

Lecturers can request inspection copies – please contact sales@rsc.org for further information.



Registered Charity No. 207890

RSCPublishing

www.rsc.org/books

Environmentally benign one-pot multi-component approaches to the synthesis of novel unsymmetrical 4-arylacridinediones

Guan-Wu Wang* and Chun-Bao Miao

Received 20th March 2006, Accepted 6th September 2006

First published as an Advance Article on the web 21st September 2006

DOI: 10.1039/b604064k

The solvent-free and aqueous conditions used give good yields that cannot be achieved in organic solvents. The current process provides a simple and green method to obtain a variety of novel unsymmetrical acridinediones, which may have potential biological activities.

Introduction

At the beginning of the new century, it is widely acknowledged that there is a growing need for developing environmentally benign processes in the chemical industry.^{1,2} Many of the traditional volatile organic solvents are ecologically harmful, and nonconventional reaction media for benign chemical technologies are highly sought after. Among these reaction media, the best solvent is no solvent, and if a solvent is needed, then water is preferred.¹ The state of the art in the use of alternative reaction media for green, sustainable organic synthesis has been described.¹ Solvent-free reactions have many advantages such as reduced pollution, lower costs and simplicity.³ Water is nontoxic, nonflammable, abundantly available and inexpensive. Thus, water as the reaction medium is generally considered as a cheap, safe and environmentally benign alternative to 'synthetic' solvents. Furthermore, due to the low solubility of common organic compounds in water, the use of water as solvent often makes the purification of products very easy by simple filtration or extraction.⁴

4-Aryl-1,4-dihydropyridines (1,4-DHPs) have proved to be valuable as drugs for the treatment of cardiovascular disorders,⁵ and constitute an important class of calcium channel blockers.⁶ It is well established that slight structural modification on the DHP ring may result in remarkable change of pharmacological effect.^{7–10} With a 1,4-DHP parent nucleus, acridine-1,8-diones have been shown to have very high lasing efficiencies¹¹ and used as photoinitiators.¹² Many acridinediones have been synthesized by the reactions of aldehydes with two equivalents of 1,3-cyclohexanedione or 5,5-dimethyl-1,3-cyclohexanedione and appropriate amines *via* various methods.¹³ However, all these compounds belong to symmetrical acridinediones **A** or **B** (Fig. 1) which contain two identical cyclohexanone rings fused to the DHP rings. To the best of our knowledge, the acridinediones of type **C**, the dihydropyridine ring linking two unsymmetrical cyclohexanone rings, have not been reported. As a continuation of our research devoted to the development of green organic chemistry by performing reactions under solvent-free conditions¹⁴ or by using water as reaction medium,¹⁵ herein we

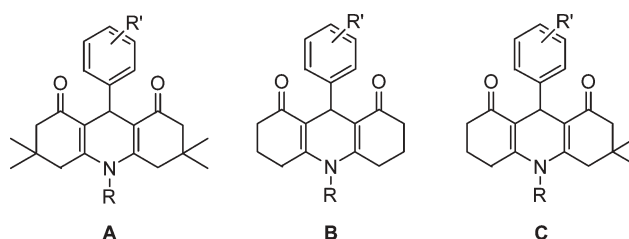
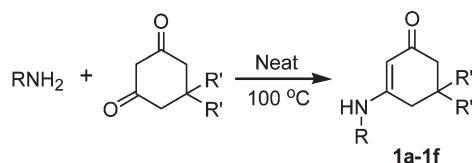


Fig. 1 Acridinediones **A**, **B** and **C**.

report a versatile, environmentally friendly, one-pot, and multi-component synthesis of acridinediones of type **C**.

Results and discussion

Enaminones are versatile and readily obtainable reagents, and their chemistry has received considerable attention in recent years.¹⁶ Our strategy of synthesizing the unsymmetrical acridinediones of type **C** was through the reaction of a preformed enaminone with a 1,3-cyclohexanedione derivative and an aldehyde. Representing amines, that is, ammonia (ammonium acetate as the source), methylamine as the aliphatic amine and 4-methylphenylamine as the aromatic amine, were selected for our study. The preparation of enaminones **1a–f** was commonly achieved by refluxing the reaction mixture in an aromatic solvent, with the removal of the produced water by azeotropic distillation.¹⁷ We found that enaminones **1a–f** could be obtained in good to excellent yields by heating the neat mixture of the corresponding amine and 1,3-cyclohexanedione or 5,5-dimethyl-1,3-cyclohexanedione at 100 °C for 10–30 minutes (Scheme 1). The reaction times and yields for solvent-free synthesis of enaminones **1a–f** at 100 °C are listed in Table 1.



- 1a:** R = H, R' = CH₃; **1d:** R = H, R' = H;
1b: R = CH₃, R' = CH₃; **1e:** R = CH₃, R' = H;
1c: R = 4-CH₃Ph, R' = CH₃; **1f:** R = 4-CH₃Ph, R' = H

Scheme 1 The preparation of enaminones **1a–f**.

Hefei National Laboratory for Physical Sciences at Microscale and Department of Chemistry, University of Science and Technology of China, Hefei, Anhui 230026, P. R. China. E-mail: gwang@ustc.edu.cn; Fax: +86-551-360-7864

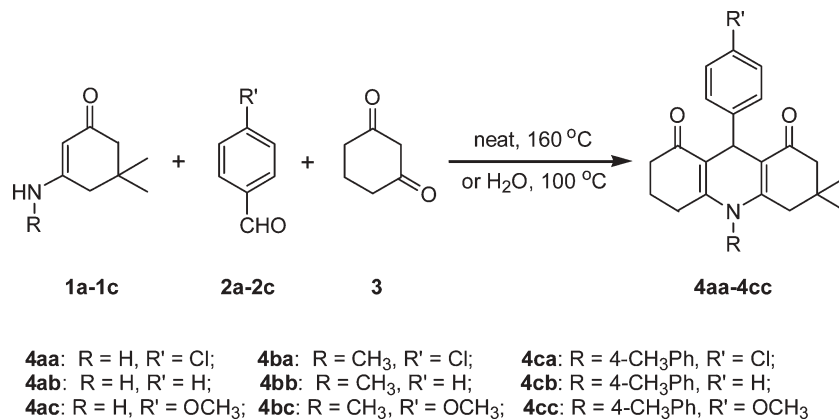
Table 1 Reaction times and yields for solvent-free synthesis of enamines **1a–f** at 100 °C

Entry	Product	Time/min	Yield (%)	Mp(ref)/°C
1	1a	10	95	165–167 (165–166.5 ^{17a})
2	1b	30	90	153–154.5 (153–154.5 ^{17a})
3	1c	30	96	203–204 (203–204 ^{17b})
4	1d	10	90	132–134 (133 ^{17c})
5	1e	30	88	67–68 (67–67.5 ^{17d})
6	1f	30	92	142–143 (140–142 ^{17e})

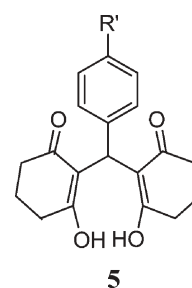
To our satisfaction, a mixture of equimolar amount of enamines **1a–c**, aromatic aldehydes **2a–c** and 1,3-cyclohexanone **3** was allowed to react in refluxing water for 3–10 h, the expected unsymmetrical acridinediones **4aa–cc** were obtained in 71–87% yields (Scheme 2). Comparable product yields were achieved by just heating the reactants at 160 °C for 2–5 min under solvent-free conditions. The reaction times and yields for the reactions of **1a–c** with **2a–c** and **3** under solvent-free conditions at 160 °C and in refluxing water conditions are collected in Table 2. As shown in Table 2, R' group on the phenyl ring did not affect the reactivity of **2a–c**. However, the reactivity of **1a–c** is slightly higher when R is H.

As can be seen from Table 2, to reach comparable yields the solvent-free reactions needed shorter reaction time than the aqueous reactions, but required higher reaction temperature. If the mixture of the reactants was heated under solvent-free conditions at a lower temperature than 160 °C, there was large amount of undesired product 2,2'-(arylmethylene)bis-(3-hydroxy-2-cyclohexen-1-one) (**5**, Fig. 2) formed by the condensation reaction of 1,3-cyclohexanedione **3** and aldehydes **2a–c**. Take entry 7 as a typical example, 2,2'-[(4-chlorophenyl)methylene]bis-(3-hydroxy-2-cyclohexen-1-one) was isolated in 64% yield and the desired product **4ac** was obtained only in 24% yield based on **3** when the reaction was operated at 100 °C for 10 h. This example exhibited the special effect of water compared with solvent-free conditions, as well as organic solvents (*vide infra*).

To demonstrate the advantages of the reactions in water, selected reactions were conducted in organic solvents for comparison. The reactions of **1a–c** with **2a** and **3** in dioxane (100 °C), toluene (100 °C) and ethanol (refluxing) were chosen as the model reactions, and their yields are listed in Table 3.

**Scheme 2** The synthesis of the unsymmetrical acridinediones **4aa–cc**.**Table 2** Reaction times and yields for the synthesis of **4aa–cc** under solvent-free or aqueous conditions

Entry	Product	Neat at 160 °C		In water at 100 °C		Mp/°C
		Time/min	Yield (%)	Time/h	Yield (%)	
1	4aa	2	87	3	87	237–238
2	4ab	2	87	3	87	242–244
3	4ac	2	85	3	89	248–250
4	4ba	5	80	10	77	233–234
5	4bb	5	70	10	72	197–198
6	4bc	5	75	10	71	193–194
7	4ca	5	75	10	72	287–288
8	4cb	5	74	10	73	254–256
9	4cc	5	77	10	75	244–246

**Fig. 2** Structure of compound **5**.**Table 3** Product yields for the reactions of **1a–c** with **2a** and **3** in various solvents

Entry	R	R'	Solvent	T/°C	Time/h	Yield (%)
1	H	Cl	Dioxane	100	10	44 (4aa)
2	CH ₃	Cl	Dioxane	100	10	17 (4ba)
3	4-CH ₃ Ph	Cl	Dioxane	100	10	11 (4ca)
4	H	Cl	Toluene	100	10	87 (4aa)
5	CH ₃	Cl	Toluene	100	10	11 (4ba)
6	4-CH ₃ Ph	Cl	Toluene	100	10	8 (4ca)
7	H	Cl	Ethanol	80	10	46 (4aa)
8	CH ₃	Cl	Ethanol	80	10	12 (4ba)
9	4-CH ₃ Ph	Cl	Ethanol	80	12	34 (4ca)

The yields in organic solvents were generally lower than those in refluxing water due to the formation of byproducts.

By comparison of the data in Tables 2 and 3, it is obvious that the yields under both solvent-free and in water conditions

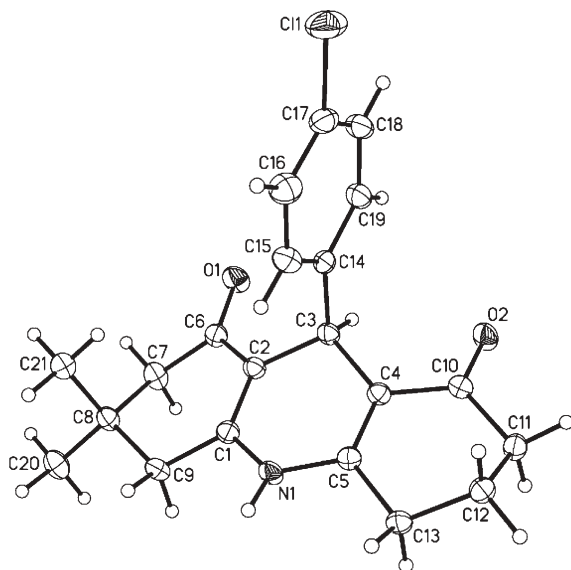


Fig. 3 ORTEP diagram of compound **4aa**. Ellipsoids are plotted at the 40% probability level.

are higher than those in organic solvents. During our solvent-free reaction processes, we observed that the reaction mixtures first turned into a uniform liquid phase, and then into the solid products. Scott and co-workers have presented examples of efficient solventless organic reactions attributed to the formation of eutectic melts.^{3c,3d} In our case, the melting points of all starting materials except for **1b** and **1c** are lower than 160 °C. Therefore, the formed uniform liquid phase at 160 °C—due to either a simple melt or a eutectic melt—facilitated the solvent-free reactions, which occurred at extremely high concentrations of the starting materials, and thus afforded higher reaction rates and higher yields than those in organic solvents. The employed starting materials are partially soluble in water. The aqueous reactions performed better than the reactions in organic solvents, probably due to the beneficial hydrophobic effect/solvophobicity and hydrogen bonding in water, as described previously.^{4b,18}

It should be mentioned that the reactions of enaminones **1d–f** with aldehydes **2a–c** and 5,5-dimethyl-1,3-cyclohexanedione, under solvent-free conditions at 160 °C or in refluxing water,

afforded rather complex mixtures containing some **4aa–cc**. Furthermore, similar phenomena were observed for the four-component reaction mixtures of aldehydes, 1,3-cyclohexanone, 5,5-dimethyl-1,3-cyclohexanone and amines under the same conditions. It seems that the combination of **1a–c**, **2a–c** and 1,3-cyclohexanedione is the only good route to the one-pot multi-component synthesis of unsymmetrical acridinediones **4aa–cc**.

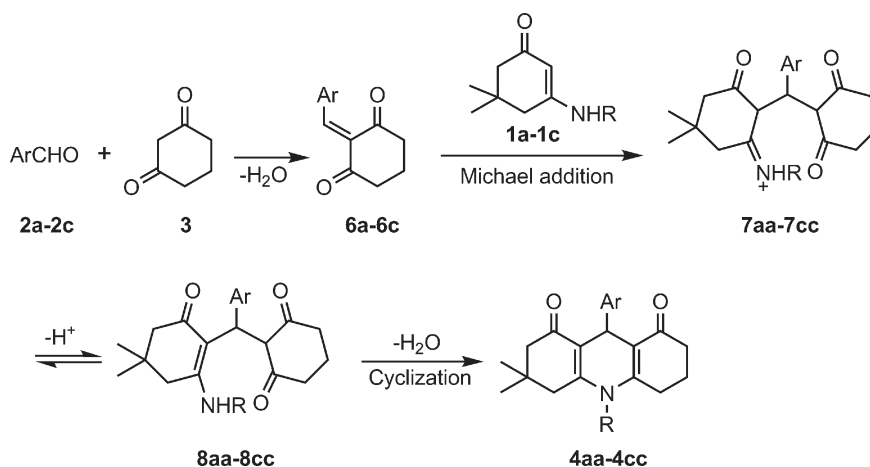
The identification of acridinediones **4aa–cc** is unequivocally ascertained by ¹H NMR, ¹³C NMR, FT-IR spectra and elemental analyses. The structure of **4aa** was further confirmed by X-ray crystallography (Fig. 3), which revealed a unique characteristic of this type of compounds in the solid state. According to the X-ray single crystal diffraction study, the central pyridine adopts a boat conformation and the plane of the phenyl ring is orthogonal to it (the phenyl ring makes a dihedral angle of 87.03° with the plane through the acridine moiety).

Chirality plays an important role in the biological activities of 1,4-dihydropyridines.^{8,19} Many of the synthesized 1,4-DHP calcium antagonists are asymmetric. The enantiomers of unsymmetrical 1,4-DHPs usually differ in their biological activities.¹⁹ Conformation–activity profiles for unsymmetrically substituted 4-aryl-1,4-dihydropyridines on calcium channel modulators were reported, and in the receptor-bound conformation the substituted aryl ring should be positioned axially, perpendicular to and bisecting the boat-like dihydropyridine ring.^{7c,8,20} Thus, these synthesized unsymmetrical acridinediones **4aa–cc** may have potential properties of calcium channel modulators.

A mechanism for the formation of **4aa–cc** is outlined in Scheme 3. The Michael additions of enaminones **1a–c** with **6a–c**, which are formed *in situ* from the condensation reactions of aromatic aldehydes **2a–c** and 1,3-cyclohexanedione **3**, give the intermediates **7aa–7cc**. Isomerizations of **7aa–7cc** to **8aa–8cc**, followed by intramolecular cycloadditions, and subsequent dehydrations afford compounds **4aa–cc**.

Conclusion

In summary, we have developed a rapid solvent-free method to synthesize cyclic enaminones **1a–f**. The reactions of



Scheme 3 Proposed mechanism for the formation of **4aa–cc**.

enaminones **1a–c** with aldehydes **2a–c** and 1,3-cyclohexanedione **3** under solvent-free or aqueous conditions provided a novel route to the access of unsymmetrical acridinediones **4aa–cc** with good yields for the first time. The method is endowed with several unique merits, namely, one-pot multi-component reactions, environmentally friendly conditions and simple work-up procedure. This new class of compounds might be used as new lead compounds for biological activity evaluation, especially as calcium channel regulators.

Experimental

General

Melting points were determined on an XT-4 apparatus and were uncorrected. IR spectra were taken on a Bruker Vector-22 spectrometer in KBr pellets and reported in cm^{-1} . ^1H NMR spectra were recorded at 300 MHz on a Bruker Avance-300 spectrometer in CDCl_3 with chemical shifts (δ) given in ppm relative to TMS as an internal standard. ^{13}C NMR spectra were recorded on a Bruker Avance-300 (75.5 MHz) spectrometer with complete proton decoupling, chemical shifts are reported in ppm relative to the solvent resonance as the internal standard (CDCl_3 , δ 77.16 ppm). All intensities in the ^{13}C NMR spectral data are 1C except where indicated. Elemental analyses were analyzed by a Vario ELIII elemental analyzer (for CHN).

Typical procedure for the synthesis of 1a–f under solvent-free conditions. A mixture of 5,5-dimethyl-1,3-cyclohexanedione or 1,3-cyclohexanedione (1 mmol), amine (1 mmol for NH_4OAc and 4-methylphenylamine, 4 mmol for methylamine (25–30% W/W aq. soln.) was stirred at 100 °C for a given time in a preheated oil bath (monitored by TLC). After being cooled to room temperature, the reaction mixture was purified on a silica gel column to give the desired enaminone (**1a–f**). For the reactions with methylamine, the reaction mixtures required evaporation *in vacuo* to remove volatile materials before column chromatography.

Typical procedure for the synthesis of 4aa–cc under solvent-free conditions. A mixture of an enaminone (**1a–c**, 0.5 mmol), an aromatic aldehyde (**2a–c**, 0.5 mmol) and 1,3-cyclohexanedione (56 mg, 0.5 mmol) was stirred at 160 °C for a desired time (monitored by TLC) in a preheated oil bath. After being cooled to room temperature, the reaction mixture was washed with ice-cold ethyl acetate (5 cm^{-3}) to afford pure product (**4aa–cc**). The desired products of very high purity were further achieved by recrystallization from ethanol.

Typical procedure for the synthesis of 4aa–cc in refluxing water. A mixture of an enaminone (**1a–c**, 0.5 mmol), an aromatic aldehyde (**2a–c**, 0.5 mmol) and 1,3-cyclohexanedione (56 mg, 0.5 mmol) was suspended in water (15 cm^{-3}), and the heterogeneous mixture was stirred vigorously and refluxed for a desired time (monitored by TLC). The reaction mixture was then evaporated *in vacuo* to remove water. After being cooled, the residue was washed with ice-cold ethyl acetate (5 cm^{-3}) to afford pure product (**4aa–cc**). The desired products of very

high purity were further achieved by recrystallization from ethanol.

3,3-Dimethyl-9-(4-chlorophenyl)-decahydroacridine-1,8-dione (4aa). Light yellow solid, mp 237–238 °C (from EtOH); (Found: C, 70.7; H, 6.1; N, 3.8. Calc. for $\text{C}_{21}\text{H}_{22}\text{ClNO}_2$: C, 70.9; H, 6.2; N, 3.9%); $\nu_{\text{max}}/\text{cm}^{-1}$ 3279(NH), 2954, 1644, 1625, 1603, 1482, 1364, 1234, 1185, 1135 829, 567 and 512 cm^{-1} ; δ_{H} (300 MHz; CDCl_3 ; Me_4Si) 0.98 (3H, s, CH_3), 1.09 (3H, s, CH_3), 1.92–2.08 (2H, m, CH_2), 2.13–2.50 (8H, m, CH_2), 5.07 (1H, s, CH), 5.99 (1H, br s, NH), 7.15 (2H, d, J 8.4, ArH) and 7.26 (2H, d, J 8.4, ArH); δ_{C} (75 MHz; CDCl_3 ; Me_4Si) 21.3, 27.4, 27.8, 29.5, 32.9, 33.3, 37.2, 41.5, 50.9, 113.7, 114.9, 128.3 (2C), 129.7 (2C), 131.8, 145.2, 147.4, 149.2, 195.3 and 195.5.

3,3-Dimethyl-9-phenyl-decahydroacridine-1,8-dione (4ab). Light yellow solid, mp 242–244 °C (from EtOH); (Found: C, 78.3; H, 7.1; N, 4.3. Calc. for $\text{C}_{21}\text{H}_{23}\text{NO}_2$: C, 78.5; H, 7.2; N, 4.4%); $\nu_{\text{max}}/\text{cm}^{-1}$ 3300 (NH), 2952, 1644, 1621, 1598, 1478, 1364, 1232, 1188, 1135, 982, 696 and 563 cm^{-1} ; δ_{H} (300 MHz; CDCl_3 ; Me_4Si) 0.98 (3H, s, CH_3), 1.09 (3H, s, CH_3), 1.92–2.06 (2H, m, CH_2), 2.14–2.52 (8H, m, CH_2), 5.12 (1H, s, CH), 6.14 (1H, br s, NH), 7.07 (1H, t, J 7.2, ArH), 7.19 (2H, t, J 7.2, ArH) and 7.32 (2 H, d, J 7.1, ArH); δ_{C} (75 MHz; CDCl_3 ; Me_4Si) 21.3, 27.4, 27.7, 29.6, 32.8, 33.6, 37.3, 41.4, 51.0, 113.9, 115.1, 126.1, 128.1 (2C), 128.2 (2C), 146.7, 147.8, 149.5, 195.5 and 195.7.

3,3-Dimethyl-9-(4-methoxyphenyl)-decahydroacridine-1,8-dione (4ac). Light yellow solid, mp 248–250 °C (from EtOH); (Found: C, 75.4; H, 7.1; N, 4.1. Calc. for $\text{C}_{22}\text{H}_{25}\text{NO}_3$: C, 75.2; H, 7.2; N, 4.0%); $\nu_{\text{max}}/\text{cm}^{-1}$ 3290 (NH), 2950, 1642, 1623, 1595, 1477, 1364, 1233, 1187, 1135, 1041, 980, 857, 828, 695, 574 and 523 cm^{-1} ; δ_{H} (300 MHz; CDCl_3 ; Me_4Si) 0.98 (3H, s, CH_3), 1.08 (3H, s, CH_3), 1.92–2.06 (2H, m, CH_2), 2.13–2.48 (8H, m, CH_2), 3.72 (3H, s, OCH_3), 5.06 (1H, s, CH), 6.05 (1H, br s, NH), 6.73 (2H, d, J 8.6, ArH) and 7.24 (d, 2H, J 8.6, ArH); δ_{C} (75 MHz; CDCl_3 ; Me_4Si) 21.3, 27.5, 27.7, 29.6, 32.7, 32.8, 37.3, 41.3, 51.0, 55.3, 113.6 (2C), 114.1, 115.3, 129.1 (2C), 139.3, 147.6, 149.3, 157.9, 195.6 and 195.8.

3,3-Dimethyl-9-(4-chlorophenyl)-10-methyldecahydroacridine-1,8-dione (4ba). Light yellow solid, mp 233–234 °C (from EtOH); (Found: C, 71.6; H, 6.4; N, 3.9. Calc. for $\text{C}_{22}\text{H}_{24}\text{ClNO}_2$: C, 71.4; H, 6.5; N, 3.8%); $\nu_{\text{max}}/\text{cm}^{-1}$ 2958, 1644, 1626, 1565, 1485, 1462, 1364, 1233, 1190, 1117, 1012, 973, 847, 821 and 556 cm^{-1} ; δ_{H} (300 MHz; CDCl_3 ; Me_4Si) 1.05 (3H, s, CH_3), 1.10 (3H, s, CH_3), 1.94–2.09 (2H, m, CH_2), 2.21 (2H, s, CH_2), 2.27–2.41 (3H, m, CH_2), 2.47–2.59 (1H, m, CH_2), 2.60 (1H, d, J_{AB} 16.9, CH_2), 2.77 (1H, dt, J 17.0 and 6.0, CH_2), 3.28 (3H, s, NCH_3), 5.26 (1H, s, CH), 7.14 (2H, d, J 8.7, ArH) and 7.18 (2H, d, J 8.8, ArH); δ_{C} (75 MHz; CDCl_3 ; Me_4Si) 21.7, 26.9, 28.8, 28.9, 31.6, 32.8, 33.5, 36.5, 40.8, 50.1, 115.0, 116.0, 128.3 (2C), 129.2 (2C), 131.6, 144.6, 151.0, 153.1, 195.4 and 195.5.

3,3-Dimethyl-9-phenyl-10-methyldecahydroacridine-1,8-dione (4bb). Light yellow solid, mp 197–198 °C (from EtOH); (Found: C, 78.6; H, 7.4; N, 4.3. Calc. for $\text{C}_{22}\text{H}_{25}\text{NO}_2$: C, 78.8;

H, 7.5; N, 4.2%); $\nu_{\max}/\text{cm}^{-1}$ 2954, 1640, 1633, 1564, 1474, 1450, 1372, 1322, 1230, 1188, 1115, 972, 934, 700 and 549 cm^{-1} ; δ_{H} (300 MHz; CDCl_3 ; Me_4Si) 1.05 (3H, s, CH_3), 1.10 (3H, s, CH_3), 1.94–2.12 (2H, m, CH_2), 2.22 (2H, s, CH_2), 2.27–2.44 (3H, m, CH_2), 2.47–2.57 (1H, m, CH_2), 2.60 (1H, d, J_{AB} 16.8, CH_2), 2.77 (1H, dt, J 17.0 and 6.0, CH_2), 3.27 (3H, s, NCH_3), 5.30 (1H, s, CH), 7.07 (1H, t, J 7.1, ArH), 7.17 (2H, t, J 7.4, ArH) and 7.22 (2H, d, J 6.9, ArH); δ_{C} (75 MHz; CDCl_3 ; Me_4Si) 21.5, 26.7, 28.7, 28.8, 31.6, 32.7, 33.5, 36.5, 40.6, 50.1, 115.0, 116.0, 125.9, 127.5 (2C), 128.0 (2C), 145.9, 151.1, 153.2, 195.5 and 195.6.

3,3-Dimethyl-9-(4-methoxyphenyl)-10-methyldecahydroacridine-1,8-dione (4bc). Light yellow solid, mp 193–194 °C (from EtOH); (Found: C, 75.8; H, 7.6; N, 3.7. Calc. for $\text{C}_{23}\text{H}_{27}\text{NO}_3$: C, 75.6; H, 7.5; N, 3.8%); $\nu_{\max}/\text{cm}^{-1}$ 2948, 1645, 1621, 1561, 1507, 1464, 1367, 1232, 1190, 1173, 1117, 1039, 971, 851, 821, 569 and 546 cm^{-1} ; δ_{H} (300 MHz; CDCl_3 ; Me_4Si) 1.06 (3H, s, CH_3), 1.09 (3H, s, CH_3), 1.96–2.14 (2H, m, CH_2), 2.23 (2H, s, CH_2), 2.28–2.42 (3H, m, CH_2), 2.48–2.59 (1H, m, CH_2), 2.60 (1H, d, J_{AB} 16.8, CH_2), 2.77 (1H, dt, J 17.3 and 6.0, CH_2), 3.28 (3H, s, NCH_3), 3.73 (3H, s, OCH_3), 5.24 (1H, s, CH), 6.72 (2H, d, J 8.6, ArH) and 7.15 (2H, d, J 8.6, ArH); δ_{C} (75 MHz; CDCl_3 ; Me_4Si) 21.7, 26.8, 28.8, 28.9, 31.0, 32.8, 33.4, 36.5, 40.7, 50.1, 55.3, 113.6 (2C), 115.5, 116.5, 128.6 (2C), 138.5, 150.7, 152.8, 157.9, 195.5 and 195.6.

3,3-Dimethyl-9-(4-chlorophenyl)-10-(4-methylphenyl)-decahydroacridine-1,8-dione (4ca). Light yellow solid, mp 287–288 °C (from EtOH); (Found: C, 75.5; H, 6.2; N, 3.2. Calc. for $\text{C}_{28}\text{H}_{28}\text{ClNO}_2$: C, 75.4; H, 6.3; N, 3.1%); $\nu_{\max}/\text{cm}^{-1}$ 2960, 2923, 2869, 1644, 1574, 1510, 1485, 1362, 1291, 1265, 1227, 1184, 1131, 1093, 1014, 977, 838, 769 and 723 cm^{-1} ; δ_{H} (300 MHz; CDCl_3 ; Me_4Si) 0.81 (3H, s, CH_3), 0.95 (3H, s, CH_3), 1.68–1.94 (3H, m, CH_2), 1.99–2.39 (7H, CH_2), 2.47 (3H, s, CH_3), 5.29 (1H, s, CH), 7.09 (2H, d, J 8.3, ArH), 7.21 (2H, d, J 8.3, ArH), 7.33 (2H, d, J 8.3, ArH) and 7.36 (2H, d, J 8.3, ArH); δ_{C} (75 MHz; CDCl_3 ; Me_4Si) 21.3, 21.4, 27.0, 28.5, 29.8, 32.3, 32.5, 36.9, 41.9, 50.4, 114.5, 115.4, 128.3 (2C), 129.0 (br), 129.4 (2C), 129.8 (br), 130.6 (br), 130.9 (br), 131.7, 136.5, 139.8, 145.2, 150.1, 152.1, 195.9 and 196.0.

3,3-Dimethyl-9-phenyl-10-(4-methylphenyl)-decahydroacridine-1,8-dione (4cb). Light yellow solid, mp 254–256 °C (from EtOH); (Found: C, 81.5; H, 7.0; N, 3.5. Calc. for $\text{C}_{28}\text{H}_{29}\text{NO}_2$: C, 81.7; H, 7.1; N, 3.4%); $\nu_{\max}/\text{cm}^{-1}$ 2964, 2929, 2894, 2867, 1643, 1634, 1570, 1511, 1490, 1449, 1428, 1379, 1362, 1335, 1291, 1264, 1225, 1184, 1151, 1133, 978, 849, 738, 698, 557 and 526 cm^{-1} ; δ_{H} (300 MHz; CDCl_3 ; Me_4Si) 0.73 (3H, s, CH_3), 0.82 (3H, s, CH_3), 1.71–1.90 (3H, m, CH_2), 1.99–2.40 (7H, m, CH_2), 2.47 (3H, s, CH_3), 5.33 (1H, s, CH), 7.07–7.13 (3H, m, ArH), 7.25 (2H, t, J 7.5, ArH), 7.33 (2H, d, J 7.8, ArH) and 7.42 (2H, d, J 7.3, ArH); δ_{C} (75 MHz; CDCl_3 ; Me_4Si) 21.2, 21.3, 26.9, 28.3, 29.7, 32.4 (2C), 36.8, 41.8, 50.4, 114.6, 115.5, 125.9, 127.9 (2C), 128.1 (2C), 128.9 (br), 129.6 (br), 130.5 (br), 130.7 (br), 136.5, 139.6, 146.5, 150.0, 151.9, 195.8 and 196.0.

3,3-Dimethyl-9-(4-methoxyphenyl)-10-(4-methylphenyl)-decahydroacridine-1,8-dione (4cc). Light yellow solid, mp 244–246 °C (from EtOH); (Found: C, 79.0; H, 7.2; N, 3.3. Calc. for

$\text{C}_{29}\text{H}_{31}\text{NO}_3$: C, 78.9; H, 7.1; N, 3.2%); $\nu_{\max}/\text{cm}^{-1}$ 2944, 2928, 2871, 1651, 1609, 1573, 1510, 1456, 1447, 1424, 1362, 1303, 1289, 1225, 1150, 1124, 1033, 980, 832, 738, 659, 568 and 523 cm^{-1} ; δ_{H} (300 MHz; CDCl_3 ; Me_4Si) 0.82 (3H, s, CH_3), 0.94 (3H, s, CH_3), 1.71–1.90 (3H, m, CH_2), 1.98–2.39 (7H, m, CH_2), 2.47 (3H, s, CH_3), 3.75 (3H, s, OCH_3), 5.26 (1H, s, CH), 6.79 (2H, d, J 8.6, ArH), 7.11 (2H, d, J 7.9, ArH), 7.32 (2H, d, J 7.9, ArH) and 7.34 (2H, d, J 8.5, ArH); δ_{C} (75 MHz; CDCl_3 ; Me_4Si) 21.3, 21.4, 27.0, 28.4, 29.8, 31.7, 32.5, 36.9, 41.9, 50.4, 55.3, 113.6 (2C), 114.9, 115.9, 128.9 (2C), 129.0 (br), 129.8 (br), 130.5 (br), 130.9 (br), 136.6, 139.2, 139.6, 149.8, 151.7, 157.9, 196.0 and 196.1.

Single crystal structure of 4aa. The single-crystal growth was carried out in ethanol at room temperature. X-ray crystallographic analysis was performed with a Rigaku Mercury CCD area detector (graphite monochromator, Mo K α radiation $\lambda = 0.71073$ Å). Crystal data for **4aa**: $\text{C}_{21}\text{H}_{22}\text{ClNO}_2$, light yellow, crystal dimension 0.40 × 0.30 × 0.20 mm, monoclinic, space group $P21/c$, $a = 7.1209(8)$, $b = 16.3999(19)$, $c = 15.0997(16)$ Å, $\beta = 92.716(4)^\circ$, $V = 1761.4(3)$ Å 3 , $M_r = 355.85$, $Z = 4$, $D_c = 1.342$ g cm^{-3} , $\lambda = 0.07107$ Å, $\mu(\text{Mo K}\alpha) = 0.231$ mm^{-1} , $F(000) = 752$, $S = 1.099$, $R_1 = 0.0412$, $wR_2 = 0.0963$.†

Acknowledgements

We are grateful for the financial support from the National Science Fund for Distinguished Young Scholars (20125205), Fund for Innovative Research Groups of National Science Foundation of China (20321101) and Anhui Provincial Bureau of Human Resources (2001Z019).

References

- 1 R. A. Sheldon, *Green Chem.*, 2005, **7**, 267.
- 2 P. Anastas and T. Williamson, *Green Chemistry, Frontiers in Benign Chemical Synthesis and Processes*, University Press, London, 1998.
- 3 (a) A. Loupy, *Top. Curr. Chem.*, 1999, **206**, 153; (b) K. Tanaka and F. Toda, *Chem. Rev.*, 2000, **100**, 1025; (c) G. Rothenberg, A. P. Downie, C. L. Raston and J. L. Scott, *J. Am. Chem. Soc.*, 2001, **123**, 8701; (d) G. W. V. Cave, C. L. Raston and J. L. Scott, *Chem. Commun.*, 2001, 2159.
- 4 (a) C.-J. Li, *Chem. Rev.*, 1993, **93**, 2023; (b) A. Lubineau and J. Augé, *Top. Curr. Chem.*, 1999, **206**, 1; (c) U. M. Lindström, *Chem. Rev.*, 2002, **102**, 2751; (d) C.-J. Li, *Chem. Rev.*, 2005, **105**, 3095.
- 5 F. Bossert, H. Meyer and E. Wehinger, *Angew. Chem., Int. Ed. Engl.*, 1981, **20**, 762.
- 6 (a) D. M. Stout and A. I. Meyers, *Chem. Rev.*, 1982, **82**, 223; (b) R. A. Janis and D. J. Triggle, *J. Med. Chem.*, 1983, **26**, 775.
- 7 (a) R. J. Chorvat and K. J. Rorig, *J. Org. Chem.*, 1988, **53**, 5779; (b) C. O. Kappe, W. M. F. Fabian and M. A. Semones, *Tetrahedron*, 1997, **53**, 2803; (c) D. J. Triggle, D. A. Langs and R. A. Jannis, *Med. Res. Rev.*, 1989, **9**, 123.
- 8 S. Goldmann and J. Stoltefuss, *Angew. Chem., Int. Ed. Engl.*, 1991, **30**, 1559.
- 9 B. Loev, M. M. Goodman, K. M. Snader, R. Tedeschi and E. Macko, *J. Med. Chem.*, 1974, **17**, 956.
- 10 M. Schramm, G. Thomas, R. Tower and G. Franckowiak, *Nature*, 1983, **303**, 535.

† CCDC reference number CCDC 279260. For crystallographic data in CIF or other electronic format see DOI: 10.1039/b604064k

- 11 (a) P. Shanmugasundaram, P. Murugan, V. T. Ramakrishnan, N. Srividya and P. Ramamurthy, *Heteroat. Chem.*, 1996, **7**, 17; (b) R. Popielarz, S. Hu and D. C. Neckers, *J. Photochem. Photobiol., A*, 1997, **110**, 79.
- 12 H. J. Timpe, S. Ulrich, C. Decker and J. P. Fouassier, *Macromolecules*, 1993, **26**, 4560.
- 13 (a) P. Shanmugasundaram, K. J. Prabahar and V. T. Ramakrishnan, *J. Heterocycl. Chem.*, 1993, **30**, 1003; (b) N. Srividya, P. Ramamurthy, P. Shanmugasundaram and V. T. Ramakrishnan, *J. Org. Chem.*, 1996, **61**, 5083; (c) P. Murugan, P. Shanmugasundaram, V. T. Ramakrishnan, B. Venkatachalapathy, N. Srividya, P. Ramamurthy, K. Gunasekaran and D. Velmurugan, *J. Chem. Soc., Perkin Trans. 2*, 1998, **4**, 999; (d) T.-S. Jin, J.-S. Zhang, T.-T. Guo, A.-Q. Wang and T.-S. Li, *Synlett*, 2004, 2001; (e) S.-J. Tu, Z. Lu, D. Shi, C. Yao, Y. Gao and C. Guo, *Synth. Commun.*, 2002, **32**, 2181; (f) S. Tu, C. Miao, Y. Gao, F. Fang, Q. Zhuang, Y. Feng and D. Shi, *Synlett*, 2004, 255.
- 14 (a) Z. Zhang, Y.-W. Dong, G.-W. Wang and K. Komatsu, *Synlett*, 2004, 61; (b) Z. Zhang, Y.-W. Dong, G.-W. Wang and K. Komatsu, *Chem. Lett.*, 2004, **33**, 168; (c) Z. Zhang, G.-W. Wang, C.-B. Miao, Y.-W. Dong and Y.-B. Shen, *Chem. Commun.*, 2004, 1832; (d) Z. Zhang, J. Gao, J.-J. Xia and G.-W. Wang, *Org. Biomol. Chem.*, 2005, **3**, 1617; (e) C.-S. Jia, Z. Zhang, S.-J. Tu and G.-W. Wang, *Org. Biomol. Chem.*, 2006, **4**, 104.
- 15 (a) Z. Zhang, Y.-W. Dong and G.-W. Wang, *Chem. Lett.*, 2003, **32**, 966; (b) G.-W. Wang, Z. Zhang and Y.-W. Dong, *Org. Process Res. Dev.*, 2004, **8**, 18; (c) J.-J. Xia and G.-W. Wang, *Synthesis*, 2005, 2379; (d) G.-W. Wang, C.-S. Jia and Y.-W. Dong, *Tetrahedron Lett.*, 2006, **47**, 1059.
- 16 (a) A.-Z. A. Elassara and A. A. El-Khair, *Tetrahedron*, 2003, **59**, 8463; (b) B. Stanovnik and J. Svete, *Chem. Rev.*, 2004, **104**, 2433.
- 17 (a) D. L. Ostercamp, *J. Org. Chem.*, 1970, **35**, 1632; (b) J. V. Greenhill, *J. Chem. Soc., Perkin Trans. 1*, 1976, 2207; (c) T. Putkonen, A. Tolvanen, R. Jokela, S. Caccamese and N. Parrinello, *Tetrahedron*, 2003, **59**, 8589; (d) Y. L. Chen, P. S. Mariano, G. M. Little, D. O'Brien and P. L. Huesmann, *J. Org. Chem.*, 1981, **46**, 4643; (e) K. Ramalingam, M. Balasubramanian and V. Baliah, *Indian J. Chem.*, 1972, **10**, 62; (f) M. Azzaro, S. Geribaldi and B. Vibeau, *Synthesis*, 1981, 880.
- 18 (a) R. Breslow, *Acc. Chem. Res.*, 1991, **24**, 159; (b) S. Otto and J. B. F. N. Engberts, *Pure Appl. Chem.*, 2000, **72**, 1365; (c) S. Otto and J. B. F. N. Engberts, *Org. Biomol. Chem.*, 2003, **1**, 2809.
- 19 A. Sobolev, M. C. R. Franssen, G. Duburs and A. D. Groot, *Biocatal. Biotransform.*, 2004, **22**, 231.
- 20 (a) J. J. Baldwin, D. A. Claremon, P. K. Lumma, D. E. McClure, S. A. Rosenthal, R. J. Winquist, E. P. Faison, G. J. Kaczorowski, M. J. Trumble and G. M. Smith, *J. Med. Chem.*, 1987, **30**, 690; (b) H. Hofmann and R. J. Camiraglia, *THEOCHEM*, 1990, **205**, 1; (c) G. C. Rovnyak, S. D. Kimball, B. Beyer, G. Cucinotta, J. D. DiMarco, J. Gougoutas, A. Hedberg, M. Malley, J. P. McCarthy, R. Zhang and S. Morelande, *J. Med. Chem.*, 1995, **38**, 119.

A black and white photograph of a man with glasses looking over a large stack of papers. He has a surprised or overwhelmed expression. The papers are piled high, obscuring the lower part of his face. A dark banner with white text is overlaid on the papers.

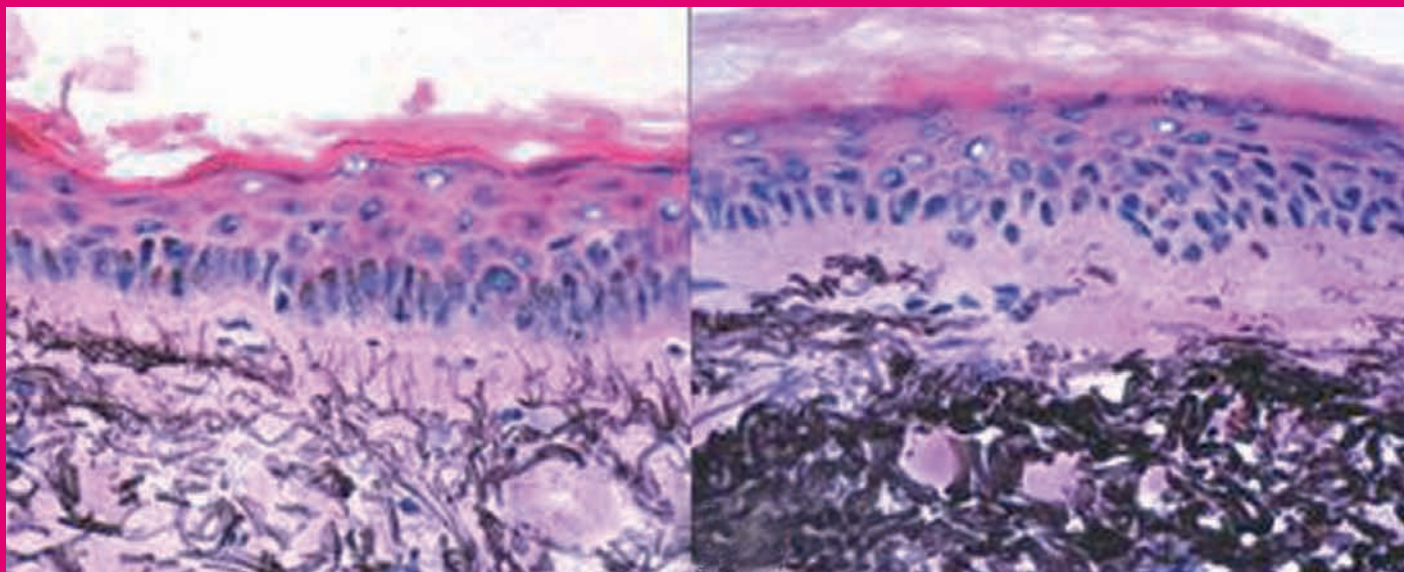
Impact factor
now
13.747!

No time to keep up with your reading?

Let *Chem Soc Rev* do the hard work for you. Our mission is to provide authoritative, accessible, succinct and reader-friendly reviews on carefully selected topics of broad and specialist interest in the chemical sciences. Highly cited and engaging to read, *Chem Soc Rev* articles are designed to highlight important primary research papers, provide concise updates of technological progress and give insight into emerging industry trends. Don't waste time scouring the literature – pick up a copy of *Chem Soc Rev* and regain back some of your precious time.

RSC Publishing

www.rsc.org/chemsocrev



Photochemical & Photobiological Sciences

The official journal of the European Society for Photobiology, the European Photochemistry Association, the Asia and Oceania Society for Photobiology and the Korean Society of Photoscience.

High-quality, peer-reviewed papers concerned with any aspect of the interaction of light with molecules, supramolecular systems or biological matter.

- Fast times to publication (typically 85 days)
- Impact factor 2.117
- High visibility – indexed in MEDLINE and ISI
- 12 issues a year



RSC online shop now open

And to celebrate we're having a sale...

The RSC online shop gives you continuous access to class leading products and services, expertly tailored to cater for your training and educational needs.

Browse: visit our shop to browse over 400 book titles, subscribe or purchase an individual article in one of our journals, register to attend a conference or one of our training events.

Gift Ideas: if you're looking for gift ideas, look no further. In our online shop you'll find everything from popular science books like *The Age of the Molecule* and the inspirational *Elegant Solutions* from award winning writer, Philip Ball, to our stunning Visual Elements wall chart and brain-teasing *Chemistry Su Doku* and *Crosswords* puzzle series.

Sale Now On: shop online during November and December and get a huge **25% discount*** on all books, puzzles/games, videos or wall charts purchased.

* Discount applied to your purchases when you check out.
Offer ends December 31st, 2006

RSC is a not for profit organisation. Revenue generated from collecting membership subscriptions, conference registration fees or through sales of our products is invested to support chemical science initiatives across the world.

Registered Charity Number: 207890